

**THE EFFECT OF PHYLLOSILICATE
MINERALOGY AND SURFACE
CHARGE ON THE RHEOLOGY OF
MINERAL SLURRIES**

A Thesis Submitted for the Degree of
DOCTOR OF PHILOSOPHY

By:

Bulelwa Ndlovu

**Department of Chemical Engineering
Faculty of Engineering and the Built Environment
University of Cape Town**

August 2013

The copyright of this thesis vests in the author. No quotation from it or information derived from it is to be published without full acknowledgement of the source. The thesis is to be used for private study or non-commercial research purposes only.

Published by the University of Cape Town (UCT) in terms of the non-exclusive license granted to UCT by the author.

‘Omnia possum in eo qui me confortat’

University of Cape Town

LIST OF PUBLICATIONS AND PRESENTATIONS

- Ndlovu, B., Forbes, E., Becker, M., Farrokhpay, S., Deglon, D. & Bradshaw, D. 2013, “A preliminary rheological classification of phyllosilicate group minerals”, *Minerals Engineering*, <http://dx.doi.org/10.1016/j.mineng.2013.06.004>
- Ndlovu, B., Forbes, E., Becker, M., Deglon, D., Franzidis, J.P. & Laskowski, J.S. 2011, “The effects of chrysotile mineralogical properties on the rheology of chrysotile suspensions”, *Minerals Engineering*, vol. 24, pp. 1004-1009.
- Ndlovu, B., Becker, M., Forbes, E., Deglon, D. & Franzidis, J.P. 2011, “The influence of phyllosilicate mineralogy on the rheology of mineral suspensions”, *Minerals Engineering*, vol. 24, pp. 1314-1322.
- Ndlovu, B., Kilickaplan, I. & Laskowski, J.S. 2010, “The rheology of aqueous suspensions of needle-like particles, International Symposium on the Fundamentals of Mineral Processing, Canadian Institute of Mining, Metallurgy and Petroleum, pp. 193-203. **ISBN: 978-926872-01-8.** (8th UBC-McGill-UA International Symposium, Conference of Metallurgists (COM), Vancouver, October 2010).
- Burdukova, E., Becker, M., Ndlovu, B., Mokgethi. & Deglon, D. 2008, “Relationship between slurry rheology and mineralogical content”, In XXIV International Minerals Processing Congress (IMPC), China, Beijing, pp. 2169-2178. **ISBN: 978-7-03-022711-9.**
- Ndlovu, B., Forbes, E., Becker, M., Farrokhpay, S., Deglon, D. & Bradshaw, D. 2013, “A preliminary rheological classification of phyllosilicate group minerals”, *Presented at Process Mineralogy '12, MEI Conferences, Cape Town, November 2012.*
- Ndlovu, B., Burdukova, E., Becker, M., Deglon, D.A., Franzidis, J.P & Laskowski, J.S. “An investigation on the effect of chrysotile shape and anisotropic properties on the rheology of chrysotile suspensions”. *Presented at XXV International Minerals Processing Congress (IMPC), Brisbane, (AUSIMM), September 2010.*
- Ndlovu, B., Becker, M., Forbes, E. & Deglon, D.A. “An investigation on the effect of muscovite and vermiculite mineralogy on the rheology of mineral suspensions”.

Presented at Process Mineralogy '10, MEI Conferences, Cape Town, November 2010.

Ndlovu, B., Becker, M, Deglon, D.A. & Franzidis, J.P. “An investigation on the effect of mineralogy and surface charge on slurry rheology”. *Presented at South African Institute of Mining and Metallurgy (SAIMM) Minerals Processing Conference, Cape Town, August 2009.*

University of Cape Town

DECLARATION

I hereby certify that the work embodied in this thesis is the result of original research and has not been submitted for another degree at any other university or institution.

Signed: _____

Bulelwa N. Ndlovu



ACKNOWLEDGEMENTS

I would like to express my sincere gratitude to the following people, who have all in their own special way provided guidance and support and without whom this project would not be possible:

- My supervisors Professor David Deglon, Dr. Megan Becker and Dr. Elizaveta Forbes, for their continued enthusiasm, assistance and mentorship throughout this study, for being an inspiration, providing constant support of my work and maintaining an open door policy. Your guidance and advice is greatly appreciated.
- The Minerals to Metals Initiative at the University of Cape Town, for their financial support of this project through the SARChi Chair in Minerals Beneficiation, and a Research Niche Area (RNA) grant from the National research Foundation.
- Professor Jean Paul Franzidis for his endless knowledge of the minerals processing industry and his invaluable pearls of wisdom.
- The staff and students of the Minerals to Metals Initiative and the Centre for Minerals Research at the University of Cape Town for their valuable and constructive advice. A special thank you to Jenni Wiese, Kenneth Maseko, Monde Bekapi, Lorraine Nkemba and Kerryn Gray for all their help in the laboratory and for making those long hours seem much shorter. To Mymoena van der Fort for her patience and willingness to assist at all times.
- The staff and students of the Julius Kruttschnitt Minerals Research Centre (JKMRC) for their support and encouragement. A special thank you to Dee Bradshaw, David Steele Saeed Farrokhpay, Kate Tungpalan and Vannie Resabel.
- The staff and students at the N.B Keevil Institute of Mining at the University of British Columbia for their assistance and advice in the early stages of the project. A special thank you to Professor Janusz Laskowski for affording me the

opportunity to perform my experimental work in a safe environment and for his technical contribution to this research project. A special thank you to Sally Finora and Pius Lo for their assistance during this time.

- Helen Divey and the analytical laboratory staff of the Department of Chemical Engineering, University of Cape Town for their help with analyses.
- Dr. Kirsten Corin (UCT) for her perseverance and assistance with the XRD analysis.
- Mrs. Miranda Waldron of the Physics Department, University of Cape Town, for her help with SEM analysis.
- Professor Dave Reid, Christel Tinguely and the staff from the Department of Geological Sciences at the University of Cape Town, for their assistance with sample preparation and EMP analysis.
- My family and friends, for their encouragement and heartfelt support from miles away. Chilufya, for his love, support and continued encouragement and for being my rock over the past couple of years.
- And finally I would like to thank my mother, Otilia Ndlovu, for her unwavering support and for being my biggest fan throughout the years, even when I least deserved it.

SYNOPSIS

Phyllosilicate minerals exist as common gangue components in many low grade ores. Often broadly classified as 'clays', this group of minerals is closely associated with several processing issues. Despite many good studies on the physico-chemical properties of phyllosilicates, there still remains a poor understanding of their suspension flow behaviour. The primary objective of this thesis was to characterise the colloidal behaviour of three commonly occurring phyllosilicates, namely muscovite, vermiculite and chrysotile in terms of their surface charge, mineralogical and resultant rheological properties. The thesis was initiated in order to gain a better understanding of the flow behaviour of these minerals within well-defined model mineral systems, with a longer term view to understanding their impact in complex mineral systems found in mineral processing circuits.

The morphological properties were investigated using scanning electron microscopy and optical microscopy. It was demonstrated that muscovite particles had a long, thin platy morphology with platelets of high aspect ratio (~40-130). Vermiculite used in this study comprised plates of a lower aspect ratio (~16-20), and a comparatively lower crystallinity than smooth muscovite platelets. Chrysotile, on the other hand, is long, thin and fibrous with a high degree of flexibility when in suspension. Compared to quartz, a non-phyllosilicate mineral with angular morphology, the phyllosilicates all demonstrated a large deviation from sphericity and regular morphology.

Conventional and non-conventional perspectives on surface charge characterisation were used to reconcile the respective charge anisotropy of the minerals used in this study. In an alternative analytical procedure, the zeta potential and potentiometric titration measurements were used in tandem to estimate the degree of charge anisotropy of each mineral, based primarily on the deviations between the point of zero charge (p.z.c) and the iso-electric point (i.e.p). Confirmatory estimations on the degree of isomorphous substitution served to approximate the pH independent component of charge on the basal planes. It was proposed that the degree of charge anisotropy increases in the order quartz < chrysotile < muscovite < vermiculite.

Surface charge distributions and likely modes of particle association were predicted for each mineral, taking into consideration the contributions from the edges and faces. In muscovite platelets, with a high aspect ratio, the charge contribution of the edge is negated by the comparatively high surface area of the faces which effectively screen out edge effects. Face-face (FF) association is the most important aspect of particle interaction here. The edges are comparatively more significant in vermiculite suspensions, albeit to a small extent, owing to their higher degree of surface charge anisotropy and lower aspect ratio. FF agglomeration is still dominant, although it is predicted that re-alignment to more complex edge-face (EF) and edge-edge (EE) structures is enhanced. Particle morphology is central to chrysotile suspension behaviour, resulting in highly entangled structures over a broad pH range.

A rheological comparison of the minerals was conducted at pH 9, with the yield stresses and viscosities evaluated at medium to high shear conditions, more closely representative of mineral processing applications (e.g. flotation cells and stirred mills). Chrysotile suspensions were characterised by the most complex rheological behaviour (highest yield stresses and viscosities) at extremely low solids concentrations. Vermiculite suspensions also had higher yield stresses and viscosities than muscovite suspensions. All phyllosilicates demonstrated more rheological complexity than non-phyllosilicate quartz suspensions at pH 9.

Binary mixtures of quartz and each phyllosilicate mineral served as preliminary simulations of real ores. It was found that the rheological complexity of muscovite and vermiculite is enhanced in the presence of quartz (antagonistic effects), likely due to the formation of additional structures. However, synergistic effects were observed for chrysotile and quartz suspensions, leading to improved flow behaviour and lower viscosities. This analysis also demonstrated the inadequacy of robust mixture design at predicting the rheological performance of mixed streams. The use of blending practices, on such a basis, is not simple for rheological forecasting.

Overall complex suspension flow behaviour decreases in the order chrysotile < vermiculite < muscovite. Suspensions containing muscovite gangue are less likely to present rheological problems. Low concentrations of chrysotile in an ore, on the other

hand, will result in high viscosities and yield stresses. This study has provided a preliminary rheological characterisation of some minerals belonging to the phyllosilicate group, with the potential for use in classification of phyllosilicate bearing ores. This serves as a contribution to ongoing and future studies aimed at better understanding this class of minerals.

Indeed the analysis of phyllosilicate minerals remains a challenge in the mineral processing industry, perhaps due to the existence of different schools of thought/theories on fundamental issues such as charge derivation and modes of particle interaction. In addition, the analysis of properties such as surface charge has, in the past been compromised by the use of conventional techniques which do not adequately take into consideration the inherent atypical morphology and charge anisotropy of these minerals. This then renders research in this field particularly difficult and to some extent subjective, dependent on the conditions of interest. The complexity of phyllosilicate behaviour is acknowledged in this work.

STATEMENT OF ORIGINALITY & CONTRIBUTION

The following outcomes are considered as original contributions from this research:

- The analysis of the surface charge properties of select phyllosilicate minerals, based on the combination of results from electrophoretic zeta potential, Roberts Mular titration and rheological measurements. The use of these different techniques allows for a comprehensive investigation which takes into account the non-spherical morphology and charge anisotropy of these minerals.
- The determination of the role of surface charge and morphology towards the overall behaviour of selected phyllosilicate minerals in their pure form and in mineral mixtures.
- A preliminary classification of selected phyllosilicate group minerals, based on their rheological properties (yield stresses and viscosities).
- A preliminary assessment of the conformational changes in selected phyllosilicate minerals upon the introduction of another mineral (quartz) with different charge and shape characteristics.
- The preliminary development of the likely modes of particle association as a function of pH (surface charge) in binary mineral systems comprising quartz and selected phyllosilicate minerals.

TABLE OF CONTENTS

LIST OF PUBLICATIONS AND PRESENTATIONS.....	v
DECLARATION.....	vii
ACKNOWLEDGEMENTS	ix
SYNOPSIS.....	xi
STATEMENT OF ORIGINALITY & CONTRIBUTION.....	xiv
GLOSSARY.....	xxvi
LIST OF SYMBOLS.....	xxviii
LIST OF ABBREVIATIONS	xxix
LIST OF ELECTRONIC APPENDICES	xxx
CHAPTER 1: INTRODUCTION	1
1.1. PROBLEM STATEMENT.....	2
1.2. OVERALL OBJECTIVES	6
1.3. KEY QUESTIONS	6
1.4. PROJECT SCOPE AND LIMITATIONS	7
1.5. STRUCTURE OF THE THESIS.....	11
CHAPTER 2: LITERATURE REVIEW	12
2.1. INTRODUCTION	12
2.2. SUSPENSION RHEOLOGY	13
2.2.1. The fundamentals of rheology.....	13
2.2.2. Rheological properties and property measurement	16
2.2.3. Rheology in the minerals processing industry.....	19
2.3. PHYLLOSILICATE MINERALS.....	22
2.3.1. Typical processing problems associated with phyllosilicate bearing ores	25
2.3.2. Current mitigation strategies for dealing with phyllosilicate bearing ores.....	27
2.4. THE MINERALOGY OF MUSCOVITE, VERMICULITE AND CHRYSOTILE.....	28
2.4.1. Muscovite mineralogy (mica group).....	28

2.4.2.	Vermiculite mineralogy (swelling clay group).....	29
2.4.3.	Chrysotile mineralogy (serpentine group)	33
2.4.4.	The effect of phyllosilicate mineralogy (morphology) on rheological behaviour	34
2.5.	PARTICLE SURFACE CHARGE	36
2.5.1.	The electrical double layer	37
2.5.2.	DLVO theory and theoretical interpretation of suspension rheological behaviour.....	38
2.5.3.	The surface charge properties of phyllosilicate minerals.....	41
2.5.4.	Measurement of surface charge.....	44
2.6.	THE MODES OF PHYLLOSILICATE PARTICLE ASSOCIATION	55
2.6.1.	Suspensions of pure minerals	55
2.6.2.	Suspensions of binary mineral mixtures	60
2.7.	SUMMARY	64
	CHAPTER 3: EXPERIMENTAL METHODS	67
3.1.	INTRODUCTION	67
3.2.	MATERIALS	67
3.2.1.	Minerals	67
3.2.2.	Solution additives	68
3.3.	MINERAL CHARACTERISATION	69
3.3.1.	Particle Size Distribution	69
3.3.2.	Powder X-Ray Diffraction	71
3.4.	MINERALOGY MEASUREMENTS	73
3.4.1.	Scanning Electron Microscopy (SEM)	73
3.4.2.	Optical Microscopy	73
3.5.	SURFACE CHARGE MEASUREMENTS	73
3.5.1.	Zeta Potential Measurements	74
3.5.2.	Potentiometric Titration Measurements.....	74
3.5.3.	Electron microprobe analysis	75
3.6.	RHEOLOGY MEASUREMENTS	76
3.6.1.	Direct yield stress measurements	79
3.6.2.	Steady stress/strain rheology measurements	81
3.7.	EXPERIMENTAL PROGRAMME	86

3.8.	STATISTICAL ANALYSIS	87
CHAPTER 4: PHYLLOSILICATE MORPHOLOGY		88
4.1.	INTRODUCTION	89
4.2.	QUARTZ MORPHOLOGY	91
4.3.	MUSCOVITE MORPHOLOGY	93
4.4.	VERMICULITE MORPHOLOGY	97
4.5.	CHRYSOTILE MORPHOLOGY.....	102
4.6.	DISCUSSION.....	104
CHAPTER 5: PHYLLOSILICATE SURFACE CHARGE		107
5.1.	INTRODUCTION	108
5.2.	SURFACE CHARGE PROPERTIES OF QUARTZ	111
5.2.1.	The zeta potential of quartz.....	111
5.2.2.	The point of zero charge of quartz.....	111
5.2.3.	Quartz charge distribution.....	113
5.3.	MUSCOVITE SURFACE CHARGE DISTRIBUTION	115
5.3.1.	The zeta potential of muscovite.....	115
5.3.2.	The point of zero charge of muscovite	116
5.3.3.	The degree of isomorphous substitution in muscovite.....	119
5.3.4.	Proposed charge distribution of muscovite particles	124
5.4.	VERMICULITE SURFACE CHARGE DISTRIBUTION.....	127
5.4.1.	The zeta potential of vermiculite.....	127
5.4.2.	The point of zero charge of vermiculite.....	128
5.4.3.	The degree of isomorphous substitution in vermiculite.....	129
5.4.4.	Proposed charge distribution of vermiculite particles.....	133
5.5.	CHRYSOTILE SURFACE CHARGE DISTRIBUTION.....	136
5.5.1.	The zeta potential of chrysotile	136
5.5.2.	The point of zero charge of chrysotile.....	137
5.5.3.	The degree of isomorphous substitution in chrysotile	138
5.5.4.	Proposed chrysotile surface charge distribution.....	141
5.6.	DISCUSSION	143
CHAPTER 6: pH Mediated Particle Interactions In Aqueous Media		146

6.1.	INTRODUCTION	147
6.2.	PARTICLE INTERACTIONS IN MUSCOVITE & VERMICULITE SUSPENSIONS (PLATY)	148
6.2.1.	Muscovite suspensions	150
6.2.2.	Vermiculite suspensions	154
6.3.	PARTICLE INTERACTIONS IN CHRYSOTILE SUSPENSIONS (FIBROUS).....	157
6.4.	DISCUSSION	159
CHAPTER 7: RHEOLOGY OF SUSPENSIONS OF PURE MINERALS		161
7.1.	INTRODUCTION	162
7.2.	ANALYTICAL APPROACH	163
7.3.	THE RHEOLOGY OF MUSCOVITE AND VERMICULITE SUSPENSIONS	166
7.4.	THE RHEOLOGY OF CHRYSOTILE SUSPENSIONS	171
7.5.	DISCUSSION	175
CHAPTER 8: RHEOLOGY OF SUSPENSIONS OF BINARY MINERAL MIXTURES.....		180
8.1.	INTRODUCTION	181
8.2.	ANALYTICAL APPROACH	182
8.2.1.	Graphing of binary mineral mixtures.....	182
8.3.	SUSPENSIONS OF MUSCOVITE-QUARTZ MIXTURES	185
8.3.1.	The rheology of suspensions of muscovite-quartz mixtures as a function of pH	185
8.3.2.	The rheology of suspensions of muscovite-quartz mixtures at pH 9.....	190
8.4.	THE RHEOLOGY OF SUSPENSIONS OF VERMICULITE-QUARTZ MIXTURES	194
8.4.1.	The rheology of suspensions of vermiculite-quartz mixtures as a function of pH.....	194
8.4.2.	The rheology of suspensions of vermiculite-quartz mixtures at pH 9.....	198

8.5.	THE RHEOLOGY OF SUSPENSIONS OF CHRYSOTILE-QUARTZ MIXTURES	200
8.5.1.	The rheology of suspensions of chrysotile-quartz mixtures as a function of pH	200
8.5.2.	The rheology of suspensions of chrysotile-quartz mixtures at pH 9	203
8.6.	DISCUSSION	205
8.6.1.	A comparison of the rheology of suspensions of phyllosilicate-quartz mixtures	208
8.6.2.	Implications on phyllosilicate mineral behaviour in real ores	209
	CHAPTER 9: CONCLUSIONS” AND RECOMMENDATIONS	213
9.1.	PHYLLOSILICATE MINERALOGY	214
9.2.	PHYLLOSILICATE SURFACE CHARGE DISTRIBUTION	214
9.3.	THE INFLUENCE OF MORPHOLOGY AND SURFACE CHARGE ON SUSPENSION RHEOLOGY	216
9.4.	THE RHEOLOGICAL BEHAVIOUR OF BINARY MIXTURE SUSPENSIONS	217
9.5.	IMPLICATIONS OF THE STUDY	219
9.6.	RECOMMENDATIONS FOR FUTURE WORK	221
	REFERENCES	223

LIST OF FIGURES

Figure 1.1 – Schematic representation of the thesis.	10
Figure 2.1 - Rheograms of different types of fluids.	14
Figure 2.2 - (a) SiO ₄ tetrahedral units and silica ‘T’ layers (b) octahedral (XO ₆) units and the difference between brucite and gibbsite ‘O’ layers.	23
Figure 2.3 - The classification of phyllosilicate group minerals.	25
Figure 2.4 - Crystallographic structure of muscovite (adapted from Fanning et al., 1989).	29
Figure 2.5 - Schematic representing the transformation of micas to swelling clays (adapted from Fanning and Keramidas, 1977).	30
Figure 2.6 - Crystallographic structure of vermiculite (adapted from Douglas, 1989). ...	31
Figure 2.7 – Layer charge differences through the transformation from micas to swelling clays (adapted from Fanning and Keramidas, 1977).	32
Figure 2.8 - Schematic of (a) mismatch between the tetrahedral and octahedral layers, resulting in (b) spiral structure of chrysotile with brucite extended on the outside and silica layer on the inside (adapted from Miller et al., 2007).	34
Figure 2.9 – The effect of solids concentration on apparent viscosity of aqueous suspensions of different morphology (Barnes et al., 1989).	35
Figure 2.10 – Development of electrical double layer on a particle in suspension.	37
Figure 2.11 - Schematic representation of the relationship between surface charge and rheological properties (Laskowski and Pugh, 1992).	40
Figure 2.12 – Schematic of the variation of free energy with particle separation according to the DLVO theory (Nasroti, 2010) and (b) the variation of free energy with particle separation at higher salt concentrations, showing the appearance of a secondary minimum (Nasroti, 2010).	41
Figure 2.13 – The zeta potential properties of the edge and face surfaces of kaolinite in the presence of 0.01M NaCl background. Edge data taken from Williams and Williams, 1978. Face ζ potentials determined by correcting data by Johnson et al., 1998 for the effect of edge ζ potential. (Johnson et al., 2000).	43
Figure 2.14 - Schematic representation of the electrical double layer, showing the difference between the zeta potential and surface charge (Alvarez-Silva et al, 2010).	46

Figure 2.15- The zeta potential and yield stress vs. pH curves for zirconia suspensions (Subbanna et al., 1998).....	48
Figure 2.16 - The normalised zeta potential and yield stress vs. pH curves for kaolinite suspensions (Johnson et al., 1998).	50
Figure 2.17 - Theoretical plot of net surface charge density of potential determining ions vs. pH (Mular and Roberts, 1966).....	53
Figure 2.18- Electrophoretic behaviour of planar (kaolinite) and tubular (halloysite) in comparison with gibbsite and silica (Miller et al., 2007).	55
Figure 2.19- The relative magnitudes of the FF, EE and EF interaction forces, F . All forces have been multiplied by the geometrically predicted interaction area ratio and then normalized by the maximum attractive EF force, F_{max} (Johnson et al., 2000).	58
Figure 2.20 – Schematic representation of the modes of particle interaction in homogeneous mineral suspensions as a function of pH and Bingham yield stress (adapted from Rand and Melton, 1977).....	58
Figure 3.1 – Cumulative size distributions of chrysotile, muscovite, montmorillonite, vermiculite and quartz.	70
Figure 3.2 - SEM micrographs used in the size estimation of chrysotile fibres.	71
Figure 3.3 - Schematic representation of the double gap measuring system used (Paar Physica MC1).....	78
Figure 3.4 – Schematic representation of the vane measuring system used (AR1500EX and Viscotester 550).	78
Figure 3.5 – (a) Haake Viscotester 550 rheometer (b) Paar Physica MC1 Rheometer and (c) AR 1500ex rheometer.	79
Figure 3.6 - Typical stress decay curve observed using the vane method.....	81
Figure 3.7 – (a) A comparison of calculated and corrected shear rate values, (b) Errors in calculated shear rate values for the narrow gap size used in the double gap geometry ...	83
Figure 3.8 - Typical rheograms observed, fitted with the Bingham model.	84
Figure 3.9 – Graphical representation of ‘critical’ phyllosilicate mineral-quartz concentration.	86
Figure 3.10 – Experimental programme for the study.....	87
Figure 4.1 - SEM micrographs demonstrating the angular morphology and dense packing of quartz particles.	92

Figure 4.2 - SEM images demonstrating the platy morphology, high aspect ratio and smooth surface structure of muscovite.	96
Figure 4.3 – Figure 4.3a to 4.3d SEM images demonstrating poor surface crystallography, swelling potential and exfoliation behaviour of vermiculite. Figures 4.3e and f show optical microscopy images of exfoliated vermiculite.....	101
Figure 4.4 - SEM images demonstrating the long, thin fibrous morphology and high degree of entanglement of chrysotile particles.	103
Figure 5.1 – A comparison of the iso-electric point (as determined by zeta potential measurement) and the point of zero charge (as determined by the Roberts Mular titration measurement) of quartz (Alvarez-Silva et al., 2010).	112
Figure 5.2 – The zeta potential of gibbsite and silica (Miller et al., 2007), compared to the electrokinetic zeta potential of muscovite (this study). The error bars represent 95% confidence interval of average values.	115
Figure 5.3 - A comparison of the iso-electric point (i.e.p) and point of zero charge (p.z.c) of muscovite. The error bars represent 95% confidence interval and the standard deviation of the average values.	119
Figure 5.4 - Ideal classification of cations according to muscovite formula.	122
Figure 5.5 - Dissipation of charge in the T and O layers.	123
Figure 5.6 - Proposed surface charge distribution of muscovite edges and faces.....	126
Figure 5.7 – The zeta potential of brucite and silica (Miller et al., 2007), compared to the electrokinetic zeta potential of vermiculite (this study). The error bars represent 95% confidence interval of average values.	127
Figure 5.8 - A comparison of the iso-electric point (i.e.p) and point of zero charge (p.z.c) of vermiculite. The error bars represent 95% confidence interval of the average values.	129
Figure 5.9 - Ideal classification of cations according to vermiculite formula.	132
Figure 5.10 - Proposed surface charge distribution of vermiculite edges and faces.	135
Figure 5.11 - The zeta potential of brucite and silica, compared to the electrokinetic zeta potential of chrysotile (Ney, 1973).	137
Figure 5.12 - A comparison of the iso-electric point (i.e.p) (Ney, 1973) and point of zero charge (p.z.c)of chrysotile (this study). The error bars represent 95% confidence interval of the average values.	138
Figure 5.13 - Ideal classification of cations according to chrysotile formula.....	140

Figure 5.14 - Proposed surface charge distribution of chrysotile particles.	142
Figure 6.1 - Proposed particle interactions of muscovite suspensions as a function of pH. The error bars represent the 95% confidence interval.	153
Figure 6.2 - Proposed particle interactions of vermiculite suspensions as a function of pH. The error bars represent the 95% confidence interval.	156
Figure 6.3 – An optical micrograph of chrysotile fibres suspended in solution. The characteristic entangling and heterocoagulation of the flexible fibres into ‘clusters’ is evident.	158
Figure 6.4 - Proposed particle interactions of chrysotile suspensions as a function of pH. The error bars represent the 95% confidence interval.	159
Figure 7.1 – Example of typical rheograms observed with the phyllosilicate suspensions. The rheograms are fitted with the Bingham model in the shear rate range where data could be analysed.	166
Figure 7.2 – A comparison of the Bingham yield stresses of suspensions of pure vermiculite, muscovite and quartz. The errors bars represent the 95% confidence interval of the average values.	167
Figure 7.3 - A comparison of the Bingham viscosities of suspensions of vermiculite, muscovite and quartz at pH 9. The errors bars represent the 95% confidence interval of the average values.	171
Figure 7.4 - A comparison of the Bingham yield stresses of suspensions of chrysotile and quartz at pH 9. The errors bars represent the 95% confidence interval of the average values.	172
Figure 7.5 - A comparison of the Bingham viscosities of suspensions of chrysotile and quartz at pH 9. The errors bars represent the 95% confidence interval of the average values.	175
Figure 7.6 - A comparison of the Bingham yield stresses of suspensions of all the phyllosilicate minerals relative to quartz, a non-phyllosilicate mineral at pH 9. The errors bars represent the 95% confidence interval of the average values.	177
Figure 7.7 - A comparison of the Bingham viscosities of suspensions of all the phyllosilicate minerals relative to quartz, a non-phyllosilicate mineral at pH 9. The errors bars represent the 95% confidence interval of the average values.	178
Figure 8.1 – Example of graphical analysis used for the binary mineral mixtures.	184

Figure 8.2 – A comparison of the yield stresses of muscovite-quartz binary mixtures to pure muscovite suspensions as a function of pH.	186
Figure 8.3 - Proposed modes of particle interaction in muscovite-quartz mixtures as a function of pH.	189
Figure 8.4 - A comparison of the (a) Bingham yield stresses and (b) Bingham viscosities of suspensions of muscovite-quartz mixtures to the predicted model and to suspensions of pure muscovite and pure quartz. The errors bars represent the 95% confidence interval of the average values.	193
Figure 8.5 - A comparison of the yield stresses of vermiculite-quartz binary mixtures to pure vermiculite suspensions as a function of pH.....	195
Figure 8.6 - Proposed modes of particle interaction in vermiculite-quartz mixtures as a function of pH.	197
Figure 8.7 - A comparison of the (a) Bingham yield stresses and (b) Bingham viscosities of suspensions of vermiculite-quartz mixtures to the predicted model and to suspensions of pure vermiculite and pure quartz. The errors bars represent the 95% confidence interval of the average values.	199
Figure 8.8 - A comparison of the (a) Bingham yield stresses and (b) Bingham viscosities of suspensions of chrysotile-quartz mixtures at pH 6 and pH 9. The error bars represent the 95% confidence interval on the average values.	200
Figure 8.9 - Proposed modes of particle association in chrysotile-quartz mixtures as a function of pH.	202
Figure 8.10 - A comparison of the (a) Bingham yield stresses and (b) Bingham viscosities of suspensions of chrysotile-quartz mixtures to the predicted model and to suspensions of pure chrysotile and quartz. The errors bars represent the 95% confidence interval of the average values.	204
Figure 8.11 – A comparison of the Bingham yield stresses and viscosities of pure mineral suspensions and suspensions of binary mixtures.	208
Figure 9.1 – Proposed charge distributions of the phyllosilicate minerals.....	216
Figure 9.2 – A graphical representation of the classification of chrysotile, vermiculite and muscovite suspension behaviour.....	219

LIST OF TABLES

Table 3.1 – P ₅₀ values of minerals as determined by Malvern Mastersizer size analysis.	70
Table 3.2 – Purity of the minerals as determined by XRD analysis.....	72
Table 3.3 - Experimental methods, conditions and variables used in surface charge characterisation of each mineral.....	74
Table 3.4 – Detailed microprobe analysis of quartz, muscovite, vermiculite and montmorillonite samples.	76
Table 3.5 - Experimental methods, conditions and variables used in the rheological characterisation of mineral suspensions.	77
Table 3.6 – A comparison of the Bingham viscosities of quartz suspensions obtained using the AR1500ex rheometer and the MC1 rheometer.	79
Table 4.1 - A summary of estimated aspect ratios of the phyllosilicates.	104
Table 5.1 - Average composition of quartz (weight %) using electron microprobe analysis. The error is a standard deviation of 3 sample populations.....	113
Table 5.2 - Distribution of cations in quartz.	114
Table 5.3 - The average composition of muscovite (weight %) using electron microprobe analysis. The error is a standard deviation of 8 sample populations.....	120
Table 5.4 - Calculated average number of cations in muscovite.....	121
Table 5.5 - Classification of cations in muscovite.	122
Table 5.6 - The average composition of vermiculite (weight %) using electron microprobe analysis. The error is a standard deviation of 8 sample populations.	130
Table 5.7 - Calculated average number of cations in vermiculite.....	131
Table 5.8 - Classification of cations in vermiculite.....	132
Table 5.9 - Typical composition of chrysotile (weight %) (Brindley and Zussman, 1957).	139
Table 5.10 - Typical number of cations in a single crystalline cell of chrysotile (Brindley and Zussman, 1957).	139
Table 5.11 - Classification of cations in chrysotile.	140
Table 5.12 – Summary of surface charge data for the minerals under study.....	143
Table 7.1 - Qualitative comparison of the rheological properties of the minerals.....	176
Table 8.1 – A summary of the rheological effects of mixing each phyllosilicate mineral with quartz.	207

GLOSSARY

Anisotropic Mineral	A mineral that has a heterogeneous surface charge distribution.
Apparent iso-electric	The iso-electric point obtained by means of an electrophoretic mobility measurement which does not directly correspond to the point of zero charge of the mineral.
Iso- electric point	The pH value at which the electrophoretic mobility of a mineral is zero (i.e.p).
Isotropic Mineral	A mineral that has a homogeneous surface charge distribution.
Net point of zero charge	The pH value at which the charge differential between different planes on a mineral surface is largest.
Phyllosilicate mineral	Layered sheet silicate mineral comprising tetrahedral and octahedral units
Point of zero charge	The pH value at which the overall surface charge of a mineral is zero (p.z.c).
Pseudo Plastic fluid	Material in which viscosity decreases with increasing rate of shear (also termed shear thinning).
Rheology	The study of flow and deformation of matter.
Shear Rate	Shear rate is a measure of the rate of shear deformation, units of $[s^{-1}]$.

Shear Stress	Shear stress is a stress state where the stress is parallel or tangential to a face of the material, as opposed to normal stress when the stress is perpendicular to the face, units of [Pa].
Van der Waals forces	Electrostatic interactions that exist between charges and multipoles. These intermolecular forces also exist between a permanent multipole on one molecule and an induced multipole on another.
Viscosity	The measure of resistance to flow of a fluid due to inter particle forces and friction between molecules, units of [Pas]
Yield stress	The initial force required to initiate flow of a suspension, units of [Pa].
Yield stress peak	The pH value at which the yield stress is at its maximum, (y.s.p).

LIST OF SYMBOLS

\mathcal{T}	- Shear stress [Pa]
\mathcal{T}_0	- Yield Stress [Pa]
η_p	- Plastic viscosity [Pas]
γ	- Shear rate [s^{-1}]
V_T	- Attractive energy [kJ/mol]
V_A	- Repulsive energy [kJ/mol]
V_R	- Total energy [kJ/mol]
ζ	- Electrokinetic potential (zeta potential) [mV]
Φ	- Surface potential [mV]
σ_0	- Net surface charge density [Coulombs/m ²]
ε	- Dielectric permittivity [Farads/m]
Z	- Valence
F	- Faraday constant
γ	- Adsorption density [cm ³ /g]
K	- Boltzmann constant
φ	- Potential decay [s^{-1}]
e	- Elementary charge [Coulombs]
n	- Electrolyte concentration [M]
T	- Absolute temperature [K]
T_{max}	- Maximum torque [Nm]
D	- Vane diameter [m]
H	- Vane height [m]
X_{quartz}	- Proportion of quartz in mixture

LIST OF ABBREVIATIONS

DLVO	Derjaguin, Landau, Verwey, Overbeek
EE	Edge-edge particle association
EF	Edge-face particle association
EQ	Edge-quartz particle association
FF	Face-face particle association
i.e.p.	Iso-electric point
IHP	Inner Helmholtz plane
O	Octahedral layer
OHP	Outer Helmholtz plane
p.z.c.	Point of zero charge
QEMSCAN	Quantitative evaluation of minerals by scanning electron microscopy
SEM	Scanning Electron Microscopy
T	Tetrahedral layer
XRD	X-ray Diffraction
y.s.p.	Yield stress peak

LIST OF ELECTRONIC APPENDICES

APPENDIX A – Material Characterisation and Statistical Analysis

- A1 E:\Appendix A\Particle Size Distribution (PSD).xls
- A2 E:\Appendix A\Powder X-ray Diffraction (XRD).pdf
- A3 E:\Appendix A\Statistical Analysis.pdf

APPENDIX B – Mineralogical Analysis

- B1 E:\Appendix B\Images.tiff

APPENDIX C – Surface Charge Analysis

- C1 E:\Appendix C\Zeta Potential measurements.xls
- C2 E:\Appendix C\Potentiometric Titration measurements.xls
- C3 E:\Appendix C\Electron Microprobe data and analysis.xls
- C4 E:\Appendix C\Calculation procedure.pdf

APPENDIX D – Rheology - Yield Stress Peaks

- D1 E:\Appendix D\Muscovite.xls
- D2 E:\Appendix D\Vermiculite.xls
- D3 E:\Appendix D\Chrysotile.xls

APPENDIX E – Rheology - Suspensions of Pure Minerals

- E1 E:\Appendix E\Quartz.xls
- E2 E:\Appendix E\Muscovite.xls
- E3 E:\Appendix E\Vermiculite.xls
- E4 E:\Appendix E\Chrysotile.xls

APPENDIX F – Rheology - Suspensions of Binary Mineral Mixtures

- F1 E:\Appendix F\Muscovite-quartz binary mixtures.xls
- F2 E:\Appendix F\Vermiculite-quartz binary mixtures.xls
- F3 E:\Appendix F\Chrysotile-quartz binary mixtures.xls

University of Cape Town

Chapter 1.

INTRODUCTION

Since the onset of civilization, the mining industry has been essential towards advances in social, economic and industrial development. The importance of the mining sector has become increasingly evident due to the unprecedented growth in population and technological advancements which have occurred over the last century. Today, it contributes towards almost every facet of the global economy, providing indispensable inputs to industries such as aerospace, agriculture, construction, communication, defence, energy, health and transport. In Africa alone, the mining industry remains a cornerstone asset, accounting for approximately 30-90% of the annual foreign export earnings in most African mining countries, and providing a significant contribution towards economic activity and job creation (Christmann, 2010).

With the rising global demand on minerals and the preferential treatment of higher quality ores, a gradual depletion in high grade mineral reserves has been observed. This has forced the mining and minerals processing industries to develop innovative methods for processing progressively complex and finely disseminated low grade ore bodies. These often require very fine grinding in order to achieve sufficient liberation of valuable minerals, rendering the recovery expensive due to higher energy and capital costs. In view of this growing problem, considerable research has been undertaken, particularly in the areas of comminution (fine grinding) and froth flotation (hydrophobic/hydrophilic separation). However, it has become apparent that at the colloidal particle sizes at which low grade ores are beneficiated, the flow properties (rheology) significantly affect the efficiency of these unit operations and the mineral suspensions tend to exhibit more complex rheological behaviour than has been observed in previous years. As a result, more and more mining companies are realising that understanding the 'optimum' rheological behaviour is central to the successful operation of their processes.

Rheology is the study of flow and deformation of matter. The importance of rheology in different aspects of the mineral processing circuit has been highlighted by many researchers (e.g. Yue and Klein, 2004; Boger, 2009; Farrokhpay, 2012). Rheological properties, simply defined as the suspension yield stress and viscosity, are of great practical importance in many mineral processing applications, as they are useful indicators of the degree of aggregation and dispersion of particles within that suspension (Luckham and Rossi, 1999; Johnson et al., 2000). Therefore, research into the fundamental understanding of the flow behaviour of mineral suspensions, particularly in the context of low grade ores, is gaining importance in the minerals processing industry.

Central to understanding the rheology of these ores is knowledge on the gangue mineralogy. Low grade ores are typically comprised of valuable minerals locked in multiple phases of unwanted surrounding gangue material. This makes the pivotal effect of gangue mineralogy on the overall suspension flow behaviour seem obvious. Nonetheless, many studies related to minerals processing applications have mainly focused on other factors such as solids concentration, particle size and temperature (Muster and Prestidge, 1995; He et al., 2004; de Kretser and Scales, 2008), and the effect of gangue mineralogy on the rheological performance is still poorly understood within this context. This is mainly because mineralogy and minerals processing have often been viewed as separate disciplines in the past, with most studies disregarding the interactive effects between the two. The mineralogy of an ore affects the resultant flow behaviour and processing.

This study aims to link aspects of applied mineralogy and rheology for a comprehensive understanding of the effects of minerals which are typically problematic during the beneficiation of low grade ores.

1.1. PROBLEM STATEMENT

Phyllosilicate group minerals exist as common gangue components in many low grade ores. Often broadly classified as ‘clays’, this class of minerals is closely associated with several

processing issues such as reduced flotation rates (Ralston and Fornaserio, 2006), complex tailings treatment (de Kretser et al., 1997) and pumping challenges (Dunn, 2004). The extensive paragenesis of phyllosilicates from weathering, sedimentation, diagenesis and hydrothermal alteration, also means that they are associated with a wide range of host rocks and mineral types. These include volcanic volatile-rich carbonatites (e.g. smectites in kimberlites along the Slave Cratons, Canada) (Boshoff et al., 2007), ultrabasic nickel laterites (e.g. serpentinites in Norseman-Wiluna Greenstone belt, Australia) (Senior and Thomas, 2005) igneous intrusions (e.g. talc in the Bushveld Complex, South Africa) (Schouwstra et al., 2000) and porphyry copper deposits (e.g. micas in Escondida, Chile). Hence, the deleterious effects of phyllosilicate minerals are ubiquitous throughout the minerals processing industry.

The problems associated with phyllosilicate bearing ores are physicochemical, and impact all facets of the mineral processing circuit; with inefficiencies arising during beneficiation, dewatering and disposal. The 'sticky' nature of phyllosilicates renders the use of conveyors, idlers and screens difficult, and the pump capacity is significantly reduced during materials handling. They also restrict percolation and limit recovery during leaching due to preg robbing (Connelly, 2011). In comminution, the grinding efficiency is lowered, making it necessary to operate the mill at lower densities (Tangsathitkulchai, 2003). High phyllosilicate ores impede the flotation kinetics, often manifest in higher reagent consumption and poorer selectivity (Schubert and Bischofberger, 1978; Schubert, 2008; Bakker et al., 2009; Shabalala et al., 2011). The risk of wall collapse and leakage is also enhanced during the treatment of high phyllosilicate tailings, resulting from their poor dewaterability (de Kretser and Boger, 1992).

Despite the abundance and adverse effects associated with phyllosilicate minerals, the mining and mineral processing industries' understanding of the issues and potential solutions for treating phyllosilicate bearing ores remains poor. In many cases, these problems are simply avoided by either not processing the ores at all, or by some operations opting to run at significantly lower solids concentrations. Slurry dilution is also frequently used to reduce medium viscosity but this puts a strain on an increasingly scarce resource, given the heightened need to mine in remote arid or desert regions. Indeed some operations have approached the processing problems by finding chemical and engineering solutions. These include the use of viscosity modifiers and the

incorporation of multi-stage cyclones, scrubbers and hydrosizers into the circuit to remove the phyllosilicates upstream (e.g. Mount Keith and Windimurra plants) (Senior and Thomas, 2005). However, in most cases there is no definitive fundamental understanding behind these solutions. As a result, such adjustments are not only highly capital intensive, but are also unsustainable as they may be unable to adapt to variations in ore mineralogy. Other solutions include blending phyllosilicate ores with more competent ores, but this approach is limited to concentrations below which the clay ore starts to cause processing problems (the ‘critical’ concentration). This concentration is strongly dependent on the phyllosilicate gangue minerals present in the ore, and the concentrations beyond which those gangue minerals will cause problems. Such information has not been clearly defined for each phyllosilicate mineral, and is further complicated by the typical occurrence of phyllosilicates as interstratified mineral mixtures, resulting in more complex systems. A better understanding, based on a fundamental analysis of phyllosilicates in their *pure* form is required for long-term solutions to these processing problems.

Most studies linking phyllosilicate minerals and their rheological behaviour in the mineral processing industry have been limited to naturally occurring ores rather than the minerals in their pure form (Wiese et al., 2007; Burdukova et al., 2008; Shabalala et al., 2011). This has often created an environment that is both difficult to control and quantify, especially when studying the effects of specific composite gangue minerals. Indeed, an extensive amount of research has been carried out on the surface charge-rheology relationships of pure phyllosilicate minerals in the geotechnical, soil and colloid science fields, with most studies confined to the clay minerals kaolinite and montmorillonite. This is primarily due to the wide use of kaolinite in the ceramics industry and the large variability, intercalation and high retention properties of montmorillonite. As a result, the analysis of the surface charge properties of these minerals is well documented (Brandenburg and Lagaly, 1988, de Kretser et al., 1997, Greene et al., 2002; McFarlane et al., 2005, Tombácz and Szekeres, 2006; Vanerek et al., 2006; Bourg et al., 2007). However, some of these studies have been angled towards other industries (e.g. nanocomposite science, ceramic manufacturing, cosmetics, paper making and soils decontamination), where the key issues are not necessarily relevant within the minerals processing context. Nonetheless, the research already conducted in these industries has demonstrated the importance of the asymmetric particle shape and anisotropic surface charge properties, to the rheological properties of this group of

minerals. This forms a solid basis for the comprehensive analysis of phyllosilicate mineral suspension rheological behaviour within the minerals processing industry, where to date, the study of these minerals in their pure form is still relatively new in its application.

This thesis focuses on the analysis of three common phyllosilicate gangue minerals, namely muscovite, vermiculite and chrysotile. Muscovite, belonging to the mica class of phyllosilicate minerals, has a platy/sheet-like morphology and is a common accessory mineral in many igneous rocks and porphyry copper deposits which are distributed extensively around the world (e.g. Kennecott, USA (North America); Escondida, Chile (South America); North Parkes, Australia (Oceania); Majdanpek, Serbia (South Central Europe); and Grasberg, Indonesia (Southern Asia)). However, despite its occurrence, there has been little research regarding its effect on the processing of these ores. Vermiculite bears close similarity to muscovite in its platy habit, but has additional expansion/swelling ability. It is typically associated with ultrabasic and basic rocks, where it occurs as an alteration product of micaceous minerals by weathering, hydrothermal alteration or percolating groundwater (e.g. Virginia, Wissahickon, USA and Foskor, Palabora, South Africa). It can also be found in volcanic volatile-rich igneous rocks and carbonatites such as the kimberlites found along the Slave Cratons in Northwest Canada. Ores containing swelling clay minerals typically present impoundment challenges during tailings treatment due to their poor compaction rates. However, due to the paragenesis of vermiculite, it has been shown to swell to a much smaller extent, with its specific effects not having been clearly defined. Chrysotile, on the other hand, is a polymorph of serpentine with a fibrous morphology and has been found to pose a major challenge in the overall processing of many nickel sulphide ores (e.g. Norseman-Wiluna, Western Australia and Jinchuan, Northwest China) by reducing the nickel grade in the concentrate either by entrainment as fine liberated particles or by true flotation as composite hydrophilic coatings on the negatively charged sulphide particles.

The research presented in this thesis is relevant to the areas of phyllosilicate (clay) mineralogy and rheological fundamental research and is of particular interest within the minerals processing context. The research aims to investigate the relationship between pulp mineralogy, particle surface charge and particle interactions on the rheology of well controlled mineral suspensions.

1.2. OVERALL OBJECTIVES

This study focuses on a fundamental investigation of muscovite, vermiculite and chrysotile suspension behaviour. The major aim of the study is to establish clear links between suspension rheology, pulp mineralogy and particle surface charge by probing the influence of factors such as particle asymmetry, aspect ratio and charge anisotropy to suspension microstructure changes. By linking the key characteristics of surface charge and mineralogical structure to variations in rheological behaviour, the study seeks to gain a detailed understanding of the mechanisms that govern the flow behaviour and interaction of these phyllosilicate minerals within the context of well-defined homogeneous (pure mineral suspensions) and heterogeneous (binary mineral mixtures) mineral systems. This will be beneficial in developing a preliminary rheological classification of the phyllosilicates studied.

It is anticipated that the outcomes of the study will offer a foundation upon which further studies on progressively complex mineral systems can be conducted. In the long term, this may be beneficial towards the classification and prediction of the rheological behaviour and process performance of phyllosilicate mineral bearing ores in different unit operations. In light of the current decline in mineral reserves, this research serves as a contribution towards ongoing studies to better process low grade ores.

1.3. KEY QUESTIONS

The objectives of this study will be met by addressing the following key questions:

1. What are the mineralogical properties (particle shape, aspect ratio, surface area) of each of the three phyllosilicate minerals (muscovite, vermiculite and chrysotile)?
2. How does the iso-electric point (as determined by zeta potential measurements) compare with the point of zero charge (as determined by titration measurements) of each mineral under study?
3. How do variations in the yield stress as a function of pH relate to

- the iso-electric point?
 - the point of zero charge?
4. What is the proposed degree of charge anisotropy and can this be confirmed by the degree of isomorphous substitution (as determined by electron microprobe analysis)?
 5. For each phyllosilicate mineral, what is the proposed surface charge distribution on the different particle planes (edges and faces)?
 6. What are the rheological properties (yield stress and viscosity) of suspensions of each pure phyllosilicate mineral?
 7. What are the dominant factors contributing towards the suspension behaviour of each mineral?
 8. How does the rheological behaviour of each phyllosilicate mineral compare to that of quartz, a 'model' mineral with simple surface charge and mineralogical properties?
 9. Does blending each phyllosilicate with quartz in binary mineral mixtures result in synergistic (improved suspension behaviour) or antagonistic (exacerbated suspension rheology) and what implications does this have on the prediction of multicomponent systems?

1.4. PROJECT SCOPE AND LIMITATIONS

- This work is a fundamental study based on phyllosilicate gangue mineralogy and rheology. For this reason, the study does not extend to real ores. Instead, it focuses on the analysis of synthetic mineral systems comprising common phyllosilicate gangue minerals. Based on a comprehensive investigation which takes the inherent properties of each mineral into consideration, the study merely serves to infer the effects that they have on complex ore behaviour.
- The use of synthetic well controlled mineral systems facilitates the analysis of phyllosilicate behaviour in systems of increasing complexity. The initial investigation of the minerals in their pure form enables a systematic analysis of the surface charge and mineralogical properties, before investigating the rheological behaviour of the pure minerals in suspension.

Having analysed the flow behaviour of the pure minerals, the rheology of binary mixtures comprising each phyllosilicate mineral and quartz is investigated. These function as preliminary simulations of 'real' ores, and give a basic indication of the interactions in suspensions containing minerals of different morphologies and surface charges.

- The three phyllosilicate minerals (muscovite, vermiculite and chrysotile) investigated in this study were selected on the basis of their relative abundance in many ores and their unique, well defined morphology and mineralogical properties; the platy structure of muscovite, the platy morphology and expansion potential of vermiculite and the fibrous nature of chrysotile.
- The mineralogical properties are important distinguishing characteristics of each phyllosilicate mineral. In this study, mineralogy refers to the particle morphology (shape), asymmetry, surface area, aspect ratio and swelling ability. Additional factors such as textural analysis and topography are not included.
- The mineralogical properties of the phyllosilicate minerals are discussed based on existing knowledge on the crystalline structure of the phyllosilicate minerals. X-ray diffraction, scanning electron microscopy and optical microscopy are used as confirmatory tests and provide information regarding the exact structure and shape of the minerals used in the study.
- Electrophoretic zeta potential and Roberts Mular titration measurements are used in tandem to estimate the degree of charge anisotropy of the minerals. In each case, data obtained from microprobe analysis is then used as a confirmatory analysis of the elemental composition. The degree of substitutions and charge distribution in the constituent basal planes can then be inferred. The intrinsic limitations associated with each measurement are taken into consideration when dealing with these phyllosilicate minerals.
- The suspension yield stress and viscosity values can be evaluated using a number of different methods which will be outlined in detail. In this study, the Bingham approximation best

provides a comparative analysis which encompasses variations in suspension rheological behaviour (and measured rheograms) over the range of studied minerals. This approximation does not take into consideration the shear thinning properties of the minerals, but instead approximates the viscosity over the entire measured range. For this reason, the shear thinning properties of the minerals are not discussed in this study. This is a limitation of this approach, particularly for the analysis of suspension behavior at low shear rate conditions as would be most appropriate in application such as particulate material settling studies. However, the approach used in this study is well suited to higher shear rate conditions at which many mineral unit processes operate and for which the study is aimed. Moreover, estimated yield stresses and viscosities are used on a comparative basis within the context of the study, and not as absolute values.

- Rheology measurements are used to estimate the suspension yield stresses and viscosities in both pure and binary mixture suspensions. In keeping within the scope of the study, only pH (surface charge) and solids concentration (quantity) are varied, keeping all other variables (e.g. particle size, temperature, ionic strength) constant in order to minimize their influence. The results of the rheological measurements, in conjunction with the titration and electrophoretic zeta potential analyses, are used to predict the different modes of particle interaction in suspension.
- The rheological analysis of phyllosilicate minerals is a complex area of research, exacerbated by the existence of several differing theories on fundamental issues. Therefore, the findings from this study are strongly related to the systems used here and several predictions and inferences are made. It is acknowledged that further analysis would be required to validate the theories made. Even so, the main objective is to demonstrate the variation in phyllosilicate suspension behaviour and this study adequately addresses this. This study forms a preliminary classification in this regard, with a large scope for further analysis in definitively defining the suspension behaviour of these minerals.

A schematic representation of the thesis is shown in Figure 1.1, highlighting the important aspects that are outlined in this study, namely mineralogy, surface charge and rheology. The aspects that are investigated and are of relevance to this study are inside the rectangle, while all other factors that are not within the scope of the study and are kept constant lie outside the rectangle.

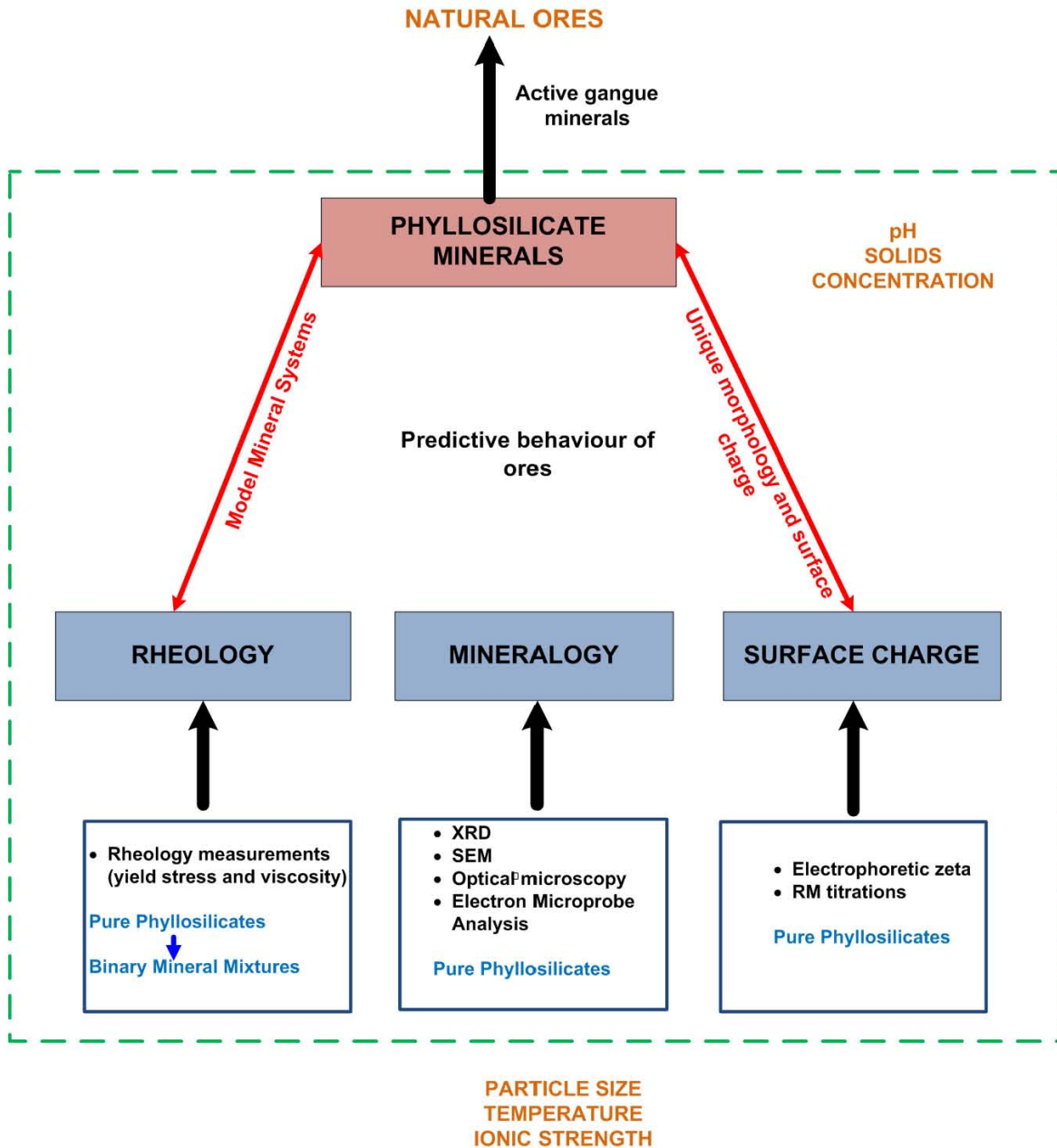


Figure 1.1 – Schematic representation of the thesis.

1.5. STRUCTURE OF THE THESIS

The body of this thesis is organized into nine chapters. Chapter 1 presents a brief background, the overall objectives, key questions and scope of the study. Chapter 2 gives a critical review of relevant literature available on the subject matter. Chapter 3 describes the materials and experimental methods used in this work, also outlining the techniques used in estimating the error in each of these tests.

The results of the study are presented and discussed in the subsequent chapters. Chapter 4 presents and discusses the mineralogy of the minerals based on the scanning electron microscope analysis. Chapter 5 discusses the surface charge characteristics of each phyllosilicate mineral, as derived from potentiometric titration, electrophoretic zeta potential, and electron microprobe measurements. In Chapter 6, predictions on pH mediated particle interactions are made, based on the rheological behaviour of the suspensions as a function of pH Chapter 7 then outlines the rheological properties of the phyllosilicate minerals in pure mineral suspensions while Chapter 8 discusses the rheological behaviour of the phyllosilicate minerals in suspensions of binary mineral mixtures.

Finally, a summarized discussion of the results is given in Chapter 9, together with the final conclusions and recommendations for further work.

Chapter 2.

LITERATURE REVIEW

2.1. INTRODUCTION

The rheological behavior of particulate fluids comprising phyllosilicate minerals such as kaolinite and montmorillonite has been an area of significant scientific and technological interest across a number of industries (Benna et al., 1999; Abend and Lagaly, 2000; Duran et al., 2000; Sakairi et al., 2005). Within the mineral processing context, the presence of phyllosilicates in hard rock has been found to have a major influence on the process selection and equipment used in the final flow sheet. Fundamental research into the rheological behaviour of these minerals is relatively new in its application to the mining and mineral processing industries and is essential towards mitigating the effects of these minerals on process performance.

The rheological behaviour of mineral suspensions is generally complicated and difficult to predict mainly due to slurry settling and wide size distributions. This is further complicated when dealing with phyllosilicate bearing mineral dispersions due to their crystallo-chemical properties which deviate from ideal spherical and isotropic charge behaviour. These properties render the use of robust analytical techniques difficult for phyllosilicate minerals since they are often more suited to ideal systems. Moreover, there is still much debate over several fundamental aspects such as the derivation of charge on the phyllosilicate particle planes and the modes of particle interaction as a function of solution pH. The existence of different theories on such foundational concepts means that research in this area may be subjective, often dependent on the preferred schools of thought.

This chapter presents a critical review of available literature applicable to the study, highlighting the importance of this work within the context of previous research that has been conducted on

the subject matter. The broad scientific foundations and theories underlying suspension rheology, phyllosilicate mineralogy, interfacial chemistry and surface charge are reviewed. This incorporates aspects of particle interaction and microstructural changes in homogenous and heterogeneous phyllosilicate mineral suspensions.

Specifically, the fundamentals of suspension rheology are outlined, highlighting the factors to be considered during analysis and measurement. The importance of rheology in the minerals processing industry is discussed, emphasizing the increasing importance of the implementation of the principles of process stream rheology for the efficiency of many unit operations. A brief outline of the problems typically experienced during the processing of phyllosilicate mineral bearing ores is then given. The mineralogical properties of the phyllosilicates under study (muscovite, vermiculite and chrysotile) are described, focusing on their distinct morphologies and additional properties as derived from their physical structures. The different schools of thought around the physico-chemical properties of phyllosilicates are also critically evaluated. A discussion on the applicability of robust conventional techniques is also presented, informing the choice of analytical techniques used in the study

2.2. SUSPENSION RHEOLOGY

2.2.1. The fundamentals of rheology

Rheology is the study of flow and deformation of matter. In practical terms, it is a study of the relationship between the applied force (shear stress [Pa]) and the resultant rate of deformation (shear rate [s^{-1}]) of a fluid element. The relationship between the two is typically represented in the form of a rheogram/flow curve. The nature of a fluid element can be highly variable within the spectrum of solid-like to liquid-like materials, with the flow behaviour within the range of elastic solids and viscous fluids. If the deformation of a substance in response to an applied stress is reversible, it is an elastic solid. However, if the deformation is irreversible, it is termed a viscous fluid. Many systems lie between the two extremes, exhibiting varying degrees of

viscoelastic behaviour. Figure 2.1 shows the typical shear stress-shear rate rheograms associated with different fluid dispersions.

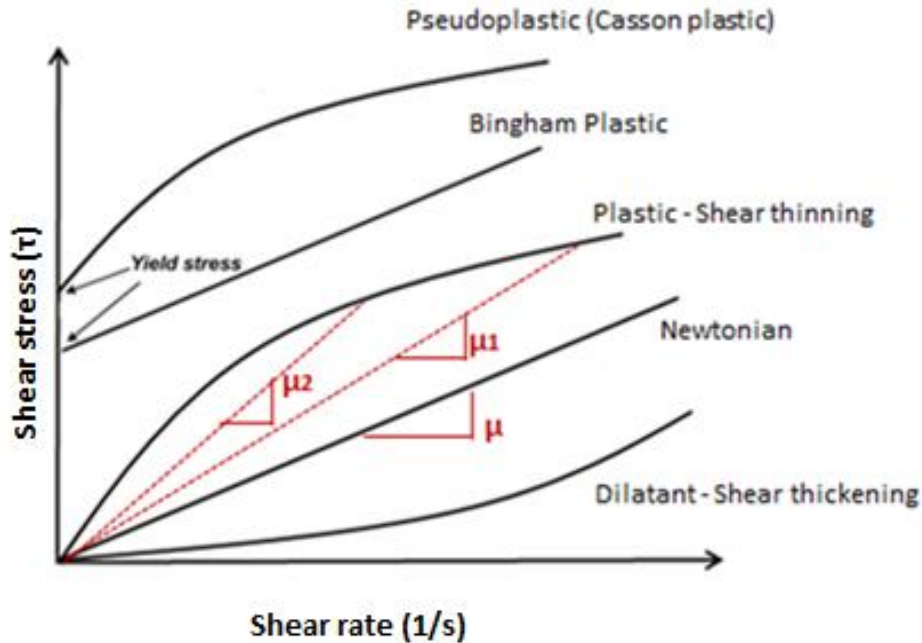


Figure 2.1 - Rheograms of different types of fluids.

Ideal viscous behaviour is typically displayed by Newtonian fluids, which are characterised by a linear relationship between the shear stress and shear rate. The ratio between the shear stress and shear rate provides an estimate of the viscosity [Pas] and is shown as μ in Figure 2.1. This rheological property, is defined as the resistance to deformation and is a measure of the internal friction of the fluid. In the case of Newtonian fluids, the viscosity is constant throughout the shear rate range. In colloidal mineral processing systems, such behaviour is most likely displayed by dilute suspensions of spherical particles in bulk Newtonian medium. However, most concentrated mineral suspensions will deviate from such behaviour and exhibit non-Newtonian (dilatant, plastic, pseudo-plastic, Bingham) fluid behaviour, where the viscosity may vary as a function of shear rate. For such suspensions, the viscosity is referred to as the ‘apparent viscosity’ at any given shear rate, as is demonstrated by μ_1 and μ_2 in Figure 2.1.

Plastic/ pseudo plastic behaviour is characterised by a reduction in apparent viscosity as the shear rate increases (shear thinning). In mineral dispersions, shear thinning may be attributed to the gradual breakdown of particle aggregates, releasing any trapped inter-aggregate bulk fluid and leading to a decrease in the effective solid concentration. This is manifest in a decrease in apparent viscosity. Shear thinning behaviour is typical of phyllosilicate particles where particles which tend to assume random orientations are progressively aligned in the direction of flow with increasing shear (Shaw, 1992; Jogun and Zukoski, 1996). Shear thinning can also be described in terms of the balance between Brownian motion and hydrodynamic forces. The Peclet number is a dimensionless number that gauges the importance of one relative to the other, and takes into consideration particle size, temperature and solvent viscosity effects. In general, the importance of Brownian motion decreases during shear thinning as the particles adopt a more flow-oriented arrangement. This is characterised by low Peclet numbers ($\ll 1$) (Brown and Jaeger, 2011).

Conversely, when hydrodynamic interactions are of less importance, this results in shear thickening dilatant behaviour. This is characterised by large Peclet numbers ($\gg 1$) and an increase in apparent viscosity with increasing shear (Brown and Jaeger, 2011). Such behaviour is most commonly observed in concentrated mineral dispersions where the shear thickening properties have been attributed to a transition from two dimensional ordered layered structures to a disordered three dimensional state at very high shear rates (Hoffman, 1972; Barnes et al., 1989; Boersma et al., 1990). The existing inter-aggregate water is also believed to act as a lubricant at low shear rates and is unable to fill the gaps created between particles at higher shear rates, resulting in increased friction between particles and increased viscosity (Cheremisihoff, 1988).

In moderately concentrated colloidal suspensions in which the net force between particles is attractive, particle-particle interactions dominate the suspension in continuous networks where the material behaves as an elastic solid. When subjected to stress, such systems resist flow until the applied stress exceeds the inherent elastic strength of the particulate network. At this critical stress, the network of interconnected particles fails and the material behaviour shifts to a more liquid-like (viscous) state with less resistance to flow (Barnes, 1999). The critical stress at which this transition occurs is termed the shear yield stress [Pa]. Suspensions where the three dimensional networked structure breaks down to a fully dispersed state are known as Bingham

plastic fluids. Here, the suspension flows as a fully viscous fluid upon yielding, unlike pseudo-plastic or dilatant fluids which demonstrate viscoelastic behaviour in this flow region with a progressive change in suspension viscosity (Johnson, 1998).

2.2.2. Rheological properties and property measurement

This study is concerned with steady shear systems, where transient time-dependent effects are minimized. The most important indicators of suspension behaviour in this case are suspension yield stress and viscosity.

2.2.2.1. Suspension yield stress

The concept of the shear yield stress, τ_y [Pa] was first devised by Bingham and Greene (1920), and has since generated much debate in rheological literature. The definition of a yield stress is far from being simple and is variously described, with descriptions such as ‘departure in linearity’ and ‘an increase in deformation without increase in stress’ having been assigned (Parker, 1991; Robinson, 1996; Collocott, 1971). Therefore, it is not a well specified quantity, which can be assigned precisely (Barnes, 1999). The true existence of a yield stress has also been debated and although this continues to be an area of discussion, there is an acknowledgement that most materials do indeed show a transition from solid to liquid-like behaviour at an applied strain, above which instantaneous flow occurs (Barnes, 1999). If this is the case, the yield stress can be viewed as the minimum force required in initiating the flow of a suspension in the limit of low shear. The concept of the yield stress, under such a definition, has proved useful in a wide range of mineral processing applications. It has, in most cases, been used as a useful indicator of changes in the degree of aggregation of suspensions and has proved beneficial in fundamental surface charge-rheology studies (Subbanna et al., 1998; Johnson et al., 2000; Addai-Mensah and Ralston, 2005).

2.2.2.2. Suspension viscosity

Viscosity, η [Pas] is a measure of the suspension resistance to flow against applied shear stress. It is a more commonly used property in mineral processing applications where it is considered a useful parameter in determining the effects of process variables such as impeller speed, process time and temperature on suspension flow behavior and subsequent process performance (Mikulášek et al., 1997; Bakker et al., 2010). The suspension viscosity term is also important towards modelling and predicting pipe fluid flow systems (Coulson and Richardson, 1999). Useful information related to the measurement and investigation of particle interactions, interfacial chemistry and system macrostructures in suspension can also be obtained from the suspension viscosity (He et al., 2009; Jayasundara et al., 2009; Senapati et al., 2010; Farrokhpay, 2012).

Although the distinction between the suspension yield stress and viscosity is often difficult in practice, they each represent different contributions towards understanding the overall suspension behaviour. For example, the design and operation of pumping systems of particulate suspensions are based on both the viscosity and yield stress values. In such an application, both the yield stress and viscosity will be important in estimating the pumping requirements, although knowledge of the yield stress may be more relevant in ensuring the successful start-up of from a static shut down condition (Sofrá and Boger, 2002).

2.2.2.3. Rheological property measurement

The measurement of suspension viscosity and yield stress is generally limited by difficulties due to aggregation and rapid settling of suspended particles (Kawatra and Bakshi, 1996). However, advances have been made to most accurately predict these properties, either directly or indirectly.

The measurement of yield stress, in particular, has been an engineering challenge for many years, as it requires the measurement of the shear stress of a fluid at shear rates approaching zero.

Indirect property measurement through Couette flow rheometry has been successfully applied to many mineral suspensions. In this case, the sample is confined between a rotating cup and a stationary bob (or vice versa). The torque is measured as a function of rotational speed, and is interpreted to determine shear stress as a function of shear rate. Smaller gap sizes are optimal for measurement, but this is commonly a challenge for many mineral processing applications where coarser particle sizes may be used. In such cases, a larger gap is required, but this then makes the property measurement subject to artifacts arising from non-uniform shearing across the annulus. Several correction factors have been proposed to account for the partially sheared and unsheared zones in this regard (e.g. Couette flow, Bingham approximation, Tikhonov approximation) (Boger, 1999; Barnes and Nguyen, 2001; Fisher et al., 2007).

Constitutive relationships can be used to approximate rheological properties based on steady shear data. Newtonian fluid behaviour is characterised by the Newtonian model (Equation 2.1a) while the Herschel Buckley model (Equation 2.1b) provides a generalised model for non-Newtonian fluid behaviour from which other non-Newtonian models can be derived. This is dependent on the presence of a yield stress and the value of the flow behaviour index which is representative of the shear thickening/thinning characteristics of the suspension. A power law model can describe both pseudoplasticity and dilatancy, depending on the value of the index. When $n > 1$, this is characteristic of dilatant fluid behaviour with shear thickening (Equation 2.1c). Conversely, a value of $n < 1$ is indicative of shear thinning behaviour (Equation 2.1d). Mineral suspensions typically exhibit pseudo plastic and Bingham behaviour (with $n < 1$ and $n = 1$ respectively and a yield value) (Equation 2.1e and Equation 2.1f). The yield value is approximated by extrapolating curves of shear stress vs. shear rate to zero or low shear, and the viscosity term is derived from the mathematical model. The accurate determination of the yield stress value from these models relies on good quality shear stress/shear rate data, and is therefore characterised with the associated error. The Bingham and Casson model are often used in the classification of the rheological behaviour of mineral suspensions (He and Forssberg, 2007)

Newtonian model:

$$\tau = \eta_p \dot{\gamma}$$

Equation 2.1a

Herschel Buckley model:	$\tau = \tau_0 + \eta_p \gamma^n$		Equation 2.1b
Power Law model:	$\tau = \eta_p \gamma^n$	$n > 1$	Equation 2.1c
Pseudo plastic:	$\tau = \eta_p \gamma^n$	$n < 1$	Equation 2.1d
Bingham Plastic model:	$\tau = \tau_0 + (\eta_p \gamma)$		Equation 2.1e
Casson model:	$\tau^{1/2} = \tau_0^{1/2} + (\eta_p \gamma)^{1/2}$		Equation 2.1f

Where τ is the shear stress, γ is the shear rate, τ_0 is the yield stress; η_p is the plastic viscosity and n is the flow behaviour index.

Nguyen and Boger, (1983) developed a direct yield stress measurement technique, which uses a vane geometry at a constant low shear rate mode ($< 1 \text{ s}^{-1}$). This technique is most applicable to concentrated suspensions and has been applied successfully in the rheological characterisation of concentrated systems (e.g. Liddell and Boger, 1996; Stokes and Telford, 2004). The major advantage of the vane technique is the minimised slip between the sample and the instrument fixture (Nguyen and Boger, 1983, 1985; Barnes and Nguyen, 2001; Fisher et al., 2007), giving a more accurate yield value particularly for structured dispersions (yield stress $> 20 \text{ Pa}$). (Alderman et al., 1991; Addai-Mensah and Ralston, 2004). The use of the vane geometry also results in less sample disturbance and structural breakdown during insertion. It has also been demonstrated through both experimental and theoretical modelling studies, that a uniform stress distribution assumption is valid for non-Newtonian fluids with a yield stress and shear rate accurately determined when using this geometry (Keentok et al., 1985; Yan and James, 1997; Fisher et al., 2007).

2.2.3. Rheology in the minerals processing industry

With its increasing importance in the mining and minerals processing industries, many operations are finding benefit in applying the principles of rheology to their operations. Increased knowledge of the factors that govern the rheology of mineral slurries leads to the enhanced ability to control flow behaviour and can be exploited by the minerals processing industry to drastically improve and optimise many unit operations, ranging from wet crushing, flotation and leaching to tailings disposal and paste backfilling. Some examples of rheology applications in the comminution, flotation and tailings disposal circuits are outlined below.

Due to the increased beneficiation of finely disseminated ore bodies, ultrafine grinding is being applied more and more in the minerals processing industry as a means to achieve sufficient liberation of valuable minerals. At the fine particle sizes generated in these mills, slurry rheology strongly affects the mill performance. It has generally been observed that very fine sizes lead to the retardation of the overall grinding process (Shi and Napier-Munn, 2002). In addition, mineral slurries tend to exhibit a wide range of rheological properties, which may change non-intuitively within different regimes in the mill (Tangsathitkulchai, 2003). This affects the process performance and makes control of the mill throughput difficult. Thus, control of rheological properties is important in optimizing performance parameters such as power draw, breakage rate, fines production, dispersant usage and particle size. It has been demonstrated that optimization of viscous effects in stirred mills reduces the proportion of oversized particles and increases throughput, product fineness and energy efficiency significantly (Boger, 1999).

In horizontal stirred mills, a good slurry fluidity (characterised by low yield stresses) produces a narrow particle size distribution by reducing the breakage of finer particles whilst maintaining sufficient breakage of coarser particles (Yue and Klein, 2004). This has significant effects on downstream processes such as flotation and dewatering. Rheology has also been useful in predicting the mechanisms of ball collision in different grinding regimes during wet ultra-fine grinding in ball mills (Tangsathitkulchai, 2003). In addition, the control and monitoring of slurry viscosity has been beneficial in advances to predict particle trajectory using positron emission particle tracking within stirred mills (Fangary et al., 2000; Govender et al., 2011). In all these applications, the control of the slurry rheology is in line with the specific requirements of the grinding media and has proved beneficial in optimising grinding performance.

Rheological investigations have also been used to provide information on the types of interactions and aggregation induced through changes in processing conditions in flotation cells. It has been demonstrated that effective fine particle flotation requires a substantial dispersion state (characterized by low apparent viscosities). This results in a reduction in turbulence damping and helps to balance out particle/bubble attachment and detachment, resulting in increased ultrafine particle floatability (Schubert and Bischofberger, 1978; Schubert, 2008). The coupling of rheology and froth flotation is also being used increasingly to improve cell hydrodynamics and fine particle flotation (Bakker et al., 2009; Gomez et al., 2010). In addition, the principles of rheology have been applied more indirectly, as a tool in investigating the mechanisms of interaction within a flotation cell, focusing particularly on the suppression of gangue-bubble attachment (Genc et al., 2010; Vasudevan et al., 2010; Patra et al., 2010). Rheological investigations have also been valuable in analysing the surface charge properties of talc, a naturally floatable gangue mineral that occurs in many base metal sulphide ores (Burdukova, 2007). This has been beneficial in advances to determine the adsorption mechanisms of talc to different polymeric depressants, thereby suppressing its recovery to the concentrate.

The mining industry continues to be one of the largest producers of waste, reporting about 90-95% of mined material to tailings (Boger, 2009). With the shift towards more energy and environmentally sustainable processes, there is a clear need to establish safe and efficient disposal methods which are also acceptable for sustainable operation of the process. Conventional 'wet disposal' practices of pumping large tonnages of mud-sand slurry residue to ponds create technical, economical and environmental problems due to the ubiquitous risk of ground water contamination, difficult rehabilitation and high costs associated with land acquisition, construction and lining of large dams. This has resulted in several incidents involving the instability and subsequent collapse of tailings dams and backfilling problems in many mining operations. In recent years, research has moved towards the pumping and semi-dry disposal of concentrated slurries. Studies by Nguyen and Boger, (1998) demonstrated how the rheological analysis of mineral slurries is useful in solving suspension handling and transportation problems. By fully characterising the yielding and viscous fluid behaviour of bauxite tailings suspensions produced in Western Australia, it was possible to design a pipeline

and predict optimum pumping conditions for the disposal system. This rheological data has been beneficial towards the development of a sustainable new semi-dry waste disposal system at Alcoa Alumina in Western Australia which now uses dry stacking techniques as opposed to wet lakes disposal. The impact of rheology on improving waste disposal in the alumina industry has been immense and these same techniques are now being applied to other industries such the coal, copper and oil sands tailings industries and have proved beneficial in this regard (Boger, 2009). This basic understanding of rheology in improving waste handling is a step towards improving problems associated with backfilling and instability of tailings dams. This is in line with the move towards environmental rheology which aims at implementing basic rheological techniques to reduce risk, recover water and reduce the footprint of suspension waste produced in the minerals processing industry.

In all these applications, an understanding of the gangue mineralogy and surface charge is beneficial towards improving the rheological effects observed in the unit operations. This is most pertinent with phyllosilicate gangue minerals which normally exhibit more complex morphologies and surface charge properties than other gangue minerals in the ore (e.g. quartz). Indeed some phyllosilicates can be less problematic than others. However, this classification has not been clearly defined yet.

2.3. PHYLLOSILICATE MINERALS

Phyllosilicate minerals comprise tetrahedral 'T' and octahedral 'O' layers which are the basic building blocks of this group of minerals. A tetrahedral layer consists of silica (SiO_4) tetrahedral units. Within each unit, four oxygen atoms are arranged symmetrically around a silicon atom. Successive tetrahedra are held together by shared apical oxygen atoms to form rings of tetrahedral 'T' layers. The ring structure of SiO_4 tetrahedra is shown in Figure 2.2a. An octahedral unit consists of a central cation in a six fold co-ordination bonded to six hydroxyl groups, resulting in an octahedral symmetry (Figure 2.2b). These hydroxyl groups are in turn linked to other surrounding metallic atoms. The cations in the octahedral unit can either be divalent (e.g. Mg^{2+}) or trivalent (e.g. Al^{3+}). When the cations are divalent, charge balance is

maintained when each cation site is occupied and each hydroxyl group is surrounded by three cations, forming a trioctahedral structure as in brucite ($\text{Mg}(\text{OH})_2$). In the case of trivalent cations, however, one out of every three cation sites is unoccupied and each hydroxyl group is then surrounded by two cations. This is the case with gibbsite ($\text{Al}(\text{OH})_3$). Such a sheet structure is known as dioctahedral. Therefore, phyllosilicate minerals can be classified as either dioctahedral or trioctahedral, depending on the constituent octahedral unit (Klein and Dutrow, 2008). The difference between brucite and gibbsite is shown in Figure 2.2b.

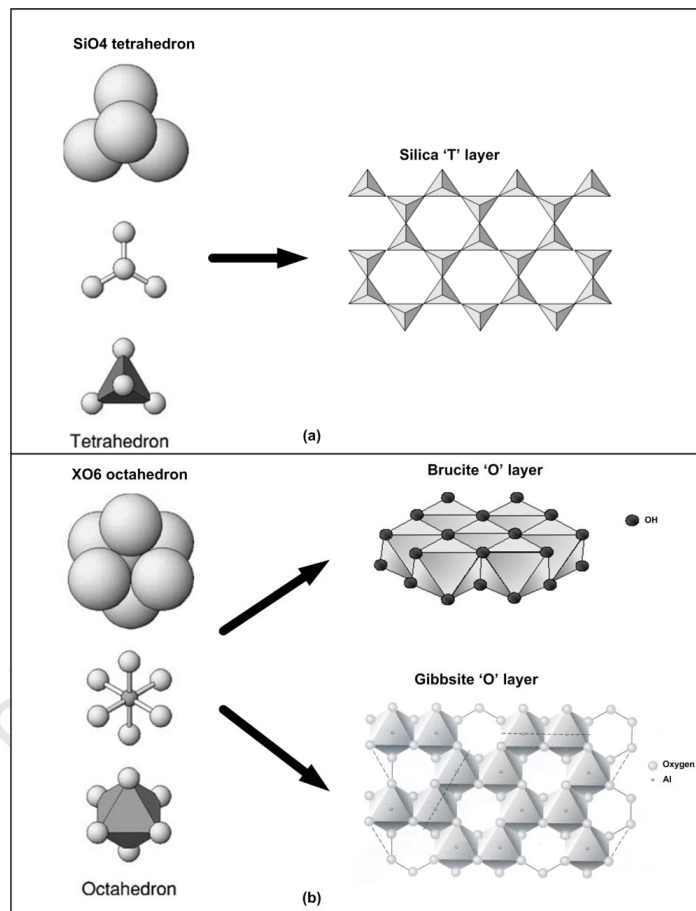


Figure 2.2 - (a) SiO_4 tetrahedral units and silica 'T' layers (b) octahedral (XO_6) units and the difference between brucite and gibbsite 'O' layers.

Variations in 'T' and 'O' layer configurations result in minerals of relatively similar structure, but with different physical and chemical properties. Consequently, there have been many different classifications of phyllosilicate minerals reported in literature (e.g. Brindley and Brown,

1980; Dixon and Weed, 1989; Klein and Hurlbut, 1993; Hurlbut and Sharp, 1998). The classification used in this thesis is in accordance with the phyllosilicate classification by Deer et al., (1992) and is shown in Figure 2.3. In this case, the phyllosilicates are grouped according to the proportion of the tetrahedral and octahedral layers, as well as the interlayer connections that may occur between successive structural units. This categorises the minerals into serpentinites, talc/pyrophyllite, micas, chlorites and clay minerals. The clay minerals can be further classified into non-swelling (kaolinites and illites), and swelling (smectites and vermiculites) clays. Alternative classifications may incorporate the chlorites into the clay mineral group (e.g. Dixon and Weed, 1989). It is worth noting that there is a distinct difference between clays and clay minerals. Clays are sediments which comprise clay minerals and accessory ‘non-clay’ minerals (Deer et al., 1992; Boggs, 2006); while clay minerals are pure sheet silicates that are responsible for the classic properties of clay, such as plasticity when wet and hardness when dry or heated (Guggenheim and Martin, 1995). By this definition, bentonite, for example, is a type of clay which is composed mostly of montmorillonite (clay mineral) and will mimic the properties of montmorillonite, but can include other non-clay minerals or phyllosilicate minerals (e.g. quartz). The difficulty with clay minerals stems from their ability to change from one form to another (interstratification), such that they typically comprise alternate layers of other clays in either ordered and regular or highly unordered and irregular sequences. In such cases, mineral identification is difficult, as they tend to mask each other.

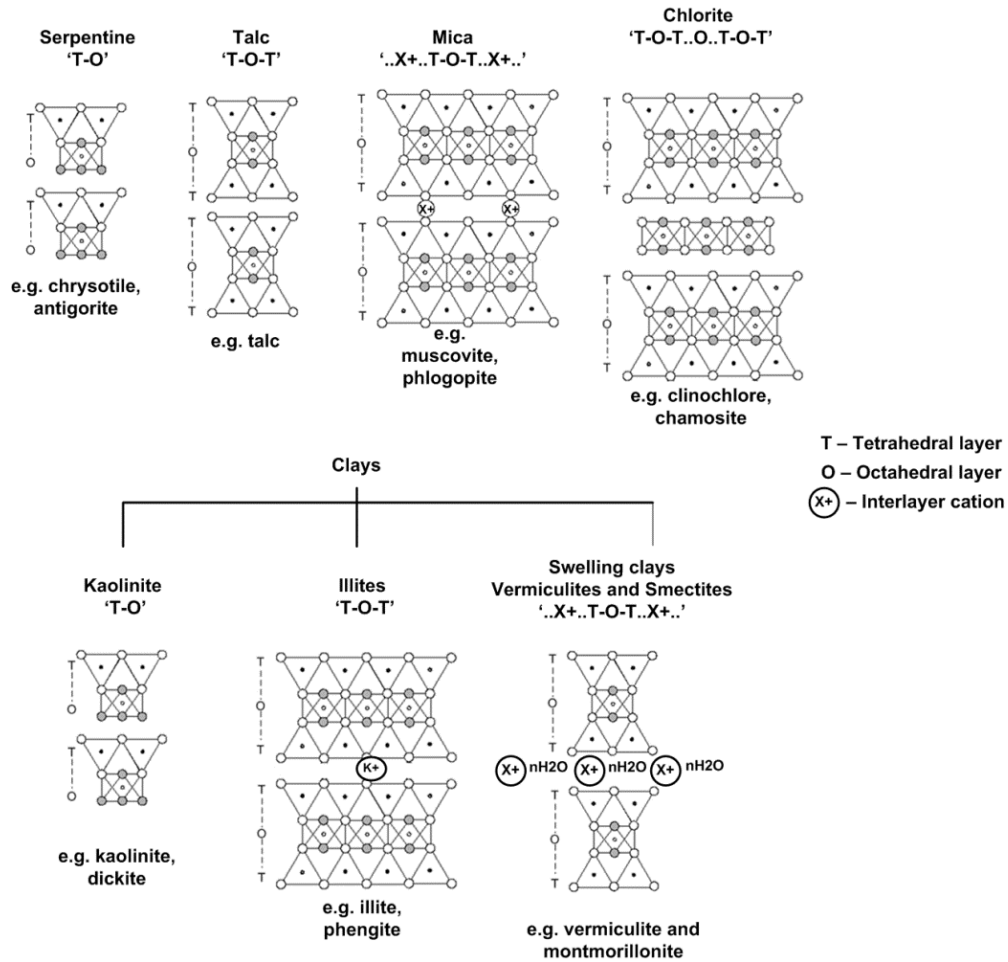


Figure 2.3 - The classification of phyllosilicate group minerals.

2.3.1. Typical processing problems associated with phyllosilicate bearing ores

Due to their wide ranging formation from argillic alterations, sedimentation and diagenesis, phyllosilicates are associated with several host rocks. Therefore, the mineral processing problems encountered are not unique to one mineral type but include gold, copper, uranium, lead zinc, iron and nickel ores. The mineral processing industry is well aware of the difficulty in treating phyllosilicate bearing ores, since they typically affect all aspects of the processing circuit, ranging from materials handling through to tailings treatment.

During materials handling, phyllosilicates stick to conveyors, idlers and screens, making the use of open stockpiles and bins highly problematic. The crushing capacity of phyllosilicate bearing

ores is very poor, often resulting in decreased throughput and grinding efficiency. In such cases, it is necessary to operate the mill at lower densities to flush out the phyllosilicates (Connelly, 2011). Due to their characteristic small particle sizes and high viscosities, phyllosilicates may also result in preg robbing and restrict percolation during leaching. Tanks are subject to overflowing because of the insufficient fall on the tanks (Tremolada et al., 2010; Farrokhpay and Bradshaw, 2012). The characteristic high surface area of phyllosilicates makes them highly reactive and responsive to changes in the processing environment during flotation. The exact mechanisms driving the behaviour of phyllosilicate particles during flotation have not been definitively defined, although it is generally believed that they affect performance through (i) slime coating on the mineral surfaces as well as air bubbles (Tao et al., 2010), (ii) higher reagent consumption, poorer selectivity and impeded flotation kinetics (Connelly, 2011a) (iii) entrainment of large quantities to the concentrate during both roughing and scavenging stages (Patra et al., 2010; Vasudevan et al., 2010; Jorjani et al., 2011) (iv) increasing pulp viscosity (Arnold and Aplan, 1986; Genc et al., 2010) and (v) increasing or decreasing the froth stability (Dippenaar, 1988; Bulatovic, 1999). During tailings treatment, high phyllosilicate bearing ores often result in tailings dams with very low water recovery rates and a high risk of wall failure and leakage. The phyllosilicates can seal the dam, preventing effective drainage and sub aerial cyclic deposition (de Kretser et al., 1997; Boger, 2009; Connelly, 2011).

It is worth noting that even with such a broad understanding of the effects of this class of minerals on process performance, phyllosilicates behave differently and in some cases their behaviour may vary from ore type to ore type. For example, studies by Hussain et al., (1996) indicated that illite and chlorite reduce coal recovery significantly (28% and 20% reduction respectively), while studies in the oil sands industry have demonstrated that the addition of illite does not have a significant effect on bitumen recovery (Kasongo et al., 2000). However, it is through its characteristic degradation to smectites and its occurrence as interstratified illite-smectite that it reduces bitumen recovery (Wallace et al., 2004). Therefore, the effects of these minerals may be ore specific.

In general, chrysotile has been found to pose a major challenge in the overall processing of many nickel sulphide ores (e.g. Norseman-Wiluna, Western Australia and Jinchuan, Northwest China)

by reducing the nickel grade in the concentrate; either by entrainment as fine liberated particles or by true flotation, as composite hydrophilic coatings on the negatively charged sulphide particles (Patra et al., 2010). It has been found that the flotation of copper porphyry ores is limited by the presence of aluminosilicates, such as kaolinite, vermiculite and muscovite, and can produce concentrates with low levels of copper grade and recovery and high levels of alumina and silica (Jorjani et al., 2011). The high alumina content in hematite ores in Australia has often been detrimental to the blast furnace and sinter plant operations, due to the prevalence of highly viscous slags and high coke rates (Ma et al., 2009).

2.3.2. Current mitigation strategies for dealing with phyllosilicate bearing ores

The processing problems associated with phyllosilicate gangue minerals have often been approached by finding short term solutions such as slurry dilution and operating at lower solids concentrations. Viscosity modifiers such as sodium pyrophosphate and caustic soda are also used in stabilising colloidal systems during milling and classification, gold carbon in pulp leaching (CIP) and flotation (Xiao et al., 1999; Mpofo et al., 2004; McFarlane et al., 2005). The application of these compounds is suggested to be mainly due to their ability to adsorb onto clay surfaces, altering the surface chemistry properties of the particles and inducing electrostatic repulsive forces and disperse systems (Doi and Edwards, 2001; Klein and Pawlik, 2005). However, these phosphate dispersants may not be stable in severe conditions such as low pH or high temperatures. Moreover, the physical aspects (morphology), which also contribute towards clay behaviour, may not necessarily be controlled by the modifiers (Vasudevan et al., 2010).

Engineering solutions include feeding directly to semi-autogeneous milling (SAG), bypassing crushing and screening to avoid problems of 'sticky' clays during secondary crushing in the comminution circuit. In mineral sands operations, the incorporation of hydrosizers upfront aids the separation of clays from the feed. Similarly, the inclusion of scrubbers early on is beneficial in clay removal to the tailings dam in dense media separation. It is worth noting, however, that the inclusion of such modifications may not necessarily improve recovery and throughput. This was observed at the Mt. McLure and Mt. Muro plants, which were specially designed for heavy

clays but still proved inoperable (Connelly, 2011). Other methods for mitigating clay effects include dilution and blending of high clay ores with less complex ores. However, these are limited to mixture concentrations below which the clay content starts to cause problems. Such information has not been clearly defined and a better fundamental understanding, particularly of the rheological properties of the different phyllosilicate minerals, is required for long-term solutions to these processing problems.

Attempts to better understand the effects of phyllosilicate minerals have, in most cases, been approached through the investigation of phyllosilicate bearing ores (e.g. Burdukova et al., 2008; Jorjani et al., 2010). Indeed analysis on such a basis may be more representative of plant behaviour. However, from a research viewpoint, the use of naturally occurring ores creates an environment that is experimentally difficult to control and quantify and control, especially when trying to better understand the specific effects of clay gangue material. In such cases, a more detailed study of the gangue minerals in simple mineral systems where specific factors such as inherent mineralogy and surface charge properties can be isolated may be beneficial.

2.4. THE MINERALOGY OF MUSCOVITE, VERMICULITE AND CHRYSOTILE

2.4.1. Muscovite mineralogy (mica group)

Muscovite [$K_2Al_4(Si_6Al_2O_{20}(OH,F)_4)$] is typically produced by the metamorphism of impure limestones. In low-grade environments, it is formed by the recrystallisation of illites ($K_{1.5-1.0}Al_4[Si_{6.5-7}OAl_{1.5-2.0}O_{20}](OH)_4$) and other clay minerals (Deer et al., 1992).

It is a 2:1 dioctahedral phyllosilicate mineral with a gibbsite O layer sandwiched between two inward pointing silica T layers to form 'T-O-T' units (Figure 2.3). Tightly held structural non-exchangeable K^+ interlayer cations exist between successive 'T-O-T' units, balancing a negative charge which is thought to be due to the isomorphous substitution of higher valence Si^{4+} cations

with Al^{3+} cations of a lower valence in the tetrahedral layer. This form of charge generation will be discussed in more detail in the following section. Successive T-O-T units are bound together by ionic bonds which form between the interlayer cations and the subsequent T-O-T unit. The whole structure can therefore be viewed as a ‘...X+_T-O-T_X+_T-O-T_X+...’ sequence. The continuous stacking of successive T-O-T units results in the platy morphology of muscovite particles which typically exist as long, thin flaky sheets. Each plate has distinct ‘T’ faces and ‘T-O-T’ edges. Figure 2.4 shows the layering of consecutive T-O-T units, drawing attention to the distinct basal planes and interlayer cations which exist between subsequent T-O-T units.

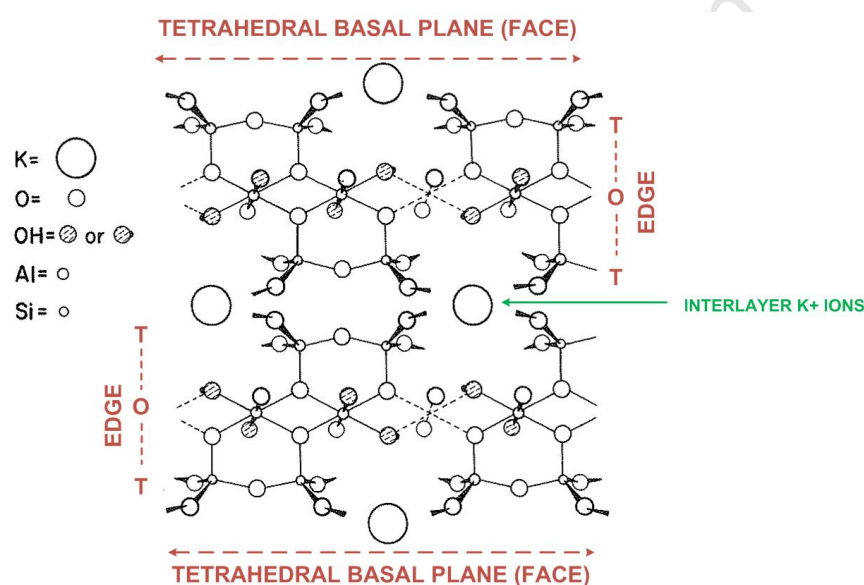


Figure 2.4 - Crystallographic structure of muscovite (adapted from Fanning et al., 1989).

2.4.2. Vermiculite mineralogy (swelling clay group)

The transformation of micas to swelling clays is well documented (Norrish, 1973; Scott and Smith, 1966; Bracke et al., 1995). Dioctahedral micas such as muscovite are normally more resistant to weathering than trioctahedral micas such as phlogopite. Micas serve as precursors to swelling clays such as vermiculite and montmorillonite, to which micas may be transformed by the replacement of the non-exchangeable interlayer K^+ cations by exchangeable hydrated cations (Fanning and Keramidas, 1977; Brindley and Brown, 1980). The weathering of micas proceeds

by the loss of K^+ ions and the increase of water and silica. The alteration occurs along cleavage planes and at crystal planes by layer and edge weathering. This results in the formation of interstratified expandible 2:1 swelling clays as shown in Figure 2.5.

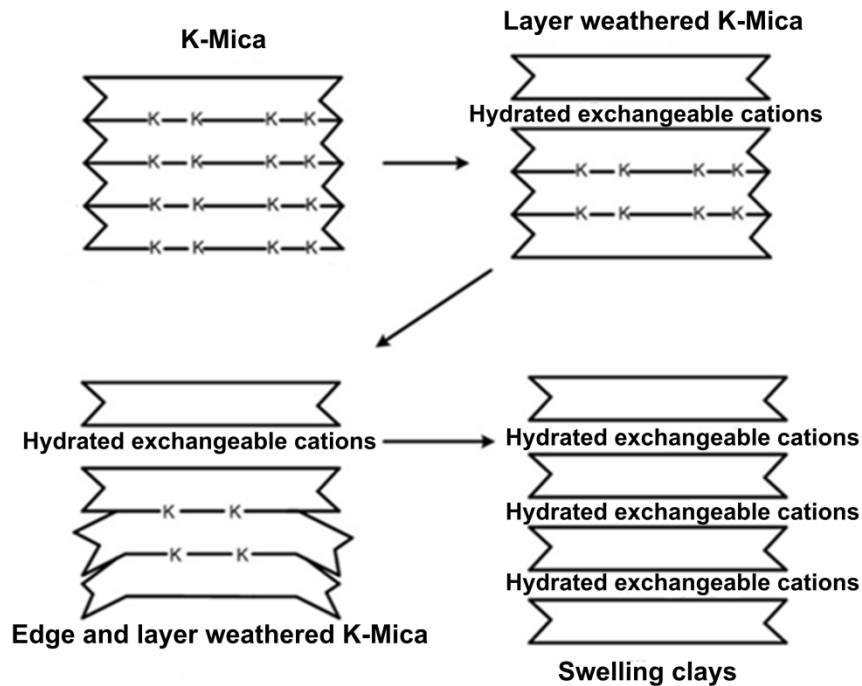


Figure 2.5 - Schematic representing the transformation of micas to swelling clays
(adapted from Fanning and Keramidas, 1977).

Vermiculite $[(Mg,Ca)_{0.6-0.9}(Mg,Fe,Al)_6[(Si,Al)_8O_{20}](OH)_4.nH_2O]$ is a trioctahedral 2:1 phyllosilicate mineral with a central brucite octahedral sheet sandwiched between two inward pointing silica tetrahedral layers forming a T-O-T configuration with distinct T faces and T-O-T edges similar to muscovite (Figure 2.4). However, in the case of vermiculite, the charge imbalance that arises due to the isomorphous substitution in the tetrahedral layer is balanced by the absorption of hydrated cations which accumulate in the interlayer region between successive T-O-T units. These interlayer cations are typically monovalent (e.g. Na^+ or Li^+ ions) and attract water molecules, forcing the adjacent sheets apart and causing the mineral to swell. Figure 2.6 shows the structure of vermiculite, with water trapped in the interlayer region between consecutive T-O-T units.

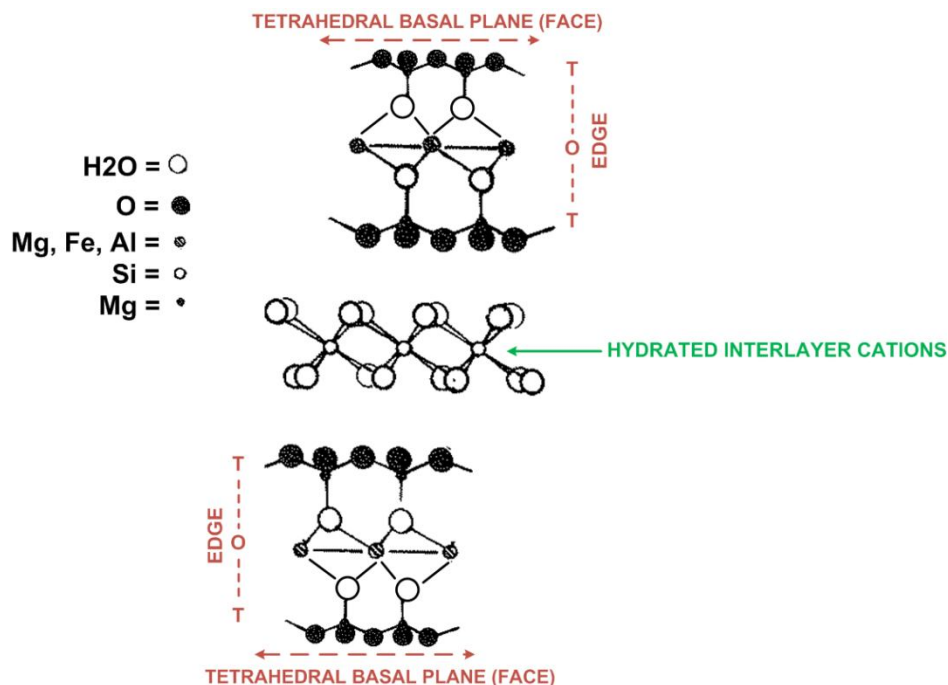


Figure 2.6 - Crystallographic structure of vermiculite (adapted from Douglas, 1989).

Vermiculite has a similar structure to smectites (e.g. montmorillonite). However, the difference between vermiculites and smectites lies in their swelling capacities. The expansion potential of swelling clays is dependent on the layer charge and the extent and location of isomorphous substitutions. As a general rule, the higher the layer charge, the less the osmotic swelling capacity. Smectites have a low layer charge (0.2-0.5 moles per unit cell) and are known for their super swelling abilities. Vermiculite, on the other hand, has a higher layer charge of 0.6-0.9 moles per unit cell (Brindley and Brown, 1980; Laird, 2006), while mica has a layer charge closest to 1.0 mole per unit cell. The increase in swelling potential related to differences in layer charge through the transformation from micas to vermiculites and smectites is demonstrated in Figure 2.7. Another distinguishing property is the location of cationic substitutions within the lattices of smectites and vermiculites. In general, most of the substitutions in vermiculite take place in the tetrahedral sheets, in the interlayer region between successive T-O-T units, such that the interaction between the charge-balancing cations and the tetrahedral sheets is strong. This limits the potential of the mineral to expand its interlayer space. In montmorillonite, however, substitutions mainly occur in the octahedral sheets, away from the interlayer spacing where balancing cations are present. Therefore, the interaction between the charge-balancing cations

and tetrahedral sheets is weak, leading to relatively large interlayer expansion (Abollino et al., 2008). For these reasons (layer charge and position of substitution), vermiculite has a lower swelling potential than smectites and in some instances has been classified as an intermediate between micas and smectites, exhibiting both platy morphology and swelling capability.

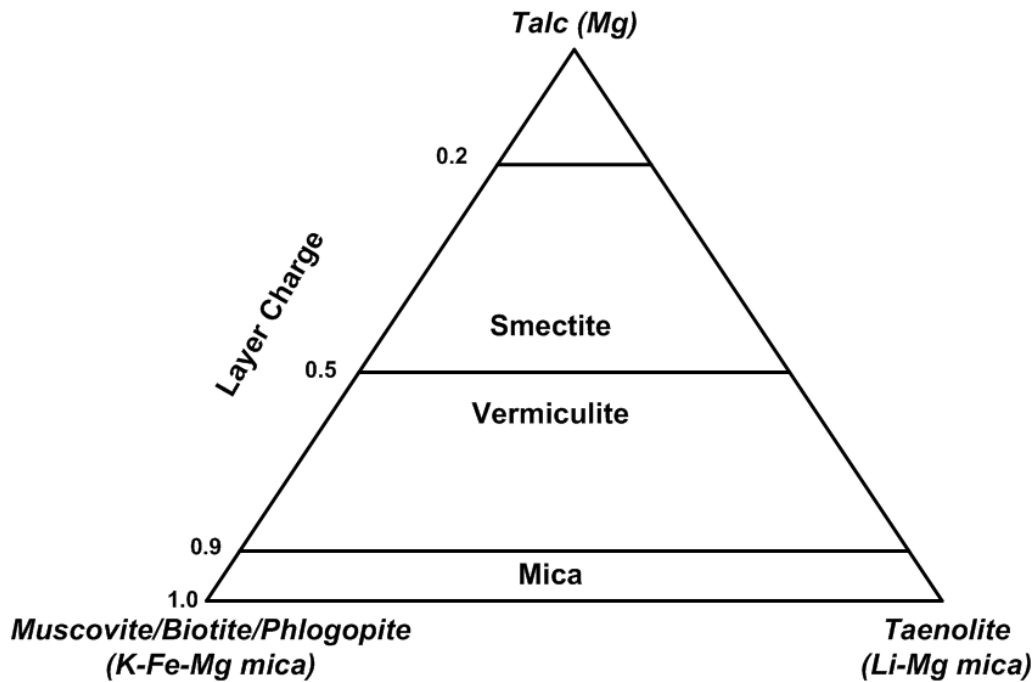


Figure 2.7 – Layer charge differences through the transformation from micas to swelling clays (adapted from Fanning and Keramidas, 1977).

At temperatures above 400°C, vermiculite has the unique ability to exfoliate. At these conditions, the heat causes the release of structural and absorbed interlayer water as steam. This causes vermiculite particles to inflate in a worm-like (vermiculare) or concertina-like manner. The spacing between adjacent plates typically accounts for one water molecule in the interlayer region (Deer et al., 2002). This is much less than in montmorillonite where swelling can, result in up to three water molecules in the interlayer region (McFarlane et al., 2005; Deer et al., 2002; Pils et al., 2007).

2.4.3. Chrysotile mineralogy (serpentine group)

Chrysotile $[\text{Mg}_3\text{Si}_2\text{O}_5(\text{OH})_4]$ is a trioctahedral magnesium silicate and is a polymorph of serpentine. It forms through the hydrothermal alteration of olivines $[(\text{Mg,Fe})_2\text{SiO}_4]$ and pyroxenes $[(\text{Ca,Na,Fe})(\text{Mn,Cr,Al})(\text{Si,Al})_2\text{O}_6]$ (Kirjavainen and Heiskanen, 2007).

Unlike symmetrical 2:1 sheet minerals such as muscovite, vermiculite and montmorillonite, serpentine minerals consists of a silica tetrahedral layer bonded to a brucite octahedral layer in a 1:1 ratio, to form T-O sheets (Figure 2.3). However, there is a mismatch between these layers, causing a strain in the T-O lattice. The adaptation of the T and O layers to this mismatch results in the formation of three polymorphs, antigorite, lizardite and chrysotile. In antigorite, the strain is relieved by the bending and periodic rotating of T layers, resulting in corrugated structures. Alternatively, the minor substitution of Al^{3+} ions for Si^{4+} ions in the T layers results in the formation of lizardite. In the case of chrysotile, however, this is relieved by the extension of the brucite O layer to form convoluted T-O tubes with the silica T layer bent on the inside and the brucite layer exposed on the outer face of the tube (Yada, 1971; Klein and Hurlbut, 1993). The bending of the T-O sheets results in long, spiral chrysotile microstructures. This internal spiral configuration means that the T-O edge occurs at the end of each tube and runs along the length of it.

The continuous curvature of chrysotile T-O microstructures results in a much more complex morphology than the familiar plate/stacked composition of most phyllosilicate minerals. Individual chrysotile particles typically have a long, thin fibrous morphology and are able to orientate themselves in several different directions when in suspension (Ney, 1973). Figure 2.8 shows the bending of the constituent T and O layers and the formation of the long thin chrysotile microfibrils.

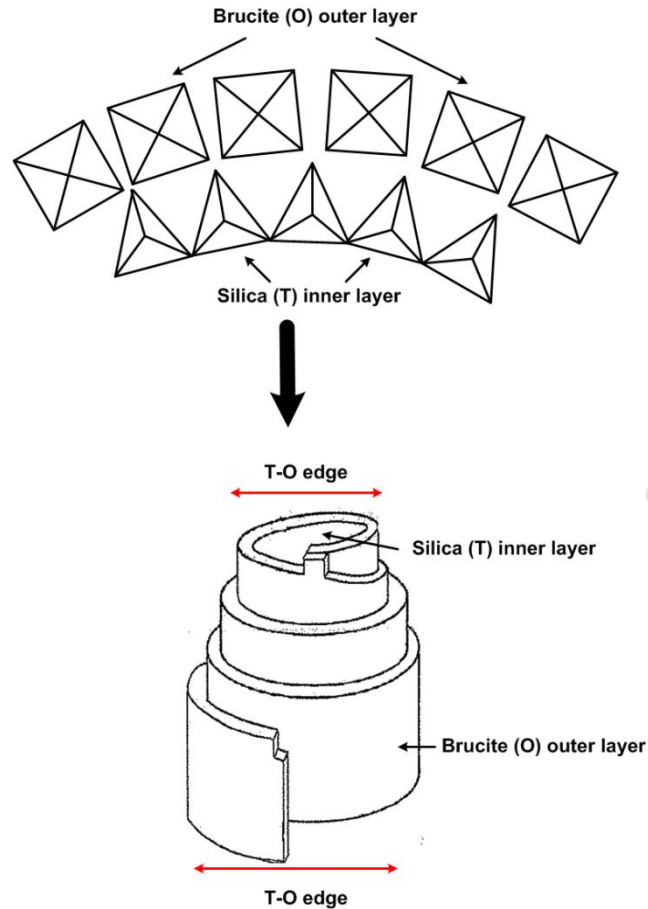


Figure 2.8 - Schematic of (a) mismatch between the tetrahedral and octahedral layers, resulting in (b) spiral structure of chrysotile with brucite extended on the outside and silica layer on the inside (adapted from Miller et al., 2007).

2.4.4. The effect of phyllosilicate mineralogy (morphology) on rheological behaviour

The derivation and mineralogical differences between the phyllosilicates under study have been demonstrated. Muscovite and vermiculite both have a platy morphology, with vermiculite characterized by its additional swelling ability. Chrysotile, on the other hand has a fibrous morphology. Particle morphology/shape plays a significant role in the rheological behaviour of suspensions of single phase minerals. It has been well established in the area of dense medium separation that suspensions of spherical particles exhibit lower viscosities than irregular shaped particles (Collins et al., 1974). Furthermore, studies by Barnes et al., (1989) demonstrated that the effect of solids concentration is much more pronounced with non-spherical particles (rods,

grains and plates) as shown in Figure 2.9. This is related to the length to diameter (L/D) ratio. A higher ratio results in mineral systems which are more non-Newtonian, with elevated apparent viscosities (Horie and Pinder, 1979). Therefore, viscosity increases with a larger deviation from spherical morphology.

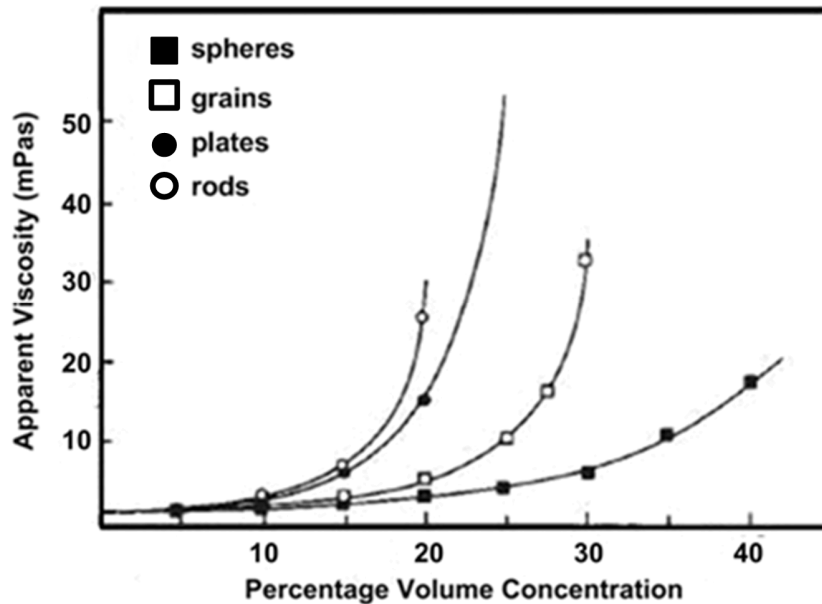


Figure 2.9 – The effect of solids concentration on apparent viscosity of aqueous suspensions of different morphology (Barnes et al., 1989).

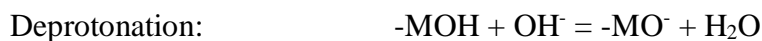
The morphology of phyllosilicate minerals is derived directly from their mineralogy. Although phyllosilicate minerals such as talc, kaolinite and montmorillonite have been studied extensively (e.g. Okuda et al., 1969; Carty, 1999; Furstenau and Huang, 2003; Bremmell and Addai-Mensah, 2005; Khraisheh et al., 2005; Burdukova et al., 2007), there has been less focus on the mica, vermiculite and serpentine groups. Moreover, no formal rheological classification of the phyllosilicate group exists. It is expected that a trend similar to that observed in Figure 2.14 would be observed, dependent on the variations in phyllosilicate morphology.

2.5. PARTICLE SURFACE CHARGE

Interfacial or surface chemistry focusses on the study of chemical reactions that occur at the solid-liquid or solid-gas interfaces (Prutton, 1994). When a particle is immersed in a suspension, it develops a surface charge through one or more mechanisms of charge generation. The particle interactions, stability and rheology of aqueous mineral suspensions are strongly dependent on the surface charge that develops (Callaghan and Ottewill, 1974; Johnson, 1998; Luckham and Rossi, 1999; Addai-Mensah and Ralston, 2004, 2005; Leong, 2005). Surface charge development occurs via a number of mechanisms, the most significant being isomorphous substitution, ionisation, differential dissolution and surface adsorption. Isomorphous substitution occurs by the substitution of higher valence ions by ions of a lower valence. This results in a permanent negative surface charge (Abend and Lagaly, 2000; Bremmell and Addai-Mensah, 2005). The ionisation of metal hydroxide amphoteric surface sites, on the other hand, is governed by the concentration of potential determining ions (H^+/OH^-) i.e. pH of the solution and occurs through the protonation or deprotonation of the surface hydroxides (Equation 2.2). In this case, the particle charge is positive at acidic conditions due to protonation, and is negative at basic pH conditions due to deprotonation (Everett, 1988). Another phenomenon that can induce surface charge is the differential dissolution (leaching) of oppositely charged ions from the surface of sparingly soluble mineral particles. This charge is also pH dependent since the extent of dissolution changes with increasing pH (Furlong et al., 1981; He et al., 2009). Finally, electrostatically driven surface adsorption of ionic species such as surfactants, organic acids and polyelectrolytes also results in the generation of surface charge (Hunter, 1981).



Equation 2.2



2.5.1. The electrical double layer

When a charged colloidal particle is dispersed in aqueous solution, regardless of the mechanism of charge acquisition, counter ions in solution will move towards it due to electrostatic attraction while co-ions are expelled. This redistribution of ions forms a diffuse layer surrounding the particle. Some of the counter ions adsorb to the surface of the particle and form a monolayer which is called the stern layer or inner Helmholtz plane. An excess amount of counter ions with some of the expelled co ions stay in an adjacent layer around the particle. A gradual decrease in the concentration of counter ions with increasing distance from the particle surface is observed, forming the diffuse layer or outer Helmholtz plane. The resulting surrounding layer of counter and co ions composed within the stern and diffuse layers is called the electrical double layer (Hunter, 1981). A schematic of the electrical double layer is given in Figure 2.10.

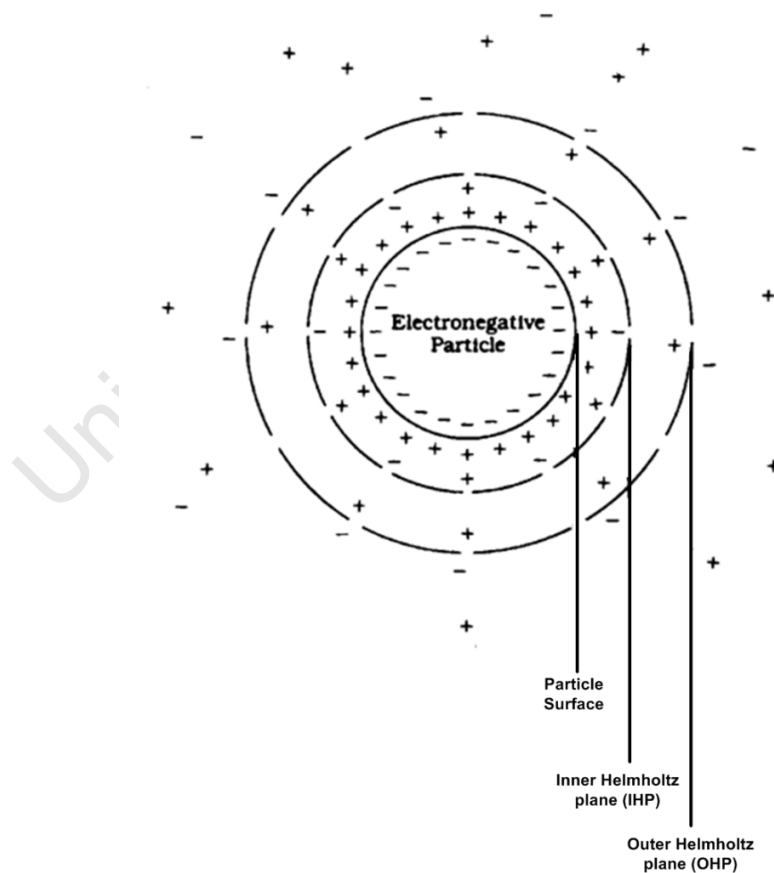


Figure 2.10 – Development of electrical double layer on a particle in suspension.

The thickness of the electrical double layer around each particle is known as the Debye length (κ^{-1}) and is represented by Equation 2.3. Here, F is the Faraday constant, ϵ is the dielectric permittivity, ϵ_0 is the permittivity of vacuum and I is the ionic strength of the electrolyte. I is defined by Equation 2.4, where Z_i and C_i are valence and concentration of the ion i present in the electrolyte

$$\kappa^{-1} = \left(\frac{RT\epsilon\epsilon_0}{2F^2I} \right)^{-1/2} \quad \text{Equation 2.3}$$

$$I = \left(\frac{1}{2} \right) \sum Z_i^2 C_i \quad \text{Equation 2.4}$$

As such, the thickness of the double layer is dependent on the concentration and valence of counter ions present in suspension. The higher the concentration and valence of counter ions, the more the double layer is compressed (Johnson et al., 2000). At high ionic concentrations, the structure of the double layer changes. Instead of two opposite diffuse layers between like-charged adjacent particles, one central layer forms, facilitating closer approach and aggregation of particles (Laskowski, 2012).

2.5.2. DLVO theory and theoretical interpretation of suspension rheological behaviour

When charged colloidal particles start to move in surrounding fluid, different interaction forces may act between particles. The forces, which are either attractive or repulsive, arise when adjacent electrical double layers overlap or undergo Brownian motion and depend on the nature and characteristics of the system and distance between adjacent particles. According to the classic DLVO theory (Derjaguin and Landau, 1941; Verwey and Overbeek, 1948), the net inter-particle force (V_T) is determined by a combination or superposition of the inter-particle double layer repulsion energy (V_R) and the van der Waals attractive energy (V_A) (Equation 2.5).

$$V_T = V_A + V_R \quad \text{Equation 2.5}$$

Van der Waals forces arise from instantaneous dipoles generated between atoms of two neighboring atoms. Each dipole generates an electromagnetic field which interacts and induces instantaneous dipoles within other adjacent atoms. The overall interaction energy between dipoles is attractive and rapidly increases in magnitude with decreasing separation between dipoles (Haymaker, 1937; Lifshitz, 1956; Israelachvili, 1985). The repulsive electrical double layer force, on the other hand, arises from electrical double layer overlap of similarly charged particles in aqueous environment when they are in close proximity of each other. Increasing the concentration of counter ions between two approaching charged surfaces increases both osmotic pressure and free energy, resulting in a repulsive force (Hogg et al., 1966).

Based on the DLVO theory, the particle interactions of colloidal dispersions may be predicted from van der Waals and electrical double layer forces. For suspensions of low electrolyte concentration, particle aggregation is a result of the contributions of the van der Waals and repulsive forces in suspension and can be related to the resultant suspension rheological behaviour. The repulsive electrical double layer forces act as a barrier against van der Waals forces to prevent aggregation. When the surface potential is zero, the attractive forces dominate over the repulsive electrical double layer forces and particles are pulled together by the van der Waals forces of attraction. At this point, fast coagulation prevails, with the formation of an interconnected network of particles with high yield stress requirements. However, in the case where the attractive forces are retarded by short range repulsion, there exists a combination of both van der Waals attraction and repulsive double layer forces, and slow coagulation of particles occurs. Conversely, at high levels of surface potential, repulsive forces are stronger than the attractive forces and the suspension exists in a strongly repulsive dispersed state of low yield stress and viscosity (Laskowski and Pugh, 1992) (Figure 2.11).

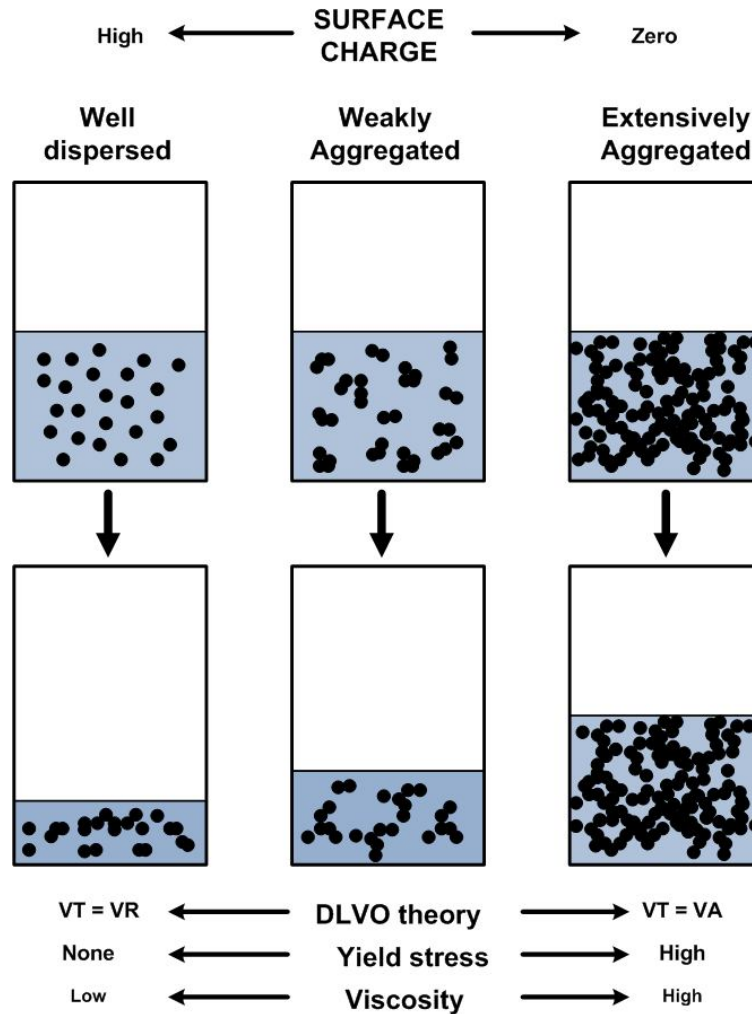


Figure 2.11 - Schematic representation of the relationship between surface charge and rheological properties (Laskowski and Pugh, 1992).

The dominance of one force over another at low electrolyte conditions is also dependent on the particle separation. Generally, van der Waals forces are dominant at shorter distances ($< 4\text{nm}$), while the net interaction energy is dominated by repulsive electrical double layer forces at longer distances ($< 100\text{nm}$). The occurrence of a maximum (V_m) at intermediate distances represents the energy barrier that must be overcome for aggregation to occur (Figure 2.12a).

Coagulation can also be induced by high electrolyte concentrations. At these conditions, V_m is reduced through compression of the double layer thickness (Equation 2.3). This reduces the

repulsive portion and leads to the formation of a secondary minimum which is low enough to promote aggregation between particles (Figure 2.12b) (Hogg, 2000).

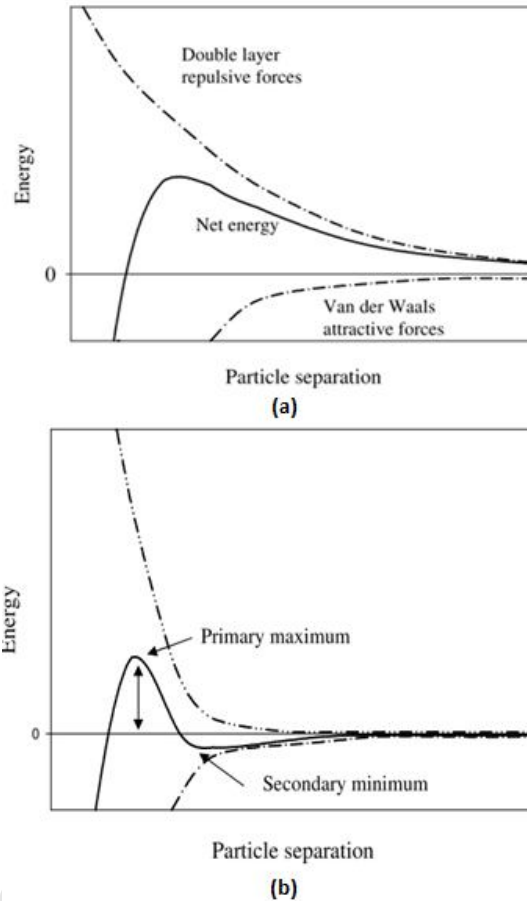


Figure 2.12 – Schematic of the variation of free energy with particle separation according to the DLVO theory (Nasroti, 2010) and (b) the variation of free energy with particle separation at higher salt concentrations, showing the appearance of a secondary minimum (Nasroti, 2010).

2.5.3. The surface charge properties of phyllosilicate minerals

The aggregation between phyllosilicate particles is more complicated primarily due to the charges that form on the different surface planes. Unlike particles with a uniform charge, the surface charge properties of layered silicates are defined based on face and edge surfaces of

different lateral dimension. This has in the past, made analysis by direct means difficult, such that the derivation of charge on the edges and faces has not been definitively defined.

Traditionally, the face surfaces are believed to carry a permanent structural negative charge due to isomorphous substitution. However, advances in electrokinetic, streaming potential and direct force measurements have revealed that the basal faces also show ionisation trends, not inconsistent with the pH dependent hydrolysis of silicon in the surface plane. This is particularly the case in the pH regime 4-8, suggesting the presence of a small amount of pH dependent negative charge (Scales et al., 1990; Nishimura et al., 1995a; Nishimura et al., 1995b). The exact contribution to the face charge of layered silicates due to either isomorphous substitution or ionisation is not clearly understood and more detailed research is warranted. However, it can be assumed that the negative charge on the basal plane is a result of both, with the magnitude dependent on the degree of isomorphous substitution and change with pH may be attributed to the pH dependent ionisation of exposed silanol groups on the surface.

The charge derivation on the edges has not been conclusively established either, but is thought to be due to the ionisation of exposed hydroxyl groups, dependent on solution pH. Therefore, in acidic solution the edge is expected to carry a positive charge, while in alkaline solution the edge is negatively charged (Schofield and Samson, 1954; Flegmann et al., 1969; Bolland et al., 1976). While there is still much debate over the derivation of charges on the different surfaces, there is common agreement in that there exists a charge separation between the edges and faces, with the faces carrying a predominantly negative charge while the charge on the edges changes from positive to negative. This charge anisotropy is shown in Figure 2.13.

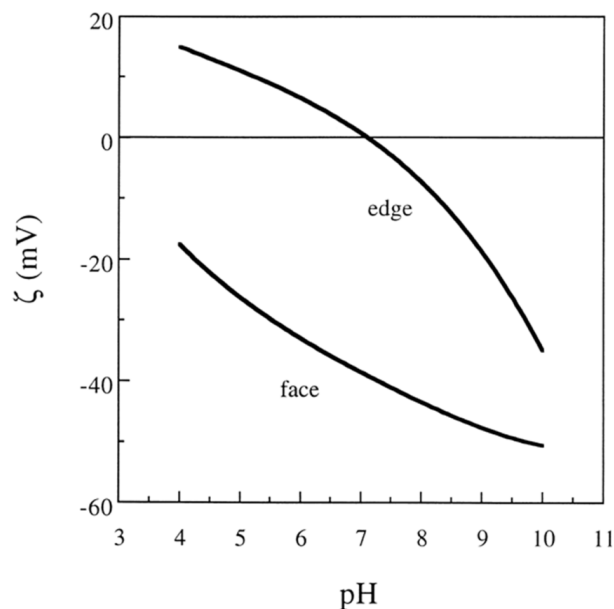


Figure 2.13 – The zeta potential properties of the edge and face surfaces of kaolinite in the presence of 0.01M NaCl background. Edge data taken from Williams and Williams, 1978. Face ζ potentials determined by correcting data by Johnson et al., 1998 for the effect of edge ζ potential. (Johnson et al., 2000).

It has been argued that the pH dependence of phyllosilicates should rather be attributed to the leaching of aluminium at low pH and precipitation to the basal plane as a more important factor rather than the edge charge effects (Furlong et al., 1981). However, this may be subject to the significance of the edge charge towards the overall particle surface charge, as defined by the thickness of the platelets and may vary from phyllosilicate to phyllosilicate.

In general, the degree of charge anisotropy is dependent on the contribution of charge from either surface. Platelets with high lateral extent (and high aspect ratios) have the surface area of the edges much smaller than the basal faces. The pH dependent charge on the edges is then considered insignificant in comparison with the predominant basal face charges (Scales et al., 1988; Scales et al., 1990; Nishimura et al., 1992; de Kretser et al., 1998). This is the case with smectite clays where it has been suggested that the total edge surface area is only ~10% compared to the basal faces (Maslova et al., 2004; McFarlane et al., 2005). In such cases, the negative electrostatic field emanating from the face would extend out sideways, screening any

positive charge developed by the edges (Callaghan and Ottewill, 1974; Tateyama et al., 1997; Solomon and Boger, 1998), such that the particles exhibit a very low degree of charge anisotropy.

However, with thicker particles (e.g. kaolinites) the edge shows a significant charge contribution and the anisotropic charge properties are more prominent. In such cases, in the absence of knowledge on the contribution of silicon hydrolysis towards the negative charge of the basal plane, the magnitude of the negative charge on this surface (degree of negativity) may be correlated only to the degree of isomorphous substitution. The degree to which isomorphous substitution occurs varies from mineral to mineral. In the case of minerals with a low degree of substitution, the faces are near neutral or only slightly negatively charged. In such cases, the minerals are likely to behave as if they were isotropic, with the overall surface charge primarily dependent on the charge of the edges. However, when there is a high degree of substitution present, the faces will carry a strong negative charge and the mineral is highly anisotropic.

2.5.4. Measurement of surface charge

2.5.4.1. Electrophoretic zeta potential measurement

The measurement of the surface charge of particles is a useful tool for investigating the nature of the surface chemistry and particle interactions within colloidal systems. The zeta potential, ζ , is a frequently used quantity that implicates the surface charge of particles and its measurement is possible through various electrokinetic methods including electrophoresis and streaming potential. The streaming potential technique, is most suitable for measuring the surface charge of macroscopic particles which have flat surfaces, where the liquid phase flows freely through stationary particles. This method is ideal for decoupling the charges on the different surfaces in phyllosilicate minerals. It has been successfully applied to muscovite (mica), whose sheet like structure allows cleavage along the basal plane into and a surface of sufficient surface area for measurement (Scales et al., 1990). However, use of this technique becomes difficult when dealing with other phyllosilicates which do not have a large enough surface area. Recent advances in the preparation of molecularly smooth surfaces through fine cutting ultramicrotome

technology, sandblasting and polishing have aided in improving the analysis of other phyllosilicates by streaming potential. This has also improved research into the use of direct atomic force measurements of the different planes of these minerals and has been applied to layered silicates such as talc and kaolinite, although these techniques still need to be perfected (Yan et al., 2011; Yin et al., 2012).

Electrophoresis, on the other hand, is based on the motion of particles within a bulk fluid of induced electrical field, and provides an overall charge estimate without isolation of charges on edges and faces. In electrophoresis, the velocity (U_E) of an isolated charged particle is measured when an electrical field with strength E is applied. A linear relationship exists between the velocity and applied electrical field strength (Hunter, 1981) (Equation 2.6).

$$U_E = \mu_e E \quad \text{Equation 2.6}$$

Where μ_e is the electrophoretic mobility of the charged particle, dependent on particle and electrolyte properties (radius, viscosity, ionic strength, pH, electric permittivity etc.). The electrophoretic mobility is typically related to the zeta potential by Smoluchowski's equation (Equation 2.7), which assumes that the particle radius (a) is large in comparison to the thickness of the electrical double layer ($\kappa a \gg 1$) (Hunter, 1981)

$$\zeta = \eta \frac{\mu_e}{\epsilon} \quad \text{Equation 2.7}$$

Where η is the viscosity and ϵ the permittivity (dielectric constant) of the suspension.

The electrophoretic measurement estimates the surface charge at the outer Helmholtz plane. This represents a measurement of the charge at the closest point of approach of the counter-ions to the surface of the particle, and not at the actual particle surface. Therefore, a discrepancy may arise between the measured zeta potential and the actual charge at the particle surface. The difference in the electrophoretic zeta potential measurement and the charge at the particle surface is shown in Figure 2.14.

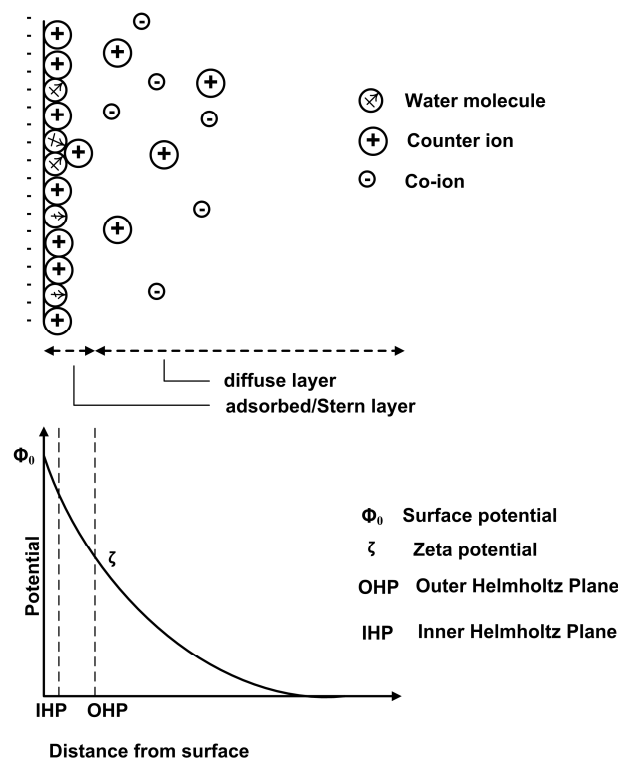


Figure 2.14- Schematic representation of the electrical double layer, showing the difference between the zeta potential and surface charge (Alvarez-Silva et al, 2010).

2.5.4.2. Application of the electrophoretic measurement to isotropically and anisotropically charged minerals

The zeta potential measurement has been widely used for the surface charge determination of both isotropically and anisotropically charged minerals. The defining property of isotropic minerals is that all surfaces of such particles are created by breaking the same bonds and the resulting mineral surfaces are homogeneous and do not vary as a function of position on the particle. Examples of such compounds are corundum (Al_2O_3) and zirconia (ZrO_2). The surface charge of these minerals arises from the ionisation of metal hydroxide amphoteric surface sites and therefore undergoes a change from positive to negative surface charge with increasing pH. When there exists an equivalent amount of positive and negative ions, the overall surface charge of the mineral is zero. The pH at which this occurs is known as the point of zero charge (p.z.c).

When estimated using the electrophoretic zeta potential measurement, this is termed the iso-electric point (i.e.p), the pH at which the zeta potential is zero.

The iso-electric point has conventionally been used to explain the colloidal behaviour of minerals suspensions. On the basis of the DLVO theory, it represents the pH at which the electrostatic repulsive forces are absent and the particle surface charge is zero (point of zero charge). Attractive van der Waals forces result in maximum particle coagulation and maximum yield stress of the mineral suspension. It has been demonstrated that for isotropically charged minerals, this p.z.c coincides with the i.e.p as determined by the zeta potential measurement, and this also corresponds with yield stress peak (Subbanna et al., 1998; Johnson et al., 2000). This relationship is demonstrated in Figure 2.15, where the yield stress peak of zirconia occurs at circa pH 5.9. This corresponds to the iso-electric point (and point of zero charge) which exist at circa pH 6. At pH conditions well away from the iso-electric point, the surface potential is high and the electrical double layer repulsion dominates over the van der Waals forces of attraction, forcing the suspension into a dispersed state (Derjaguin and Landau, 1941; Verwey and Overbeek, 1948). These suspensions are characterized by low yield stresses. As the pH moves towards the iso-electric point, the surface charge diminishes and the reduced electrostatic repulsive forces can no longer counteract the attractive forces. The system starts coagulating and the yield stress of the suspension gradually increases. Therefore, for isotropically charged minerals, the zeta measurement adequately estimates particle surface charge.

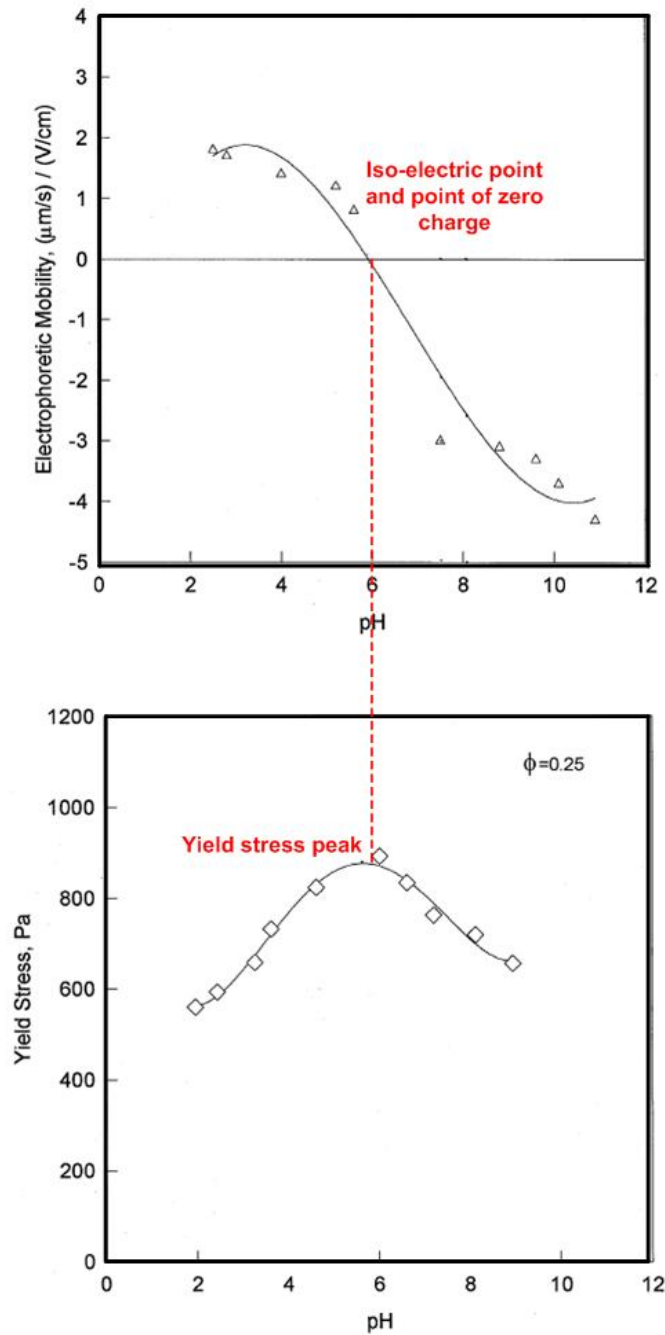


Figure 2.15- The zeta potential and yield stress vs. pH curves for zirconia suspensions (Subbanna et al., 1998).

The processes of surface charge measurement and aggregation of anisotropically charged particles is much more complicated. For such minerals, the surface charge varies with the position on the particle surface such that the zeta potential measurement is now dependent on the

plane of measurement. It has been demonstrated that for these minerals, the iso-electric point no longer corresponds with the point of zero charge or the maximum yield stress. This discrepancy has been demonstrated for kaolinite (Figure 2.16) where there exists a disparity between the yield stress peak (pH 5.5) and the electrophoretic iso-electric point (circa pH 3.6) in an anisotropically charged mineral.

The difference between the i.e.p and p.z.c for anisotropically charged minerals can be attributed to inadequacies with the zeta potential measurement itself, Since it relies on the mobility of the mineral particle in solution and makes use of Smoluchowski's equation to convert electrophoretic mobility to zeta potential (Lyklema, 1995; Burdukova et al., 2007), this equation has been specifically derived for uniformly shaped, spherical (or near spherical) particles, such that it is compromised by the shape and anisotropic character of the layered and fibrous silicates (Miller et al., 2007; Nalaskowski et al., 2007; Yin et al., 2012). Moreover, the electrophoretic mobility of particles in solution is not only a strong function of the particle surface charge, but also the orientation of the particle with respect to its motion. The lateral plane of a layered particle experiences significantly more drag than its edges making the conversion from mobility to zeta potential highly unreliable (Knecht et al., 2008).

The charge heterogeneity complicates the aggregation of particles since it is now dependent on the surface charge properties of different planes. Layered silicates can associate in edge-edge (EE), edge-face (EF) and face-face (FF) configurations, with the formation of each dependent on the balance of electrostatic interaction between adjacent particles. The formation and dominance of one mode of interaction over another is dependent on a number of factors such as electrolyte concentration, pH, aspect ratio and surface area. Therefore, for anisotropically charged minerals, the point of maximum coagulation (and yield stress) does not result through the prevalence of attractive van der Waals forces, but rather through the transition to an alignment of highest rheological complexity. For this reason, the iso-electric point is no longer indicative of the maximum yield stress of slurries of anisotropically charged minerals. In fact, it is not exactly clear what the measured iso-electric point represents. Therefore, the results of zeta potential measurements cannot be viewed in isolation and should rather be used in combination with other techniques for a comprehensive analysis of the surface charge distribution of phyllosilicates.

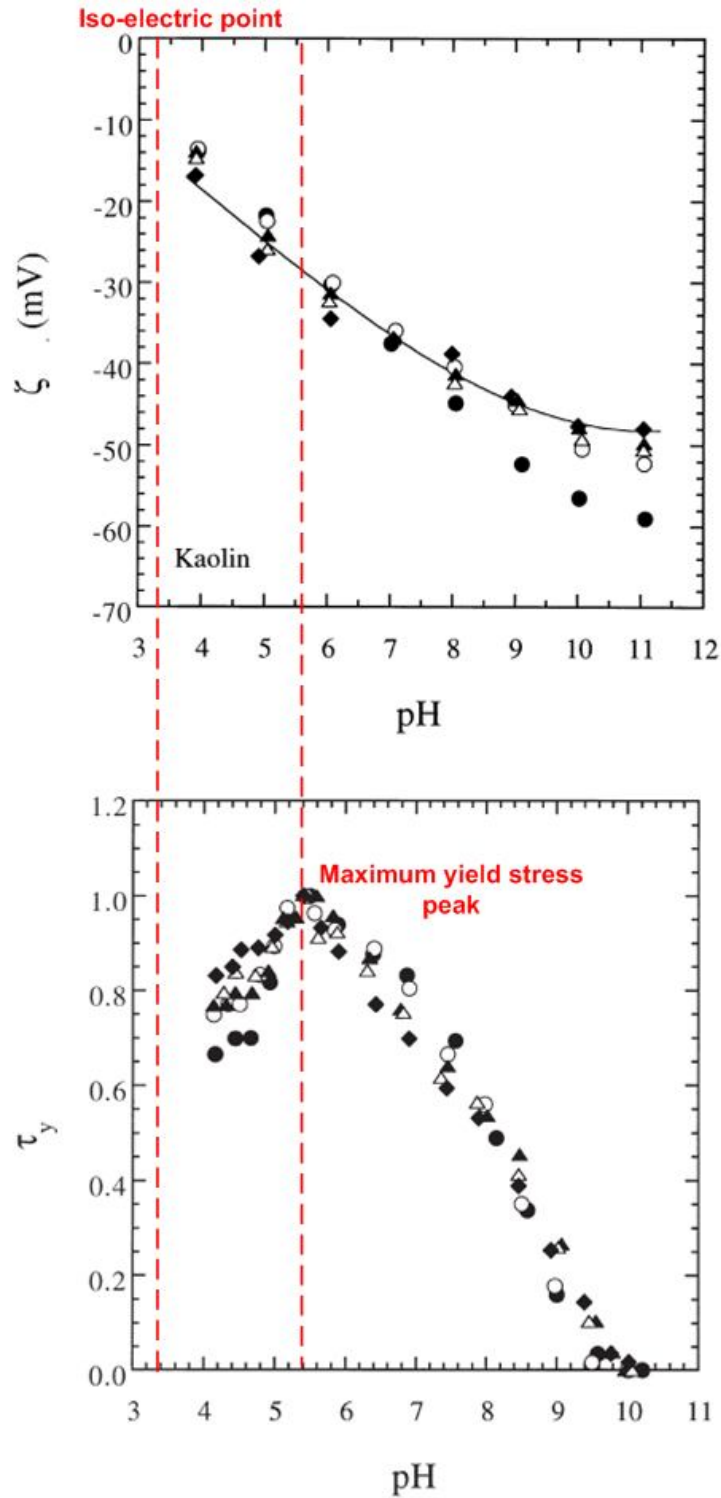


Figure 2.16 - The normalised zeta potential and yield stress vs. pH curves for kaolinite suspensions (Johnson et al., 1998).

2.5.4.3. Potentiometric titrations

Potentiometric titrations are based on the principle of ion exchange and are therefore not subject to particle morphology (Laskowski and Sobieraj, 1969; Mular and Roberts, 1966). A simplified titration method to determine the point of zero charge was developed by Mular and Roberts (1966). This technique relies on the effect of surface charge as the concentration of indifferent background electrolyte is changed, such that the only potential determining ions are the H⁺ and OH⁻ ions (as determined by changes in pH). The validity of the Roberts Mular titration method has been established experimentally by comparing the point of zero charge (as determined using Roberts-Mular potentiometric titrations) and iso-electric point (as determined using electrophoretic zeta potential measurements) of quartz (isotropically charged). Quartz is a well characterized mineral whose iso-electric point is estimated to lie within the range pH 2 to pH 3 (e.g. Prakash et al., 1999; Klein et al., 2012). The point of zero charge, estimated by the Roberts Mular titration occurs at pH 2 (Alvarez-Silva et al., 2010). The convergence of the p.z.c and i.e.p not only proves that the Roberts Mular potentiometric titration method accurately estimates the point of zero charge but also is equivalent to other potentiometric titration techniques. It has also been used to successfully demonstrate the distinction between the iso-electric point and point of zero charge for anisotropically charged minerals such as talc and chlorite (Burdukova et al., 2007).

In the Roberts Mular titration technique, the point of zero charge is based on the calculation of the net surface charge density, σ_0 which is defined as

$$\sigma_0 = \sum_i z_i F_i \gamma_i \quad \text{Equation 2.8}$$

Where F is the Faraday constant, γ is the adsorption density of potential determining ions and z is their corresponding valence (Hunter, 1981). Since the only potential determining ions are H⁺ and OH⁻ ions,

$$\sigma_0 = F (\gamma_{H^+} - \gamma_{OH^-}) \quad \text{Equation 2.9}$$

When the surface potential is zero, the background electrolyte strongly affects the surface charge according to the following equation (Hunter, 1981)

$$\sigma_0 = -\varepsilon \left(\frac{d\phi}{dx} \right)_{x=0} \quad \text{Equation 2.10}$$

Where ε is the permittivity of the dielectric and $\frac{d\phi}{dx}$ is the potential decay as given by the Debye-Huckel expression

$$\frac{d\phi}{dx} = -K\phi \quad \text{Equation 2.11}$$

$$K = \left(\frac{e^2 \sum n_i z_i^2}{\varepsilon kT} \right)^{0.5} \quad \text{Equation 2.12}$$

Where e is the elementary charge, n_i is the electrolyte concentration, K is the Boltzmann constant and T is the absolute temperature. In the Roberts Mular titration, the electrolyte concentration n_i is increased, resulting in an increase in K and the rate of potential decay $\frac{d\phi}{dx}$. This causes potential determining ions to be adsorbed onto the surface in order to maintain a constant surface potential. Since the potential determining ions are H^+ and OH^- ions, this induces a change in pH. The point of zero charge occurs when there is no change in pH (Mular and Roberts, 1966). Figure 2.17 gives a plot of the net surface charge density versus pH, demonstrating the change in pH due to an increase in ionic strength of the supporting electrolyte.

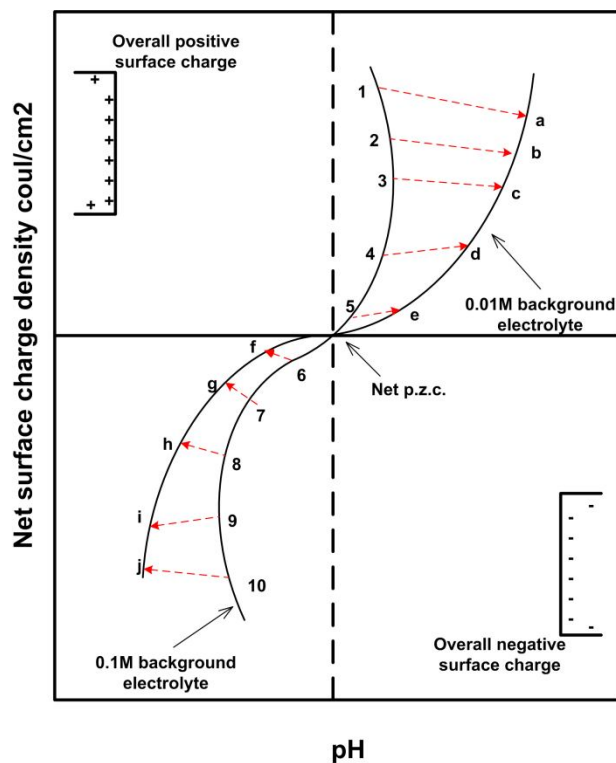


Figure 2.17 - Theoretical plot of net surface charge density of potential determining ions vs. pH (Mular and Roberts, 1966).

While the potentiometric titration provides a more accurate estimation of the point of zero charge of isotropically charged minerals, it is important to note that in the case of anisotropically charged minerals, neither the zeta potential measurements nor the potentiometric titrations give the value of the particle point of zero charge. This is due to the fact that for anisotropically charged minerals, the point of zero charge may not exist, since the edges or faces carry an electrical charge at any pH. Instead, the potentiometric titration gives a realistic estimate of the 'net' point of zero charge of the mineral. At this point, there is a balance between the positive and negative charges on edges and faces. Below the net point of zero charge, the mineral is prone to the adsorption of OH⁻ which is indicative of an overall positive charge on the mineral surface. Conversely, above the net point of zero charge, the adsorption of H⁺ ions is favoured, indicating an overall negative charge on the particle surface. The electrophoretic measurements and potentiometric titrations can be used in tandem, to provide an estimate of the degree of deviation of a mineral from isotropic behaviour, to measure the true location of the net point of zero charge

and to estimate the relative surface charge distribution of the different particle planes at a range of pH values, based on deviations between the p.z.c. and i.e.p. (Burdukova et al., 2007).

2.5.4.4. The electrophoretic zeta and titration measurements in tandem

Despite the ambiguity around the electrophoretic measurement for anisotropically charged minerals, considerable discussion on the electrokinetic characteristics and the iso-electric points, particularly of kaolinite have been reported, with most studies reporting an iso-electric point in the range pH 2.5 to pH 3.6 (Williams and Williams, 1978; Schroth and Sposito, 1997; Johnson et al., 2000; Brady and Krumhansl, 2001; Liu et al., 2001; Das, 2002; Zbik and Smart, 2002; Hong et al., 2003; Celik, 2004). Although it is not clear what this measured iso-electric point represents, it has been found to be closely related to the ratio of alumina to silica in the kaolinite, with a higher iso-electric point reported with increasing alumina content (Hu et al., 2003). Kaolinites comprise equal proportions of silica tetrahedral and gibbsite octahedral layers, and the variations in alumina content may be attributed to the degree of isomorphous substitution (Al^{3+} for Si^{4+} ions). A larger degree of substitution is likely to result in a higher iso-electric point value.

A comparison with constituent silica (T) and gibbsite (O) layers demonstrated the similarity in the electrokinetic behaviour of kaolinite to silica (Miller et al., 2007). Such behaviour is anticipated for halloysite, a tubular form of kaolinite with the silica T layer exposed on the surface (Figure 2.18). Kaolinite, on the other hand, has a planar structure and it is expected that both layers would have an equal contribution and an intermediate iso-electric point would be reported. The low iso-electric point suggests that the alumina content, although showing equivalent exposure, is not very significant towards the electrokinetic behaviour which is misleading. Conversely, surface charge density studies of kaolinite by titration have reported point of zero charge values within the range pH 4.3 to pH 4.6 (Motta and Miranda, 1989; Brady et al., 1998). This is significantly higher than that measured by electrophoresis, suggesting that the titration method may indeed better describe the surface charge properties of layered silicates.

It could also be inferred that below the measured p.z.c (pH 4.6), kaolinite particles carry an overall positive charge and are net negatively charged above this value.

When used in isolation, neither method adequately describes the charge properties of layered silicates. However, information regarding the relative degree of charge anisotropy, the apparent contribution of constituent layers and the overall particle charge at certain conditions can be better surmised by using a combination of both methods.

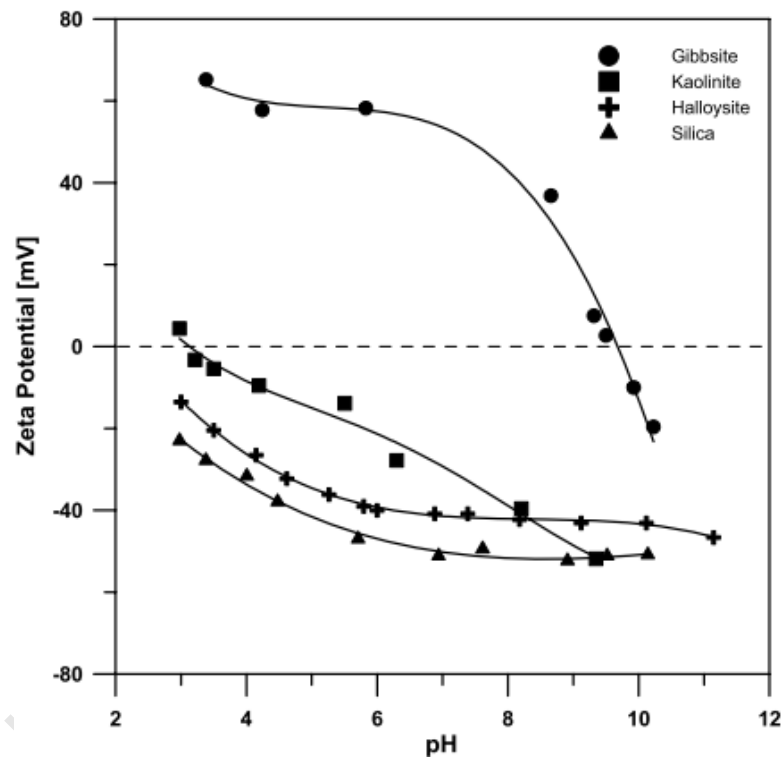


Figure 2.18- Electrophoretic behaviour of planar (kaolinite) and tubular (halloysite) in comparison with gibbsite and silica (Miller et al., 2007).

2.6. THE MODES OF PHYLLOSILICATE PARTICLE ASSOCIATION

2.6.1. Suspensions of pure minerals

Contemporary approaches to phyllosilicate colloid and rheological behaviour are based on the DLVO theory, where competing electrical double layer and van der Waals forces determine whether the mineral suspensions will be stabilized (in sol form) or coagulated (in gel form) (Nasser and James, 2006). The mode of particle interaction with phyllosilicates is further complicated by their anisotropic surface charge distribution. The mechanism by which surface charge on the clay face is generated, be it as a result of substitution in the octahedral or tetrahedral layers is of importance, as are both the thickness (aspect ratio) and lateral dimensions of the plates (Tateyama et al., 1997).

Conventional theories in colloidal and clay science have identified three main modes of particle association for platy minerals. Platelets can associate in face-face (FF), edge-edge (EE) and edge-face (EF) configurations, with the formation of each dependent on the balance of electrostatic interaction between the planes of adjacent particles (Van Olphen, 1951; Rand and Melton, 1977; Luckham, Rossi, 1999). EE and FF association may occur due to the high repulsive potential between basal surfaces (faces and edges respectively). EF association, on the other hand, is a result of the attractive forces between oppositely charged planes. Conversely, repulsive forces between similar charged planes result in a dispersed state. The yield stress has been used as a sensitive indicator of the degree of coagulation and can be used as an index of changes in the mode of particle-particle interaction. FF association leads to the formation of lamellar structured aggregates (tactoids) of low apparent volume per plate. This is manifest in low suspension yield stresses. EF and EE associations, on the other hand, lead to three dimensional 'house of cards' structures where the volume occupied/swept out by an individual particle is maximized, and the apparent volume fraction of the suspension is also a maximum. This results in more rheologically complex suspensions (Rand and Melton, 1977; Lagaly and Zeisner, 2003).

Due to the individual physico-chemical characteristics of platy phyllosilicates, the particle-particle aggregation mode that occurs in a solution is highly dependent on the suspension pH. Resolution of changes in particle orientation of kaolinite particles with pH has been achieved using the electrical double layer theory by Hogg et al., (1966), and takes into consideration geometrically predicted interaction area ratios. Figure 2.19 shows the relative magnitudes of the

face-face, edge-face and edge-edge interaction forces, F normalized by the maximum edge-face force (F_{max}). These can be used to rationalize the yield stress properties. At low pH, many particles are expected to interact in an edge-face manner due to the strength of the edge-face attraction. However, interactions between the face surfaces are also predicted to be significant due to the aspect ratio (~10 for kaolinites). As the pH rises, the edge-face force becomes progressively more attractive, and the face-face force less attractive, driving particle reorientation in order to allow further edge-face association to occur. This generates an increase in the yield stress. At still higher pH, the edge-face attraction has been predicted to diminish and the 'house of cards' structure is disrupted. A corresponding decrease in yield stress results. Edge-edge association is predicted to increase as the face-face and edge-face interactions decrease. At high pH, interaction forces between all surfaces are either repulsive or zero and a completely dispersed system is expected (Johnson et al., 2000).

Van Olpen (1951) proposed a change in particle aggregation from edge-face at low pH conditions to edge-edge and dispersion at higher pH conditions. This model is schematically represented in Figure 2.20, demonstrating the corresponding changes in suspension yield stress.

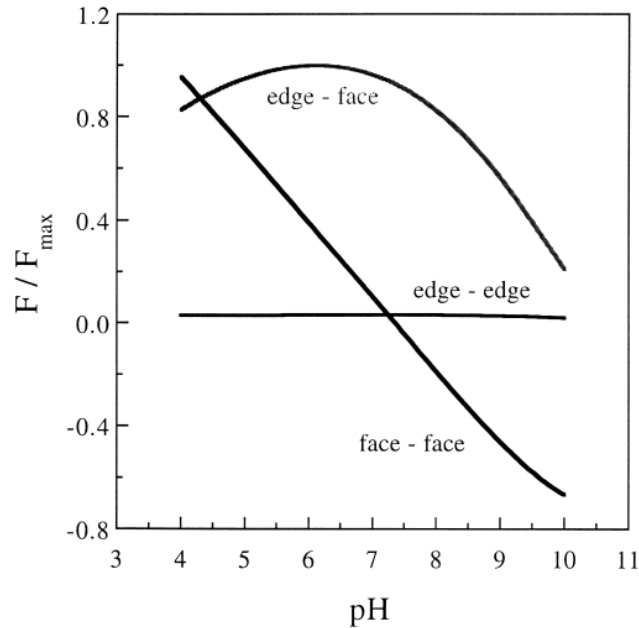


Figure 2.19- The relative magnitudes of the FF, EE and EF interaction forces, F . All forces have been multiplied by the geometrically predicted interaction area ratio and then normalized by the maximum attractive EF force, F_{max} (Johnson et al., 2000).

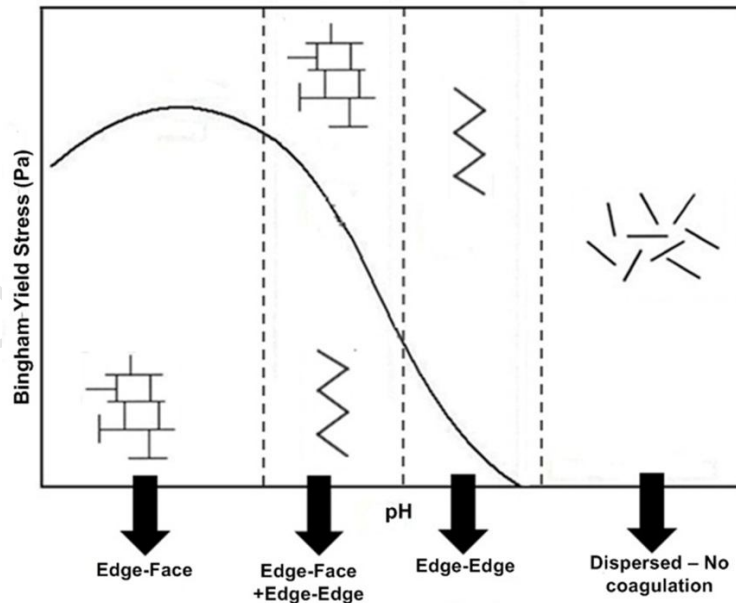


Figure 2.20 – Schematic representation of the modes of particle interaction in homogeneous mineral suspensions as a function of pH and Bingham yield stress (adapted from Rand and Melton, 1977).

This form of particle interaction has since been used in explaining colloidal properties of platy minerals by many researchers (James and Williams, 1982; Permien and Lagaly, 1994; Johnson et al., 1998; Benna et al., 1999; Lagaly and Zeisner, 2003; Burdukova et al., 2007; Gupta et al., 2011; Yin et al., 2012). However, there has been some debate over the existence of edge-face interactions and the application of this model to all phyllosilicates, particularly at low pH conditions (M'Ewen and Pratt., 1957; de Kretser et al., 1998). Primary reasons for these objections lie in the fact that many measurements supporting the concept of edge-face interactions have been conducted in basic pH conditions (>pH 8), most likely above the iso-electric point of the edge surface. Theoretically, the suspension pH must be lower than the edge iso-electric point for a positive charge and edge-face interactions to occur. Although the exact iso-electric point of most phyllosilicates has not been definitively defined, estimates from investigations on non-crystalline alumina and silica surfaces as well as from direct AFM measurements estimate the edge iso-electric point at a pH between pH 6 and 8 (Gupta and Miller, 2010). Similarly, the edge i.e.p. of magnesium silicates such as talc has been estimated to lie in the range pH 8 to pH 9 based on a combination of surface charge and electron microprobe analyses (Burdukova et al., 2007). While the edges may carry a slight positive charge above the iso-electric point, it is most likely mediated by the presence of any humic substances in the system within a natural clay environment (de Kretser et al., 1998).

Even so, compelling evidence for the existence of edge-face interactions in kaolinite suspensions has been observed by a number of researchers with some of the most recent being Gupta and Miller, (2010) and Gupta et al., (2011). In these studies, interaction forces between exposed alumina and silica surfaces were interrogated using AFM surface force and CryoSEM measurements. FF interactions were predicted at low pH conditions (pH 3) , a combination of FF and EF and EE interactions at intermediate pH values and EE and EF interactions showing a more porous structure were observed at even higher pH conditions (pH 7).

Such behaviour would be expected on the basis of the increased thickness of kaolinite platelets relative to their lateral extent. In this case, the edge shows a significant charge contribution and the relatively high degree of charge anisotropy likely results in the formation of edge-face interactions. In contrast, platelets with high lateral extent have the surface area of the edges much

smaller than the basal faces. The pH dependent charge on the edges is considered insignificant in comparison with the predominant basal face charges due to screening effects and the particles are not strongly anisotropically charged (Scales et al., 1988; Scales et al., 1990; Nishimura et al., 1992; de Kretser et al., 1998; Callaghan and Ottewill, 1974; Tateyama et al., 1997; Solomon and Boger, 1998). The most important aspect of colloidal behaviour in this instance is FF agglomeration. Changes in rheological behaviour with pH in such cases may be attributed to subtle misalignment of the FF agglomeration whose increased thickness may then give rise to EF and EE aggregation.

In addition to variations with pH, it has also been suggested that the particle surface and crystallinity play a decisive role in particle interaction. Herein, the assumption of ideal long, thin platy morphology is challenged; primarily due to the unpredictable nature of mineral formation such as sedimentation, fragmentation or lateral intergrowth, rendering the formation of molecularly smooth minerals less likely (Deer et al., 1992). Instead phyllosilicate platelets can exist as poorly ordered structures, with subhedral flakes (islands) attached on the basal faces of larger particles (Zbik and Smart, 1998; Zbik et al., 2010). This results in composites of small areas of the faces between steps of exposed edge sites. As a result, it cannot be assumed that the extensive faces are flat or that the edges are insignificant. These surface properties provide adsorption sites and predominantly promote EE bridging flocculation, with some EF aggregation also likely upon shearing (Du et al., 2010).

There is, therefore, no definitive and conclusive model in support of the existence of one dominant mode of particle interaction. Indeed all factors, charge anisotropy, particle asymmetry, aspect ratio and crystallinity are important toward the type of particle aggregation and most probably result in a combination of FF, EE and EF interactions. The relevance of one factor over another (and the dominance in the mode of aggregation) is most likely dependent on the physico-chemical properties of the mineral of interest.

2.6.2. Suspensions of binary mineral mixtures

2.6.2.1. Mixture design for blending practices in minerals processing

As previously mentioned, blending is a technique that is used in mitigating the effects of one 'bad' ore by mixing it with a more competent ore. This is a standard technique that has been used extensively in food processing and pharmaceutical industries for researching mixtures. Although this form of analysis is a mature discipline in other industries, the outcomes of its application to the minerals processing industry have often been contradictory due to intrinsic differences in ore metallurgical properties (e.g. grade, grindability index etc.). The effect of blending on rheological performance has not been previously investigated but is of relevance in predicting ore suspension behaviour of blended ores.

Standard practices in blending are based primarily on robust strategies of mixture design used in other industries. Herein, prediction of performance of a mixture is based on additive effects of each constituent with the mixture. This means that the prediction on metallurgical performance is often equivalent to the weighted average sum of each component in the blend. For example, the recovery of an ore in a blend is considered equal to the recovery of the pure ore multiplied by its mass fraction. However, when performance of the blends is controlled by one of the constituents, non-additive synergistic or antagonistic effects occur. When synergistic/ antagonistic effects are observed, the suspension behaviour is then most likely due to additional colloidal interactions which cannot be statistically or mathematically predicted by simply adding the effects of each component. In rheological systems, these non-additive effects are best explained by considering the modes of particle association in the binary mineral mixtures.

Despite the theoretical and practical importance of understanding the modes of particle association in mineral mixtures, few systematic studies have been conducted in this area, particularly in the rheological context. This has been due to the theoretical difficulties associated with the hydrodynamics of non-spherical minerals. Consequently, the few studies which have been conducted have focused mainly on spherical particles with uniform sizes in a laminar velocity gradient. For example, rheological studies of two binary mineral mixtures (nickel oxide-quartz and nickel oxide-haematite) conducted by Otsuki et al.(2011) demonstrated that

electrokinetic zeta potential measurements of the binary mixtures can be used to explain the rheological and heterocoagulation behaviour that occurs in suspension. In addition, the nature of the particle-particle interactions within each binary mixture could be explained by the DLVO theory.

However, within a phyllosilicate mineral-quartz binary mixture, the type of coagulation is complicated by the size and charge dissimilarities between the phyllosilicate mineral and quartz particles. The theoretical difficulties associated with using the electrophoretic zeta potential measurement for the analysis of phyllosilicate minerals have already been discussed. Therefore, phyllosilicate mineral-quartz binary mixtures are not as easily amenable to such analyses. The charges of all minerals in suspension must be considered when predicting the modes of particle interaction in suspensions of these binary mixtures.

Within such binary mineral mixtures comprising phyllosilicate and non-phyllosilicate components (e.g. quartz), the formation of particle interactions is likely to occur through additional face-quartz (FQ), edge-quartz (EQ) and quartz-quartz (QQ) associations (James and Williams, 1982). The particle interactions that will occur will depend on the charges of the edges and faces of the phyllosilicate mineral as well as the surface charge of the non-phyllosilicate mineral. The prevalence of the face and edge charge will also depend on the aspect ratio, surface area and crystallinity considerations as discussed.

The analysis of mixtures containing phyllosilicates is further complicated by dissolution of ions from the mineral surface. Studies by He et al., (2009) used a combination of zeta potential, dissolution and rheological measurements to demonstrate the significance of leaching of mineral ions towards particle aggregation. The presence of Cu^{2+} species due to oxidation and dissolution of chalcocite at low pH conditions, and its subsequent re-precipitation at higher pH's was seen to result in unexpected hetero-aggregation, manifest in a marked increase in shear yield stress of the mixture suspensions (antagonistic effects) for measurements conducted from a low to high pH relative to a high to low pH. Such aggregation is a result of enhanced particle interactions facilitated by the cementation of aggregates by the leached species, and is not incorporated into robust mixture design analysis.

Therefore, the prediction of rheological performance of a blended stream is very complicated for phyllosilicate-bearing suspensions. However, such knowledge is necessary for the correct application of this technique. As a starting point, the evaluation of robust blending techniques for the rheological prediction of binary mineral systems is required.

University of Cape Town

2.7. SUMMARY

The fundamentals of suspension rheology and mineral surface charge have been reviewed. In both cases, these have been discussed in terms of their application to ideal spherical minerals of uniform surface charge properties and phyllosilicate minerals with characteristic non-spherical and anisotropic charge properties. The deviation from ideal mineral behavior, based on phyllosilicate mineralogy has been demonstrated. This renders the analysis of phyllosilicate minerals using robust techniques (e.g. zeta potential) and theories (e.g. application of DLVO theory to colloidal behavior) difficult, and it is often required to adapt these for their analysis.

The literature review has also demonstrated that different theories exist on fundamental issues such as charge derivation on the edges and faces of phyllosilicates and the modes of particle interaction as a function of pH. These are often based on differences in particle mineralogical properties such as aspect ratio, surface area, crystallinity and morphology. Indeed all these properties are important and should be considered when analyzing each mineral. There is no definitive and conclusive model in support of the existence of one dominant mode of particle interaction. The alignment of particles (and the dominance in the mode of aggregation) is most likely dependent on the physico-chemical properties of the mineral of interest, and each mineral must be considered individually. This is the approach that is taken in this study and while reference is made to existing theories, this study attempts not to get locked into one single school of thought, taking into consideration the inherent properties of each mineral.

The processing problems that are often associated with phyllosilicate bearing ores have been outlined, with reference to specific operations, demonstrating the need to better understand the colloidal behavior of this class of minerals. An extensive amount of research has been conducted on the kaolinite, smectite and talc groups, but this has mainly been within the context of other industries. Comparatively fewer studies have been conducted on the mica, vermiculite and serpentine groups. A fundamental understanding of this class of minerals within the context of minerals processing is warranted. In particular, a rheological classification of these minerals may

prove beneficial, as the distinction in phyllosilicate mineral behavior has not been definitively defined.

In this study, the influence of differences in phyllosilicate mineralogy and surface charge properties on rheological performance will be investigated. Phyllosilicate mineralogy will mainly be studied in terms of differences in particle morphology, aspect ratio, surface area and surface structure (crystallinity). This will be supplemented by existing knowledge of the studied minerals. The surface charge properties will be investigated via a combination of zeta potential and potentiometric titration measurements. It is believed that more valuable information can be obtained by using these methods in tandem rather than in isolation. Traditional theories of charge derivation on edges and faces will be used as the platform for charge analysis on the edges and faces in this study. In the absence of knowledge on the contribution of the pH dependent charge, the charge on the faces will mainly be attributed to the pH independent component as derived by isomorphous substitution. The degree of isomorphous substitution will be quantified based on the elemental composition of the minerals and will be used to substantiate theories on charge anisotropy based on differences in the measured iso-electric point (as derived from the zeta potential measurement) and the point of zero charge (as derived from the potentiometric titration measurement). The rheological response will be evaluated in terms of the suspension viscosity and yield stress values.

The study will first investigate the phyllosilicates in their pure form, for an understanding of their distinct surface charge, mineralogical and surface charge properties at pH conditions which are typically used during processing operations. Binary mineral mixtures comprising quartz and each phyllosilicate mineral will then be used as preliminary simulations of real ores. These will serve to demonstrate the changes in rheological behavior of phyllosilicate multi-component systems as is the case in ore composition. The binary mixture behavior will be evaluated using robust synergistic/antagonistic indicators based on comparison with a predictive response derived from concentration contributions from each mineral. Predictions on the likely modes of particle association will then be made. It must be noted that these predictions are merely inferred, based on the charge properties of the minerals and it is acknowledged that further research would be

required to validate the theories made. However, this serves as a preliminary evaluation of phyllosilicate behaviour in binary mixtures and its analysis by robust blending methods.

The interplay between phyllosilicate mineralogy, surface charge and rheology will be established within single mineral and binary mineral systems. In both cases, a rheological classification will be provided. This will serve as an indicator of likely changes in colloidal behavior in systems of increasing complexity, albeit on a fundamental level.

University of Cape Town

Chapter 3.

EXPERIMENTAL METHODS

3.1. INTRODUCTION

In order to achieve the objectives of the study it was necessary to design and perform experiments in which it would be possible to establish the particle mineralogy and surface charge properties of each mineral and then determine their effects on suspension rheology.

The phyllosilicate minerals (muscovite, vermiculite and chrysotile) were investigated individually, and compared to quartz, a well-studied non-phyllosilicate mineral. The materials used and their pre characterisation are described in Sections 3.2 and 3.3 respectively. Section 3.4 outlines the methods used to investigate the mineralogy, the surface charge measurements are discussed in Section 3.5 and the rheological techniques are outlined in Section 3.6. A summary of the experimental programme is then presented in Section 3.7. Finally, Section 3.8 outlines the statistical analysis tools used in the study.

3.2. MATERIALS

3.2.1. Minerals

It has been well established that exposure to chrysotile (asbestos) in its dry form enhances the likelihood of inhalation of fibres, and has been linked to serious lung diseases including asbestosis, lung cancer or mesothelioma (Lee et al., 2008). Due to the hazardous nature of chrysotile, the necessary safety precautions were taken when handling it. All the experimental work was conducted in a specially built, well ventilated laboratory, with the proper personal

protective equipment worn at all times. These specialised facilities were provided at the N.B Keevil Institute of Mining Engineering of the University of British Columbia (UBC). The experimental work on muscovite, vermiculite and montmorillonite was conducted in the Department of Chemical Engineering at the University of Cape Town (UCT).

Chrysotile from Vermont, USA was supplied in rock form by Wards Minerals. Muscovite was obtained in a pre-ground form from Magic Minerals, Northern Cape, South Africa. Vermiculite is usually supplied in an exfoliated form. However, in this condition, the structure has already been altered and was unsuitable for this study. Therefore, vermiculite was handpicked from Agnes ore samples (Mpumalanga, South Africa) under controlled laboratory conditions. Quartz used during experiments at the University of British Columbia was sourced from Alfa Aesar, Canada, and that used at the University of Cape Town was supplied by Kiln Contracts, Western Cape, South Africa. Both were obtained in a pre-ground form.

3.2.2. Solution additives

In all tests 0.01M sodium chloride (NaCl) solution was used as a background electrolyte. The electrolyte concentration at which double layer compression is likely has not been definitely defined, although it has been estimated at monovalent salt concentrations as low as 0.015M and as high as 0.2M for swelling clays (van Olphen, 1977; Brandenburg and Lagaly, 1988; Luckham and Rossi, 1999). A concentration of 0.01M NaCl in its initial state may well be very close to the threshold for weak double layer based coagulation and this could be exceeded given the total ion concentration with dissolution of ions from mineral surfaces, particularly at low pH conditions. This is taken into consideration when discussing the results at these conditions. This concentration provides a controlled environment, where aggregation could be predominantly monitored by variations in attractive and repulsive forces as determined by the DLVO theory.

The solution pH was modified as required using solutions of hydrochloric acid (HCl) and sodium hydroxide (NaOH).

3.3. MINERAL CHARACTERISATION

3.3.1. Particle Size Distribution

The effect of particle size on suspension rheology has already been well established and is not within the scope of this study. Therefore, it was important to maintain relatively similar size distributions for all minerals under investigation. Samples of muscovite and vermiculite were pre-ground (50g samples at a time) in a titanium ring mill for 20 and 30 seconds respectively. A wet Malvern size analysis was conducted on subsamples which were considered significantly representative of the batch samples of each mineral. In each case, the representative samples were conditioned in 5% sodium hexametaphosphate (Calgon) dispersant, and pre-dispersed in an ultrasonic bath at room temperature for 10 minutes to avoid agglomeration. The particle size distributions of the minerals were determined using a Malvern Mastersizer (manufactured by Malvern, United Kingdom), yielding P_{50} values as shown in Table 3.1. These are considered sufficiently similar for the purposes of this study. The cumulative size distributions are shown in Figure 3.1.

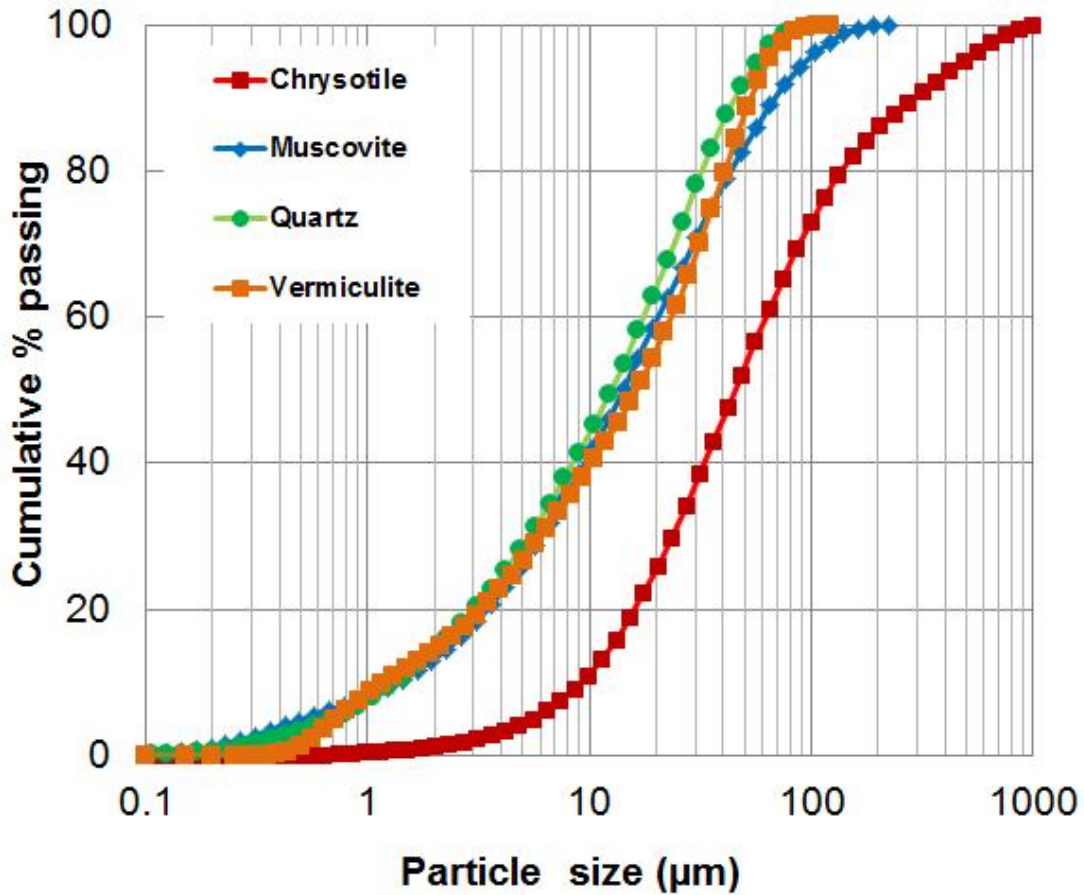


Figure 3.1 – Cumulative size distributions of chrysotile, muscovite, montmorillonite, vermiculite and quartz.

Table 3.1 – P₅₀ values of minerals as determined by Malvern Mastersizer size analysis.

Mineral	P ₅₀ (µm)
Muscovite	14
Vermiculite	16
Quartz	12

Chrysotile was wet ground in water, using a ceramic ball mill. However, its fibrous nature made size reduction difficult, with prolonged grinding resulting in long, thin fibres. Therefore, when the size of the resultant particles was estimated using a Malvern Mastersizer, a P₅₀ of 45 µm was obtained (Figure 3.1). It must be noted, however, that the Malvern Mastersizer uses light scattering analysis which estimates the size of particles by equating their volume to that of a

sphere of equivalent volume (equivalent sphere theory) (Rawle, 2011). This is misleading for irregular shaped particles, and the inaccuracy of this measurement becomes further exaggerated with a larger deviation from sphericity, as in the case of chrysotile fibres. For this reason, scanning electron microscopy was used to provide a more accurate size approximation. Figure 3.2 shows some scanning electron micrographs which were used for size estimation. A more detailed discussion on the aspect ratios of chrysotile and the other minerals is given in Chapter 4.

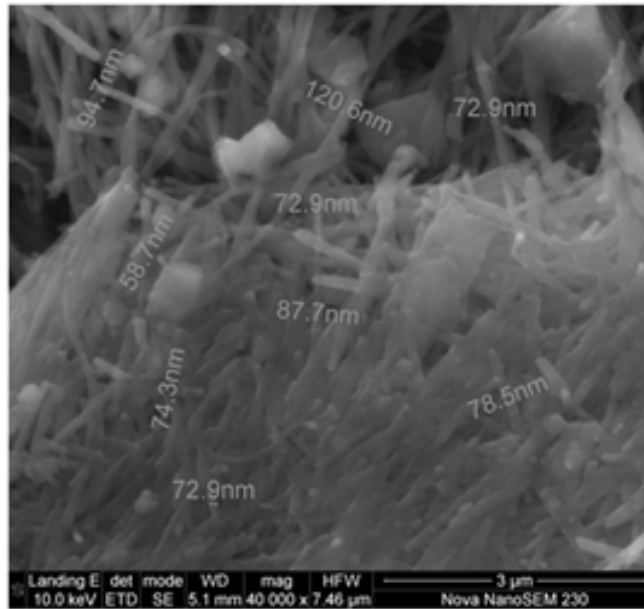


Figure 3.2 - SEM micrographs used in the size estimation of chrysotile fibres.

3.3.2. Powder X-Ray Diffraction

Powder X-ray diffraction was used for the routine determination of the purity of each mineral. The structural diversity of phyllosilicate clay minerals makes their identification difficult. This is due to the formation of extraneous organic, carbonates or iron compounds (cementing agents) which often occur and obscure peaks and result in increased peak intensity which is undesirable for XRD analysis (Brindley and Brown, 1980). Therefore, chemical pretreatment was necessary prior to X-ray diffraction. In this study, the chemical pretreatment proposed by Jackson, (1973) was used. This is a widespread and accepted three-step procedure which has been used to successfully limit and reduce the amount of non-clay materials during soil analysis (Brewster,

1980; Hasselov et al., 2001; Srodon, 2006; Deng et al., 2009). The procedure involved washing the suspensions through sodium acetate (CH_3COONa) at pH 5, soaking it in hydrogen peroxide (H_2O_2) and finally shaking through with distilled water.

In all cases, the minerals were micronized in ethanol using a McCrone microniser before XRD analysis. This method reduces particle size to micrometer size, yielding small particle and uniform phase distributions. It also results in the least damage to crystalline structure which is ideal for XRD analysis.

XRD spectra were obtained using a Bruker D8 Advance powder diffractometer with Vantec detector. Samples were run with fixed divergence slits, using Cobalt- $K\alpha$ radiation. The phases were identified using Bruker Topas 4.1 software and the relative phase amounts (weight %) were estimated using the Rietveld method. Since this method takes only crystalline phases into account, residual amorphous content was determined indirectly by spiking each sample with corundum (20% weight fraction), a well used internal standard, prior to analysis. The relative weight fractions were normalised to 100% thereafter. The relative purities of the minerals are shown in Table 3.2.

Table 3.2 – Purity of the minerals as determined by XRD analysis.

Mineral	Purity (Weight %)	Goodness of fit
Corundum (standard)	100	1.99
N.Cape muscovite	100	4.02
Agnes vermiculite	91.1	2.43
W.Cape quartz	100	2.68

It must be noted that in the case of chrysotile, size reduction of the fibres could not be achieved by micronising, and XRD analysis of this mineral was not possible.

3.4. MINERALOGY MEASUREMENTS

3.4.1. Scanning Electron Microscopy (SEM)

The structure of each mineral was examined under a Nova Nano scanning electron microscope (manufactured by FEI, Oregon, USA). This provided detailed images which showed the distinct morphology of the minerals at high resolution.

The expansion potential of vermiculite was investigated by conducting SEM analysis on untreated and pre-treated samples. Pre-treatment involved the hydration of samples in 0.01M NaCl solution for 24 hours, facilitating full swelling of the particles. The expanded minerals were then dried at room temperature (23°C) overnight. At this temperature, water molecules in the interlayer region are not driven off but the samples are sufficiently dry for SEM analysis (Deer et al., 1992).

3.4.2. Optical Microscopy

Optical microscopy was used to observe any visible interactions occurring between particles. Very dilute suspensions were prepared in 0.01M NaCl solution and placed in a petri dish using a pipette. Images were viewed under transmitted light with an Olympus BX600 microscope, fitted with an Olympus U PMTVC digital camera (both manufactured by Olympus, Tokyo, Japan).

3.5. SURFACE CHARGE MEASUREMENTS

The surface charge properties of the minerals were investigated using zeta potential and Robert Mular potentiometric titration measurements. Electron microprobe analysis was used to measure the elemental composition of the minerals from which the degree of isomorphous substitution could be estimated. The experimental conditions and variables used in these techniques are summarized in Table 3.3. The experimental methods are discussed individually thereafter.

Table 3.3 - Experimental methods, conditions and variables used in surface charge characterisation of each mineral.

Measurement	Conditions	Variables
<i>Electron Microprobe Analysis</i>	Accelerating voltage: 15kV Probe current 20nA Peak counting time : 10s Background counting time : 5s Spot size: 5-10µm Standardisation: amphibole	
<i>Zeta Potential</i>	Sample volume : 1ml Background electrolyte : 0.01mol dm ⁻³ NaCl pH modifiers : HCl and NaOH	pH 3 to pH 11
<i>Potentiometric Titration</i>	Sample mass : 2g Sample volume : 50ml Background electrolyte : 0.001 - 0.1 mol dm ⁻³ NaCl	Initial pH : pH 3 to pH 11

3.5.1. Zeta Potential Measurements

The zeta potential measurements were performed using a Malvern Zetasizer (manufactured by Malvern, United Kingdom). For each mineral, a suspension of 0.25 g in 500 ml of 0.01M NaCl solution was prepared, from which 9 aliquots of 25 ml each were collected. The particles in these samples were assumed to be representative of the well-mixed bulk solids. Each aliquot was adjusted to a pre-determined pH (between pH 3 and pH 11), ensuring homogeneity in each sample throughout the preparation. 1 ml samples of each aliquot were then pipetted into cuvettes and placed in the Zetasizer for analysis. The pH at which the zeta potential is zero is the iso-electric point of the mineral.

3.5.2. Potentiometric Titration Measurements

The point of zero charge of each mineral was determined using the Roberts Mular titration method. This method works on a principle of ion exchange, with the pH measured at different ionic strengths of the solution (Mular and Roberts, 1966). Suspensions consisting of 1.00 g samples of each mineral in 50 ml of 0.001M NaCl were prepared, with each suspension adjusted

to a different pH value (ranging from pH 3 to pH 11). The ionic strength of each solution was then raised from 0.001M to 0.1M by the addition of the appropriate amount of dry NaCl crystals. The pH of the resulting solution was then measured to give a final pH. The difference in the initial and final pH values (ΔpH) is plotted against the final pH. The pH value at which ΔpH is zero indicates the point of zero charge of each mineral.

3.5.3. Electron microprobe analysis

The elemental composition of each mineral was determined using electron microprobe analysis. This technique has been widely used in mineralogy applications to calculate the exact formula of minerals (Deer et al., 1992). It has also been used to determine the degree of isomorphous substitution occurring in phyllosilicate minerals (Burdukova, 2007). The method works by focussing a beam of electrons onto a mineral surface, resulting in the emission of x-rays with a wave length specific to every individual compound. It must be noted that electron microprobe analysis is unable to accurately quantify the intensity of light elements such as hydrogen (H^+), lithium (Li^+) and helium (He^+), and these are not accounted for.

Using polished ore mounts or polished thin sections of each mineral, analysis was conducted with a Jeol-JXA-8100 Superprobe (manufactured by Jeol Ltd, Japan). The samples were analysed using an accelerating voltage of 15kV and probe current of 20nA, with counting times of 10s and 5s for peak and background times respectively. The spot size of the electron beam was approximately 5-10 μm . This beam size was suitable for the analysis of quartz, muscovite, vermiculite and montmorillonite. However, the long, thin fibrous morphology of chrysotile rendered electron microprobe analysis inappropriate since the width of the fibres (less than 0.1 μm) was much smaller than the beam size. Consequently, an electron microprobe analysis of chrysotile could not be conducted.

In-house amphibole and garnet specimens from the Department of Geological Sciences at the University of Cape Town were used for the standardisation of the phyllosilicate minerals and quartz respectively. For each mineral, analyses were conducted on 8 sample populations, from

which an average composition was calculated. The average composition of each mineral, as determined by microprobe analysis is shown in Table 3.4.

Table 3.4 – Detailed microprobe analysis of quartz, muscovite and vermiculite samples.

Compound	Quartz		Muscovite		Vermiculite	
	Average	Std. deviation	Average	Std. deviation	Average	Std. deviation
SiO ₂	99.7	0.3	46.3	0.2	38.7	0.9
K ₂ O	0.0	0.0	10.3	0.1	3.3	1.6
Na ₂ O	0.0	0.0	0.6	0.1	0.7	0.3
CaO	0.0	0.0	0.0	0.0	1.1	0.3
Al ₂ O ₃	0.1	0.1	35.6	0.1	14.9	0.4
FeO	0.0	0.0	3.0	0.2	7.5	0.5
MgO	0.0	0.0	0.8	0.0	21.5	1.0
Total	99.9		96.6		87.7	

Since H⁺ ions cannot be detected, it was not possible to estimate the amount of water contained in each mineral using microprobe analysis. This amount was determined experimentally using dehydration. Two samples (5.00–6.00g) of each mineral were pre-dried at 110°C for four hours, before roasting in a furnace at 950°C over a period of 48hours. At these temperatures, all constitutional crystalline and interlayer water is driven off (Deer et al., 1992). The amount of water was calculated as the difference in mass before and after roasting.

The exact chemical formula of each mineral was determined by balancing the detected cations present in the sample with the oxygen content of the associated oxide. This calculation procedure is simple but consists of a number of steps which are outlined in Appendix A. This procedure is also described in detail by Deer et al., (1992).

3.6. RHEOLOGY MEASUREMENTS

This study was not aimed at transient time dependent behaviour of the phyllosilicates. As a result, the rheological analysis was performed using steady shear systems, with the transient effects minimized. The rheological parameters used to characterize the mineral suspensions were the yield stress τ_y and viscosity η . In investigating the effect of pH on the rheology of phyllosilicate suspensions, the yield stress was measured using the vane technique as developed by Nguyen and Boger, (1983). Yield stress and steady shear viscosity data for the rheology of

pure mineral suspensions and suspensions of binary mineral mixtures as a function of solids concentration was obtained using stress/ strain measurements. The experimental conditions and variables used are summarized in Table 3.5. A detailed discussion of each experimental method is then given.

Table 3.5 - Experimental methods, conditions and variables used in the rheological characterisation of mineral suspensions.

Measurement	Conditions	Variables
<i>Direct Yield Stress Measurement</i>	Background electrolyte : 0.01mol dm ⁻³ NaCl pH modifiers : HCl and NaOH <i>Solids concentration (by volume)</i> Muscovite : 70% Vermiculite : 50% Chrysotile : 2%	pH 3 to pH 11
<i>Stress/strain Measurement</i>	Background electrolyte : 0.01mol dm ⁻³ NaCl Shear rate range : 10s ⁻¹ to 400s ⁻¹ <i>Pure mineral suspensions</i> pH: natural pH (9-10)	<i>Solids concentration (by volume)</i> Quartz : 10 - 40% Muscovite : 10 - 35% Vermiculite : 10 - 30% Chrysotile : 0 - 0.8%
	<i>Binary Mineral mixtures</i> <i>(i) Preliminary tests</i> pH: natural pH (9-10) Concentration: 30% total solids by volume <i>(ii) Secondary tests</i> Concentration: 30% total solids by volume <i>Critical phyllosilicate-quartz concentration</i> Muscovite - quartz : 24% muscovite/6% quartz Vermiculite-quartz : 21% vermiculite/9% quartz	<i>Phyllosilicate concentration (by volume)</i> Muscovite-quartz : 0% - 30% Vermiculite-quartz : 0 - 30% Chrysotile : 0% - 2% pH 3 to pH 11

As previously mentioned, the experimental work in this study was split between the University of British Columbia and the University of Cape Town. The rheological analyses of muscovite and vermiculite suspensions were conducted at the University of Cape Town. Tests on muscovite suspensions were performed using a Paar Physica MC1 rheometer (manufactured by Anton Paar, Germany). The measuring geometry used was a double gap cylinder, with a gap size of 0.5 mm, as shown in Figure 3.3. During the course of the study, a second rheometer (AR1500EX

(manufactured by Thermal Analysis, Germany), with a standard vaned rotor geometry was purchased and used for the remainder of the experimental work. This geometry is comprised of four thin rectangular blades welded to a thin, rigid, central, cylindrical shaft at right angles to each other and is represented schematically in Figure 3.4. Rheology tests on chrysotile suspensions at the University of British Columbia were performed using a Haake Viscotester 550 (manufactured by Thermo Fischer Scientific, Germany), also with a vaned rotor geometry.

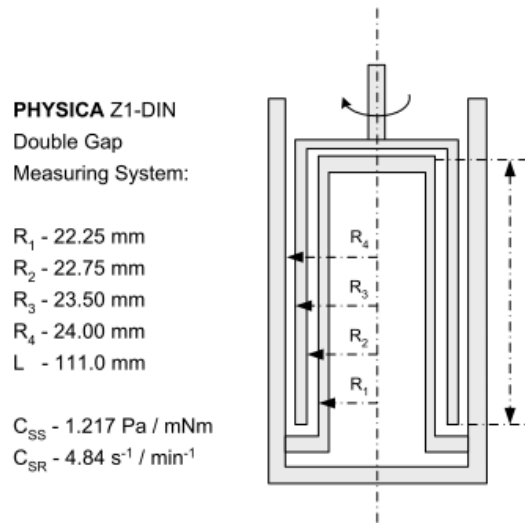


Figure 3.3 - Schematic representation of the double gap measuring system used (Paar Physica MCI).

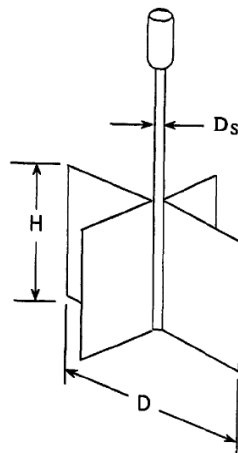


Figure 3.4 – Schematic representation of the vane measuring system used (AR1500EX and Viscotester 550).

Although different rheometers were used at the University of Cape Town, the comparability and reliability of the results was determined by performing tests on pure quartz suspensions. A comparison of the Bingham viscosities (over the shear rate range 0 to 400 1/s) that were obtained using the different rheometers is shown in Table 3.6. These were considered adequately similar and demonstrated the consistency in the results between the rheometers. The rheometers used throughout the study are shown in Figure 3.5.

Table 3.6 – A comparison of the Bingham viscosities of quartz suspensions obtained using the AR1500ex rheometer and the MC1 rheometer.

% solids (by volume)	AR1500ex	MC1	
10	0.001	0.001	Bingham viscosity (Pas)
20	0.005	0.006	
30	0.011	0.013	



Figure 3.5 – (a) Haake Viscotester 550 rheometer (b) Paar Physica MC1 Rheometer and (c) AR 1500ex rheometer.

3.6.1. Direct yield stress measurements

The effect of pH on the yield stress of pure phyllosilicate mineral suspensions was investigated using the direct yield stress measurement developed by Nguyen and Boger, (1983). This method

requires the torque measurement of structured dispersions of high yield stress. The slurry concentration used is dependent on the intrinsic properties and varied from mineral to mineral, as shown in Table 3.5. It was not necessary to use equivalent concentrations as these tests merely served to demonstrate the change in suspension behaviour as a function of pH for each mineral.

The tests were conducted in batch systems with samples prepared by dispersing the minerals in 0.01M NaCl suspension at initial pH conditions within the range pH 3 to pH 11. Individual samples were made up at each pH. This prevented aggregation due to the subsequent re-precipitation of leached ions at higher pH conditions had the tests been conducted on a single sample from low to high pH (He et al., 2009). The samples were allowed to rest for 36 hours, while monitoring the suspension pH. Preliminary tests indicated that it was reasonable to assume full structural recovery after 12 hours, following any initial breakdown during preparation. The vane was then inserted into the sample and rotated at a constant low shear rate of 0.1rpm for 150 seconds with the torque trace measured. This low rotational speed is necessary to avoid the influence of viscous resistance and instrument inertia (Nguyen and Boger, 1985; Barnes and Nguyen, 2001). Moreover, reasonable reproducibility could be obtained by inserting the vane slowly into the sample to measure the recovered yield stress, indicating that any artefacts arising from inserting the vane could be considered negligible or constant.

Figure 3.6 shows a typical complete stress decay curve obtained in these tests. In each case, the torque increased sharply until it showed a peak value when the flow behaviour of the suspension changed, after which the torque decreased slowly to an asymptotic value. At each pH condition, the maximum torque is regarded as the point of yielding and is used in the determination of the yield stress, taking into consideration the dimensions of the vane used as shown in Equations 3.1 and 3.2. For each mineral, 3 sweeps of tests (over the range pH 3 to pH 11) were conducted. Each measurement point presented in the results represents an average of three individually prepared and measured samples at that pH value.

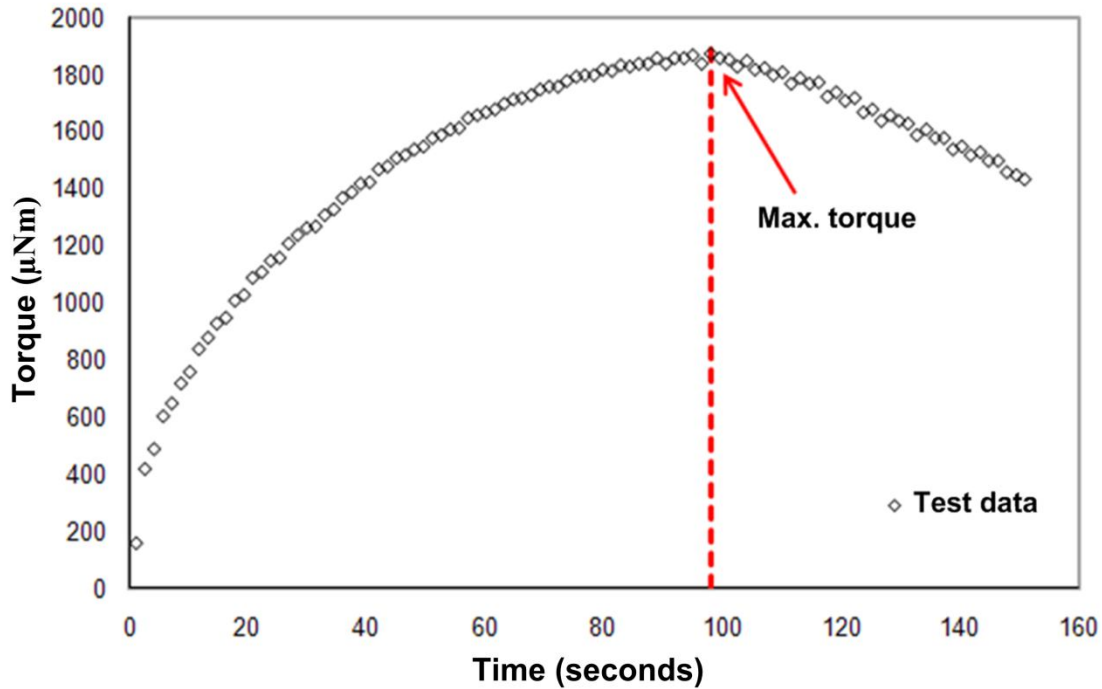


Figure 3.6 - Typical stress decay curve observed using the vane method.

$$\tau = KT_{max} \quad \text{Equation 3.1}$$

$$K = \left[\frac{\pi D^3}{2} \left(\frac{H}{D} + \frac{1}{3} \right) \right]^{-1} \quad \text{Equation 3.2}$$

τ - Shear stress (Pa)

H = height of the vane (m)

T_{max} - Maximum torque (Nm)

D = diameter of the vane (m)

3.6.2. Steady stress/strain rheology measurements

The yield stress and viscosity values of pure phyllosilicate and phyllosilicate-quartz slurries were measured as a function of solids concentration. Attempts were made to use the vane technique to directly measure shear yield stress values for all the minerals. However, this was not possible as most of the values at low concentration were well below the measuring limit for this method (i.e. 15 to 20Pa) (Nguyen and Boger, 1983; Barnes and Nguyen, 2001). Therefore the steady

stress/strain technique was used for all flow curve analysis and low shear yield stress measurements.

Tests using the Paar Physica MC1 rheometer with double gap geometry demonstrated non-Newtonian behaviour. However, the estimation of the shear rates by the Anton Paar software is based on Newtonian fluid behaviour and needs to be corrected for non-Newtonian behaviour. Shear rate correction may be performed using a number of approximations including the simple shear Couette (Barnes et al., 1989; Estelle, 2008), power law (Krieger, 1968), Bingham fluid approximation (Nguyen and Boger, 1987; Estelle et al., 2008) and Tikhonov regularisation (Leong and Yeow, 2003), depending on the Couette geometry and configuration. In this case, the gap could be classified as narrow, since $1/\alpha > 0.97$ (where α is the ratio of the cup radius (R_c) to the bob radius (R_b)) (Barnes et al., 1989; Estelle et al., 2008; Steffe, 1996). For such cases, it can be assumed that the system approaches simple shear Couette flow, with a uniform shear rate across the gap. The shear rate values can be accurately calculated using Equation 3.3 (Steffe, 1996).

$$\gamma = \frac{\Omega R b}{R_c - R_b} = \frac{\Omega}{\alpha - 1} \quad \text{Equation 3.3}$$

A comparison of the shear rate values calculated by the Newtonian approximation in the Anton Paar software and the corrected values using the simple shear Couette flow (Equation 3.3) was conducted. This is shown in Figure 3.7. The corrected shear rates yielded values that were within 1% of the calculated values (Figure 3.7b). These were considered adequately similar for the purposes of this study and the rheometer calculated values were used for further analysis.

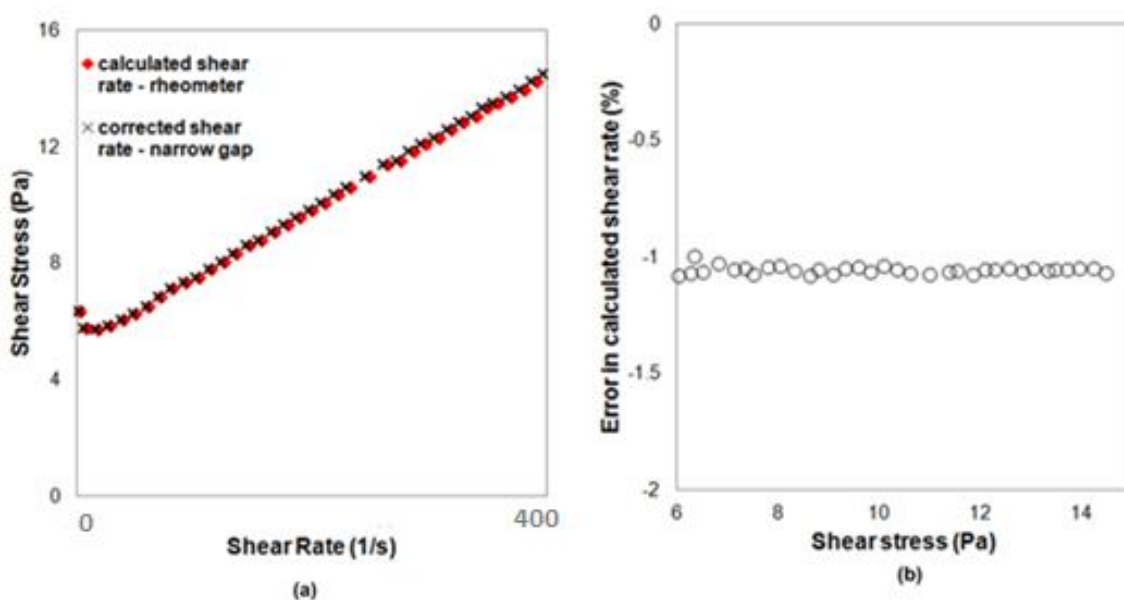


Figure 3.7 – (a) A comparison of calculated and corrected shear rate values, (b) Errors in calculated shear rate values for the narrow gap size used in the double gap geometry .

Suspensions were prepared at varying solids concentrations (and ratios for mixtures) in 0.01M NaCl solution. Each slurry sample ($\sim 50 \text{ cm}^3$) was pre-sheared at a high shear rate of 400 s^{-1} . Preliminary tests showed hysteresis loops when readings were taken at increasing and decreasing rates of shear. This was overcome by performing continuous ascendant and descendant shear viscosity runs until both could be represented by a common curve. At this point, the system was assumed to be shear equilibrated. The stress/ strain tests were then conducted in a shear rate controlling regime, within the range 0.1 s^{-1} to 400 s^{-1} over 90 seconds.

The resulting rheograms demonstrated pseudo plastic viscoelastic shear thinning behaviour, with a gradual decrease in suspension viscosity with shear rate. Ideally, the shear thinning index, as derived by the Herschel Buckley model (Equation 2.1b), would best quantify the rheological behaviour at these conditions. However, a comparison on this basis was limited by the analysis across the three phyllosilicates, each with different flow characteristics. The high degree of variability of data in this region in some suspensions made reproducibility difficult and estimation using this method erroneous. Therefore, with the aim of obtaining a comparative analysis of the studied phyllosilicates, this method could not be used. Instead the Bingham model

was used (Equation 2.1e). Using data in the region $> 40\text{-}50\text{s}^{-1}$, the yield stress and viscosity values could be estimated by extrapolation to zero shear rate. However, this model assumes fully viscous flow upon yielding and does not account for the curvature of the flow curve at low shear rate data. This data is indicative of the degree of structural breakdown with shear. Nonetheless, the Bingham approach is still well suited to higher shear rate conditions ($> 20\text{s}^{-1}$) at which many mineral unit processes operate and for which the study is aimed. Moreover, estimated yield stresses and viscosities are used on a comparative basis within the context of the study, and not as absolute values. Rheological analysis on the basis of the Bingham model most accurately provided a comparative analysis of muscovite, vermiculite and chrysotile.

Figure 3.8 gives an example of a typical rheogram obtained, with the Bingham model used in the calculation of the Bingham yield stress and viscosity of the slurry.

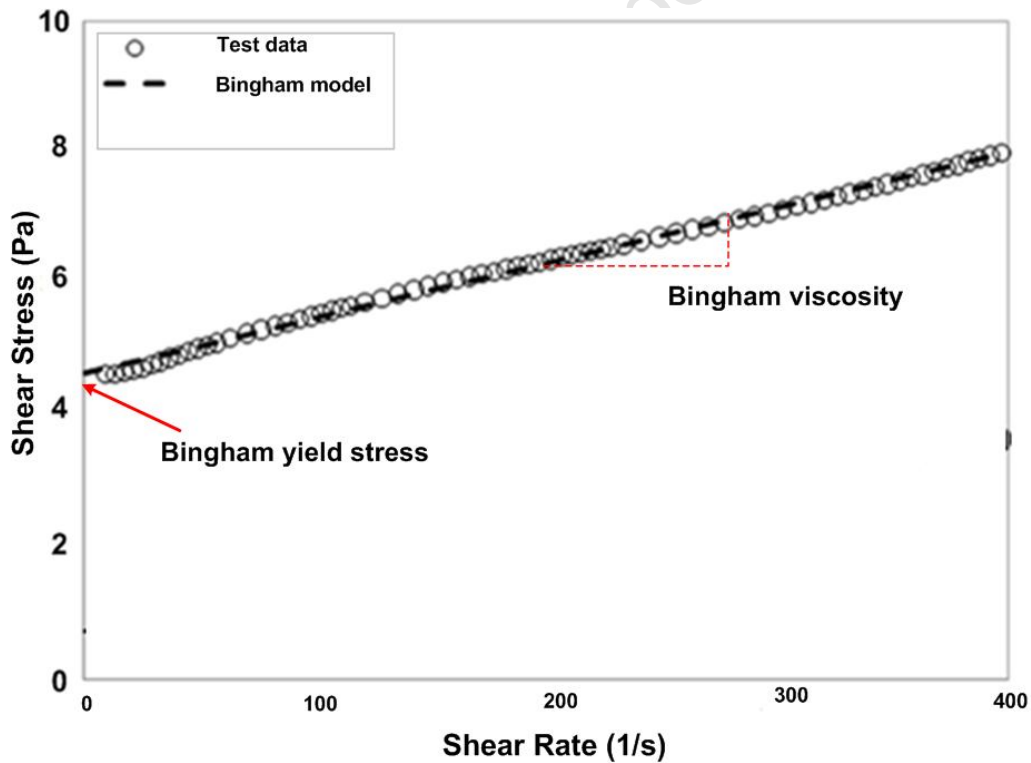


Figure 3.8 - Typical rheograms observed, fitted with the Bingham model.

3.6.2.1. Pure Mineral Suspensions

The rheology of pure mineral suspensions was investigated as a function of solids concentration at the natural pH (circa pH 9). In each case, suspensions were made up at varying concentrations within the limitations of the measuring equipment. The range of concentrations over which measurements were taken for each mineral is shown in Table 3.5.

3.6.2.2. Suspensions of binary mineral mixtures

The rheology of suspensions of binary mixtures comprising quartz and each phyllosilicate mineral was initially investigated at the natural pH. These tests were used to investigate the changes in phyllosilicate flow behaviour upon the addition of another mineral at conditions of known surface charge. The tests were conducted on slurries with 30% total solids concentration (on a volume basis), varying the phyllosilicate mineral to quartz ratio until the suspensions were too viscous for further measurement. The range of phyllosilicate-quartz concentrations over which measurements were taken for each binary mixture is dependent on the intrinsic properties of the mineral mixture and is shown in Table 3.5.

Having estimated the rheological behaviour of binary mineral mixtures, it was now possible to measure the changes in flow behaviour as the surface charge properties of the minerals in the mixture were altered. This was done by conducting stress/strain tests over the range pH 3 to 11, using HCl and NaOH to change the solution pH accordingly. Similarly, experiments were conducted using slurries of 30% total solids content. However, these were performed at a fixed phyllosilicate mineral-quartz concentration, termed the 'critical' concentration. This concentration was determined from preliminary measurements on the binary mineral mixtures (at the natural pH) and is defined as the point at which the rheological properties of the slurry increase exponentially. This point was chosen on the basis that it represents the most responsive concentration for the investigation of slight changes in surface charge which can result in sudden improvements (or vice versa) in rheological behaviour. The determination of the critical

concentration is shown in Figure 3.9. These concentrations varied for each phyllosilicate mineral-quartz mixture and are shown in Table 3.5.

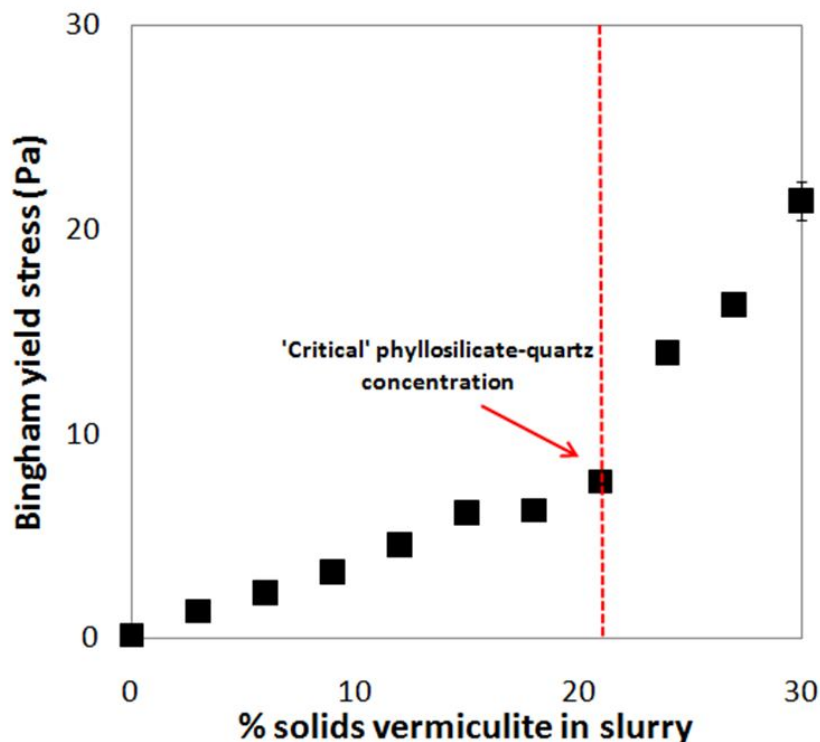


Figure 3.9 – Graphical representation of ‘critical’ phyllosilicate mineral-quartz concentration.

3.7. EXPERIMENTAL PROGRAMME

The experimental programme was divided into 3 phases. The first phase investigated the morphology and surface charge properties of each mineral. With a good understanding of the distribution of charge on the different mineral basal planes, the rheology of pure mineral suspensions could be studied in the second phase. Having estimated the surface charge, morphological and rheological properties of the pure minerals, it was now possible to estimate the rheological behaviour of the phyllosilicates within a synthetic ‘ore’. This was done in the third phase using well controlled simplified binary mineral systems comprising quartz and each phyllosilicate mineral. The experimental programme and outcomes of the measurements performed in this study are summarized in Figure 3.10.

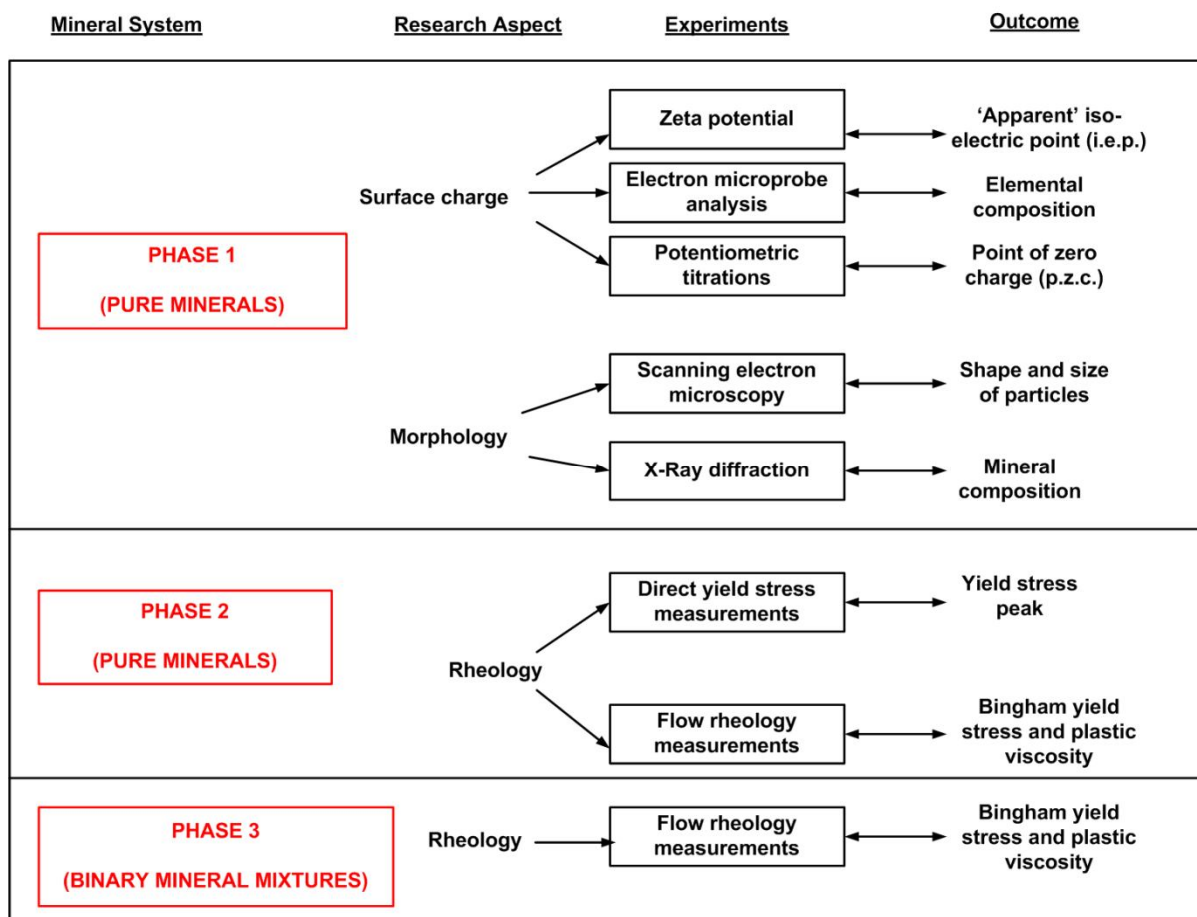


Figure 3.10 – Experimental programme for the study.

3.8. STATISTICAL ANALYSIS

Surface charge and rheology experiments were conducted in triplicate using fresh samples for each measurement for reproducibility and error analysis. Each measurement point presented in the results represents an average of individually prepared and measured samples. Standard deviation, 95% confidence interval and regression analysis were used as routine statistical analytical tools. The details of these methods are outlined in Appendix A.

Chapter 4.

PHYLLOSILICATE MORPHOLOGY

Summary

The surface morphological properties of muscovite, vermiculite and chrysotile have been investigated. These were compared to quartz, a non-phyllsilicate mineral. Quartz particles demonstrated an angular morphology which facilitates close packing into low volume clusters. Muscovite particles, on the other hand, displayed a long, thin platy morphology, with high aspect ratios in the range 40-120 estimated. The muscovite particles also had smooth basal surfaces, which likely enhance alignment of plates along the faces. Conversely, vermiculite surfaces showed prominent crystallographic steps on the basal cleavage planes, resulting in 'micro-island' formation. Some smoother platelets were observed in the vermiculite sample but these showed occasional step lines and were characterized by thicker edges and lower aspect ratios than in muscovite. The swelling potential of vermiculite was also observed, demonstrating expansion by either intercrystalline or interlayer swelling. Chrysotile particles characteristically demonstrated a long, thin fibrous morphology. The flexibility of these fibres results in a high degree of entanglement into knotted meshes. In all cases, the irregular morphology enables packing into high voluminous structures when compared to quartz. The morphological properties observed in each case are in agreement with what has been observed in previous morphological studies of the minerals under investigation.

4.1. INTRODUCTION

Due to their ubiquitous nature, phyllosilicates exert significant influence on the processing of many ores. The particle size, shape and surface charge characteristics play a pivotal role in defining the overall particle interactions in suspensions containing phyllosilicate minerals. Phyllosilicate particles deviate from ideal spherical and isotropic surface charge properties, and this contributes towards the overall colloidal stability and rheology of the mineral suspensions.

Of particular interest in this chapter is the morphology of muscovite, vermiculite and chrysotile particles. The movement of a particle in a liquid medium is largely dependent on shape, since it will experience different levels of drag dependent on its lateral dimensions. This affects the particle orientation, packing and flow behaviour of mineral suspensions. For this reason, suspension rheology is more pronounced with a larger deviation from sphericity, with higher yield stresses and viscosities observed in suspensions containing platy and rod shaped particles relative to spherical particles (Barnes et al., 1989).

Analysis of the particle morphology in this chapter is performed using scanning electron micrograph (SEM) imaging. One cannot make inferences on the particle networks and agglomeration behavior of the minerals from the images, given the highly randomized structure that arises from the capillary forces as samples dry during preparation for SEM analysis. However, the differences in particle packing behaviour and resultant apparent volumes can be deduced, given the differences in particle shape.

The particle morphology also provides information on the aspect ratio, which in the case of phyllosilicates, is important in understanding the significance of the edge charge relative to the basal plane. The aspect ratio in this case is defined as the ratio of the *length* of the basal plane to the *thickness* of the edge, and is best estimated from the SEM images. The estimates made here are compared to existing literature. This is then vital for the prediction of the likely modes of particle interaction which drive the colloidal behaviour of the minerals in suspension. Particles with a high aspect ratio comprise faces with a large lateral extent and surface area relative to the

edges. In such cases, it can be assumed that the charge on the edge is insignificant and the most important aspect of colloidal behaviour in this instance is dependent on the face characteristics (Scales et al., 1990; Tateyama et al., 1997; de Kretser et al., 1998). Conversely, in particles with a low aspect ratio the charge on the edges contributes towards the overall charge and subsequent particle interactions and suspension rheology (Gupta et al., 2011). Particle crystallinity will also contribute towards the type of particle alignment and subsequent suspension rheology. Highly crystalline particles have smooth surfaces which enhance alignment along their basal planes. Particles of low crystallinity, on the other hand, comprise complex 'rough' surface structures and particle alignment is compromised by the randomised formation of surface microstructures (Zbik and Smart, 1998, Du et al., 2010; Zbik et al., 2010).

Indeed the mineralogical and shape characteristics of muscovite, vermiculite and chrysotile have been widely investigated, particularly within the context of geological and nanocomposite science applications. Therefore, the purpose of this chapter is to characterize the specific materials at hand, as a result of the procedures employed in this work. These can then be compared to existing literature on each mineral. Many conventional analytical methods (such as electrokinetic zeta potential and Malvern size analysis) are theoretically based on the premise of spherically shaped particles. The typical non-spherical morphology of phyllosilicate minerals renders the application and results of these robust methods potentially misleading, especially when viewed in isolation. Therefore, knowledge of the particle morphology is essential, prior to surface charge analysis and for a comprehensive rheological investigation. The results of this chapter can then be used in the interpretation of results based on these robust analytical techniques in the following chapters.

4.2. QUARTZ MORPHOLOGY

Figure 4.1 shows SEM images of quartz used in this study. The micrographs show that quartz consists of a combination of angular particles. Sharpened wedge-like particles (A) are observed, with some hexagonal (Hx) and cubic (Cu) particles also present. The morphological analysis of quartz particles has been used widely as a tool in understanding the complex history and paragenesis of ore deposits within the geological and soil science industries. Fine quartz particles have been found to exhibit same source-indicative features, with variations in morphology resulting from differences in the grouping of tetrahedra during paragenesis. This leads to the transformation of silica polymorphs from one form to the other, resulting in different crystalline forms (Deer et al., 1992).

The quartz morphologies observed here are indicative of grains formed through glacial drift. Such particles are characteristically pointed (angular) and wedge-like, and their surfaces are characterized by mechanically produced features such as breakage blocks and conchoidal fractures into a random combination of polygonal particles as observed in Figures 4.1a, b and c. Conversely, quartz grains which have been derived from weathering environments typically display sub spherical and well-rounded morphologies (Leschak and Ferrell, 1988). While the morphology may be, in part, related to the paragenesis, it must be noted that the observed morphology is also likely a result of the breakage mechanism, where in some cases the morphology may also be a result of randomized breakage during size reduction. Therefore, the variations in particle size and shape observed is indicative of some randomized breakage in the quartz used.

Even so, the majority of individual particles (angular, hexagonal or cubic) comprise thick dimensions, with the lateral extent comparable to its thickness, and low aspect ratios can be assumed.

It can be assumed that when in suspension and at low levels of surface charge, the most efficient arrangement of such particles occurs by the close packing of congruent particles (Laskowski and

Pugh, 1992). Smaller particles are likely to fill the spaces between large particles, resulting in dense clusters of randomly oriented particles.

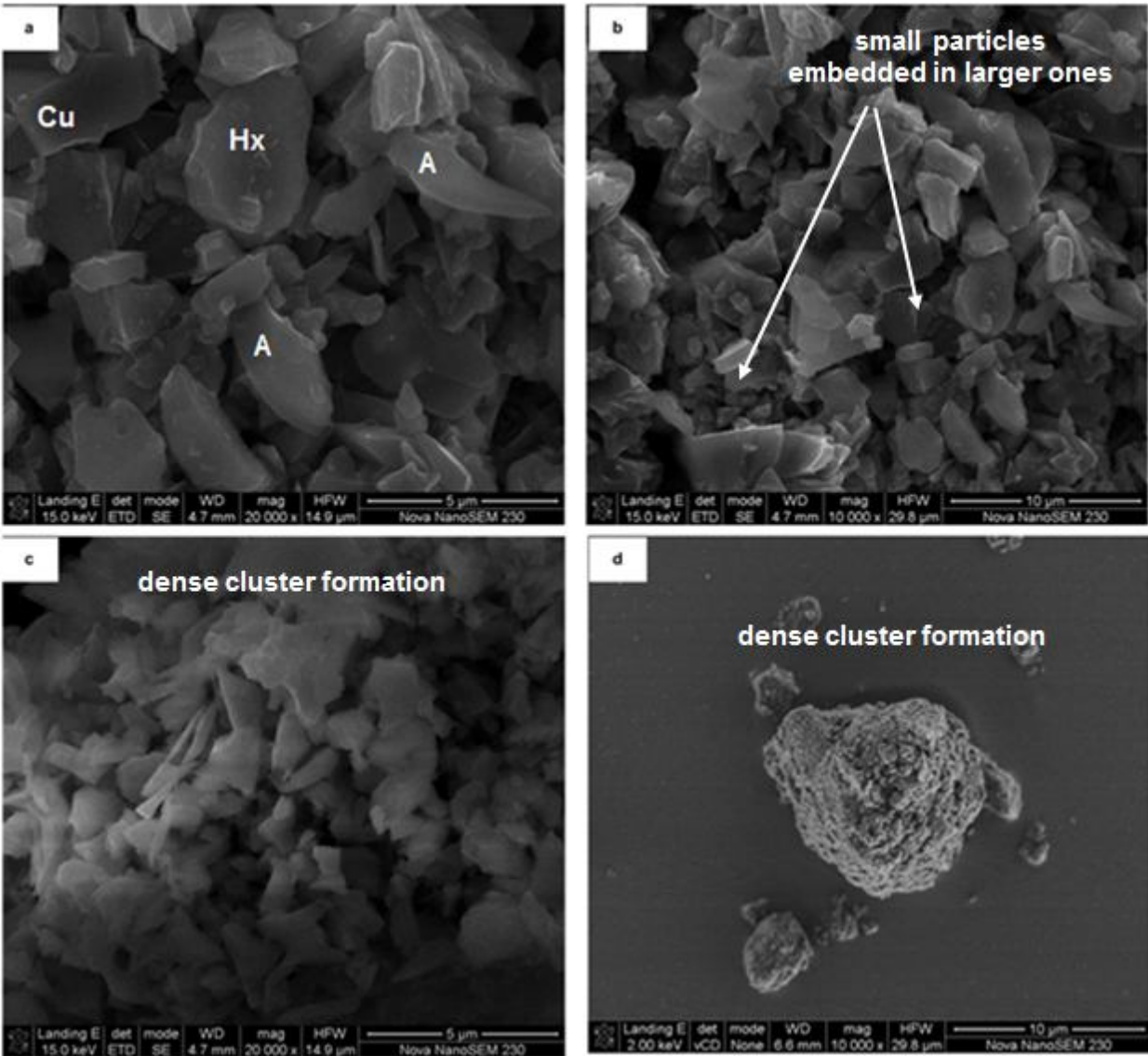


Figure 4.1 - SEM micrographs demonstrating the angular morphology and dense packing of quartz particles.

4.3. MUSCOVITE MORPHOLOGY

Several reports on the surface morphology of micas and micaceous vermiculites have been published (e.g. Jackson et al., 1973; Jackson and Sridhar, 1974; Barabaszova and Valaskova, 2013). However, in most of these studies, the micas used have often undergone chemical pre-treatment in accordance with their application as nanocomposite materials (e.g. as organofillers, biopolymers, ceramics etc.). These treatments, however mild, have been shown to cause alteration of micas and make comparison with the muscovite used in this study of little value (Protz and St. Arnaud, 1964; McKeague and Day, 1966; Arshad et al., 1972). Studies which have used natural micas, on the other hand, have often separated these from residual soils, and have analysed them in their untreated state as a means to characterize the stages of alteration within naturally weathered micas (Tarzi and Protz, 1978; Roth et al., 1968; Newman and Brown, 1969). Although the micas used in this SEM analysis have not been subjected to any form of chemical treatment, they have undergone mechanical pre-grinding, a requirement of the other analytical techniques used in the later stages of the investigation. This then makes factors such as particle size and irregularities due to grinding important.

The scanning electron micrographs shown in Figure 4.2 give an indication of the morphological characteristics of the muscovite used. In general, the muscovite samples consisted of long, thin platelets. The majority of particles existed as layers of platelets, with perfectly intact edges (Figure 4.2a and b). Since the analysis was conducted on dry samples, the stacking of platelets cannot be attributed to the preferred orientation of particles arising from surface charge characteristics as would be expected in aqueous media. It may be, in part due to the friction process that occurs between the grinding media and muscovite particles during size reduction. This causes spreading of the surface flakes in directions parallel to the shearing movement and likely results in thinning and superimposition of the plates.

Figure 4.2b and c give clearer images of individual plates within stacks of platelets. In general, each sheet comprises faces of high lateral extent, with thin edges. Slanted, step like and irregular edges on muscovite particles were common, a likely artifact of the mechanistic size reduction

procedures. This also results in heterogeneity in the size of plates within the sample (Figure 4.2d). Even so, the long platy morphology is maintained upon grinding. This is characteristic of micaceous minerals whose breakage mechanism has been shown to occur through cleavage along the basal plane into smooth, finer plates (Deer et al., 1992).

Based on Figure 4.2b and c, aspect ratios in the range 40 to 120 can be estimated. This estimate is based on particles of lateral extent within the range $3\mu\text{m}$ to $25\mu\text{m}$, which accounts for approximately 60% of the sample (based on the particles size distribution Figure 3.1). Indeed smaller and larger platelets may fall outside this range, although it can be assumed this estimation is representative of the bulk sample. This estimation is also in agreement with previous estimates on muscovite aspect ratio, which have approximated that the basal face area can be up to 50 or 80 times that of the edge area (Nasroti, 2010; Deer et al., 1992). With such high aspect ratios, it is often assumed that the edge surface is relatively insignificant compared to the face basal plane. In such cases, the edge contribution towards particle surface charge and subsequent modes of particle interaction can be considered negligible and the most important aspect of colloidal behaviour is then dependent primarily on the face basal plane (Maslova et al., 2004; Nishimura et al., 1992; He e al., 2009; Callaghan and Ottewill, 1974).

Irregular shaped patchy deposits (detritus) are observed on the basal surfaces of numerous particles. In some particles, the coating material was deposited irregularly over the entire basal plane, giving a spongy or roughened appearance. In others, it took the appearance of a hard crust (Figure 4.2b and c). However, careful examination shows that the coating material is merely deposited and is not embedded within the basal surfaces of the platelets. Studies by Roth et al (1966, 1968) examined similar coatings on micaceous minerals and found them to be a combination of Fe_2O_3 , Al_2O_3 and SiO_2 . The same can be assumed in this case, and can be confirmed through elemental analysis in the following chapter. The muscovite platelets have smooth, highly crystallised surfaces. This is characteristic of muscovite (and most micas). It is just this property, together with its sheet-like structure that renders muscovite amenable to techniques such as streaming potential and direct force measurements (Scales et al., 1990).

Although the muscovite particles shown in the scanning electron micrographs mostly exhibit a platy morphology, these plates tend to be more brittle than other clay minerals such as talc (Fanning et al., 1989). The characteristic frayed or flaky nature of muscovite edges can be seen in Figure 4.2e. The edges of the concomitant plates are rounded and corrugated, a likely consequence of the frangible properties of these sheets during shearing.

Finally Figure 4.2f demonstrates the random stacking of platelets within a cluster. Although it is most likely attributable to the capillary forces which arise during sample preparation, such packing behaviour and the heterogeneity in particle orientation into different directions is facilitated by the asymmetric morphology of muscovite sheets. This results in clusters of notably higher volume than in quartz particles (Figure 4.1). Such structures of a higher volume are likely to result in more complex suspension flow characteristics.

University of Cape Town

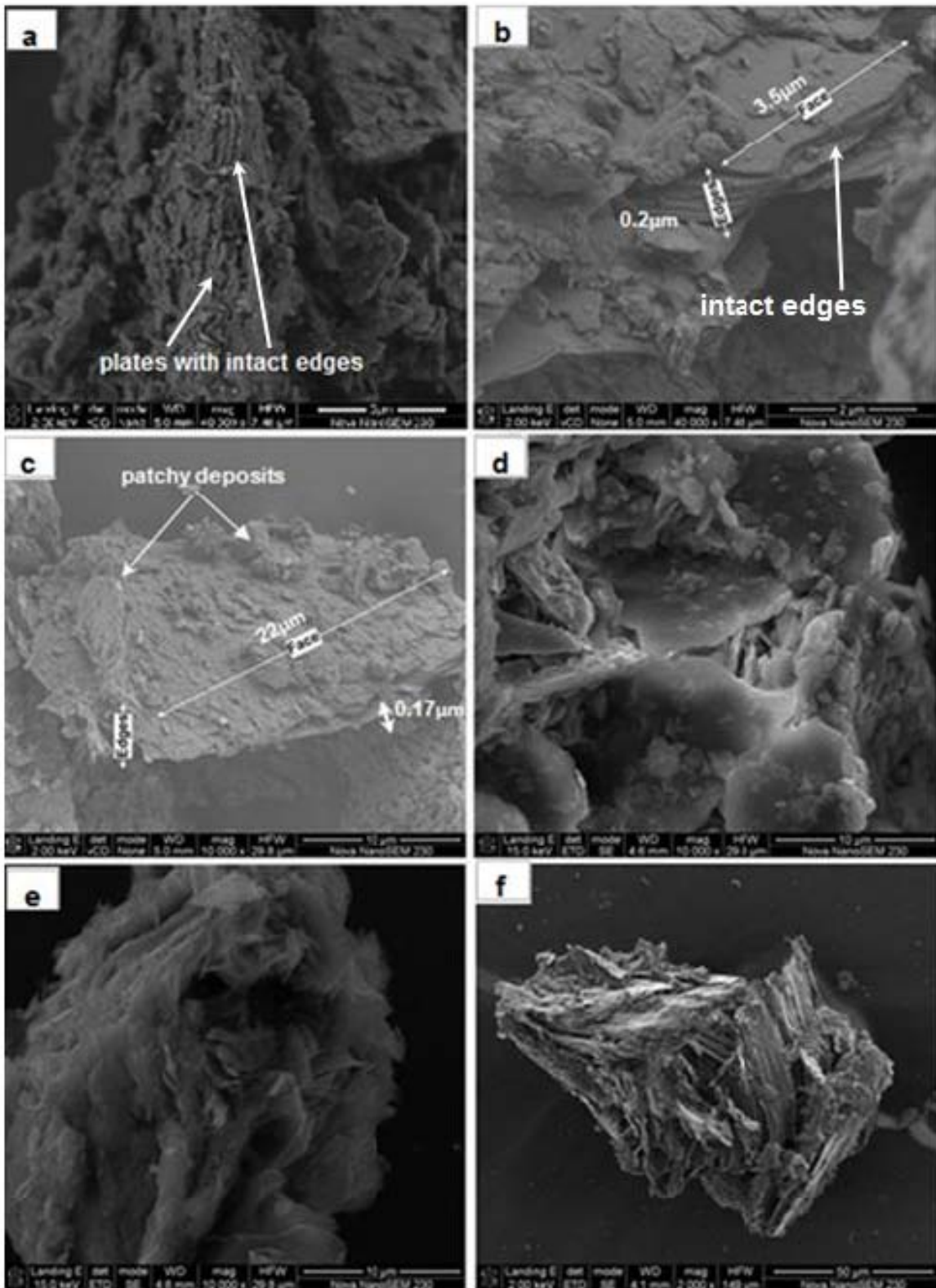


Figure 4.2 - SEM images demonstrating the platy morphology, high aspect ratio and smooth surface structure of muscovite.

4.4. VERMICULITE MORPHOLOGY

The paragenesis of vermiculite from micas has been discussed in detail in Chapter 2, section 2.4.2. Vermiculite is an alteration mineral arising from the replacement of interlayer potassium (K^+) ions by hydrate cations. This alteration may be complete or partial, and as such vermiculites are often classified as intermediates between micas and smectites, bearing morphological similarities to both groups.

Vermiculite typically exhibits a platy morphology and has a swelling habit when immersed in suspension. It is also known to exfoliate at high temperatures. In an attempt to demonstrate these distinguishing characteristics, different methods of sample preparation were used prior to SEM analysis. The SEM images of vermiculite particles, as derived from different treatment procedures, are shown in Figure 4.3. Figure 4.3a and b show SEM images of vermiculite particles after size reduction. These particles have not undergone any other form of pretreatment and are indicative of the vermiculite structure prior to suspension in aqueous media. The swelling ability of vermiculite was investigated using pre-hydrated vermiculite particles. The hydration procedure was conducted prior to SEM analysis and is described in the previous chapter. Drying the samples at room temperature produced particles that were adequately dry for SEM analysis, without destroying the structure or driving out the interlayer water molecules (which are removed at temperatures $> 100^\circ\text{C}$). The resulting SEM images are shown in Figure 4.3c and Figure 4.3d. Finally, Figure 4.3e and f show high resolution hand specimen images of vermiculite particles that were heated to 400°C , and then cooled down rapidly. Such treatment induces thermal exfoliation of the particles.

Examination of the SEM images of untreated vermiculite particles showed that the vermiculite used here could be classified into two major categories; those consisting of larger ‘macroscopic’ particles (Figure 4.3a) or those consisting of smaller ‘microscopic’ vermiculite (Figure 4.3b). This is a common morphological characteristic that has been observed for natural vermiculites from South Africa such as this and is also typical of vermiculites from other localities including Chester Pennsylvania, Libby Montana and Llano, Texas (Basset, 1963; Venkata and Jackson,

1963) The most common feature among particles from either size fraction is their appearance as plates or flakes, demonstrating that the platy morphology is conserved upon size reduction. The surfaces of the larger platelets have comparatively smooth morphology, with occasional folds or step lines along the basal surface ends. These folds, indicated by arrows in Figure 4.3a, in many cases, are at 60° or 120° and appear to give rise to minor fractured edges seen on the face basal surfaces. Similar step lines have been observed by other researchers and have been identified as prism angles of micas which are physical manifestations of the phyllosilicate structure which contains sheets of tetrahedra sharing 3 neighboring oxygens (Verma, 1956; Venkata and Jackson, 1963). Studies by Raman and Jackson, (1963) associated such smooth morphological features within a vermiculite sample with the presence of potassium ions in the interlayer region. Although the ionic content of this particular site was not measured individually, the bulk elemental composition of the vermiculite used in this study was found to contain 3.3% K_2O . These results are discussed in more detail in the next chapter. As one of the major changes in the transformation of mica to vermiculites is the replacement of interlayer potassium ions by hydrated cations (e.g. Na^+ ions), the presence of K^+ ions is then indicative of partial alteration of mica to vermiculite. The presence of interstratified mica-vermiculite inclusions is common in natural vermiculites (Deer et al., 1992). On this basis, together with the characteristic prism angles, the smooth areas observed within vermiculite samples (and shown in this micrograph) can be assumed to contain partially weathered mica cores within the sample (Jackson, 1963).

Even so, the platelets observed are comparatively thicker than was observed in muscovite platelets, with aspect ratios estimated in the range 16-20 (based on dimension estimates in Figure 4.3a). The edges, in this case, are likely to have more of a contribution towards the overall surface charge and colloidal behavior properties than in muscovite, although the face basal plane will still have a dominant role.

While some of the vermiculite surfaces show smooth morphology, Figure 4.3b brings out the complexities and micro morphological structure variations of vermiculite surfaces. The surfaces observed here are no longer even, but show discontinuity of layers and marginal buckling, with indications of prominent crystallographic steps and micro-islands of small particles lodged on top of larger ones, much in contrast to the smooth surfaces previously observed in Figure 4.3a.

This phenomenon has been studied by several researchers in relation to the crystal growth of vermiculite, and has been attributed to the replacement with hydrated cations and to lattice expansion during weathering (Burns and White, 1963; Raman and Jackson, 1963; Kishk and Barshad, 1969; Barabaszova and Valaskova, 2013). This leads to heterogeneity of the interlayer population, whose ionic size differences would cause a strain on the structural layers, manifest in a low crystalline roughened appearance as seen in Figure 4.3b. The discontinuity of the layers has also been attributed to the shrinkage of the layers when K ions are lost from mica interlayers, which may cause the layers to break at intervals of a few microns. The aspect ratios of these particles is then harder to estimate although the ‘layering’ and buckling of layers results in platelets with an increased thickness.

The SEM images of pre-hydrated samples are shown in Figure 4.3c and d. These particles do not represent the structural properties of fully hydrated vermiculite particles, due to the partial hydration that is required for SEM analysis. However, in the absence of CryoSEM technology which more accurately facilitates the analysis of “in situ” hydrated structures, this method merely seeks to inform of any structural changes, if any, upon partial hydration. In Figure 4.3c, the platy morphology of vermiculite particles is further demonstrated. In its hydrated form, the layering of sheets is still evident, although the platelets are not as tightly stacked and the edges no longer intact, with the appearance of a separation between adjacent layers. This is in agreement with studies on the swelling mechanisms of smectites which have postulated that swelling occurs by the penetration of water in the interlayer region, resulting in plate separation (Laird, 2006). In fact, it has been estimated that the maximum amount of water taken up by natural vermiculites corresponds to two layers of water molecules in each available space (Deer et al., 1992). Figure 4.3d demonstrates the swelling and stacking characteristics of smaller platelets. The poor crystalline surface structure is still evident here, with surface irregularities attributable to cracked edges and stacking of smaller platelets on larger ones. However, the platelets are clearly more swollen in structure, resulting in a spongy appearance. The swelling also seems to smooth out the surface, albeit to a small extent. From this SEM image, expansion leads to the transformation from polygonal structures into fuller, more ‘rounded’ structures. This indicates that expansion may also occur by inter crystalline swelling. Expansion, either by inter crystalline or interlayer swelling results in spatially larger structures. The stacks that are formed occupy markedly higher

volumes upon expansion, and this affects their hydrodynamic and flow characteristics in suspension.

Figures 4.3e and f show images of exfoliated vermiculite particles. These images show that expansion in these samples occurred by the buckling of structural layers in the direction perpendicular to the cleavage planes. This resulted in the separation of plates in a concertina-like manner. Expansion occurs due to the rapid generation of steam which cannot escape without contortion of the layers and can result in expansion of up to 30 times the original volume (Deer et al., 1992). The exfoliation process converts dense vermiculite flakes into lightweight porous granules containing innumerable air layers. Exfoliated vermiculite is light and clean to handle, has a high insulation value, acoustic-insulating properties and will absorb and hold a wide range of liquids. It is this property that makes it useful in low heat conductivity; thermal heating applications such as brake linings and high temperature insulation. It also provides baffle against impact shock when used in packaging (Abollino et al., 2008)

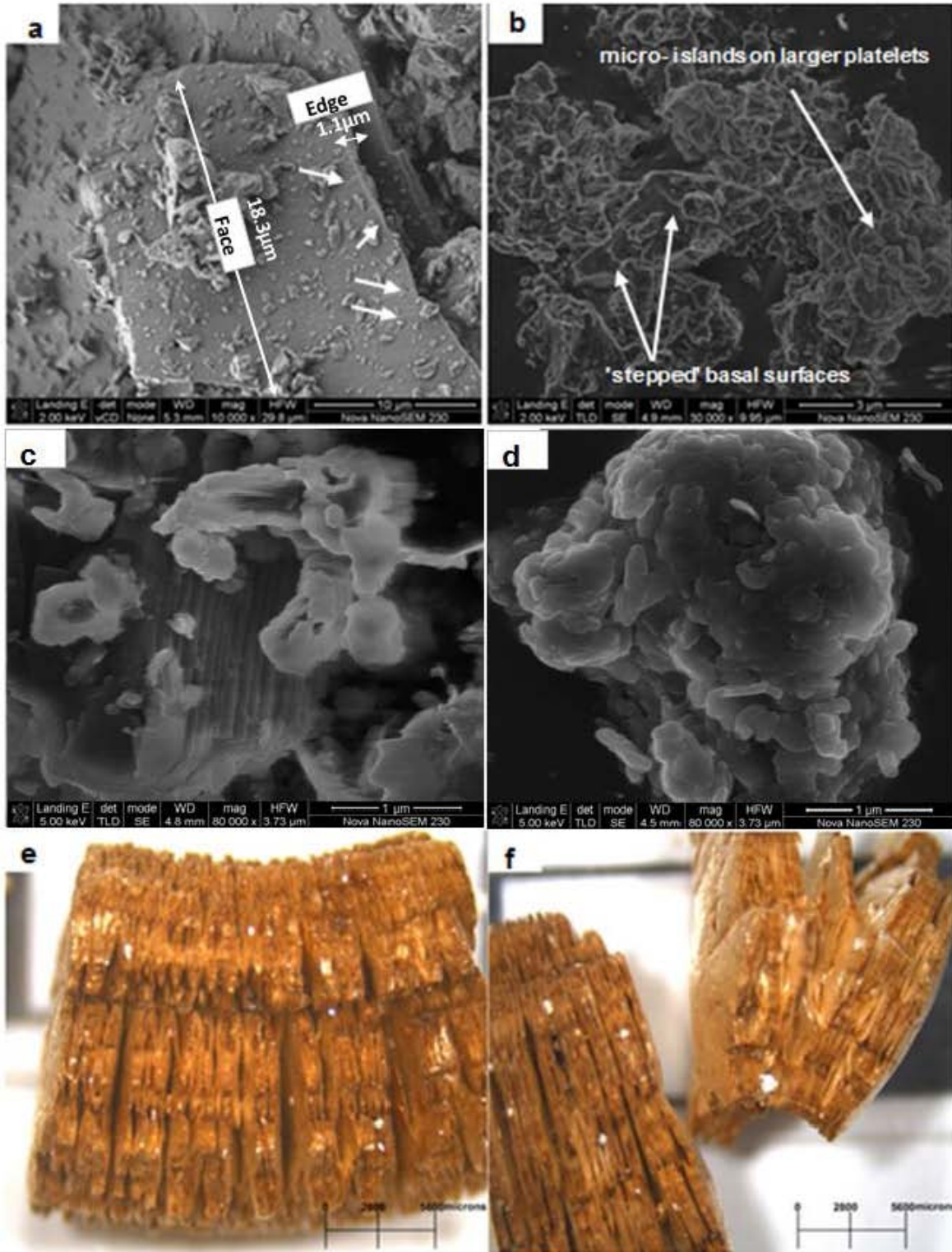


Figure 4.3 – Figure 4.3a to 4.3d SEM images demonstrating poor surface crystallography, swelling potential and exfoliation behaviour of vermiculite. Figures 4.3e and f show optical microscopy images of exfoliated vermiculite.

4.5. CHRYSOTILE MORPHOLOGY

Figure 4.4 shows the SEM images of chrysotile used in this study. Figures 4.4a and 4.4b, in particular, show images of individual chrysotile particles, demonstrating their long, thin fibrous morphology. Based on Figure 4.4b, it can be approximated that each fibre is about 100 μm long and 0.1 μm thick (aspect ratio 1000). This is significantly higher than was observed in both muscovite and vermiculite, demonstrating the extreme morphology of chrysotile. Needless to say, that the edge contribution towards the apparent surface charge characteristics is negligible due to the extremely high aspect ratios. Figure 4.4a also demonstrates the flexibility of chrysotile fibres since the structure is bent. Together with the long, thin morphology, the high degree of flexibility contributes towards a significantly large effective volume that each individual fibre will ‘sweep’ across when in suspension, despite the comparatively low actual volume of the fibres.

The large surface area and flexibility of each fibre enhances the probability of particle-particle interaction such that individual fibrils are easily entangled both within themselves and with adjacent fibres. This leads to the formation of packets of fibres knotted in an intricate mesh of intertwined fibres as observed in Figures 4.4c and d.

Figures 4.5e and 4.5f show SEM images of entangled chrysotile fibres, with particles of a different morphology entrapped within the mesh. These particles do not present a platy or lath-like morphology of antigorite and lizardite, which are most likely to be present with chrysotile. The identity of the particles could not be definitively verified, but can be assumed to be solid material or impurities which arise during sample preparation. Even so, this gives an indication of the degree of entanglement which is prevalent even in the presence of minerals of a different morphology. This suggests that within a heterogeneous mineral system, particles of a different shape are likely to get trapped in the fibres, such that their colloidal behaviour is ‘masked’ by that of chrysotile.

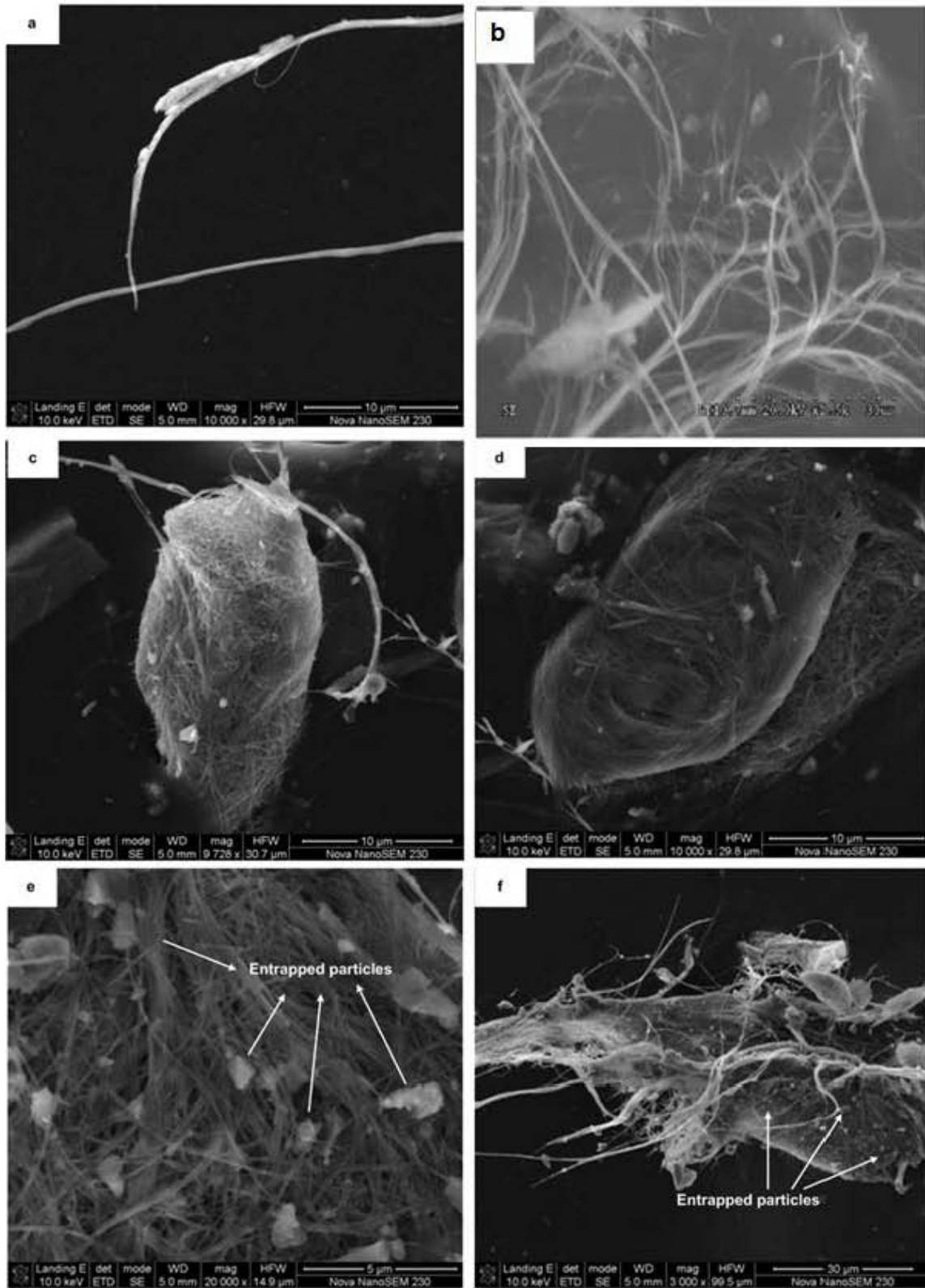


Figure 4.4 - SEM images demonstrating the long, thin fibrous morphology and high degree of entanglement of chrysotile particles.

4.6. DISCUSSION

The morphological properties of quartz, muscovite, vermiculite and chrysotile have been investigated using SEM analysis.

Quartz particles are angular in shape, existing in a combination of hexagonal and cubic particles. The phyllosilicates, on the other hand, all present much more complex morphological properties, with muscovite and vermiculite exhibiting characteristic platy morphology. Chrysotile, on the other hand, has a long thin fibrous morphology. In each case, the surface structures and aspect ratios have been estimated. Table 4.1 gives a summary of the estimated long and short axial dimensions and aspect ratios.

Table 4.7- A summary of estimated aspect ratios of the phyllosilicates.

	Short axis (μm)	Long axis (μm)	Estimated aspect ratio
Muscovite	0.17	22	40 - 130
Vermiculite	1.1	18.3	16 - 20
Chrysotile	0.1	100	1000

Indeed a clear difference in the aspect ratios of the phyllosilicates under study is observed. Muscovite platelets have higher aspect ratios than vermiculite. It is therefore expected that the role of the edge is almost insignificant, since the surface area of the edge is comparatively much smaller than that of the face. This is perhaps more prominent in muscovite where the smooth basal planes facilitate alignment along the basal surfaces. The most important aspect of colloidal behaviour in this case, is most likely basal face agglomeration. This type of aggregation may be more complicated in vermiculite due to the observed prominent crystallographic steps with edge surfaces exposed on the basal cleavage of some surfaces. This may enhance bridging along the edge surfaces of micro-islands on the basal plane. The observed surface characteristics of vermiculite are likely to result in more complex suspension flow behaviour than muscovite suspensions.

The fibrous nature of chrysotile differs from the platy morphology observed in muscovite and vermiculite, with extremely high aspect ratios observed for individual fibres. The effect of this morphology is evident in the high degree of entanglement. It is highly likely that the disentangling of these clusters into separate fibres is extremely difficult and complex suspension flow behaviour is probable.

In all cases, particle agglomeration is likely to result in more voluminous structures than in quartz suspensions. Indeed all the minerals observed here are not perfect crystals. Therefore, it should not be expected that they will behave in a manner that is expected of perfectly crystalline particles with perfect edges and faces. This then puts into question the applicability of robust techniques such as the zeta potential measurement as the sole means to estimate the surface charge properties of the phyllosilicates.

This method is well suited to particles with a homogeneous surface charge and spherical shape, such that the exact significance of the zeta potential distribution and iso-electric point is questionable for minerals with a large deviation from charge anisotropy and spherical morphology (Rasmusson et al., 1997; Miller et al., 2007). Ideally, correction of the zeta potential measurement, and accurate estimation of the overall surface charge of anisotropically charged minerals, would require knowledge of the relative charge density and surface area of the different planes. Such information is attainable for minerals with a sheet-like structure, allowing perfect cleavage into a 'molecularly smooth' surface for use in streaming potential and AFM measurements (Scales et al, 1990; Yin et al., 2012). Ergo, surface charge estimation by these techniques may be applicable to muscovite platelets which have been shown to have a smooth surface structure. However, this would be more complicated in some vermiculite particles of low crystallinity with poorly ordered stepped structures or in the analysis of chrysotile with its extreme fibrous morphology. Some researchers have attempted to calculate the charge distribution of asymmetric particles from zeta potential data, using an estimation of the aspect ratio (Williams and Williams, 1978; O'Brien and White, 1978; Delgado et al., 1986). However, these too have often relied on an assumption of perfect planes, as well as the accurate estimation of the aspect ratio using scanning electron microscopy (SEM) analysis, which on its own does not provide a sufficiently adequate quantitative estimate. In the absence of the knowledge of

these quantities, the electrokinetic measurement merely provides an average zeta potential value which can be very misleading if viewed in isolation. Therefore, in this study, it is best to rely on bulk techniques, while supplementing conventional measurements e.g. zeta potential with titrations for a more comprehensive and comparative analysis. The application of these techniques in this study is explained in more detail in following chapters.

University of Cape Town

Chapter 5.

PHYLLOSILICATE SURFACE CHARGE

Summary

The degrees of charge anisotropy of quartz, muscovite, vermiculite and chrysotile have been investigated using a combination of zeta potential and potentiometric titration techniques. This was correlated to the degree of isomorphous substitution which served as a proxy for the negative charge on the basal plane. Quartz is isotropically charged as demonstrated by a similarity in measured iso-electric point (estimated from the zeta potential measurement) and point of zero charge (estimated from the potentiometric titration). A deviation in these values is observed for the phyllosilicates, a characteristic of anisotropically charged particles. However, the difference in these values is not significant for muscovite (i.e.p = pH 5.4; p.z.c. = pH 4.6) and chrysotile (i.e.p = pH 10.5; p.z.c. = pH 8.2), suggesting that the minerals are only weakly anisotropically charged. Taking into consideration the high aspect ratios previously observed for muscovite and chrysotile, it is not likely that charge anisotropy will play a decisive role in the structures that form in suspension, with face interactions likely to dominate in muscovite. Vermiculite, on the other hand demonstrated a higher deviation in the measured i.e.p (pH 3.3) and p.z.c (pH 8.4) values with high negative charge contribution from isomorphous substitution (~30%). The degree of charge anisotropy in this case may be enhanced by the observed stepped edge sites on vermiculite surfaces. In addition to predominant face interactions, edge interactions may also occur in suspension.

5.1. INTRODUCTION

The surface charge characteristics play a pivotal role in defining the net interaction energy, colloidal stability and rheology of phyllosilicates in aqueous media. The interplay between phyllosilicate surface charge, particle interactions and suspension rheology has been widely investigated, particularly within the context of kaolinite and montmorillonite (e.g. Brandenburg and Lagaly, 1988, de Kretser et al., 1997, Greene et al., 2002; McFarlane et al., 2005, Tombácz and Szekeres, 2006; Vanerek et al., 2006; Bourg et al., 2007). However, there exists some debate around the nature of particle interactions that are likely to occur in suspension and fundamental research in this area is still warranted. Such an understanding would be beneficial in regulating the interfacial chemistry and colloidal behavior of phyllosilicates at industrially relevant processing conditions.

The inconclusiveness around the modes of phyllosilicate particle interaction may be in part attributed to the obscurity around the derivation of charge on the constituent edges and faces. The edges are generally believed to carry a pH dependent charge, determined by the protonation and deprotonation of exposed amphoteric groups, while the charge on the faces has been largely attributed to isomorphous substitution of higher valence ions with ions of a lower valence, rendering the basal planes permanently negatively charged (Williams and Williams, 1978; McFarlane et al., 2005; Vanerek et al., 2006; Miller et al., 2007; Nalaskowski et al., 2007; Yin et al., 2012). However, a pH dependent charge not inconsistent with the hydrolysis of silicon in the basal plane has also been evidenced (Scales et al., 1990). The relative contributions of the pH dependent and independent charge towards the overall charge of the basal plane has not been established. It is, however, acknowledged that the faces of phyllosilicates carry a negative charge over the range pH 3 to pH 10 (Luckham and Rossi, 1999; Rand and Melton, 1977; Johnson et al., 2000), where the pH independent charge may contribute towards the degree of negativity on the faces while the pH dependent charge may be more important in determining the change in this negative charge with pH. Regardless, a charge separation exists between the edges and faces resulting in anisotropically charged particles.

The surface charge analysis of phyllosilicates has also largely been compromised by the use of the zeta potential measurement which has traditionally been applied as a sole means to characterise phyllosilicate charge in many studies (e.g. Johnson et al., 1998; Fuerstenau and Huang, 2003; Bremmell and Addai-Mensah, 2005). The inapplicability of techniques such as AFM and streaming potential across the range of minerals studied in this work has been discussed. With the inapplicability of such techniques, the magnitude and differentiation of charge on the edges and faces cannot be accurately estimated. Moreover, the pH dependent charge contribution towards basal plane charge cannot be accounted for. However, the degree to which isomorphous substitution occurs in the basal plane can be estimated, based on the elemental composition of the minerals. The isomorphous substitution contributes towards the magnitude of the negative charge on the basal planes. In the case of minerals with a low degree of substitution, the faces are likely to be neutral or only slightly negatively charged. In such cases, the minerals are likely to behave as if they were isotropically charged; or weakly anisotropically charged. However, when there is a high degree of substitution present, the faces will carry a strong negative charge and the mineral is highly anisotropically charged. The degree of isomorphous substitution can then be used as an indicator of charge anisotropy. The degree of charge anisotropy is then important in predicting the expected modes of particle interaction, taking into consideration other factors such as aspect ratio, asymmetry and surface area estimated from particle morphology. At conditions of similar (and low) aspect ratio, the alignment into more rheologically complex structures (e.g. edge-face structures) is more likely in particles with a higher degree of charge anisotropy.

This study does not seek to dispute or investigate any theories around the derivation of charge on the different surfaces of the phyllosilicates under study, or to determine the distribution of charge on edge and face surfaces. Instead, based on the aforementioned theories of charge derivation on edges and faces, this chapter aims at *estimating the degree of charge anisotropy* using a combination of techniques which although unable to delineate the charge on the edges and faces, are not restricted by morphological properties and are applicable to all minerals under study.

This chapter proposes the use of the traditional zeta potential measurement and Roberts Mular titration technique in tandem. The incongruity of the zeta potential measurement is demonstrated

through deviations between the measured iso-electric point (as determined by the zeta potential measurement) and point of zero charge (as determined by the potentiometric titration) for minerals with a significant deviation from charge and morphological isotropy. For isotropically charged minerals, the iso-electric point and point of zero charge occur at the same value while these values may differ for anisotropically charged particles. However, if the faces are near neutral, the mineral behaves as if it were isotropically charged and the point of zero charge does not deviate greatly from the iso-electric point. Therefore, the difference between the iso-electric point and point of zero charge is used as an indicator of the degree of charge anisotropy (or deviation from isotropic charge behavior), where a large deviation is indicative of a large degree charge anisotropy. This then ties in with an estimation of the degree of isomorphous substitution in the basal plane in approximating the pH independent contribution of the basal surface charge. This calculation procedure is based on elemental data and is used extensively in mineral chemistry, ion distribution and chemical formula estimates in the mineralogical context. The details of this calculation can be found in Deer et al., 1992.

The analytical procedure taken here does not claim that any one method is better than the other, or that any one method can be used alone for charge estimation. The shortcomings of the zeta potential measurement have been discussed. The potentiometric titration is able to provide information on the charge state above and below the p.z.c., without quantifying the charge at any pH. Calculation of the degree of isomorphous substitution is a quantitative measure, not directly linked to colloidal properties in aqueous media (such as the hydrolysis of surface layers). However, the combined use of these techniques may serve as a better indicator of charge anisotropy rather than the common use of the zeta potential measurement in isolation, and may offer a surface charge estimation where analytical techniques are limited by particle morphology particularly in the case of highly asymmetric and anisotropically charged minerals

5.2. SURFACE CHARGE PROPERTIES OF QUARTZ

5.2.1. The zeta potential of quartz

Quartz (SiO_2) is a simple oxide built from the linked SiO_4 tetrahedra. The surface charge properties of this mineral have been studied extensively using electrophoretic zeta potential measurements. Figure 5.1 shows the zeta potential of quartz reported by Alvarez-Silva et al (2010) in their studies to validate the Roberts Mular titration. An iso electric point value $< \text{pH } 3$ was reported and is within the range that is typically reported in literature for quartz $\text{pH } 1.6 - 3.5$ (Gupta and Miller, 2010, Koopal et al., 1998)

5.2.2. The point of zero charge of quartz

A comparison with the point of zero charge as determined by the Roberts Mular potentiometric titration is shown in Figure 5.1. A point of zero charge value of $\text{pH } 2$ was observed, demonstrating agreement with the iso-electric point. This is a characteristic property of isotropically charged minerals and is indicative of a uniform surface charge that does not vary as a function of position on the particle surface. This also indicates that the electrophoretic zeta potential measurement adequately represents the surface charge properties of quartz. It has been well established that quartz is negatively charged at conditions greater than $\text{pH } 3$ (e.g. Otsuki et al., 2012). The measured point of zero charge is in agreement with this.

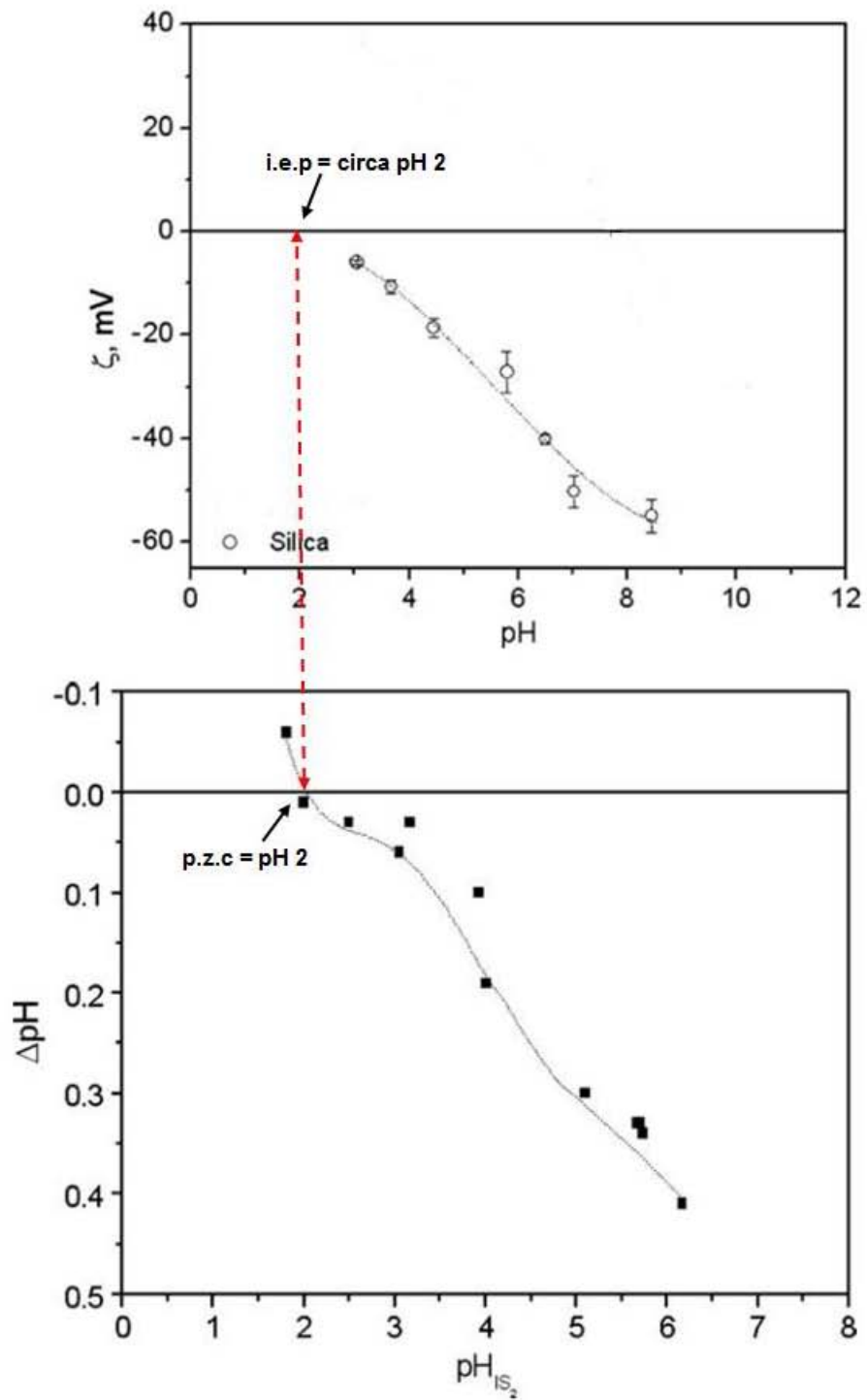


Figure 5.1 – A comparison of the iso-electric point (as determined by zeta potential measurement) and the point of zero charge (as determined by the Roberts Mular titration measurement) of quartz (Alvarez-Silva et al., 2010).

5.2.3. Quartz charge distribution

The charge on quartz particles has been attributed to the protonation and deprotonation of amphoteric sites. Based on the similarity between the iso-electric point and point of zero charge, and also given the extensive amount of research that has been conducted on quartz (and silica), neither isomorphous substitution nor charge anisotropy is expected in this case. In fact, it has been well established that charge development in quartz occurs through the protonation and deprotonation of silanol amphoteric groups (e.g. Johnson et al., 2000; Otsuki et al., 2012), which results in a pH dependent charge as observed in Figure 5.1. However, the following analysis is necessary to demonstrate the difference in its application to isotropically charged minerals (as is the case with quartz) relative to subsequent anisotropically charged minerals.

The elemental composition of quartz from electron microprobe analysis is given in Table 5.1, showing that quartz predominantly consisted of silicon dioxide (SiO_2) and smaller amounts of other oxides (potassium oxide (K_2O), calcium oxide (CaO), aluminium oxide (Al_2O_3) and iron oxide (FeO). These oxides are generally due to either small inclusions of other minerals or fluid inclusions within quartz (Breeman and Buurman, 1998). However, these occur in relatively insignificant amounts and can be assumed to be negligible.

Table 5.1 - Average composition of quartz (weight %) using electron microprobe analysis. The error is a standard deviation of 3 sample populations.

Compound	Weight %	Standard deviation
<i>SiO₂</i>	99.7	0.32
<i>K₂O</i>	0.01	0.01
<i>CaO</i>	0.01	0.00
<i>Al₂O₃</i>	0.09	0.07
<i>FeO</i>	0.02	0.02
<i>Total</i>	99.8	

From this data, a calculation of the distribution of cations could be conducted and compared to the ideal formula of quartz (SiO_2). The results of the calculation are shown in Table 5.2.

Table 5.2 - Distribution of cations in quartz.

Cation	No. cations in formula		Charge		Charge deficit
	Ideal	Experimental	Ideal	Experimental	
Si^{4+}	1.00	1.00		4.00	0
K^+	-	0.00		0.00	
Ca^{2+}	-	0.00		0.00	
Al^{3+}	-	0.00		0.00	
Fe^{2+}	-	0.00		0.00	
Total	1.00	1.00	4	4	

Table 5.2 shows that Si^{4+} ions completely fill all available cation sites such that there is no isomorphous substitution and resultant charge imbalance. On this basis, it can be deduced that the formula of quartz does not deviate from the ideal formula (SiO_2). Therefore, the charge of quartz is entirely due to the protonation/deprotonation of silanol amphoteric groups exposed on the mineral surface and the charge varies with pH as shown in Figure 5.1. Below the p.z.c ($< pH$ 2), the silanol groups are protonated (to form $Si-OH_2^+$) and quartz is positively charged. Above the p.z.c ($> pH$ 2), deprotonation of the silanol groups occurs (to form $Si-O^-$), resulting in negatively charged quartz particles.

5.3. MUSCOVITE SURFACE CHARGE DISTRIBUTION

5.3.1. The zeta potential of muscovite

Muscovite comprises silica T and gibbsite O layers in a 2:1 ratio, forming plates with distinct T faces and T-O-T edges. The T and O layers will both have an effect on the overall charge behavior of the edges and faces. The surface charge properties of the face basal planes are dictated by the surface charge of the silica T layers, while the surface charge of the edge is dependent on both the silica T and gibbsite O layers where the T layers would have twice the effect of the O layer. The overall zeta potential of muscovite is dependent on the relative contribution of each layer and surface. The zeta potential of muscovite used in this study was measured and compared to gibbsite and silica zeta potential data previously derived by Miller et al., (2007). This comparison is shown in Figure 5.2.

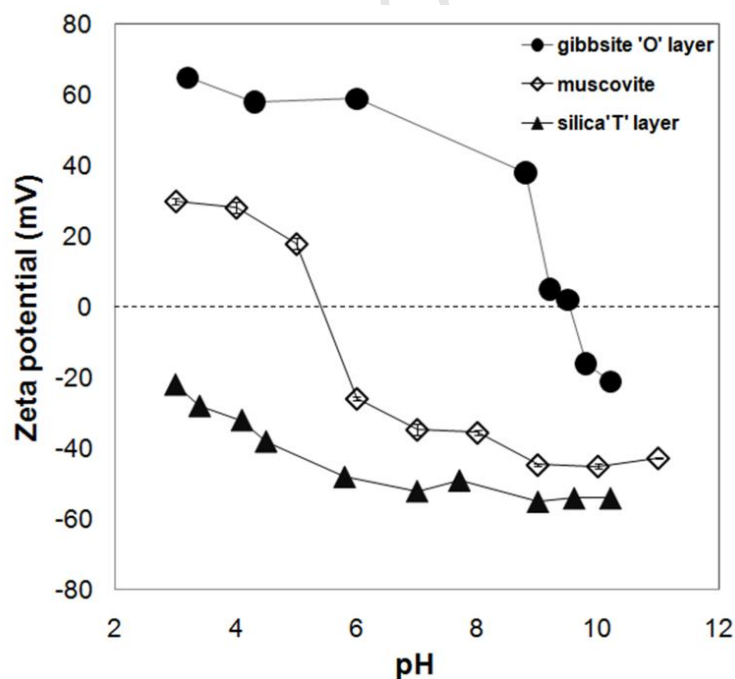


Figure 5.2 – The zeta potential of gibbsite and silica (Miller et al., 2007), compared to the electrokinetic zeta potential of muscovite (this study). The error bars represent 95% confidence interval of average values.

The muscovite data shows a negative zeta potential in the majority of the tested pH range. The zeta potential is negative in the neutral to alkaline pH range, the magnitude of which decreases with decreasing pH. An iso electric point is indicated at pH 5.4, which is in good agreement with reported data for muscovite particles in dilute suspension with low Al^{3+} concentrations (Lyons et al., 1981; Pashley, 1985). Studies which have reported higher i.e.p. values (~pH 7 to pH 8) have often ascribed the shift to the leaching of multivalent ions e.g. Al^{3+} in the acidic range, subsequent hydrolysis and specific adsorption onto surfaces with increasing pH (Hunter, 1981; Nasroti, 2010). The same trend has been observed with kaolinite particles as they systematically shift from kaolinite-like to alumina-like behavior (Johnson et al., 1998). Since the zeta potential measurements at each pH were conducted on individually prepared samples in this study, this minimized the effects of subsequent adsorption of leached ions onto the same surfaces with pH increment. Even so, pH induced leaching and surface modification in samples in the acidic range is still likely. Therefore, although largely attributable to particle surface protonation, mainly of the edge surface hydroxyl groups, the positive zeta potential below the i.e.p is also a result of instantaneous interfacial chemistry modification of surfaces and leaching of hydrolysed divalent and trivalent cations (Lyons et al., 1981; Pashley and Israelachvili, 1984). The importance of the O layer and edge charge in this pH range is evidenced by the positive zeta potential data observed in both the muscovite and gibbsite surfaces.

Above the i.e.p, negative zeta potential is measured. The observed negative zeta potential of the particles has been largely attributed to the negative charge of the muscovite silica basal faces (Pashley, 1985; Nishimura et al., 1992). This is evident in the comparison shown in Figure 5.2, where the zeta potential behaviour of muscovite shows significant similarity with the silica plane in this pH range. However, a difference in magnitude of the negative charge is observed, likely due to the deprotonated silanol and aluminol groups at the pH dependent edge sites at alkaline pH.

5.3.2. The point of zero charge of muscovite

In order to determine the validity of the measured zeta potential as a true representation of the surface charge of muscovite as a function of pH, the zeta potential measurement results are compared to the potentiometric titration results as shown in Figure 5.3.

A comparison of the potentiometric titration and zeta potential curves shows that the measured point of zero charge ($\text{pH } 4.6 \pm 0.3$) is not equivalent to the electrophoretic iso-electric point ($\text{pH } 5.4 \pm 0.7$) of muscovite. However, the values do not differ greatly from each other and are in fact within a 95% confidence interval of each other. Therefore, although a difference is observed, it is not significantly large. Indeed, the disparity observed demonstrates the inconsistency between the electrophoretic zeta and titration measurements, albeit to a small extent in this regard. While the Roberts Mular titration method negates any complications associated with particle morphology, the application of the electrophoretic zeta potential measurement to muscovite is compromised due to theoretical complications associated with the hydrodynamics of platy particles in solution, and also due to the known charge anisotropy of the different surfaces (Burdukova, 2007; Miller et al., 2007; Nalaskowski et al., 2007; Yin et al., 2012). However, the small disparity observed in the i.e.p and p.z.c values indicates that the zeta potential measurement is not highly erroneous for muscovite particles, and could potentially be attributed to the natural variation between experiments.

It has been well established that muscovite comprises edges and faces of different charge properties (Fanning and Keramidas, 1977; Scales et al., 1990; Nasroti, 2010). Therefore, the charge anisotropy in itself is not under question here. It is the degree of anisotropy, as indicated by its analogous charge behaviour to isotropically charged minerals (as evidenced by the similarity in the p.z.c. and i.e.p) that is of interest. The relative contributions of either face or edge to the overall surface charge are important towards determining whether a particle will be near isotropically charged or strongly anisotropically charged. When one plane is dominant (due to larger surface area contributions), the particle is likely to exhibit surface charge properties similar to that of an isotropically charged mineral, dependent mainly on the charge properties of the dominant plane. In this case, the measured i.e.p and p.z.c values are likely to be within the same range of each other. The similarity in the i.e.p and p.z.c values of muscovite indicate that

muscovite is only weakly anisotropically charged and this may be due to the dominance of the face plane relative to the edges.

It must be noted that for anisotropically charged minerals (either weakly anisotropic or strongly anisotropic), the absolute point of zero charge does not exist since the edges or faces carry an electrical charge at any pH. Therefore, the measured point of zero charge determined by the potentiometric titrations in this case does not represent the pH where the overall charge of muscovite is zero, but rather a net point of zero charge at $\text{pH } 4.6 \pm 0.3$ where there is a balance between the positive and negative charges on basal edges and faces. It also gives an indication of the overall charge of muscovite particles above and below this value (Mular and Roberts, 1966).

Below $\text{pH } 4.6 \pm 0.3$, ΔpH is positive owing to the removal of OH^- ions in solution, which is indicative of an overall positive muscovite surface. Conversely, at pH values above pH 4.6, ΔpH is negative due to the removal of H^+ ions from solution for adsorption onto negatively charged muscovite particles. Therefore, although the potentiometric titration curve does not provide a numerical estimate of the magnitude of the surface charge of muscovite, it does indicate that muscovite has a net negative charge at conditions $> \text{pH } 4.6$, which agrees strongly with the measured zeta data.

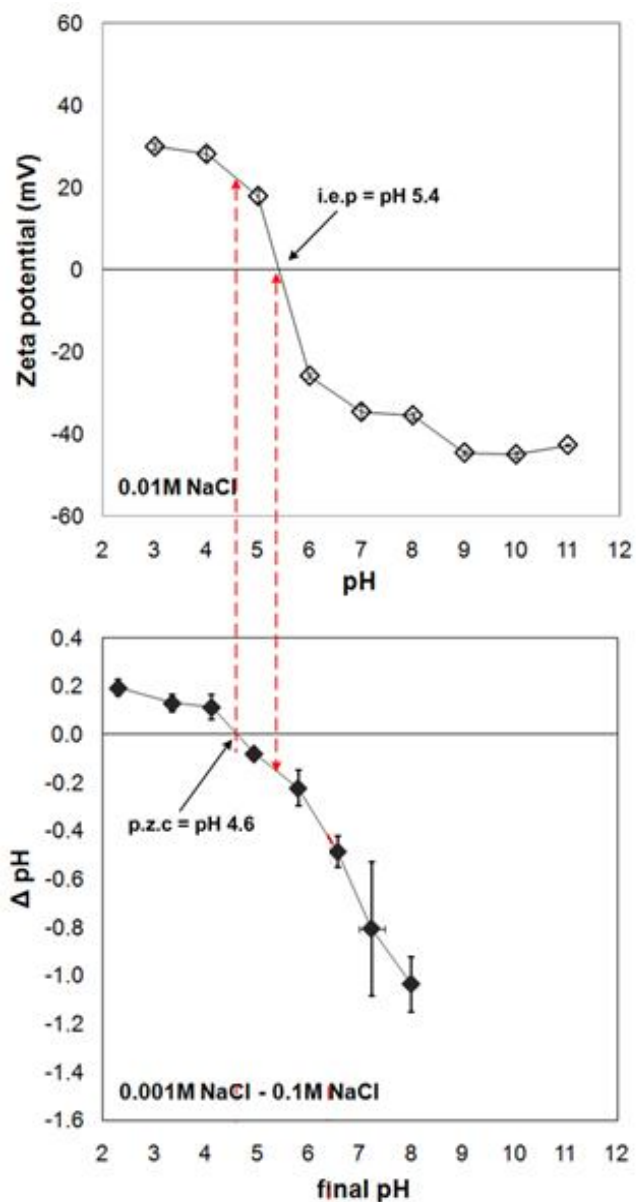


Figure 5.3 - A comparison of the iso-electric point (i.e.p) and point of zero charge (p.z.c) of muscovite. The error bars represent 95% confidence interval and the standard deviation of the average values.

The low degree of charge anisotropy suggested by the similarity in the i.e.p and p.z.c values can be verified by examining the degree of isomorphous substitution.

5.3.3. The degree of isomorphous substitution in muscovite

If muscovite is indeed weakly anisotropically charged, this can be related to a low degree of isomorphous substitutions in the octahedral and tetrahedral layers. Electron microprobe data analysis was used to determine the degree of substitution in these layers. This analysis has been used in a similar manner to determine the presence of a negative charge on the basal planes of talc (Burdukova, 2007).

The measured average elemental composition of muscovite as determined by electron microprobe analysis is presented in Table 5.3.

Table 5.3 - The average composition of muscovite (weight %) using electron microprobe analysis. The error is a standard deviation of 8 sample populations.

Compound	Weight %	Standard deviation
SiO₂	46.3	0.19
K₂O	10.3	0.15
Na₂O	0.62	0.08
Al₂O₃	35.6	0.11
FeO	2.97	0.16
MgO	0.83	0.01
H₂O	4.01	0.01
Total	100	

The results show that the muscovite sample consisted of SiO₂ and Al₂O₃ which is expected due to its constituent silica (SiO₄) and gibbsite (Al(OH)₃) layers. Smaller amounts of other oxides (K₂O, MgO, Na₂O and FeO) were also detected. These constitute cations which take part in isomorphous substitutions in the tetrahedral and octahedral layers. The amount of crystalline water was found to be 4.01% (by weight) using a dehydration measurement.

From the measured compositional data, the number of cations in muscovite could be determined. Table 5.4 shows the average number of each type of cation in muscovite.

Table 5.4 - Calculated average number of cations in muscovite.

Cation	No. cations in formula
Si^{4+}	6.67
K^+	1.90
Na^+	0.17
Al^{3+}	6.05
Fe^{2+}	0.36
Mg^{2+}	0.18
OH	4.00

In order to classify the cations according to those in the tetrahedral layer, octahedral layer and interlayer region, a comparison with the ideal formula of muscovite was used. According to the ideal formula of muscovite $[K_2Al_4[(SiAl)_8O_{20}](OH,F)_4]$, there are 8 cation sites available in the tetrahedral layer, 4 cation sites in the octahedral layer and 2 interlayer cation sites. In the tetrahedral layer, Si^{4+} ions may be substituted by Al^{3+} ions in some cation sites while Al^{3+} ions occupy all the cation sites in the octahedral layer and K^+ ions can be assigned to the interlayer region (Figure 5.4). Indeed aluminium is likely to exist in various forms in aqueous solution, each with different charges, viz. Al^{3+} , $AlOH^{2+}$, $Al(OH)_2^+$ and various polymeric forms. Therefore, it may be difficult to know the relative proportions of these forms that will balance the negative surface charge. However, the assumption that aluminium balances the charge in the form Al^{3+} appears valid due to its greater charge which makes it preferentially adsorbed relative to the other forms. Moreover, early studies on the nature of isomorphous substitution in kaolinite reached the same conclusion, based on small amounts of Al^{3+} ions in the extract solutions, even at low pH levels, suggesting adsorption by the mineral structure (Bolland et al., 1976).

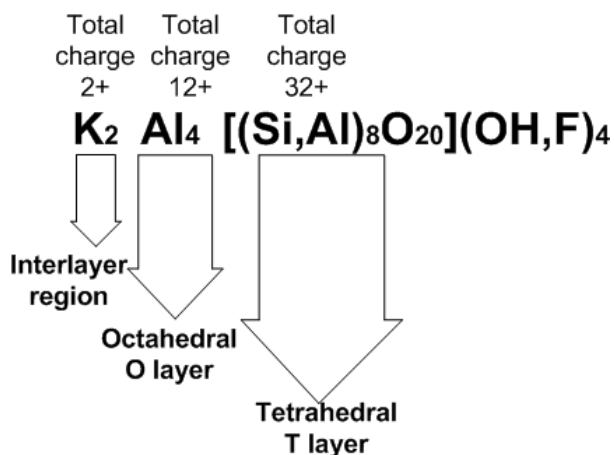


Figure 5.4 - Ideal classification of cations according to muscovite formula.

Although the values of the cations determined experimentally rarely add up exactly to the ideal formula, a comparison with the ideal formula facilitates a classification of cations into the different layers. The distribution of cations in muscovite is shown in Table 5.5.

Table 5.5 - Classification of cations in muscovite.

Cation	Mean no. cations		Charge		Charge deficit	
	Ideal	Experimental	Ideal	Experimental		
Si⁴⁺	6	6.67		26.68	-1.33	Tetrahedral layer
Al³⁺	2	1.33		3.99		
Total	8	8	32	30.67		
Mg²⁺	-	0.18		0.36	3.24	Octahedral layer
Fe²⁺	-	0.36		0.72		
Al³⁺	4	4.72		14.16		
Total	4	5.26	12	15.24		
Na⁺	-	0.17		0.17		Interlayer cations
K⁺	2	1.9		1.9		
Total	2	2.07	2	2.07		

The classification shows that the Si⁴⁺ cations (6.67) do not adequately fill all 8 available cation sites in the tetrahedral layer. Therefore Al³⁺ ions occupy the remaining sites. This means that there is isomorphous substitution of Si⁴⁺ ions by Al³⁺ ions in the T layer, resulting in a charge deficiency (-1.33). Similarly, in the octahedral layer Fe²⁺ and Mg²⁺ ions occur with Al³⁺ ions

resulting in a positive charge deficiency. The resultant charges in both layers indicate that the edges and faces of muscovite are permanently positively and negatively charged respectively. However, studies on clay minerals talc and kaolinite have proven that in the T layer, the charge in the replaced tetrahedron is distributed between the surrounding 3 surface oxygens (the fourth one being bonded to an octahedron), resulting in the localized charge distribution and permanent negative charge contribution to the faces. In the O layer, on the other hand, the positive (or negative) charge deficiency is dissipated over the complete framework of 10 oxygens of the 4 tetrahedra bonded to the deficient octahedron. Therefore, the charge resulting from isomorphous substitution in the O layer is degenerated throughout the mineral structure and is not the likely source of the charge on the edges (Brindley, 1980, Meunier, 2005) (Figure 5.5). Instead, the charge on the edges is largely due to aluminol (Al-OH) and silanol (Si-OH) amphoteric groups which are situated at the broken edges and exposed hydroxyl-terminated planes of phyllosilicate minerals, and are amenable to pH changes (Figure 2.17).

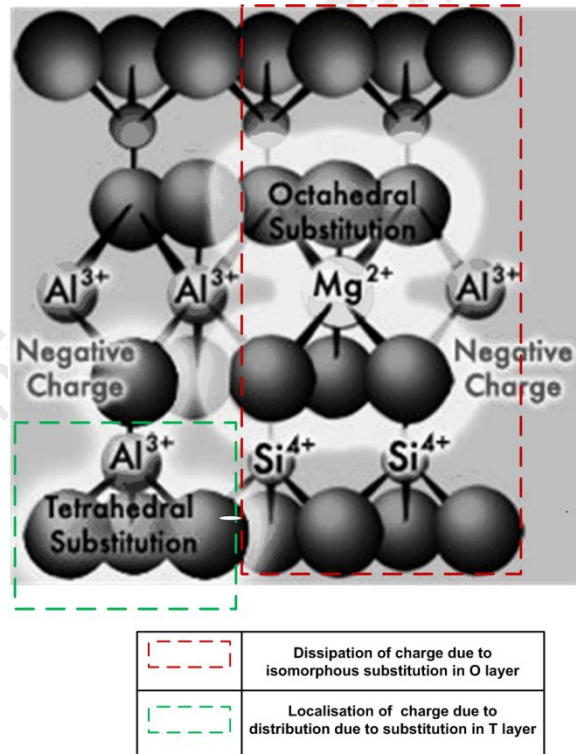


Figure 5.5 - Dissipation of charge in the T and O layers.

On this basis, the charge deficiency from the substitutions in the T layer results in the permanent negative charge contribution towards the charge of muscovite faces. This substitution accounts for 16% of the cations in the T layer and is in agreement with the degree of substitution that has been reported to range between 12.5 % and 25% for muscovite from other deposits (Deer et al, 1992).

The results also show that the interlayer cations mostly comprised of K^+ , with smaller amounts of Na^+ ions. These ions compensate the charge resulting from the substitutions in the tetrahedral and octahedral layers. Based on the distribution of cations, the exact formula of the muscovite sample is $(K_{1.9}, Na_{0.1}) (Al_{3.6}, Fe_{0.4}, Mg_{0.2}) [Si_{6.7}Al_{1.3}O_{20}](OH,F)_4$.

5.3.4. Proposed charge distribution of muscovite particles

It has been concluded from the present work that isomorphous substitution takes place in the T layers of muscovite, resulting in a pH independent charge which contributes towards the negative charge of the basal planes. Based on the small deviation in the measured iso-electric point and point of zero charge, it is believed that the basal planes are not strongly negatively charged. A charge distribution can be proposed, based on these findings.

It is proposed that the faces carry a negative charge throughout the pH 3-11 regime. The magnitude of this charge is thought to be determined by the degree of isomorphous substitution. Therefore, within the context of this study, the muscovite faces are only slightly negatively charged. The presence of a pH dependent negative charge is also expected, assumed to be a result of the hydrolysis of Si-O-Si groups to yield an ionisable form of the silanol groups, in a manner similar to silica systems. It is expected that this charge is most important in the range pH 4- 8, as is the case with silica itself (Bolland et al., 1976; Scales et al., 1990).

The charge on the edges undergo a change from positive to negative, attributable to the pH dependent protonation and deprotonation of exposed amphoteric groups. Protonation reactions will occur below the edge p.z.c. while deprotonation will occur above the edge p.z.c. The

measured overall p.z.c. (pH 4.6) can be used, not as locator of the edge p.z.c but rather as a range below which the edge p.z.c cannot occur. The overall p.z.c. itself reflects a balance between positive and negative charges on the mineral surface and may indicate the pH at which the charge differential between the edge and face is greatest. Therefore, at pH 4.6, the negative charge on the faces must be balanced by a positive charge on the edges, and the edges must still be positively charged at this condition. The edge p.z.c cannot occur below pH 4.6, but is likely to exist at a pH much higher than the overall p.z.c (> pH 4.6). Estimation of edge p.z.c. from a weighted average based on the T-O-T crystal structure of muscovite particles yields a value in the range pH 4.2 to pH 4.8, which lies too close to the measured overall p.z.c. (pH 4.6). An estimation on such a basis has also proved erroneous in calculating the p.z.c. of kaolinite particles. Instead, variations in the $\text{Al}_2\text{O}_3/\text{SiO}_2$ ratio have been shown to have some influence on the measured p.z.c., with a higher Al_2O_3 content generally resulting in a higher p.z.c. (Hu et al., 2003; Hu and Liu, 2003; Miller et al., 2007). Therefore, based on the Al_2O_3 and SiO_2 compositions presented in Table 5.3, an edge p.z.c in the range pH 5.5 to pH 6 is estimated. However, these may not be the only determining components, especially since additional charge balancing ions also exist and are likely to contribute towards the overall edge charge, albeit to a smaller extent. Predictions of the edge p.z.c. based on direct force measurements (which are inclusive of all surface ions) have reported the point of zero charge of the edge of muscovite particles in the range pH 7 to pH 8 (Yan et al., 2011) while sedimentation tests have estimated the edge p.z.c in the range pH 5.8 to pH 6.8 (Sverjensky, 1994). These techniques generally estimate the edge p.z.c in the range pH 6 to pH 8. A highly simplified schematic representation of the proposed charge distribution, based on the measurements performed on muscovite particles in this study is given in Figure 5.6.

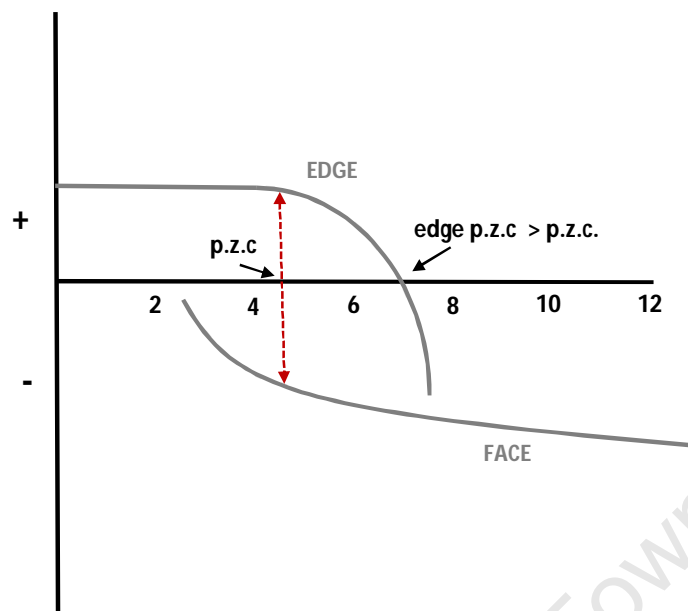


Figure 5.6 - Proposed surface charge distribution of muscovite edges and faces.

It must be noted that although the proposed charge distribution demonstrates the charge anisotropy in the edges and faces, the contribution of the edge charge to the overall surface charge is minimal due to the high aspect ratio and small area of the edges in muscovite platelets. At low indifferent electrolyte concentrations, the negative electrostatic field emanating from the face plane spills over onto the edge surfaces, and as a result the positively charged edge is swamped by the negative electrostatic field (Tateyama et al., 1997). This is manifest in a muscovite zeta potential trend similar to the silica face as observed in Figure 5.2.

5.4. VERMICULITE SURFACE CHARGE DISTRIBUTION

5.4.1. The zeta potential of vermiculite

Vermiculite has a T-O-T structure similar to muscovite. However, the octahedral layer in this case is brucite and the interlayer cations are both exchangeable and hydrated. The surface charge properties of the edges are dependent on the surface potential of the constituent silica T and brucite O layers, while the surface charge of the faces is dependent on the charge properties of the silica T layer. The zeta potential of vermiculite used in this study was measured and compared to brucite and silica zeta potential data previously derived by Miller et al., (2007) (Figure 5.7).

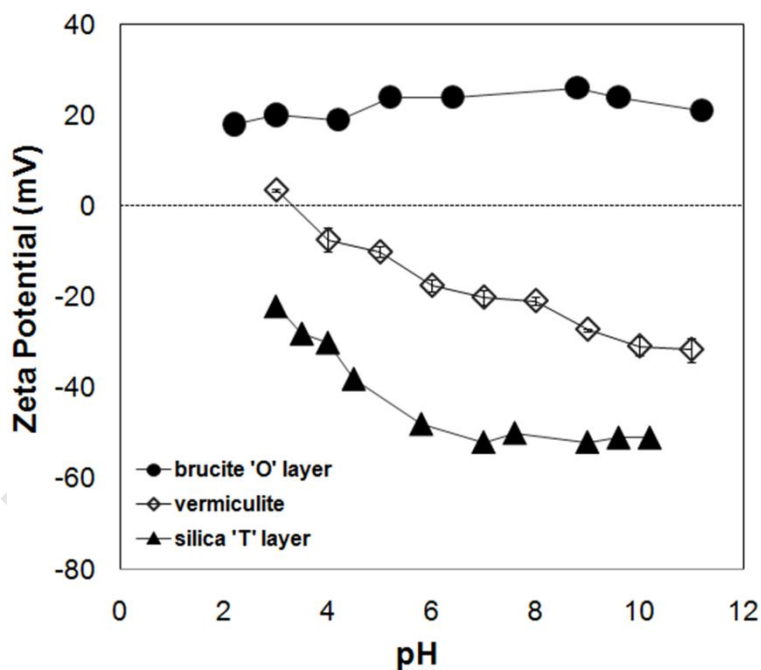


Figure 5.7 – The zeta potential of brucite and silica (Miller et al., 2007), compared to the electrokinetic zeta potential of vermiculite (this study). The error bars represent 95% confidence interval of average values.

The results show that vermiculite particles are predominantly negatively charged throughout the tested pH range. An iso electric point was measured at pH 3.3. At pH conditions less than this,

the particles are only slightly positively charged. Above this, the zeta potential is negative, the magnitude of which becomes increasingly negative throughout the neutral and alkali pH range.

Similar to muscovite, the negative zeta potential of the particles can be largely attributed to the negative charge of the basal planes, derived from the pH dependent charge consistent with the hydrolysis of silicon in the surface plane as well as the pH independent permanent negative charge resulting from isomorphous substitution (Lyons et al., 1981; Pashley and Israelachvili, 1984; Nishimura et al., 1992). Within vermiculite, the positive charge of the constituent brucite O layer likely counteracts the negative charge of silica T faces, resulting in the observed reduction in magnitude of the negative charge in vermiculite relative to silica. The edge also likely contributes to the overall negative charge of vermiculite via the deprotonated silanol and aluminol groups. The zeta measurement for brucite shown in Figure 5.7 shows no i.e.p value, although this has been estimated close to pH 11 and pH 12 (Pokrovsky and Schott, 2004).

5.4.2. The point of zero charge of vermiculite

In order to investigate the applicability of the zeta potential measurement to vermiculite and also to estimate whether vermiculite deviates largely from isotropic charge behaviour, the zeta potential data can now be compared to the potentiometric titration measurement results.

This comparison is shown in Figure 5.8.

The potentiometric titration results show a point of zero charge measured at pH 8.4. This differs significantly from the measured iso electric point, which was estimated at pH 3.3. Indeed, this observed deviation between the i.e.p and p.z.c is characteristic of anisotropically charged minerals (Alvarez-Silva et al., 2010), validating the presence of edges and faces of significantly different charge properties. From the measured p.z.c, it can be inferred that at conditions $< \text{pH } 8.4$ (below the p.z.c), vermiculite particles carry a net positive charge. Above this ($> \text{pH } 8.4$), the particles carry a net negative charge. This is contradictory to the zeta potential data which indicated an overall negative charge at conditions $> \text{pH } 3.3$. This inconsistency then demonstrates the erroneous nature of the zeta potential measurement whose applicability to anisotropically

charged minerals has been questioned (Yin et al., 2012). This is more the case with strongly anisotropically charged minerals.

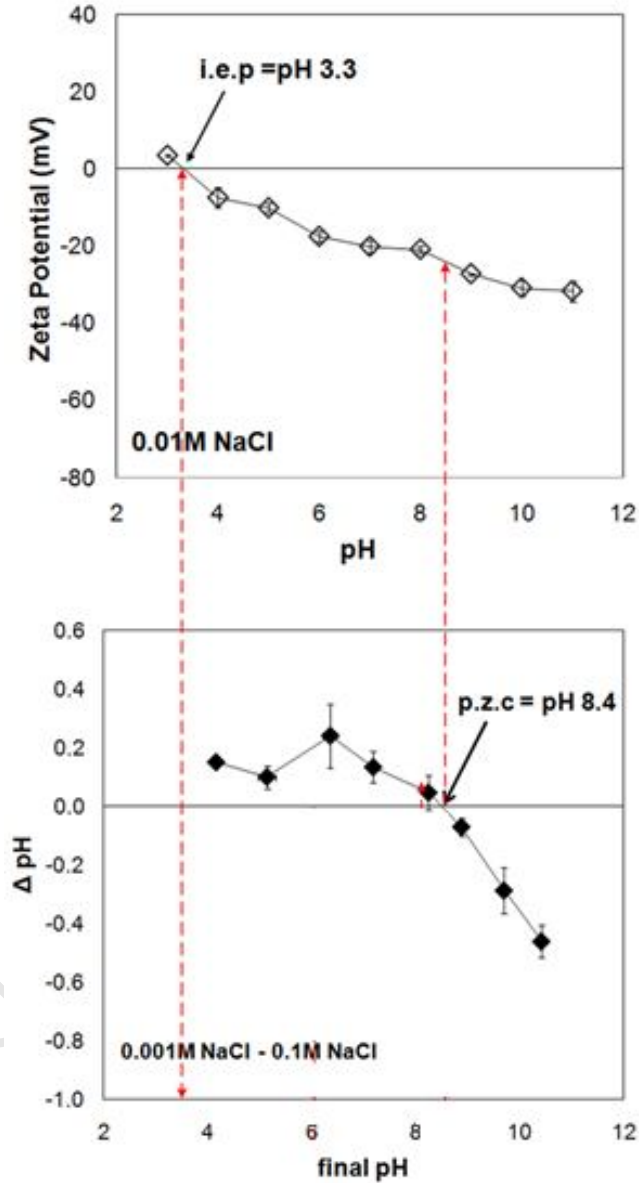


Figure 5.8 - A comparison of the iso-electric point (i.e.p) and point of zero charge (p.z.c) of vermiculite.

The error bars represent 95% confidence interval of the average values.

5.4.3. The degree of isomorphous substitution in vermiculite

The large deviation between the i.e.p and p.z.c suggests that vermiculite will likely demonstrate a large deviation from isotropic particle charge behaviour and is strongly anisotropically charged. This is further probed by investigating the degree of isomorphous substitution, as a possible source of negative charge on the basal planes.

A similar analysis to that conducted for muscovite was done to determine the degree of isomorphous substitution and exact formula of vermiculite. Table 5.6 gives the average elemental composition of the key constituents.

Table 5.6 - The average composition of vermiculite (weight %) using electron microprobe analysis. The error is a standard deviation of 8 sample populations.

Compound	Weight %	Standard deviation
SiO₂	38.72	0.88
K₂O	3.30	1.62
Na₂O	0.72	0.31
CaO	1.08	0.31
Al₂O₃	14.90	0.39
FeO	7.47	0.54
MgO	21.51	1.05
H₂O	9.53	0.11
Total	97.2	

The results show that vermiculite mainly consisted of SiO₂ and MgO, which constitute the silica T and brucite O layers. Al₂O₃ and FeO were also detected, and these constitute the Al³⁺ and Fe²⁺ ions which take part in isomorphous substitutions in the tetrahedral and octahedral layers. Variable amounts of detected Na₂O and CaO represent elements in the interlayer region. The proportion of water was determined by dehydration measurements and was estimated at 9.53%. This represents the water molecules which settle in the interlayer region as well as constitutional crystalline water and is in accordance with the amount of water which is taken up by most natural vermiculites (7 – 12% by weight). This corresponds to two layers of water molecules in each available space (Deer et al., 1992). It must be noted that an imbalance in total weight

fraction was observed when dealing with vermiculite, but this can be attributed to the high variability of water content in swelling clays.

Table 5.7 shows the calculated average number of each cation in vermiculite.

Table 5.7 - Calculated average number of cations in vermiculite.

Cation	No. cations in formula
Si^{4+}	5.83
K^+	0.63
Na^+	0.21
Ca^{2+}	0.17
Al^{3+}	2.64
Fe^{2+}	0.94
Mg^{2+}	4.83
OH	4.00

The ideal formula can now be compared to the actual number of cations in vermiculite. According to the ideal formula of vermiculite, there are 8 cation sites available in the T layer, 6 cation sites in the O layer and 0.6-0.9 cation sites the interlayer region. In the T layer, Al^{3+} ions may substitute for Si^{4+} ions while the Mg^{2+} cations are mainly substituted by Fe^{2+} and Al^{3+} ions in the octahedral layer. Mg^{2+} is the most common interlayer cation, although Ca^{2+} or Na^+ ions also occur (Figure 5.9).

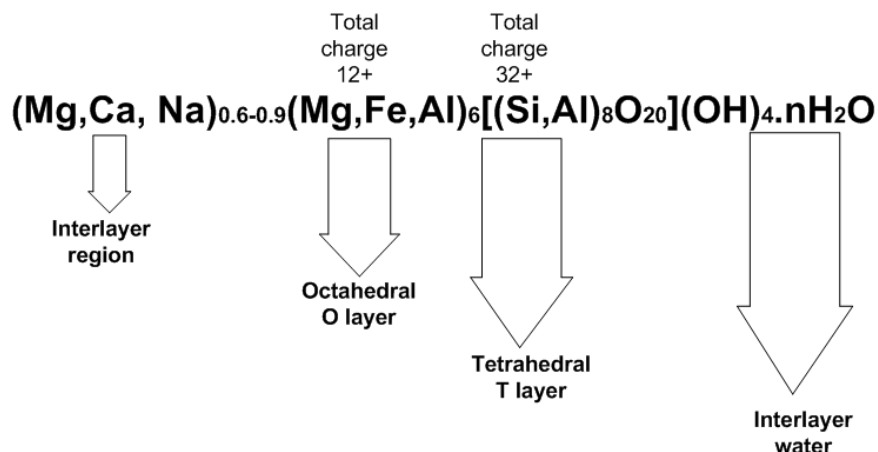


Figure 5.9 - Ideal classification of cations according to vermiculite formula.

The classification of cations according to those in the interlayer region, tetrahedral and octahedral layers is shown in Table 5.8.

Table 5.8 - Classification of cations in vermiculite.

Cation	Mean no. cations		Charge		Charge deficit	
	Ideal	Experimental	Ideal	Experimental		
Si^{2+}		5.83		23.32	-2.17	Tetrahedral layer
Al^{3+}		2.17		6.51		
Total	8	8	32	29.83		
Mg^{2+}		4.59		9.18	0.47	Octahedral layer
Fe^{2+}		0.94		1.88		
Al^{3+}		0.47		1.41		
Total	6	6	12	12.47		
Ca^{2+}		0.17		0.34	1.66	Interlayer cations
Mg^{2+}		0.24		0.48		
Na^+		0.21		0.21		
K^+		0.63		0.63		
Total	0.6-0.9	1.25	1.2-1.8	1.66		

The results show that there is isomorphous substitution in the tetrahedral layer, with some Al^{3+} ions filling available cation sites. The substitution accounts for about 28% of the cations in the tetrahedral layer. This means that isomorphous substitution accounts for almost a third of the

cations in the T layer. This is a significantly higher degree of substitution than is typically observed in kaolinite and talc (and that calculated for muscovite), whose degree of substitution has been reported as <10% (Deer et al., 1978; Deer et al., 1992). This means that there is a higher contribution to the negative charge by isomorphous substitution in vermiculite. Hence the faces carry a stronger negative charge and a high charge separation is likely to be observed with the edges.

Fe^{2+} and Al^{3+} ions substitute for Mg^{2+} ions in the octahedral layer, but the resultant charge is dissipated throughout adjacent oxygen atoms and tetrahedra of the deficient octahedral layer and is not localized to the O layer (Figure 5.6). Mg^{2+} , Ca^{2+} , K^+ and Na^+ ions are the main exchangeable interlayer cations. On this basis, the exact formula of vermiculite is $(\text{Mg}_{0.2}, \text{Ca}_{0.2}, \text{Na}_{0.2}, \text{K}_{0.6})[(\text{Mg}_{4.6}, \text{Fe}_{0.9}, \text{Al}_{0.5})(\text{S}_{5.8}, \text{Al}_{2.2})\text{O}_{20}](\text{OH})_{4.5} \cdot 5.5 \text{H}_2\text{O}$.

5.4.4. Proposed charge distribution of vermiculite particles

Given the disparity in the measured i.e.p and p.z.c. values and the higher degree of isomorphous substitution in vermiculite, it can be estimated that vermiculite particles will have a higher degree of charge anisotropy than muscovite. In fact, based on the degrees of isomorphous substitutions (16% in muscovite and 28% in vermiculite), it can be assumed that the basal planes of vermiculite carry a negative charge of a higher magnitude (almost double) than muscovite.

In comparison to muscovite, it is proposed that vermiculite basal planes carry a strong negative charge, arising primarily from isomorphous substitution in the T layer. A pH dependent charge also contributes to the negative charge in a manner similar to muscovite.

The charge on the edge is pH dependent, also attributable to the protonation and deprotonation of amphoteric groups. At the measured overall p.z.c., pH 8.4, the edges are expected to carry a strong positive charge to balance the negative charge on the faces. Most studies in literature on vermiculite surface charge tend to quote the zeta potential i.e.p. rather than the p.z.c or edge

p.z.c., such that estimation and comparison of the edge p.z.c. is difficult. For this reason, the edge p.z.c. can only be approximated above pH 8.4, based on the findings of this study.

An overall p.z.c. value at pH 8.4 suggests that the overall charge is net positive up to pH 8.4. This would either require a very large positive charge or a large edge surface area to counteract the negative faces. This seems unlikely when one considers vermiculite to have a smooth surface structure similar to muscovite. However it has been shown in the previous chapter, and in morphological studies on vermiculite that the surfaces tend to have small step edge sites attached to basal planes of larger platelets, resulting in a 'roughened' structure. The additional step edge sites result in a larger number of exposed edge sites, contribute to the total surface area and generate a pH dependent positive charge across the surface at certain pH conditions. This may result in an enhanced edge contribution (Zbik and Smart, 1998; Du et al., 2010; Zbik et al., 2010). The fewer the step edge sites, the smoother the surfaces and the lower the edge contribution. These platelets are more likely to behave in a manner similar to muscovite platelets where the negative face charge screens out the edge charge effects.

A highly schematic representation of the proposed surface charge distribution of vermiculite faces and edges is shown in Figure 5.10.

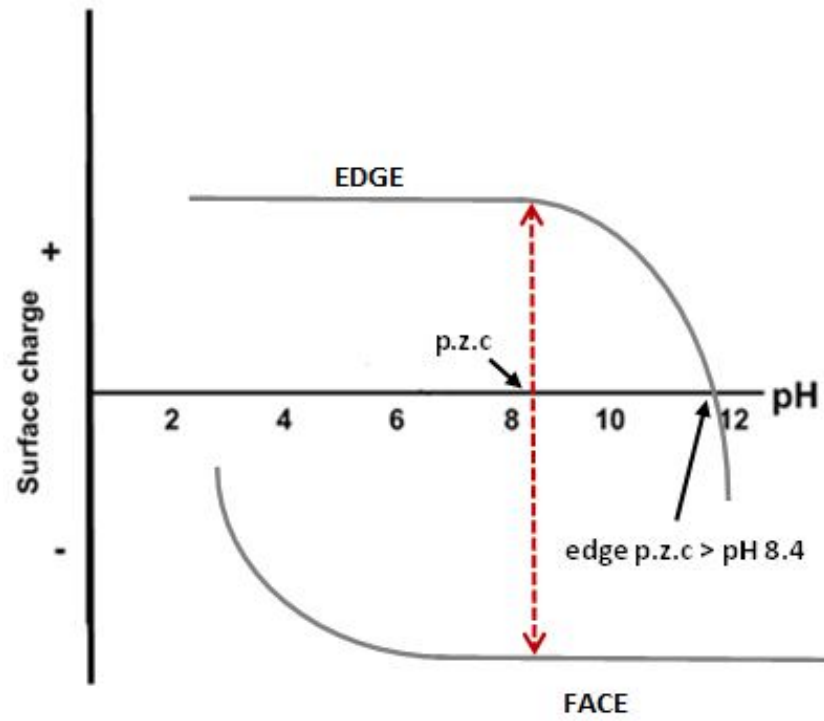


Figure 5.10 - Proposed surface charge distribution of vermiculite edges and faces.

5.5. CHRYSOTILE SURFACE CHARGE DISTRIBUTION

5.5.1. The zeta potential of chrysotile

Chrysotile differs from muscovite and vermiculite in that it has a long, thin fibrous morphology and comprises equivalent amounts of silica T and brucite O layers. These are curled in a tube-like structure, with the brucite layer exposed on the outside and the silica layer on the inside. T-O edges occur at the end of each tube and run along the length (see Figure 2.13). Therefore, the charge on the edges is dependent on the charges of both the silica and brucite layers, while the charge along the tube length is due to the charge of the exposed brucite layer.

The comparison of the zeta potential of chrysotile relative to that of brucite and silica was conducted by Ney, (1973) and is shown in Figure 5.11. Since the brucite and silica layers exist in equal proportions and carry sufficiently strong opposite charges, one might expect that the chrysotile zeta potential would undergo a change from positive to negative, as dictated by the magnitude of the zeta potential of both the silica and brucite layers. However, the zeta data shows that chrysotile is strongly positively charged over a broad pH range, with an iso-electric point estimated at circa pH 10.5. The zeta potential values of chrysotile decrease only when the zeta potential of the brucite layer becomes less positive. In this way, the zeta potential trend of chrysotile predominantly follows that of the brucite layer, indicating that brucite is the overall determining factor for the surface potential of chrysotile particles. This is expected since brucite forms the outer layer of chrysotile fibres and measurement along this plane is enhanced by the characteristic long, thin fibrous morphology.

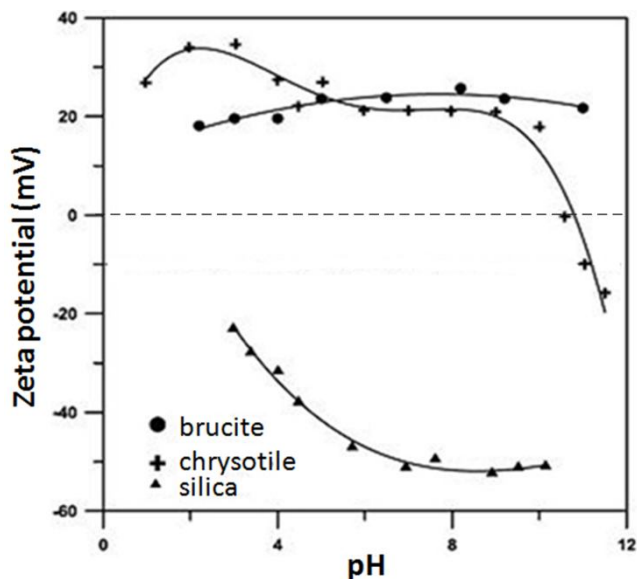


Figure 5.11 - The zeta potential of brucite and silica, compared to the electrokinetic zeta potential of chrysotile (Ney, 1973).

5.5.2. The point of zero charge of chrysotile

A comparison between the potentiometric titration and zeta potential data shows a difference in the measured point of zero charge (pH 8.2) and iso electric point (pH 10.5) (Figure 5.12). Again, this disparity can be attributed to the application of the zeta potential measurement which although generally complicated by charge anisotropy may be compromised more by the hydrodynamics associated with the extreme long, thin fibrous morphology which deviates greatly from spherical morphology (for which the zeta potential measurement is best suited) in this case. Even so, both analytical techniques indicate that chrysotile particles carry a net positive charge in the majority of the pH range. Below the net point of zero charge (pH 8.2), chrysotile particles carry a net positive charge. Above this, they carry a net negative charge. The agreement in this regard, may be attributed to the tubular morphology and exposure of the brucite layer such that measurement is mostly limited to this plane

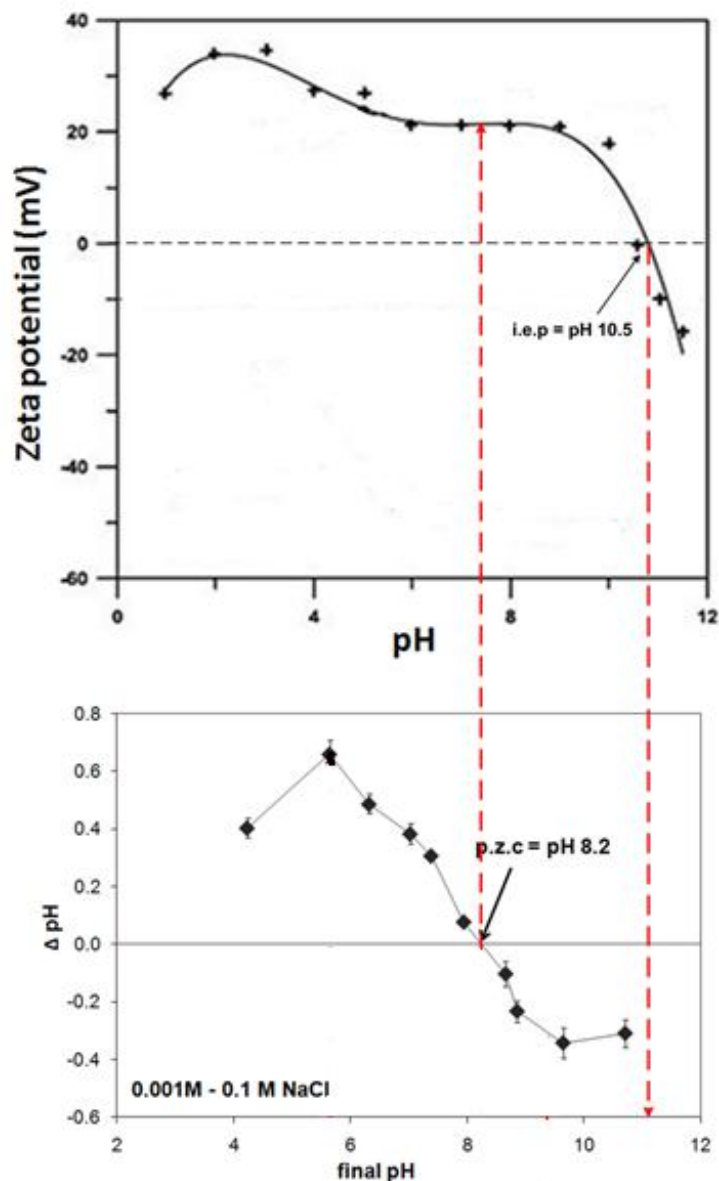


Figure 5.12 - A comparison of the iso-electric point (i.e.p) (Ney, 1973) and point of zero charge (p.z.c) of chrysotile (this study). The error bars represent 95% confidence interval of the average values.

5.5.3. The degree of isomorphous substitution in chrysotile

The long thin morphology of chrysotile fibres rendered electron microprobe analysis inappropriate, such that the composition of chrysotile is estimated based on the average composition of natural chrysotile specimens as previously determined by Brindley and Zussman

(1957). Table 5.9 gives the average elemental composition of chrysotile, demonstrating that it mainly comprises SiO_2 and MgO , as expected from its concomitant brucite and silica layers.

Table 5.9 - Typical composition of chrysotile (weight %) (Brindley and Zussman, 1957).

Compound	Weight %
SiO_2	41.83
Fe_2O_3	1.29
MnO	1.08
Al_2O_3	0.30
FeO	0.08
MgO	41.39
H_2O	13.66
Total	99.63

Using the same procedure as for muscovite and vermiculite, the calculated number of cations is shown in Table 5.10. Table 5.11 then shows the categorization of these cations into the tetrahedral and octahedral layers based on the ideal formula of chrysotile which is presented in Figure 5.13.

Table 5.10 - Typical number of cations in a single crystalline cell of chrysotile (Brindley and Zussman, 1957).

Cation	No. cations in formula
Si^{4+}	1.99
Fe^{3+}	0.05
Mn^{2+}	trace
Al^{3+}	0.02
Fe^{2+}	trace
Mg^{2+}	2.88

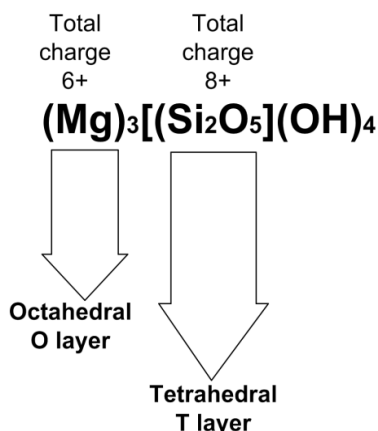


Figure 5.13 - Ideal classification of cations according to chrysotile formula.

Table 5.11 - Classification of cations in chrysotile.

Cation	Mean no. cations		Charge		Charge deficit	
	Ideal	Experimental	Ideal	Experimental		
Si^{4+}	2.00	2.00	8.00	7.99	0.00	Tetrahedral layer
Al^{3+}	-	1.50E-03		4.50E-03		
Total	2.00	2.00	8.00	8.00		
Mg^{2+}	3.00	2.90	6.00	5.80	0.00	Octahedral layer
Fe^{3+}	-	0.05		0.14		
Fe^{2+}	-	0.00		0.00		
Mn^{2+}	-	0.00		0.00		
Al^{3+}	-	0.02		0.06		
Total	3.00	2.97	6.00	6.00		

The results show that there is typically hardly any isomorphous substitution in the tetrahedral layer of chrysotile. In fact, the principal substitutions which may occur are in the octahedral layer, with minor replacement (less than 1% of cations in octahedral layer) of Mg^{2+} ions with Al^{3+} , Fe^{3+} , Fe^{2+} and Mn^{2+} ions, with full charge compensation leading to no resultant charge deficiency. This minimal substitution is mainly because isomorphous substitutions exacerbate the structural misfit between the tetrahedral and octahedral layers and therefore most natural specimens of chrysotile do not deviate from the ideal formula (Deer et al., 1992).

5.5.4. Proposed chrysotile surface charge distribution

Since there is no isomorphous substitution in the octahedral and tetrahedral layers, the charges on the tube lengths and edges are purely due to the dominant plane of measurement for each surface.

Since the tubes curl in such a way to expose the brucite layer on the outside (Figure 2.13), it is expected that the charge on this site will be similar to brucite. The outer layers are expected to carry a positive charge over a broad pH range, the magnitude of which is greatest in the range pH 6 to pH 9. This charge becomes less positive at alkali conditions greater than pH 9. The charge on either edge, on the other hand, is expected to undergo a change from positive to negative. The overall p.z.c, pH 8.2, represents the pH at which the charge differential between the tube length and edges is greatest. Therefore, the edge p.z.c must lie at a pH less than pH 8.2. An estimation of the edge p.z.c based on the weighted average between the p.z.c values of silica and brucite predicts an edge p.z.c in the range pH 6.5 to pH 6.7. Since there is little/no isomorphous substitution in the T and O layers, an estimation on this basis seems more adequately accurate when applied to chrysotile than in muscovite or vermiculite where additional ion speciation due to substitution may contribute towards the charge on the different surfaces. Figure 5.14 gives a highly simplified schematic representation of the proposed surface charge distribution of chrysotile fibres.

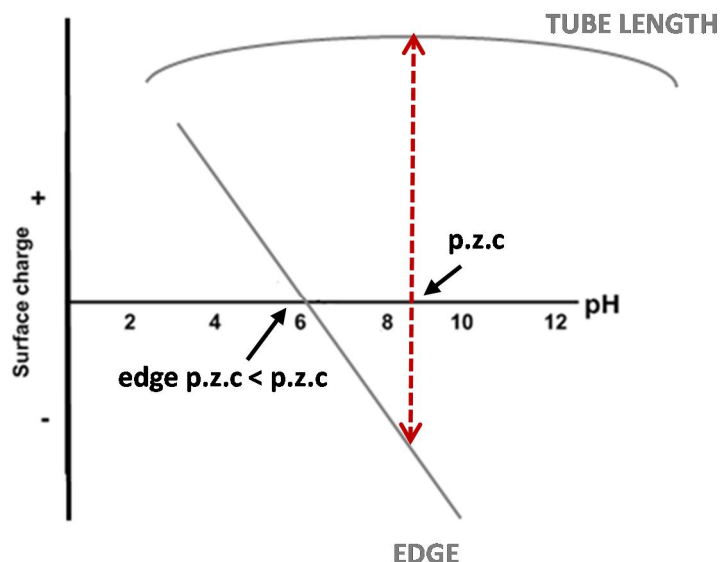


Figure 5.14 - Proposed surface charge distribution of chrysotile particles.

It must be noted that although it has been suggested that chrysotile is anisotropically charged, the structure results in the brucite outer layer being more exposed than the silica layer. Moreover, with the high aspect ratio of the fibres, the charge on the tube length is more pronounced than on the tube edges. Therefore, although individual fibres may be anisotropically charged, the dominance of the brucite layer is important and results in the seemingly near isotropic behaviour, which is manifested by the small divergence in the apparent iso-electric point, net point of zero charge. This also concurs with the combined results of the electrophoretic and zeta potential measurements which indicated a net positive charge.

Given the high aspect ratio of individual fibres, it seems unlikely that the charge on the edge of an individual fibre could ever counteract the charge on the tube length. Due to the high degree of entanglement that occurs in suspension, the charge differential could be more representative, not in terms of fibre-fibre interactions but with regards to interactions between fibre clumps, in which case the p.z.c. may reflect a balance between clumps of fibres. However, this is all speculative and the long, thin morphology and flexible nature of chrysotile fibres render the surface charge analysis of chrysotile challenging. The charge distribution serves as a description of charge, based on the measurements used in this study.

5.6. DISCUSSION

The degree of charge anisotropy of each mineral has been estimated, based on a comparison of the zeta potential and potentiometric titration data. This was then correlated to the degree of isomorphous substitution, which served as a proxy for the degree of negativity on the basal plane and hence the degree of charge anisotropy. A summary of the measured p.z.c, i.e.p and cations in T layers due to isomorphous substitution is given in Table 5.12.

Table 5.12– Summary of surface charge data for the minerals under study.

	Quartz	Muscovite	Vermiculite	Chrysotile
Iso-electric point (pH)	2	5.4	3.3	8.2
Point of zero charge (pH)	2	4.6	8.4	10.5
Cations due to isomorphous substitution (%)	0	16	28	<1
	Isotropically charged	weakly anisotropically charged	strongly anisotropically charged	weakly anisotropically charged

Based on the similarity in the p.z.c and i.e.p values, quartz is isotropically charged. The consistency between the two illustrates the appropriate application of the zeta potential measurement for adequately accurate estimation of its charge properties. Together with the comparatively regular morphology observed in the previous chapter (relative to the phyllosilicates), the isotropic charge properties of quartz render it appropriate as a model system against which the colloidal behaviour of the phyllosilicates can be measured.

All the phyllosilicates show a deviation in the measured i.e.p and p.z.c values. This is characteristic of anisotropically charged particles and is expected since they comprise edges and faces of different charge properties. However, the difference between these values is quite small for muscovite, and this is supported by a comparatively low degree of isomorphous substitution. Vermiculite, on the other hand, shows a large deviation in the i.e.p and p.z.c values which corresponds to a much higher degree of isomorphous substitution. In fact, the degree of isomorphous substitution in vermiculite is almost double that measured in muscovite. Assuming similar contribution of pH dependent charges, this suggests that the overall negative charge on

the basal plane and indeed the degree of charge anisotropy is almost twice as much in vermiculite compared to muscovite. For this reason, muscovite is only 'weakly anisotropically charged' while vermiculite is 'strongly anisotropically charged'.

Charge anisotropy is important in defining the mode of particle interaction that is likely to occur in suspension, where strongly anisotropically charged minerals are more likely to form rheologically complex structures at conditions where the edges and faces are oppositely charged relative to weakly anisotropically charged minerals. However, the effect of charge anisotropy cannot be viewed in isolation in such a manner. The observed differences in charge anisotropy and indeed the significance of this charge separation must be related to the surface area and aspect ratios of the particles. It has been shown in the previous chapter that muscovite exists predominantly as long, smooth expansive sheets with high aspect ratios. This renders the edge charge more or less insignificant and the charge is most likely predominantly defined by the basal planes of marginally higher surface area. This also explains the observed near similarity in the measured p.z.c and i.e.p values since muscovite is likely to behave as if it were isotropically charged. The edges are not likely to play a decisive role in the colloidal behaviour. Here, the interactions between faces will be a dominant factor.

Vermiculite particles, on the other hand, were seen to occur as a combination of comparatively 'thicker' platelets of lower aspect ratio and as platelets with roughened surfaces of broken stepped edges. Although the platelets may have relatively higher aspect ratios than in muscovite, the basal plane is still dominant and face interactions are likely to play an important role in the structures which form in suspension. The presence of exposed edges, may however enhance the influence and relevance of the edge charge. In fact, the overall positive charge in the majority of the pH range ($< \text{pH } 8.3$) suggests a strong positive edge charge, of greater magnitude than the negative face charges, and this may be due to the presence of multiple edge sites. By this analysis, the charge anisotropy may be of significance for vermiculite and interactions between both edges and faces are likely to play a role in the suspension colloidal behaviour.

The importance of charge anisotropy in this case of chrysotile may be of even less significance, owing to the extremely high aspect ratio of the fibres. Surface charge effects may play a more decisive role between entangled structures than between individual fibres.

Chapter 6.

pH Mediated Particle Interactions In Aqueous Media

Summary

The likely modes of particle interaction in muscovite, vermiculite and chrysotile suspensions have been predicted as a function of solution pH. FF agglomeration is the most important aspect of colloidal behaviour for the platy minerals - muscovite and vermiculite. Interactions between faces are likely to dominate due to the low basal surface charge which promotes FF approach. This mode will prevail over others due to the large aspect ratio of the face to edge surface area. This translates to low apparent volume per plate and low suspension yield stress and viscosity. FF interaction forces are expected to diminish with a pH shift to alkali conditions and the particles re-orientate to allow association in EF/EE association. The maximum in the yield stress peak may be attributed to a likely transition from FF alignment to randomised EF/EE networks of the highest apparent volume. At even higher pH conditions, the net interaction EF, EE and FF forces diminish due to increasing electrostatic repulsion, approaching zero upon complete dispersion. Fibrous chrysotile particles, on the other hand, are easily entangled and form high yield stress suspensions over a broad pH range (pH 4 to pH 11). The surface charge of the edge and 'face' sites in this instance merely serve to increase the degree of entanglement in the range pH 5.5 to pH 9.

6.1. INTRODUCTION

The rheological behavior of a suspension is essentially determined by the forces that control the spatial arrangement and dynamics of the suspended particles. When under the predominant influence of repulsive forces, the particles tend to be positioned as far from each other as possible. Such suspensions are deflocculated and will be characterized by little/no yield stress. Conversely, aggregates will form when particle interactions are dominated by van der Waal forces of attraction. The aggregated structures immobilize the suspension medium and give rise to a suspension yield stress, the magnitude of which is dependent on the mode of particle association.

Clay studies have identified three modes of particle interaction, namely face-face (FF), edge-face (EF) and edge-edge (EE) as the main forms of interaction for platy minerals, with defined edge and face surfaces. These have different rheological characteristics, with FF aggregates forming lamellar tubular structures of low apparent volume and low suspension yield stress and viscosity. EE and EF aggregates, on the other hand, form rheologically complex voluminous structures with high suspension yield stresses and viscosities. Therefore, the aggregate structure plays an important role in explaining the rheological behaviour of phyllosilicate suspensions as a function of pH.

Particle characteristics such as morphology, size and surface area will also greatly affect the mode of particle association that is likely to occur in suspension. High electrolyte concentrations compress the electrical double layer and may elevate or depress the suspension yield stress, dependent on the solution pH and aggregate modification.

In this chapter, the particle interactions that are likely to form in muscovite, vermiculite and chrysotile suspensions as a function of pH are proposed. These are discussed in terms of the morphological properties and developed surface charge distributions in previous chapters. The proposed interactions will also be debated against existing theories of phyllosilicate aggregate formation.

6.2. PARTICLE INTERACTIONS IN MUSCOVITE & VERMICULITE SUSPENSIONS (PLATY)

One of the most debated aspects of the colloidal behaviour of phyllosilicates with a platy morphology is over the mode of particle interaction that is responsible for the yield stress trends observed as a function of pH. Many studies in this area have established the form of the pH-Bingham yield stress curve, originally postulated by van Olpen (1951) (Figure 2.24) (James and Williams, 1982; Permien and Lagaly, 1994; Johnson et al., 1998; Benna et al., 1999; Johnson et al., 2000; Lagaly and Zeisner, 2003; Burdukova et al., 2007; Yin et al., 2012). As such, this has been the basis of many studies focused on surface chemistry- rheology relationships. By this model, EF association should occur at $\text{pH} < \text{edge p.z.c}$, EE association in the pH region close to the edge p.z.c. and, provided the solid concentration is not too high, deflocculation at $\text{pH} > \text{edge p.z.c}$ (Rand and Melton, 1977). EF interactions are believed to be the dominant mode of particle interaction, resulting in a maximum in the yield stress peak as a function of pH (Luckham and Rossi, 1999).

This concept has been successfully applied in explaining the influence of electrolytes on rheological characteristics, and has also been beneficial in the development of methods to estimate edge p.z.c values in kaolinite dispersions (Schofield and Samson, 1954; Rand and Melton, 1977; Johnson et al., 1998). However, the applicability of this model, and in particular the presence of EF interactions at low pH conditions in montmorillonite suspensions has been questioned. Primary reasons for these objections lie in the fact that many measurements supporting the concept of edge-face interactions have been conducted in basic pH conditions ($>\text{pH } 8$), most likely above the iso-electric point of the edge surface (e.g. Miano and Rabaioli, 1994). Theoretically, the suspension pH must be lower than the edge iso-electric point for a positive charge and edge-face interactions to occur (de Kretser et al., 1998). Results in contrast to van Olpen's model were initially contended by Norrish (1954) who suggested that a more likely explanation for the gelation in montmorillonite suspensions may be the mutual repulsion of the particles as a result of interactions between their electrical double layers, rather than the formation of EF interactions. The absence of EF interactions, particularly at low pH has since

been disputed and demonstrated by other researchers (e.g. M'Ewen and Pratt, 1957; de Kretser et al., 1998). In some of these studies, the existence of FF and EE coagulated structures in the regions postulated by van Olpen, (1951) has been established, but there has been little evidence for EF aggregates (Rand et al., 1978).

A likely explanation for the observed differences between kaolinite and montmorillonite has been attributed to the high aspect ratio of montmorillonite platelets relative to kaolinite particles. Due to the small area of the edge, the electrostatic attraction between the edge and the face is small compared to the repulsion between faces when two particles approach perpendicular to each other, such that EF association is unlikely (Rand et al., 1978). Moreover, it is expected that the face double layer will extend out sideways, screening out any positive charge developed by the edges such that invariant mobility is predominantly due to the basal faces and FF agglomeration (Callaghan and Ottewill, 1974; Tateyama et al., 1977). This is supported by Secor and Radke (1985) who found by numerical simulation that the electrostatic field from the basal plane may spill over to dominate the positive edge surface. Bourg et al. (2007) also showed that the negative electric field from the basal plane of a disc shaped clay mineral near the edge surface is mainly controlled by the particle thickness. This does not exist in kaolinite particles, with their edges of comparatively substantial surface area. Therefore, compelling evidence for the existence of EF interactions in kaolinite suspensions is expected. In fact, van Olpen's model cannot be deemed as wrong, but rather that its applicability is limited by aspect ratio considerations.

Another consideration that must be made in determining the modes of particle association is the surface crystallinity. Investigations on the effects of kaolinite surface structure by Zbik and Smart (1998) and Zbik et al., (2010) demonstrated that kaolinites can exist as poorly ordered structures, with stair step subhedral flakes and exposed broken edges on the basal faces of larger particles. These low crystalline particles were seen to promote EE and EF aggregation, while smoother platelets resulted in more compact FF associations upon settling. (Du et al., 2010). This suggests that complexities in the surface structure of phyllosilicates may also be important in determining the aggregate structures that form at low, medium and high pH values (Gupta et al., 2011).

Therefore, this is an area where fundamental research is still warranted. However, significant factors that should be considered in predicting the particle interactions in muscovite and vermiculite suspensions in this study are

- (1) The colloidal behaviour of muscovite suspensions is a result of the structural buildup of smooth, high aspect ratio platelets.
- (2) The colloidal behaviour of vermiculite suspensions is a result of the structural buildup of high aspect ratio platelets. The presence of poorly ordered, low crystalline particles comprising micro-islands and individual crystallites attached to the basal surfaces of larger platelets may also affect the structures that form in vermiculite suspensions.
- (3) The aspect ratio, coupled with interaction forces will result in suspensions with a combination of FF, EF and EE aggregates, depending primarily on the solution pH.
- (4) The use of 0.01M NaCl as a background electrolyte enhances double layer compression and screens out the repulsion between like charged particles to allow closer approach of particles and subsequent coagulation.

6.2.1. Muscovite suspensions

The yield stresses of concentrated suspensions of muscovite were measured using the direct yield stress measurement technique devised by Nguyen and Boger, (1983). Measurements were conducted over the range pH 3 to pH 10. The yield stress curve is shown in Figure 6.1. The curve shows a steady increase in suspension yield stress through the acidic pH range, with a yield stress peak observed at circa pH 6.5. A decrease in yield stress to pH 10 is observed thereafter.

It has already been proposed that muscovite particles are weakly anisotropically charged, with the faces carrying a negative charge that is comparatively lower than in vermiculite particles. On the basis of the high aspect ratio of muscovite platelets, it is expected that at low pH, the negative charge emanating from the face plane spills over the edge surfaces and as a result, the positively charged edge is swamped by the negative electrostatic field (Callaghan and Ottewill, 1974; Chang and Sposito, 1994; Tateyama et al., 1997; Gupta et al., 2011). At low electrolyte concentrations, there is a very high potential barrier to close particle approach. However, a

background electrolyte concentration of 0.01M NaCl may well fall at the threshold for weak double layer compression and facilitates close approach and coagulation. Compression of the electrical double layer occurs to a point where the particles are predicted to fall into a deep secondary minimum (Figure 2.17b) (Tateyama et al., 1997; de Kretser et al., 1998). At pH values below the edge p.z.c (estimated at circa pH 7 for muscovite) the system of lowest free energy is one in which particles are associated in a FF fashion (Rand and Melton, 1976). This is in agreement with more recent findings by Gupta et al., (2011), who used a combination of potentiometric data and surface force measurements to determine the DLVO interactions and to demonstrate that FF aggregation showed favorable interaction in acidic solutions. It is therefore anticipated that the muscovite particles will orientate themselves dominantly in a FF arrangement, forming lamellar tactoids or quasi crystals at conditions less than the edge p.z.c (pH 7) (Gupta et al., 2011; Schofield and Samson, 1954). The net result is a low number of flow units and an overall low apparent volume structure in muscovite suspensions. This translates to the low suspension yield stresses observed at low values pH in the muscovite yield stress curve.

As the pH is increased, the FF force is expected to diminish and the particles re-orientate to allow association into EF and EE interactions (Rand and Melton, 1976). This transition has been validated by calculations on DLVO interactions and has been attributed to the progressive growth of tactoids into thicker edge surfaces, promoting charge anisotropy and subsequent EE and EF aggregate formation (Gupta et al., 2011). In accordance with van Olphen's model, EF association should occur at $\text{pH} < \text{edge p.z.c}$ (i.e. $< \text{pH } 7$) and EE association should occur in the pH region closer to the edge p.z.c. Therefore, although the muscovite particles are expected to predominantly exist in FF arrangement below pH 7, the progressive transition to more complex EF and EE particle association occurs as the pH increases. The volume fraction of particles is obviously constant, but the volume occupied or swept out by an individual particle is maximized through the transition from a 'card pack' structure to a more voluminous 'house of cards' structure, resulting in a net increase in the apparent volume and yield stress of the suspension (Tateyama et al., 1997). The maximum in the yield stress peak observed at pH 6.5 may be a result of a likely transition from FF alignment to randomized EF or EE aggregates of the highest apparent volume.

As the pH is increased further ($> \text{pH } 7$), there is a reduction in the magnitude of the surface charge density on the edge surfaces and a reduction in the FF and EF interaction forces is observed. At pH values close to the edge p.z.c, the edges can either carry a weak negative or positive charge, while the faces maintain their weak negative charge. This would result in EE association (van Olphen, 1963; Schofield and Samson, 1954). The presence of EE aggregates as the predominant mode of particle interaction in this pH range has been confirmed in kaolinite and montmorillonite suspensions using CryoSEM imaging analysis and viscoelastic measurements (Gupta et al., 2011). At even higher pH conditions, ($> \text{pH } 8$), the net EE, EF and FF interaction forces are expected to decrease due to the increasing electrostatic repulsion between like-charged edges and faces. This results in the observed reduction in suspension yield stress in Figure 6.1. Complete dispersion will occur when the net interaction forces are repulsive, and a negligible shear yield stress is measured.

In this way, the yield stress trend for muscovite can be explained. It must be noted that although Figure 6.1 designates specific modes of interaction to different pH regimes, in the case of high concentrations of anisotropically charged and asymmetrically shaped particles, exclusive existence of one mode of interaction is unlikely.

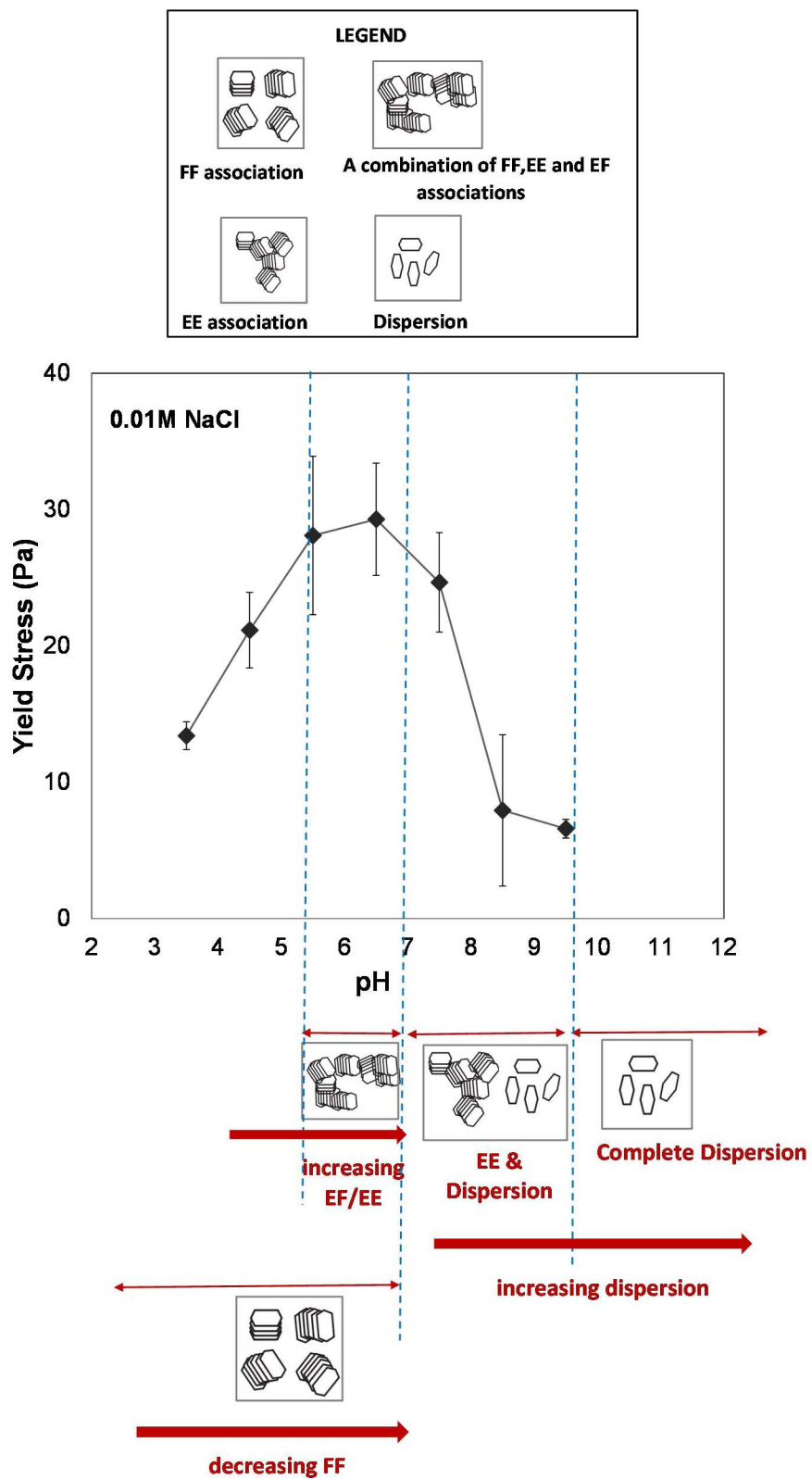


Figure 6.1 - Proposed particle interactions of muscovite suspensions as a function of pH. The error bars represent the 95% confidence interval.

6.2.2. Vermiculite suspensions

The yield stress curve for vermiculite suspensions as function of pH is given in Figure 6.2. The curve shows that vermiculite suspensions are characterised by low yield stresses at low acidic pH conditions (\leq pH 4). The yield stresses increase steadily with an increase in solution pH. Unlike muscovite, vermiculite particles do not have a single peak value for the point of maximum yield stress. Instead, there exists a pH range, pH 6 to pH 8, over which vermiculite aggregation is most apparent. Upon further increase in pH, a decrease in the suspension yield stress is observed.

It has been proposed that vermiculite particles are strongly anisotropically charged, with faces that carry a negative charge of comparatively higher magnitude than muscovite. Vermiculite platelets, although of a lower aspect ratio than muscovite, still have a high lateral extent relative to thickness. Moreover, the attachment of smaller platelets onto larger basal plane surfaces in some particles results in more amorphous surfaces than in muscovite.

It is anticipated that vermiculite particles will orient themselves predominantly in a FF manner at pH values less than the edge p.z.c. For vermiculite particles, this was broadly estimated at a pH $>$ pH 8.4 (the overall p.z.c of vermiculite particles). This estimate is in agreement with the yield stress curve which shows a reduction in suspension yield stress above pH 8.4, with the yield stress values approaching negligible values at pH greater than pH 11. Therefore, the edge p.z.c of vermiculite can be assumed to be in the range pH 8.4 $<$ edge p.z.c $<$ pH 11. Similar to muscovite, the potential for FF agglomeration in this range is enhanced by the use of 0.01 M NaCl background electrolyte.

It is expected that progressive growth of the lamellar tactoids throughout the acidic pH range will result in thicker edges such that EF and EE interaction forces are enhanced with increasing pH. The net result is an increase in voluminous structures as pH increases. The presence of already poorly ordered platelets contribute to the random orientation of particles during transformation to EF and EE structures, as has been shown in the sedimentation of poorly ordered kaolinites (Du et al., 2010). Therefore, the transformation to EF and EE formation may be enhanced in vermiculite suspensions. This, coupled with the high charge anisotropy between edges and faces, is likely to

result in a higher proportion and stronger EF and EE structures than in muscovite suspensions. The maximum yield stress in the range pH 6 to pH 8 may be attributed to region over which transition from FF to EE and EF structures results in networks of highest apparent volume.

Above this pH, FF and EF interaction forces are expected to diminish as the charge differential between edges and faces decreases. EE associations are most likely to exist in this range. The observed decline in the suspension yield stress at alkali pH conditions can be attributed to the onset of dispersion which results from increasing electrostatic repulsion between negatively charged edges and faces. Based on the yield stress curve data, complete dispersion is expected to occur at $\text{pH} > \text{pH } 11$ where negligible yield stresses are observed.

The yield stress curve of vermiculite suspensions with the proposed modes of particle association as a function of pH is shown in Figure 6.2.

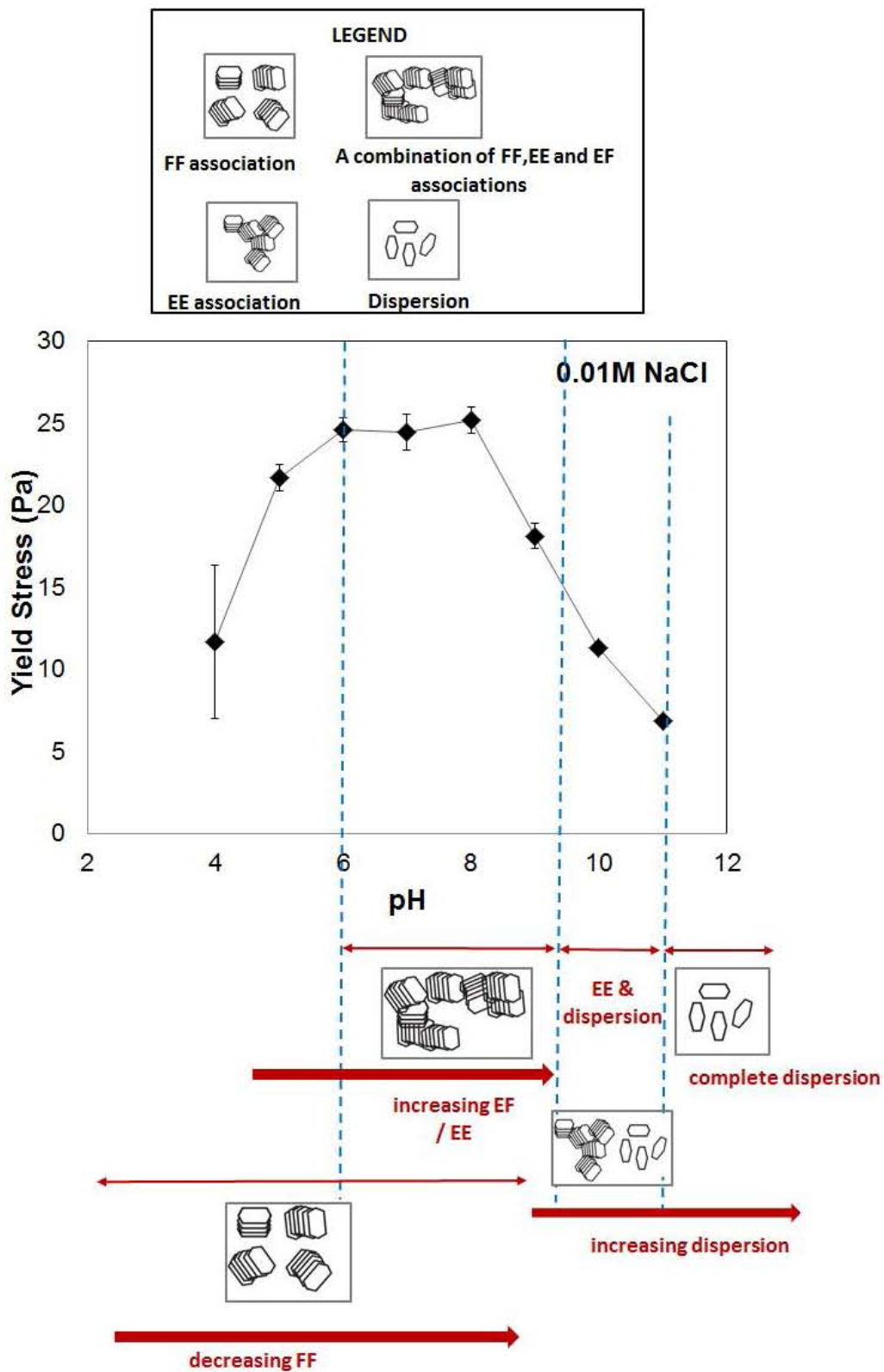


Figure 6.2 - Proposed particle interactions of vermiculite suspensions as a function of pH. The error bars represent the 95% confidence interval.

6.3. PARTICLE INTERACTIONS IN CHRYSOTILE SUSPENSIONS (FIBROUS)

The yield stress curve of chrysotile suspensions as a function of pH is shown in Figure 6.3. The curve shows that chrysotile suspensions are characterized by extremely high yield stresses throughout a broad pH range (pH 4 to pH 11), indicating that although rheological behaviour in this case may be affected by surface charge, it may not play a primary role. The long, thin morphology and high degree of flexibility of the fibres enhances the probability of particle interactions, resulting in the naturally occurring entangled meshes. Since this is a physical property, it is not dependent on solution pH and fibres are entangled throughout the pH range, resulting in structures with high yield stresses. The surface charge properties may play a role, not so much in determining the orientation of particles as was observed with the platy minerals, but rather in the degree of entanglement that occurs with pH variation.

The degree of entanglement in this case is then dependent on the magnitude of the interaction forces between fibre ends and tubular surfaces. As a result, the changes in suspension yield stress occur in three distinct regions. In the first region (between pH 4 and pH 5.5), yield stress increases with increasing pH. In this pH range the net interaction force is retarded by the electrostatic repulsion between like charged sites. However, as the magnitude of the positive charge on the edges decreases with increasing pH, attractive forces become stronger and the suspension yield stresses increase. The tangled formation of chrysotile fibres in suspension is real and observable and not just postulated. This is evidenced by the optical micrograph of chrysotile fibres suspended in water (Figure 6.3). Here, the randomized entanglement is observed.



Figure 6.3 – An optical micrograph of chrysotile fibres suspended in solution. The characteristic entangling and heterocoagulation of the flexible fibres into ‘clusters’ is evident.

In the second region, the yield stress reaches a maximum and plateaus at the highest yield stress values between pH 5.5 and pH 9. A comparison of the chrysotile yield stress and zeta potential curve (Figure 5.12) shows that the yield stress peak range (pH 5.5 to 9) coincides with the region over which the zeta potential is also at an equilibrium, suggesting that surface charge plays a role in the modes of particle association that occur in suspension. The edge p.z.c (start of the range over which yield stress is maximum) represents the pH at which attractive forces between fibre edges and ‘faces’ become dominant due to oppositely charged sites and the overall p.z.c (circa end of the range of maximum yield stress) represents the pH at which the charge differential is greatest. Therefore, in this range, which the charge differential and interaction forces between the fibre edges and ‘faces’ is greatest and intra clump fibre-fibre entanglement is enhanced. Surface charge may also play a role in promoting coagulation between fibre clumps (inter-clump entanglement).

In the last region, a significant decrease in yield stress between pH 9 and pH 11 is observed. Here, interaction forces begin to decline due to lessening of the positive charge on the fibre ‘faces’. The net result is a decline in the suspension yield stress.

The changes in degree of entanglement in chrysotile suspensions as a function of pH are shown in Figure 6.4.

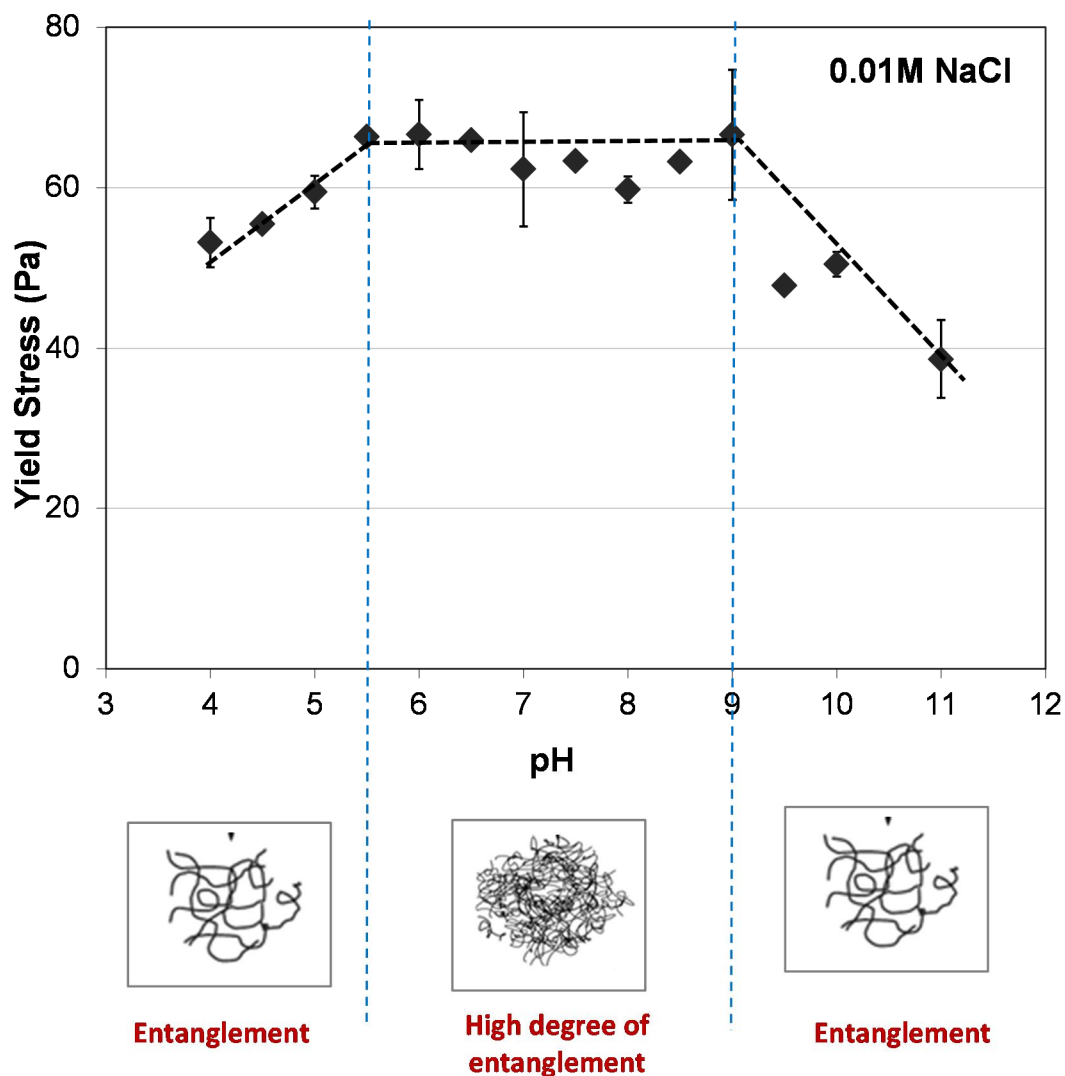


Figure 6.4 - Proposed particle interactions of chrysotile suspensions as a function of pH. The error bars represent the 95% confidence interval.

6.4. DISCUSSION

The orientation of muscovite, vermiculite and chrysotile particles has been predicted as a function of pH. Indeed surface charge is important in defining the modes of particle interaction that are most likely to occur in suspension. The more complex the structure formed, the higher the suspension yield stress.

Face-face (FF) agglomeration is the most important aspect of colloidal behaviour for the platy minerals muscovite and vermiculite, specifically in the acidic pH range. The preferential alignment of particles in this manner is enhanced by the high aspect ratio of the particles. Therefore, these particles are expected to be predominantly oriented in a FF fashion, with a gradual progression to randomized EF and EE aggregation. Vermiculite surfaces are poorly ordered relative to smooth muscovite platelets and it is anticipated that this will promote the alignment into EF and EE aggregates, effectively resulting in more rheologically complex suspension behaviour. The prevalence of FF agglomeration, particularly in the acidic pH range is contrary to van Olpen's original model, which predicts EF aggregation at these conditions. However, van Olpen's model is still valid in the alkaline pH region, where EF alignment is favored with an increased edge thickness (and hence edge charge and overall charge anisotropy).

Chrysotile behaves in a different manner to the platy minerals. The high degree of entanglement is a consequence of the high aspect ratio and flexibility of the fibres in suspension such that charge anisotropy effects merely serve to exacerbate the degree of entanglement and resultant suspension flow behaviour.

The rheological behaviour and subsequent rheological problems experienced during the aqueous processing of phyllosilicate bearing suspensions will depend on the pH at which the operation is run. Most unit operations in the mineral processing industry are run in the range pH 8 to pH 9. This is also the natural pH of most silicates, and certainly that of the phyllosilicates under study. An indication of the expected suspension rheological behaviour can be approximated, albeit on a preliminary level.

Chapter 7.

RHEOLOGY OF SUSPENSIONS OF PURE MINERALS

Summary

The rheological properties of suspensions of each phyllosilicate mineral at pH 9 have been investigated. These have been compared to quartz suspensions as a means to demonstrate deviations in flow behaviour from isotropically charged regular shaped minerals. The observed rheological behaviour is in agreement with the predicted modes of particle association. Quartz suspensions are characterised by the lowest yield stresses and viscosities. Vermiculite suspensions, on the other hand, have higher yield stresses than muscovite, presumably due to a higher charge anisotropy and aspect ratio effects. However, both minerals are characterized by low suspension viscosities at high shear rates. The long, thin morphology and flexibility of chrysotile fibres results in suspensions with extremely high yield stresses and viscosities at low concentrations (< 1% solids by volume). The rheology of the minerals in their pure form becomes increasingly complex in the order quartz < muscovite < vermiculite < chrysotile, suggesting that, on a weight by weight basis, muscovite bearing suspensions are least likely to present rheologically related issues within the context of high shear mineral processing operations.

7.1. INTRODUCTION

The surface charge and morphological properties of all the minerals under study have been analysed and discussed. As a result, conformational changes as a function of pH have been proposed for each mineral. These estimations have been made, taking into consideration the contributions of factors such as aspect ratio, the degree of charge anisotropy, particle morphology and effective volume effects.

Having estimated the likely modes of particle association through the acidic to alkaline pH range, it is now possible to analyse the rheology of suspensions of each pure mineral at a fixed pH. This creates a well-controlled environment in which the surface charge distributions and orientation of particles have been proposed. In each case, it is expected that the rheological behaviour can then be explained or linked to the estimated form of particle interaction at that pH condition. In this work, analysis of the suspension behaviour is conducted at pH 9. This is the natural pH of many silicates and is a common pH condition at which many flotation systems are operated. Therefore, analysis at this pH gives a good preliminary approximation of the rheological behaviour of the minerals when in suspension within an industrial context. It must also be noted that the applicability of this work is aimed at high shear mineral aqueous processing operations such as in flotation and comminution. Therefore, the rheological analysis in this chapter is conducted mainly within the context of high shear rate regimes.

The rheological behaviour of suspensions of each phyllosilicate mineral is explained in terms of the suspension Bingham yield stress and Bingham viscosity. The choice of this analytical technique is elucidated in the following section. The rheological properties of suspensions of each phyllosilicate mineral are compared to those of quartz suspensions. It has been well established that this mineral is not likely to present rheological problems when present in dilute suspensions. Therefore, it serves as a good reference material for non-complex rheological behaviour. Comparison with quartz, in this case, provides a 'standard' against which the rheological properties of all the phyllosilicates can be pegged. This then facilitates a rheological classification of the phyllosilicates under study, albeit on a preliminary basis.

7.2. ANALYTICAL APPROACH

The rheological analysis in this work has not investigated the time dependent behaviour of phyllosilicate minerals in suspension. Instead, it has focused on the analysis of steady shear data at which transient stress or time relationships were minimized. Indeed, the thixotropic (and antithixotropic) time dependent suspension behaviour of phyllosilicate minerals is of practical importance in the mineral processing context from the handling or processing of ‘rested’ material viewpoint (e.g. during tailings handling) and also in analyzing particulate material settling behaviour. In these applications, the time dependent properties have been beneficial in understanding the microstructural formation and deformation characteristics of minerals (e.g. de Kretser et al., 1998; Du et al., 2010). However, this study was more interested in the flow behavioral properties of the phyllosilicates in dynamic systems of high shear, as would be applicable in e.g. a flotation cell. Therefore, the discussion and analysis in this chapter is not focused on the rate of structural breakdown over time, but rather on the high shear-dependent flow phenomena of the phyllosilicate suspensions.

The rheological behaviour of the suspensions was investigated as a function of solids concentration, such that the suspensions under investigation varied from extremely dilute to highly concentrated. As a result, the direct yield stress measurement derived by Nguyen and Boger (1983), was not applicable throughout the studied range of concentrations, since it is most appropriate in analyzing slurries of high yield stress (circa $> 20\text{Pa}$) (Nguyen and Boger, 1983; Nasroti, 2010). Therefore, estimation of the rheological properties (of all suspensions) was best achieved through the application of constitutive rheological relationships (Equation 2.1), from which the yield stress and viscosity terms could be derived.

The rheograms observed in this study exhibited pseudo plastic behaviour with the prominence of a yield stress with increasing concentration. In a typical pseudo plastic rheogram, at low shear rates (e.g. in the lower one third of a rheograms in a $0\text{-}300\text{ s}^{-1}$ cycle), suspension structure resists deformation, and sometimes, flow does not even occur until destruction of the internal networks

is completed (Barnes, 1999). In this region, viscosity decreases steadily with increasing shear (shear thinning). Such behaviour has been attributed to

- (a) Structural degradation due to hydrodynamic effects where the rate of particle dissociation is greater than the rate of association,
- (b) The release of trapped inter aggregate bulk fluid leading to a gradual decrease in effective volume concentrations and
- (c) The progressive alignment of particles into the direction of flow (Triantafillopoulos and Smith, 1998).

At higher shear rates, internal structure breaking due to shear competes with structure-forming due to the increased frequency of collision between particles, such that viscosity changes are less prominent. This is the region of interest in this study.

Ideal characterization of pseudo plastic behaviour at both low and high shear rates may be best achieved using the Herschel Buckley model (Equation 2.1b). This model allows prediction of the suspension yield stress, viscosity and shear thinning index, which from a fundamental viewpoint are each indicative of the suspension flow behaviour at different shear conditions. The suspension yield stress is estimated at *zero shear* and is the initial force required to initiate flow of a suspension. It is indicative of the complexity of the free forming structures in suspension. The viscosity and shear thinning index quantify the degree of structural breakdown with shear or energy input, where the shear thinning index is indicative of the degradation and progressive alignment of particles into the direction of flow. Shear thinning is more prominent in the low shear region. As shear is increased, shear thinning becomes less evident and viscosity changes are less prominent. Under such conditions, it can then be assumed that the suspension viscosity is indicative of the ease of flow of the suspensions at *high shear* rates. This is more representative of unit operations within the mineral processing industry. Therefore, the Herschel Buckley model facilitates rheological analysis of pseudo plastic fluids from yielding to flow at high shear rates.

Indeed such an analysis would have been ideal for the pseudo plastic behaviour observed. However, characterization of the low shear rate range was often compromised by the noisy shear stress/shear rate data observed in some suspensions (particularly in chrysotile and vermiculite

suspensions). This made application of the Herschel Buckley model and derivation of the shear thinning index across the entire range of studied minerals difficult. In order to obtain a comparative analysis, and to maintain uniformity, it was decided that rheological characterization of the rheograms would exclude the regions of noisy data (typically $< 50\text{s}^{-1}$). With low shear rate/ stress data excluded from the analysis, the rheograms were now more accurately described by the Bingham model (Equation 2.1e). In this model, a characteristic shear thinning index of 1 is assigned to all suspensions. The Bingham yield stress is approximated by a linear regression to zero shear and the Bingham viscosity is given by an average of the shear stress/shear rate gradient over the analysed shear rate range.

Indeed there are some shortcomings to this approach and these include

- (1) The overestimation of the yield stress value due to the nature of the linear approximation which does not take into account the curvature that may be present at low shear rates,
- (2) It does not facilitate comparison of the shear thinning index for different suspensions such that information regarding structural deformation, particularly at low shear rates, is not adequately represented.
- (3) It estimates a viscosity over a predominantly high shear rate range and in that way may be more representative of moderate to high shear induced flow behaviour.

The limitations of such an approach are of more significance in studies aimed at underpinning the mechanisms of structural degradation or particle alignment of particulate material with shear (e.g. understanding structural changes induced by raking processes for bed density estimations) or at low shear (e.g. during the analysis of settling material). However, this study is aimed at characterizing moderate to high shear flow behaviour which is more characteristic within the flotation or comminution context. Moreover, the study seeks to merely compare and detect any relevant trends or differences from one phyllosilicate to another. The approach employed here, through application of the Bingham model, adequately achieves this. The derived yield stress and viscosity values need not be treated as absolute values, but must rather be considered as comparative approximations within the context of this study. By this application, the Bingham

yield stress is an indicator of the degree of complexity of the structures that form in suspension (attributable to physico-chemical properties) of one mineral relative to another and the Bingham viscosity is simply a predictor of the flow properties of the suspension, as applied to pumping, grinding and mixing. These therefore have strong implications for the processes of flotation and comminution from both energy requirements and process efficiency.

Figure 7.1 gives examples of typical rheograms observed with the Bingham model fitted to estimate the Bingham yield stress and viscosity.

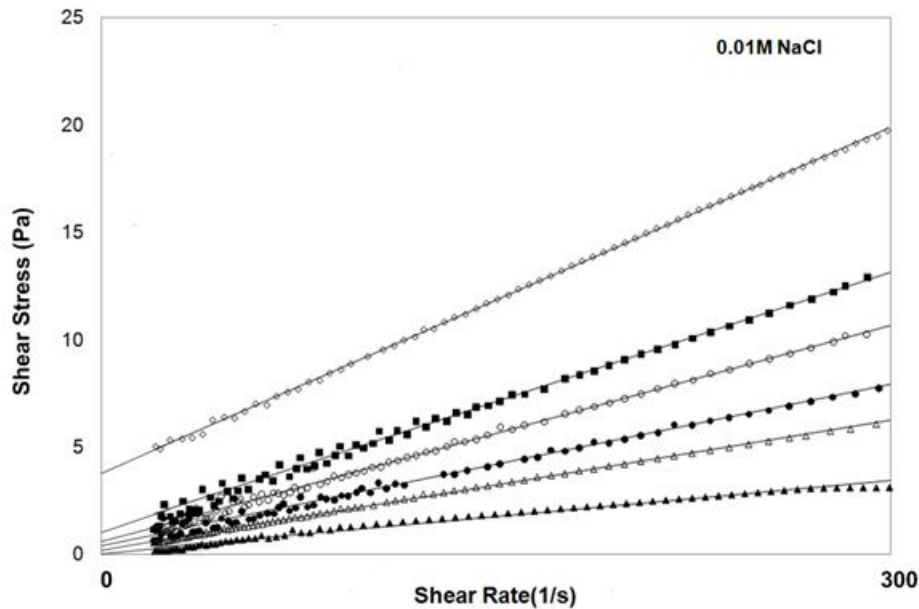


Figure 7.1 – Example of typical rheograms observed with the phyllosilicate suspensions. The rheograms are fitted with the Bingham model in the shear rate range where data could be analysed.

7.3. THE RHEOLOGY OF MUSCOVITE AND VERMICULITE SUSPENSIONS

Rheology tests were conducted on suspensions of increasing concentrations of pure muscovite and vermiculite at pH 9. The rheograms exhibited pseudo plastic behaviour and were fitted with

the Bingham model as a means to estimate the Bingham yield stress and Bingham viscosity as has been discussed. These were compared with quartz suspensions, whose rheology was also measured at pH 9. It has been demonstrated that quartz is isotropically charged and has a more regular morphology than the phyllosilicates. Therefore, this comparison serves to demonstrate the rheological differences that may result due to these dissimilarities. A comparison of the Bingham yield stresses of suspensions of pure muscovite, vermiculite and quartz as a function of solids concentration at pH 9 is shown in Figure 7.2.

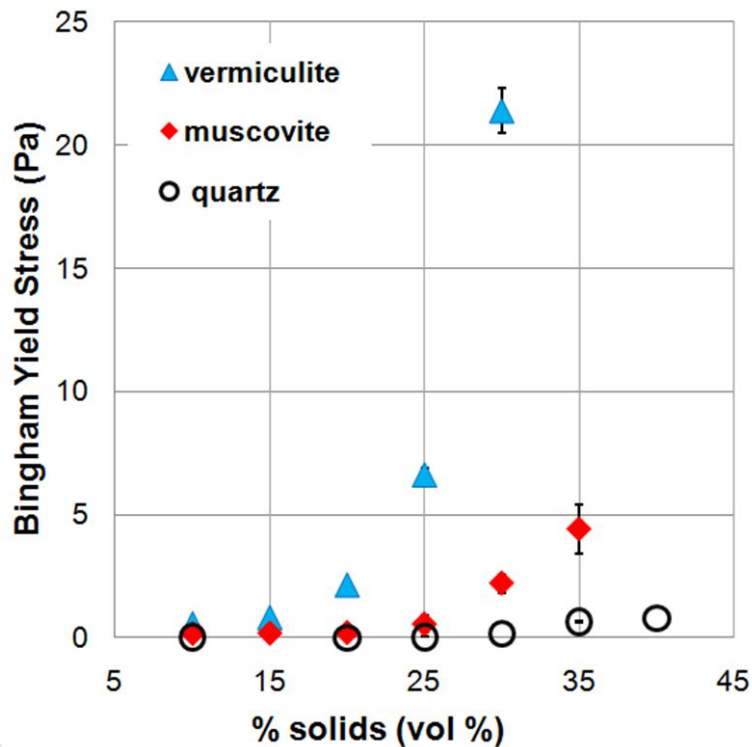


Figure 7.2 – A comparison of the Bingham yield stresses of suspensions of pure vermiculite, muscovite and quartz. The errors bars represent the 95% confidence interval of the average values.

The yield stress is the initial force required to initiate flow of a suspension and is an indicator of the complexity or strength of the formed network structures. A high yield stress indicates an intricate static network structure which requires a large force to effect deformation and movement in the direction of flow. For all minerals, the results show a characteristic exponential increase in suspension yield stress with solids concentration. As the concentration of particles in suspension increases, so does the probability of particle interaction. This enhances the likelihood

of aggregation, resulting in suspensions of increasing yield stresses. Suspension rheology, at low solids concentration is primarily dictated by the particle-liquid interfacial interactions. Under shear, there is enough liquid phase between particles to lubricate them, and the interaction between particles is mainly conducted by the liquid. With increasing solids content, however, the mean distance between particles decreases and particle-particle interactions and hydrodynamic effects influence the flow (Prestidge, 1997).

The results show that suspensions of vermiculite are characterised by the highest Bingham yield stresses, followed by suspensions of muscovite and finally quartz. In particular, vermiculite suspensions have high yield stresses (up to 20 Pa), muscovite suspensions have low but present yield stresses ($< 5\text{Pa}$) and quartz suspensions have little to no yield stresses ($< 1\text{Pa}$). The differences in the yield behaviour of these minerals suggests that the conformation of particles in vermiculite suspensions results in the formation of more complex structures than in muscovite which in turn forms more complex aggregates than in quartz suspensions. This can be supported by considering the estimated particle interactions of the different minerals at pH 9.

The surface charge analysis of quartz has demonstrated that quartz particles are strongly negatively charged at pH 9 (Figure 5.1). The p.z.c (and i.e.p) of these particles occurs at around pH 2. To re-iterate, for isotropically charged minerals, this is the pH condition at which maximum particle aggregation is expected. Particle aggregation decreases with a larger deviation from the p.z.c value. Therefore, since pH 9 lies well away from the p.z.c., particle aggregation is less likely. At a fixed solids concentration, dispersed particles will occupy a certain portion of the total volume available, which consequently is excluded from occupation by the continuous phase. The effective volume is directly proportional to the size and shape distribution of the dispersed phase. For the colloidal sizes and angular particle morphology displayed by quartz particles, it is expected that individual particles are easily mobilized. The motion of the particles will also depend on the surrounding immobilized double layer which is dragged along the particles' path line. It must be remembered that the overall background electrolyte of 0.01M NaCl may well be on the threshold for double layer compression and weak coagulation, such that close particle approach is enabled and random coagulation may be a possibility. Therefore, it is expected that at pH 9, mutual repulsion between adjacent negatively charged particles results in a

dispersed state, with the possibility of electrolyte induced random coagulation. Therefore, suspensions characterised by little or no yield stresses are likely in quartz suspensions.

On the other hand, it has been proposed that vermiculite particles are comparatively strongly anisotropically charged, with a p.z.c value at pH 8.4 (Figure 5.8). While FF aggregation is a dominant factor, particularly at acidic pH conditions, the development of EF and EE interactions in suspension is expected at pH 9 (Figure 6.2). The proportion of these aggregates is enhanced by the high charge anisotropy of particles. Moreover, pH 9 is close to the measured p.z.c. of vermiculite particles, which although not representative of the point of maximum aggregation in this case, is indicative of the point at which there exists a close balance between positive and negative charges. This then increases the strength of aggregates that form in suspension. Therefore, at pH 9, vermiculite suspensions are expected to comprise a combination of FF, EE and EF aggregates, with a relatively higher proportion of EE and EF structures in suspension, as FF aggregation forces diminish. The platy shape of vermiculite particles results in high effective volume effects. This, together with the randomised coagulation attributed to the electrolyte concentration, most likely results in the higher suspension yield stresses observed.

In the case of muscovite, however, it was proposed that the faces carry a weaker negative charge than vermiculite, owing to a lower degree of isomorphous substitution. The p.z.c. value was estimated at pH 4.6 (Figure 5.3). This is far from pH 9, indicating that it is unlikely that both positive and negative charges are present. Furthermore, since pH 9 is above the p.z.c value point, this indicates that muscovite particles carry an overall negative charge at this condition. This suggests that there are three possible modes of particle-particle association for muscovite:

- (1) Both edges and faces could be negative, resulting in an entirely dispersed system characterised by very low yield stresses;
- (2) The edges could have a near neutral charge, while the faces maintain their weak negative charge. This would result in edge-edge coagulation with low yield stresses and
- (3) Finally and most likely, a combination of both dispersion and weak edge-edge coagulation could take place concurrently in suspension at pH 9 (Figure 6.1).

However, it has been explained that surface charge anisotropy effects are of less relevance in muscovite suspensions due to the high aspect ratio of muscovite platelets, which largely negates edge charge contributions. In this case, FF agglomeration is of more significance than in vermiculite, particularly at acidic pH conditions. Therefore, although EE aggregates may start to form at higher pH, the proportion of these structures may well be much less than in vermiculite. Therefore, lower suspension yield stresses are expected in muscovite suspensions. With a low proportion of EE aggregates, a mostly dispersed system is likely at pH 9. However, it must also be noted that with high aspect ratio systems, it is possible that even for a dispersed system, a low yield stress might be exhibited due to crowding effects from the asymmetric particles and the net increase in the number concentration of particles and associated inter-particle interactions for high aspect ratio particles versus more spherical particles at the same volume concentration. This contributes towards the higher yield stresses of muscovite suspensions compared to quartz.

The yield stress differences observed in Figure 6.2 can be attributed to the particle interactions occurring in suspension. A comparison of the Bingham viscosities of the suspensions of pure vermiculite, muscovite and quartz upon shearing is shown in Figure 7.3.

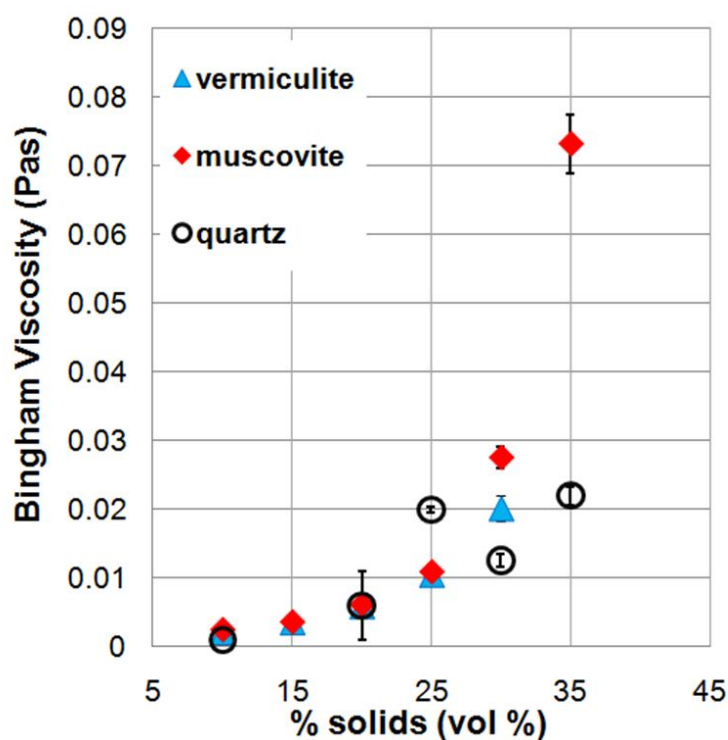


Figure 7.3 - A comparison of the Bingham viscosities of suspensions of vermiculite, muscovite and quartz at pH 9. The errors bars represent the 95% confidence interval of the average values.

The results show that the Bingham viscosities of vermiculite, muscovite and quartz are very similar, with few discernible differences. The viscosities of vermiculite and muscovite now fall within the range of viscosities of quartz suspensions. Since quartz is a simple mineral which is known not to present rheological problems (Johnson et al., 2000), this demonstrates that muscovite and vermiculite suspensions have low viscosities at high shear conditions.

7.4. THE RHEOLOGY OF CHRYSOTILE SUSPENSIONS

It has been proposed that the tube lengths of chrysotile particles are positively charged, while the charge on the tube ends changes from positive to negative (Figure 5.14). The high degree of entanglement between chrysotile fibres has also been demonstrated (Figure 4.4). A rheological

analysis is used to investigate how these properties affect the flow characteristics of chrysotile in suspension.

Rheology tests were conducted on chrysotile suspensions at pH 9. The tests were done as a function of solids concentrations and the resultant rheograms were fitted with the Bingham model. Figure 7.4 shows a comparison of the calculated Bingham yield stresses of chrysotile and quartz suspensions at increasing solids concentrations.

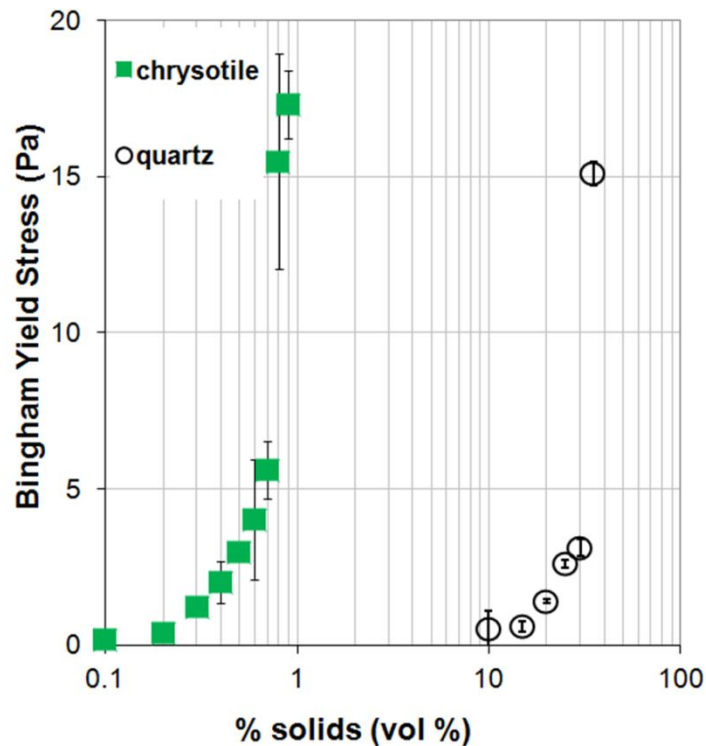


Figure 7.4 - A comparison of the Bingham yield stresses of suspensions of chrysotile and quartz at pH 9. The errors bars represent the 95% confidence interval of the average values.

It must be noted that when performing the rheological tests on pure chrysotile suspensions, the high degree of entanglement and viscous nature of the suspensions made use of a magnetic stirrer particularly difficult. Homogeneity of the suspensions was best achieved by consistently stirring the suspension manually prior to testing. This type of mixing is not as effective as that achieved when using a mechanical stirrer which regulates uniformity throughout the sample. Therefore, when the tests were conducted, a relatively larger variance was observed in the calculated yield stresses and viscosities. This is reflected in the error bars. Nonetheless, these

represent 95 % confidence interval and the values within this range are considered to adequately represent the yield stresses and viscosities of the entire sample at a given concentration.

Figure 7.4 shows that rheology tests in chrysotile suspensions were confined to concentrations less than 1% solids by volume. Most mineral suspensions do not typically exhibit rheological complexities at such low concentrations. However, the results show that chrysotile suspensions exhibit Bingham behaviour, with the clear appearance of a yield stress at concentrations as low as 0.3% solids by volume. This type of behaviour differs greatly from most minerals as demonstrated in quartz whose suspensions are only comparable at much higher concentrations (20% solids by volume). This means that within a chrysotile suspension comprising less than 1% solids by volume, the type of particle aggregation is much more complicated than in a quartz suspension comprising 20% solids. The results indicate that the network structures that form in chrysotile suspensions are much more complex than in quartz suspensions, despite a higher particle concentration in quartz suspensions.

Based on surface charge data, it has been proposed that the degree of charge anisotropy between the tube ends and tube length is large at pH 9 (Figure 5.14). This enhances the degree of particle interaction, with pH 9 falling in the region of maximum suspension yield stress (Figure 6.3). Furthermore, at this pH (pH 9), chrysotile particles are close to the net point of zero charge (pH 8.23), which is representative of a state of high charge anisotropy and suspension yield stress. Therefore, a high degree of particle entanglement is expected in chrysotile suspensions at pH 9, while quartz suspensions are expected to exist in a dispersed state. Hence one would naturally expect chrysotile suspensions to have higher viscosities and yield stresses than quartz suspensions. However, the differences in the degree of aggregation or dispersion alone cannot account for the vast order of magnitude difference between the rheological properties of these two suspensions. At such low concentrations, the change in the yield stress of suspensions with the increasing degree of aggregation can be expected to be in the range of a factor of 2–10, depending on the mineral (Burdukova et al., 2007; Johnson et al., 2000). In this case however, the differences in rheological behaviour are immeasurable due to the differences in solids concentrations and the type of aggregation that occurs in chrysotile suspensions. If surface charge was greatly significant to the aggregation, this would result in tube length–tube end

particle association. However, it has been demonstrated that the conformation of chrysotile particles is very random, with fibres orientated in any direction (Figure 4.4). On this basis, the type of aggregation in chrysotile suspensions cannot be largely due to surface charge effects.

The unique behaviour of chrysotile can only be attributed to its long, thin morphology. The high aspect ratio associated with this geometry has previously been demonstrated to exacerbate the flow properties (Barnes et al, 1989). However, it is more the flexibility of the fibres that results in the problematic behaviour of chrysotile. This results in the entangling of fibres both within themselves and with adjacent fibres, leading to the formation of intricate networks or 'balls' of intertwined fibres. Although the actual volume of particles in suspension may be low, the volume swept by a single fibre is large, such that effective volume effects, in this case, are significantly escalated.

The high yield stress values observed for chrysotile suspensions are indicative of a static network structure. An analysis of the viscosities is required to understand the ease of flow of these structures at high shear conditions. A comparison of the Bingham viscosities of suspensions of chrysotile and quartz is given in Figure 7.5.

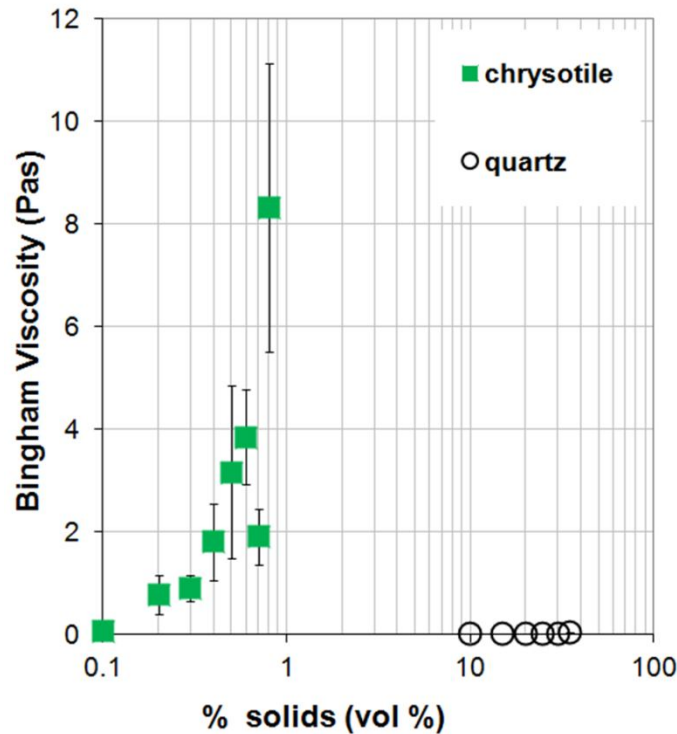


Figure 7.5 - A comparison of the Bingham viscosities of suspensions of chrysotile and quartz at pH 9. The errors bars represent the 95% confidence interval of the average values.

The results show that chrysotile suspensions have much higher viscosities (about 100 times more in magnitude) than quartz suspensions. The trends observed here are similar to what was observed in the yield behaviour. However, the differences between chrysotile and quartz are more apparent in the viscosities. This comparison suggests that while particles in quartz suspensions flow relatively freely at high shear conditions, there is a high degree of particle-particle interaction in chrysotile suspensions and this poses a high resistance to deformation and flow, even at high shear rates. This is expected since the fibres are highly entangled.

7.5. DISCUSSION

The rheological properties of suspensions of each phyllosilicate mineral at pH 9 have been investigated. These have been compared to quartz suspensions as a means to demonstrate deviations in flow behaviour from isotropically charged, regular shaped minerals.

Knowledge on the suspension yield stresses have given an indication of the relative degrees of complexity of the network structures that form in suspension, while the viscosities have been used to infer the ease of flow of the pure minerals at high shear conditions. The differences in rheological properties of these minerals have been largely explained in terms of their morphological and surface charge properties. A qualitative comparison of the rheological characteristics of the minerals, related to differences in their physico-chemical properties is given in Table 7.1.

Table 7.13- *Qualitative comparison of the rheological properties of the minerals. Anisotropy refers to charge anisotropy.*

Mineral	Morphology	Anisotropy	Bingham yield stress	Bingham viscosity
Quartz	Simple	None	Low	Low
Muscovite	Platy	Slight	Moderate	Low
Vermiculite	Platy	High	High	Low
Chrysotile	Fibrous	Slight	Very High	High

The differences in rheological behaviour of vermiculite and muscovite are in good agreement with the estimated modes of particle association for each mineral in the previous chapter. Indeed, the higher suspension yield stresses exhibited by the vermiculite suspensions supports the prediction of more complex network structures in vermiculite than muscovite. However, both minerals exhibit low suspension viscosities similar to quartz suspensions at high shear rates. Conversely, chrysotile fibres form extremely complex structures, with high yield stresses. These suspensions have high viscosities even at high shear rates, demonstrating the dramatic effect of chrysotile fibrous morphology.

A comparison of the rheological behaviour of all the phyllosilicate minerals in this study relative to non-phyllosilicate quartz suspensions is given in Figures 7.6 and 7.7. Figure 7.6 shows a comparison of the Bingham yield stress and Figure 7.7 gives a comparison of the Bingham viscosities. This serves to provide a preliminary classification of the rheological behaviour of the phyllosilicates in their pure form. Such a classification is foundational in understanding the

changes in rheological behaviour of the minerals when present in more complex mineral systems.

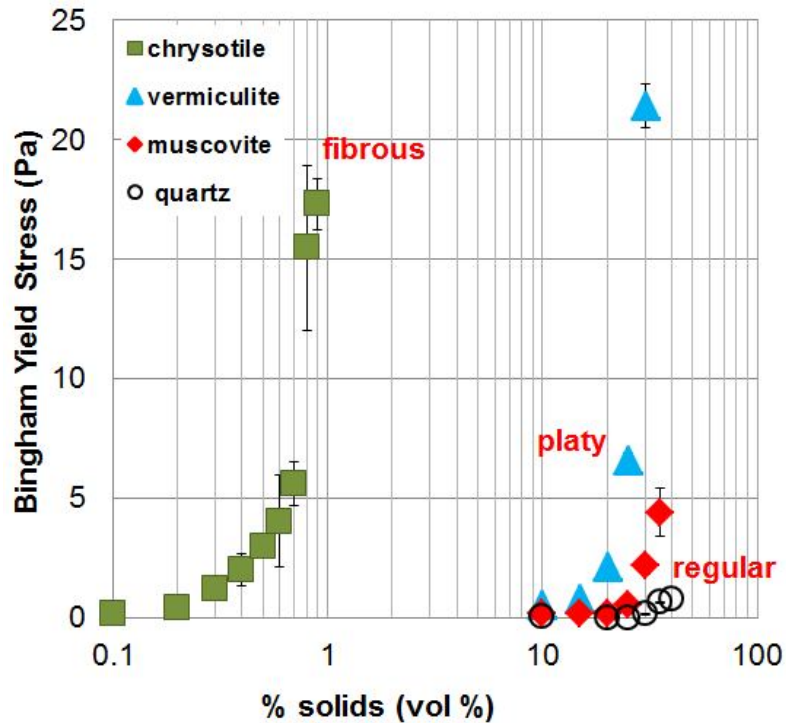


Figure 7.6 - A comparison of the Bingham yield stresses of suspensions of all the phyllosilicate minerals relative to quartz, a non-phyllosilicate mineral at pH 9. The errors bars represent the 95% confidence interval of the average values.

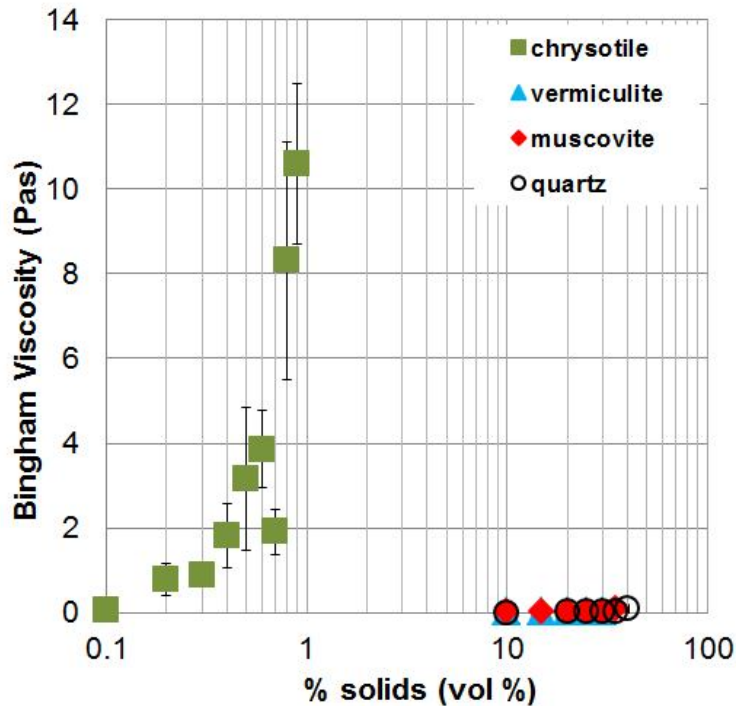


Figure 7.7 - A comparison of the Bingham viscosities of suspensions of all the phyllosilicate minerals relative to quartz, a non-phyllosilicate mineral at pH 9. The errors bars represent the 95% confidence interval of the average values.

Figure 7.6 further demonstrates that suspension rheological effects are more pronounced in phyllosilicate minerals. Taking into consideration morphological effects, the comparison demonstrates that the degree of complexity increases in the order 'spherical' < platy < fibrous. This trend is in agreement with findings by Barnes et al (1989) who used synthetic material to demonstrate the rheological effects of particles of different morphologies. Although his studies did not take into consideration additional factors such as flexibility, the comparison shows the importance of morphological effects.

Figure 7.7 demonstrates that chrysotile forms the most rheologically complex suspensions, characterised by the highest yield stresses and showing the largest deviation from simple rheological behaviour observed in quartz suspensions. Since the rheology can be attributed to its fibrous morphology, the results demonstrate the dramatic effects of the morphology and flexibility of the fibres. Vermiculite, on the other hand, shows a high charge anisotropy resulting in higher yield stresses than muscovite which shows the least deviation from non-phyllosilicate

behavior at pH 9. On the basis of the combined yield stress and viscosity results, the rheological behaviour of the phyllosilicate minerals becomes more complex in the order muscovite < vermiculite < chrysotile.

Based on the rheological classification observed here, it can be inferred that from a rheological viewpoint, muscovite bearing suspensions are less likely to present viscosity related processing issues than vermiculite and chrysotile bearing suspensions, with chrysotile bearing suspensions resulting in the most problematic suspension behaviour. The high viscosities and yield stresses observed in this case are likely to enhance the formation of viscous zones in stirred mills and result in an overall retardation in the grinding process. In flotation, the high viscosities are likely to result in an increase in turbulence dampening and a reduction in bubble attachment and detachment. Indeed, this has not taken into consideration, the effects of the minerals on factors such as froth stability, entrainment and hydrophobicity, and the minerals may well present different effects on comminution and flotation applications in this regard. However, their influence based on rheological performance can be inferred here.

Indeed the rheological behaviour of these slurries may change in the presence of other minerals, due to interactions resulting from differences in morphologies and surface charge properties, and this can be studied, on a preliminary basis, through the analysis of controlled binary mineral systems.

Chapter 8.

RHEOLOGY OF SUSPENSIONS OF BINARY MINERAL MIXTURES

Summary

The rheological properties of suspensions of binary mixtures comprising quartz and each phyllosilicate have been investigated. In each case, the yield stress trends were analysed as a function of pH and compared to the constituent pure phyllosilicate. Vermiculite – quartz and chrysotile –quartz mixtures have yield stress trends similar to pure vermiculite and chrysotile respectively, demonstrating their dominance in binary mixture suspension behaviour. Muscovite-quartz mixtures, on the other hand show a deviation from pure muscovite yield stress trend, owing to the relatively lower degree of muscovite rheological complexity. The synergistic (improved rheology) and antagonistic (exacerbated rheology) effects of adding quartz have also been investigated. Muscovite–quartz and vermiculite-quartz mixtures show antagonistic effects, suggesting that the phyllosilicate suspension flow behaviour is exacerbated through the addition of quartz. In the case of chrysotile, however, the yield stresses are not significantly affected by the presence of quartz particles, although synergistic effects are observed in the suspension viscosities. This suggests that the complex rheological characteristics of chrysotile-bearing suspensions can be improved through blending techniques. The application of robust mixture designs to predicting rheological behaviour is not simple and consideration must be made to the interaction between particles in multicomponent systems. There remains a large scope for study in making mixture design experiments more applicable to rheological performance predictions.

8.1. INTRODUCTION

The rheological properties of pure suspensions of each phyllosilicate have been investigated. In each case, the rheological characteristics have been discussed in terms of the surface charge and physical properties of the minerals e.g. morphology, aspect ratio, surface area. As a result, a rheological classification of the pure phyllosilicates has been established. Such a categorisation provides a foundational understanding of the differences in phyllosilicate behaviour, albeit on a preliminary basis. However, ore suspensions typically comprise composite particles locked in multiple phases of mineral mixtures. Therefore, the analysis of heterogeneous mineral systems is necessary for a better approximation of phyllosilicate-bearing ore behaviour. Indeed a lot more research is still required in trying to establish a full understanding of the deleterious effects of phyllosilicate minerals within ores and careful analysis and monitoring of phyllosilicate behaviour from a simplistic foundational state to increasingly complex mineral systems may be beneficial in achieving this.

This chapter sets out to investigate the changes in rheological behaviour of the phyllosilicates when present in well characterised binary mineral mixtures containing quartz and each phyllosilicate mineral. It has been demonstrated in previous chapters that quartz does not cause any rheological problems associated with irregular shape or charge anisotropy and results in suspensions with comparatively lower yield stresses and viscosities (at the conditions used in this study). Nonetheless, its presence may well alter the flow behaviour of phyllosilicate minerals in suspension either through changes in structural forming mechanisms or simply by replacement with a less rheologically complicated material. These binary mixtures are sufficiently simple to examine and serve as preliminary simulations of ‘real’ multicomponent ore systems.

Similar to the pure phyllosilicate mineral suspensions, this rheological analysis is aimed at high shear systems of relevance in the mineral processing industry. The main aim of this chapter is to determine whether the inclusion of other minerals at these conditions improves or exacerbates the suspension rheology, as estimated through changes in suspension yield stress and viscosity. As such, any changes in the rheological classification of the phyllosilicates from pure to binary

mineral systems are noted. Inferences on the interactions that are likely to occur between quartz and the phyllosilicates are made in formulating possible reasons for changes in the rheological behaviour. It must be noted though that this is not the main focus of this chapter and it is acknowledged that additional confirmatory analysis would be required to validate the theories made on particle interaction.

A secondary aim of this chapter is to probe the applicability of techniques used in mixture design experiments. These are often used as a basis for blending practices. Blending is typically used as a means to mitigate the effects of a ‘poor’ performing ore by mixing it with a more competent ore. Estimations on the metallurgical performance are mostly made based on the additive effects of the constituents. In this chapter, the accuracy of such an approach for rheological projections is evaluated. The approaches typically used in mixture design experiments and that taken here are explained further in the following section.

8.2. ANALYTICAL APPROACH

8.2.1. Graphing of binary mineral mixtures

The application of mixture design for blending is a mature discipline in other industries such as pharmaceuticals. The increased use of blending practices in mineral processing has prompted the adoption of robust techniques used in other industries and mixture design is now increasingly used to predict metallurgical performance of blended streams (e.g. Yan and Eaton, 1994; Rubiera et al., 1999; Vuthaluru et al., 2003; Zhong et al., 2005). Herein, the predicted metallurgical response is based on the weighted average sum of that for the pure minerals in the mixture. Following this approach, the rheological response of each phyllosilicate-quartz binary mixture in this chapter, is evaluated by simply adding the yield stress/viscosity values of the pure minerals (phyllosilicate and quartz) at a given ratio to produce a summed value (Equation 8.1). Such an approach takes into account the characteristic non-linear yield stress/viscosity – solids concentration relationship since it is based on non-linear pure mineral behaviour. The actual measured mixture behaviour can then be compared against this predicted additive value. If the

measured yield stress/viscosity value falls above this predicted value, then the prediction underestimates the rheological behaviour. Instead, the suspension behaviour is exacerbated. In this study, this is termed an antagonistic effect. Conversely, if the measured yield stress/viscosity value falls below the prediction, improved suspension behaviour is observed. The phyllosilicate and quartz are said to have synergistic effects.

$$\tau_{mixture} = \tau_{quartz} + \tau_{phyllosilicate}$$

$$\eta_{mixture} = \eta_{quartz} + \eta_{phyllosilicate}$$

Equation 8.1

$\tau_{mixture}$ - yield stress of the binary mixture

τ_{quartz} - yield stress of pure quartz at a volume fraction equivalent to its proportion in the mixture.

$\tau_{phyllosilicate}$ - yield stress of pure phyllosilicate at a volume fraction equivalent to its proportion in the mixture.

$\eta_{mixture}$ - viscosity of the binary mixture

η_{quartz} - viscosity of pure quartz at a volume equivalent to its proportion in the mixture.

$\eta_{phyllosilicate}$ - viscosity of pure phyllosilicate at a volume equivalent to its proportion in the mixture.

A schematic of this approach is shown in Figure 8.1. The suspensions are compared at pH 9, at which the rheological properties of the pure minerals have already been analysed. The rheological properties are plotted as a function of solids concentration, with the primary and secondary X axes representative of the phyllosilicate and quartz concentrations in each mixture respectively and the Y axes showing the rheological properties (Bingham yield stress/viscosity). The actual measured mixture behaviour is plotted and compared with the predicted values.

The binary mixtures were investigated using suspensions with a total concentration of 30% solids by volume, varying only the proportion of the phyllosilicate mineral and quartz within the mixture. This means that analysis is conducted within the limits of pure quartz suspensions (30%

quartz, 0% phyllosilicate by volume) and pure phyllosilicate suspensions (30% phyllosilicate, 0% quartz by volume) with intermediate phyllosilicate-quartz proportions. This covers the range over which phyllosilicate content within an ore is typically observed, and allows analysis from low phyllosilicate bearing to high phyllosilicate bearing suspensions. It has been demonstrated in the previous chapter, that at 30% solids by volume, all the phyllosilicates exhibit pseudo plastic behaviour in their pure form, with measurable yield stresses and viscosities. Quartz suspensions, on the other hand, have extremely low yield stresses ($\ll 1\text{Pa}$). From a rheological perspective, yield stresses of such a low magnitude may be considered negligible with no claim of a real yield stress. However, this is considered to be representative of quartz suspension behaviour in multicomponent systems and its contribution is evaluated by comparing the rheological properties of suspensions of each pure phyllosilicate mineral to pure quartz and the concomitant binary mineral mixture.

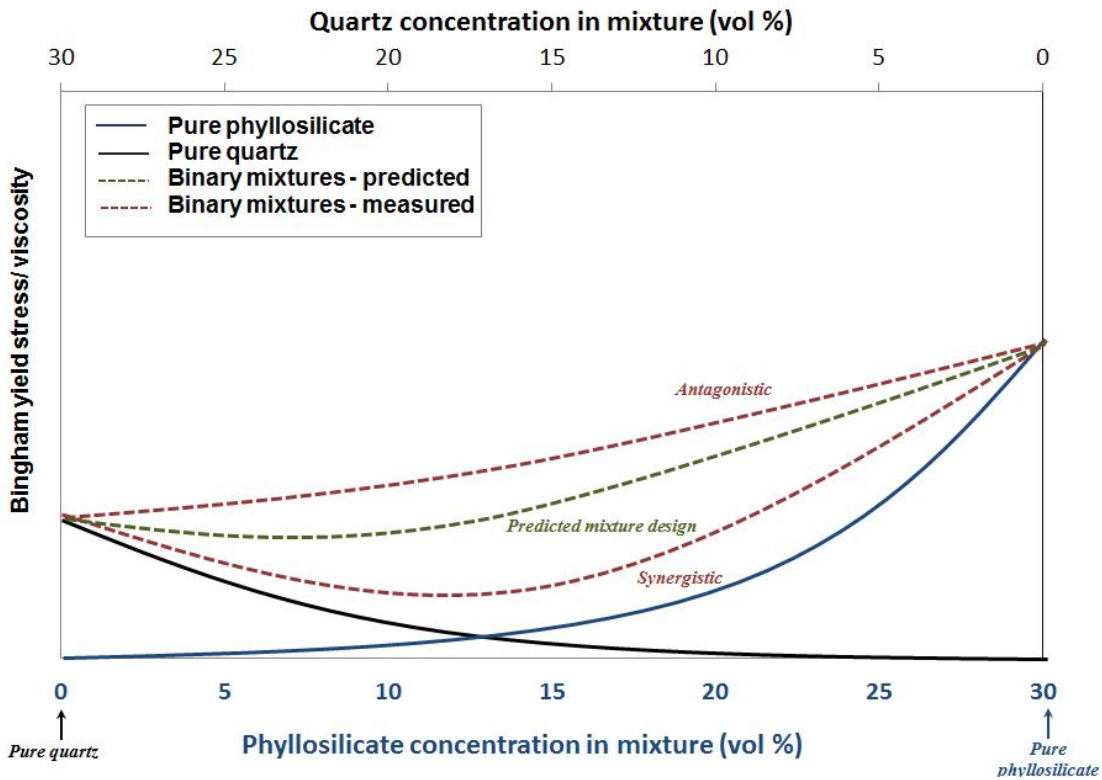


Figure 8.1 – Example of graphical analysis used for the binary mineral mixtures.

For each binary mixture, the yield stress trend is initially investigated as a function of pH, with the yield stresses evaluated using the direct yield stress vane measurement technique. Similar to the pure mineral suspensions, tests on the binary mixtures were conducted on individual batch samples at each pH, rather than entire pH sweeps on a single sample. This served to isolate the interaction effects between phyllosilicate and quartz particles from additional colloidal effects resulting from the re-precipitation (at higher pH) of previously leached ions in the acidic pH range (He et al., 2009). In each case, tests were conducted at a pre-determined ‘critical’ phyllosilicate-quartz concentration (Table 3.5). Inferences on the particle interactions that are likely to occur in the binary mixture suspensions are made as a function of pH.

In each case, the rheological behaviour of the mixtures is then analysed at pH 9, where the synergistic/ antagonistic effects are investigated using the analytical approach previously described.

8.3. SUSPENSIONS OF MUSCOVITE-QUARTZ MIXTURES

8.3.1. The rheology of suspensions of muscovite-quartz mixtures as a function of pH

The rheological properties of suspensions of muscovite-quartz mixtures were measured over the range pH 3 to 11. Tests were conducted on individual muscovite-quartz mixtures with a concentration of 80% muscovite and 20% quartz within a 30% solids by volume mixture (i.e. 24% muscovite, 6% quartz). Therefore, the suspensions represented in Figure 8.2 comprise a much higher proportion of muscovite relative to quartz. It has also been demonstrated in Chapter 7 that muscovite suspensions are more rheologically complex than quartz suspensions. It is therefore expected that the rheology of the binary mixture suspensions (and the yield stress curves) will closely resemble or be largely driven by the muscovite in the mixture. For this reason, Figure 8.2 compares the yield stress curves of the muscovite-quartz binary mixtures to that of pure muscovite. This comparison serves to determine whether a shift in the yield stress peak or yield stress trend of muscovite is observed within the binary mixtures. Since this comparison is more qualitative rather than quantitative, normalized yield stress values are used

as per Johnson et al., (1998). From a simplistic viewpoint, a similarity in the yield stress curves (and yield stress peaks) is indicative of the dominance of muscovite within the mixture, and suggests that the presence of quartz is of little or no significance. Conversely, a deviation in the yield stress peak suggests that the addition of quartz adequately alters the rheological behaviour of the phyllosilicate mineral.

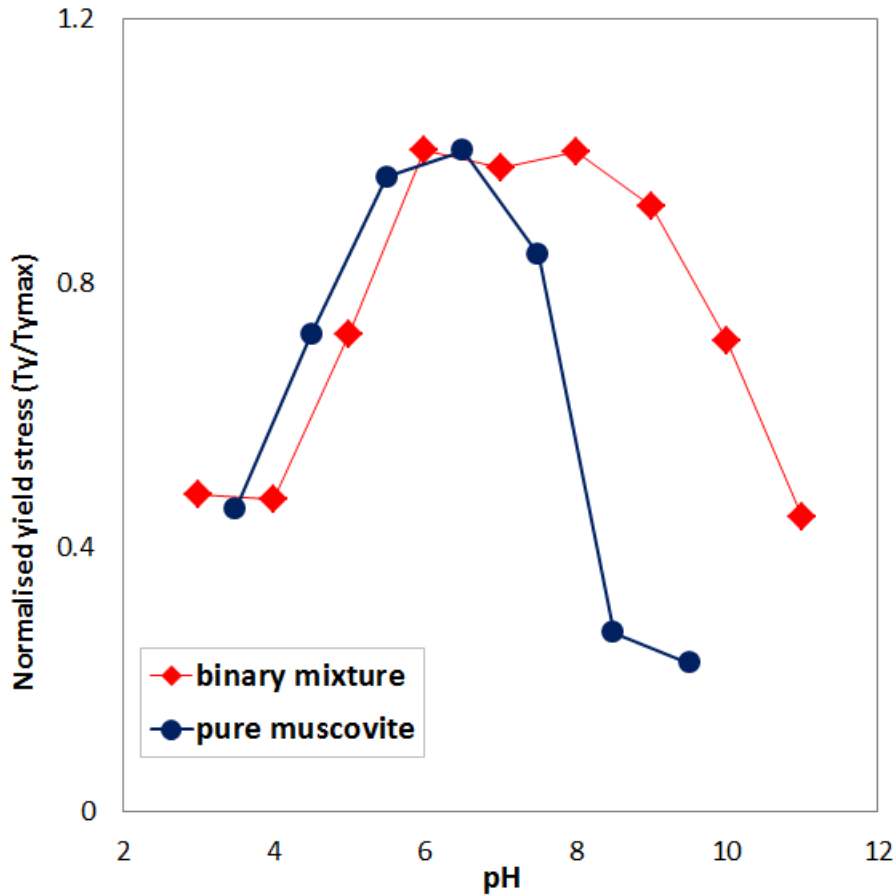


Figure 8.2 – A comparison of the yield stresses of muscovite-quartz binary mixtures to pure muscovite suspensions as a function of pH.

The yield stress curve of the binary muscovite-quartz mixtures shows a steady increase within the acidic pH range (pH 3 to pH 6), with a yield stress peak between pH 6 and pH 8. Thereafter, suspension yield stress decreases through the alkaline pH range. Where the yield stress peak of pure muscovite suspensions occurred at pH 6.5, the binary mixture suspensions are characterized

by the highest yield stresses between pH 6 and pH 8. Indeed the yield stress peak of pure muscovite suspensions falls within this range. However, it is not representative of the entire region and a clear shift in the yield stress peak is observed. This can be attributed to the presence of quartz particles and can be explained by inferring possible additional particle-particle interactions over this region.

The dominance of face-face (FF) particle alignment in muscovite suspensions, particularly in the acidic pH range (pH 3 to 6) has been proposed and discussed in Chapter 6. As the pH is increased, progressive realignment to (edge-edge) EE and (edge-face) EF aggregates is expected resulting in an increase in suspension yield stress. Maximum aggregation between adjacent quartz particles (QQ), on the other hand, is expected in the region of the i.e.p (pH 2 to 3), after which particles become increasingly negatively charged, realigning into a low volume dispersed state. Therefore, by considering the interactions between like minerals in isolation, the interaction (repulsion) between adjacent quartz particles is expected to reduce the suspension yield stress while the progressive formation of FF aggregates between muscovite particles increases the suspension yield stress in the acidic pH region.

The observed increase in the yield stress curve over the range pH 3 to 6 of the binary mixtures demonstrates similarity to muscovite behaviour, suggesting the predominance of FF arrangements and their progressive realignment into EE and EF aggregates with pH. The significance and contribution of the (positive) edge charge is enhanced through the stacking of layers in FF aggregates and this promotes charge anisotropy not only between the edges and faces of FF aggregates but also with negatively charged quartz particles. The pronounced anisotropy of muscovite-quartz aggregates could result in preferential edge-quartz (EQ) association, while EF and EE particle associations between muscovite particles may still occur as originally predicted and as dictated by changes in the charge of the faces and edges of muscovite particles. Moreover, EQ interactions could act as 'binding agents' holding adjacent EE and EF structures together. Such interactions would be similar to those proposed by He et al., (2009) who proposed enhanced cementation and proliferation of aggregates by binding mediated interactions in suspension. This would result in unexpected hetero-aggregation, manifest in marked increases in shear yield stresses of the suspensions. Such aggregation may be a result of

a combination of interactions including electrostatic/charge patch attraction and van der Waals attraction between oppositely charged quartz particles and muscovite edges (He et al., 2009).

Therefore, although the maximum in the yield stress peak between pH 6 and 8 is still likely a consequence of a combination of transition from FF alignment to randomized EE and EF alignment in muscovite particles the observed shift in the yield stress peak may be attributed to interactions between quartz and muscovite particles, through the possible formation of EQ interactions. As pH is increased, > pH 9, muscovite edges and faces are negatively charged and a progressive transition to a dispersed state is expected. The synergistic or antagonistic effects of these additional interactions are investigated further in the next section. The proposed modes of particle association between muscovite and quartz particles, over the range pH 3-11 are shown in Figure 8.3.

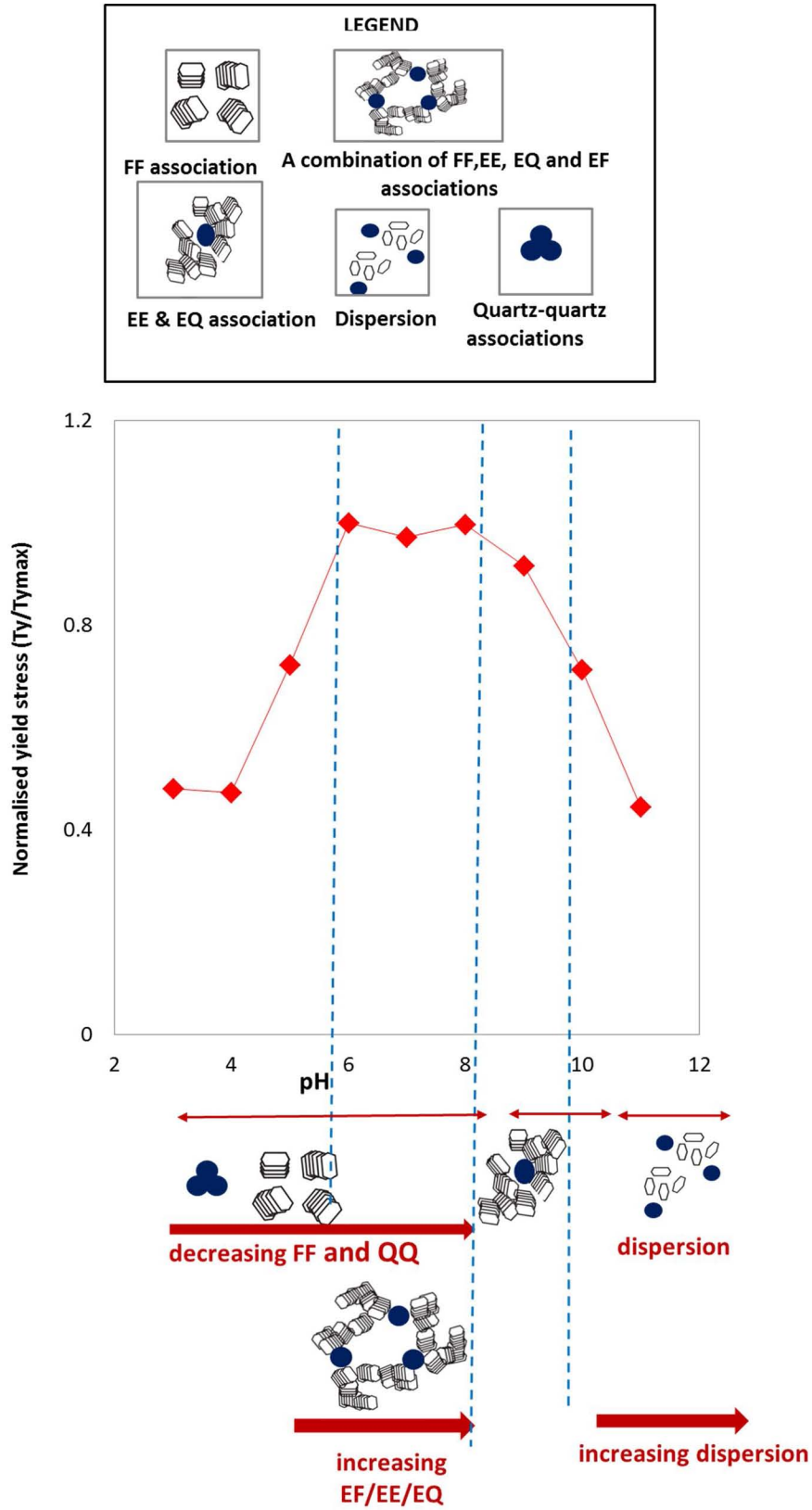


Figure 8.3 - Proposed modes of particle interaction in muscovite-quartz mixtures as a function of pH.

8.3.2. The rheology of suspensions of muscovite-quartz mixtures at pH 9

Having proposed and discussed the modes of particle interaction that may occur between muscovite and quartz particles as a function of pH, it is now possible to investigate whether the addition of quartz improves (has synergistic effects) or exacerbates (has antagonistic effects) on the suspension rheology. The rheological properties of muscovite-quartz suspensions at different mixture ratios were investigated and compared to suspensions of quartz and muscovite at pH 9. Figure 8.4a gives a comparison of the suspension yield stresses while the viscosities are presented in Figure 8.4b. At each mixture ratio, the rheological properties are predicted, based on the additive effects of the pure mineral components at that concentration (Equation 8.1). This is compared to the actual measured yield stress/viscosities, with a higher yield stress/viscosity indicative of antagonistic effects and a lower yield stress/viscosity of synergistic effects.

It has been proposed that at pH 9, muscovite suspensions comprise a combination of dispersed particles, with the possibility of weakly aggregated EE structures resulting from the pronounced edge effects due to the progressive stacking of platelets in FF aggregates at lower pH conditions. These suspensions have been shown to be characterized by low (but present) yield stresses. Quartz suspensions, on the other hand, most likely comprise a completely dispersed system of comparatively negligible yield stress. In addition to these modes of particle association, it has been suggested that binary mixtures of these two result in the formation of additional EQ interactions. Therefore, a predominantly dispersed suspension with the possible formation of EE and EQ aggregates may be likely in muscovite-quartz suspensions.

A comparison of the pure mineral suspensions to the binary mixtures shows that at any given concentration, the binary mixtures (predicted or measured) are characterized by higher yield stresses/viscosities than pure muscovite and quartz suspensions. To re-iterate, the measurements on the binary mixtures were conducted at varying proportions of muscovite and quartz within a 30% total solids concentration. Therefore, at any given point, the yield stress/viscosity value of the binary mixtures represents the rheology of a 30% solids suspension. The rheology of the pure minerals, on the other hand, was measured as a function of solids concentration. Thus, on comparing the pure suspensions to the binary mixtures, a pure muscovite suspension of e.g. 20%

solids by volume contains only muscovite particles. However, a binary mixture comprising 20% muscovite will contain an equivalent volume concentration of muscovite particles as in the pure suspension, but will also contain an additional 10% by volume concentration of quartz particles to make a total solids concentration of 30 % v/v. It is therefore expected that the binary mixtures will have higher yield stresses/viscosities than the pure minerals, not necessarily only due to the development of more complex structures, but also due to higher volume concentration effects. Since the predicted values are based on additive effects (which take into consideration the volume contributions of each mineral component), the effects of the structures formed are then approximated by a comparison of the predicted and actual rheological properties of the binary mixtures.

At the varying mixture concentrations, the rheological properties of quartz suspensions are negligible in comparison to muscovite suspensions (particularly yield stresses). Therefore, it is expected that the rheology of the binary mixtures will closely resemble that of pure muscovite, and the presence of quartz would be of little rheological significance. This would mean that within the mixture, quartz behaves as a benign component. However, the results show that the measured rheological properties of the mixtures are significantly higher than pure muscovite suspensions, suggesting that suspension behaviour is dependent on both quartz and muscovite in the mixture, and not entirely driven by the muscovite.

A comparison of the predicted to the measured rheological behaviour shows that the measured yield stresses and viscosities do not correspond with those predicted using standard mixture design techniques, indicating that a prediction of this form may be erroneous in this application. Instead, the measured values are higher than predicted. Since the predicted values are based on the volume contributions of either mineral, this then suggests that the observed rheological behaviour is not only a result of higher volume concentrations in the mixtures but is also due to the formation of more rheologically complex structures, manifest in elevated yield stresses and viscosities. By this evaluation, the interaction of muscovite and quartz in binary mixtures results in antagonistic effects.

This concurs with the proposed formation of EQ structures which if they do occur, result in aggregates of significantly higher volume due to the linking of adjacent EE structures in suspension. Higher yield stress requirements and viscosities are expected for such structures. Even so, the binary mixture suspensions are still characterized by low yield stresses ($< 1\text{Pa}$) and viscosities ($< 0.025\text{ Pas}$) which are within the same range as pure quartz suspensions (at high shear conditions). Therefore, although suspension rheology may be exacerbated through the addition of quartz, this is not to a large extent in the case of muscovite.

University of Cape Town

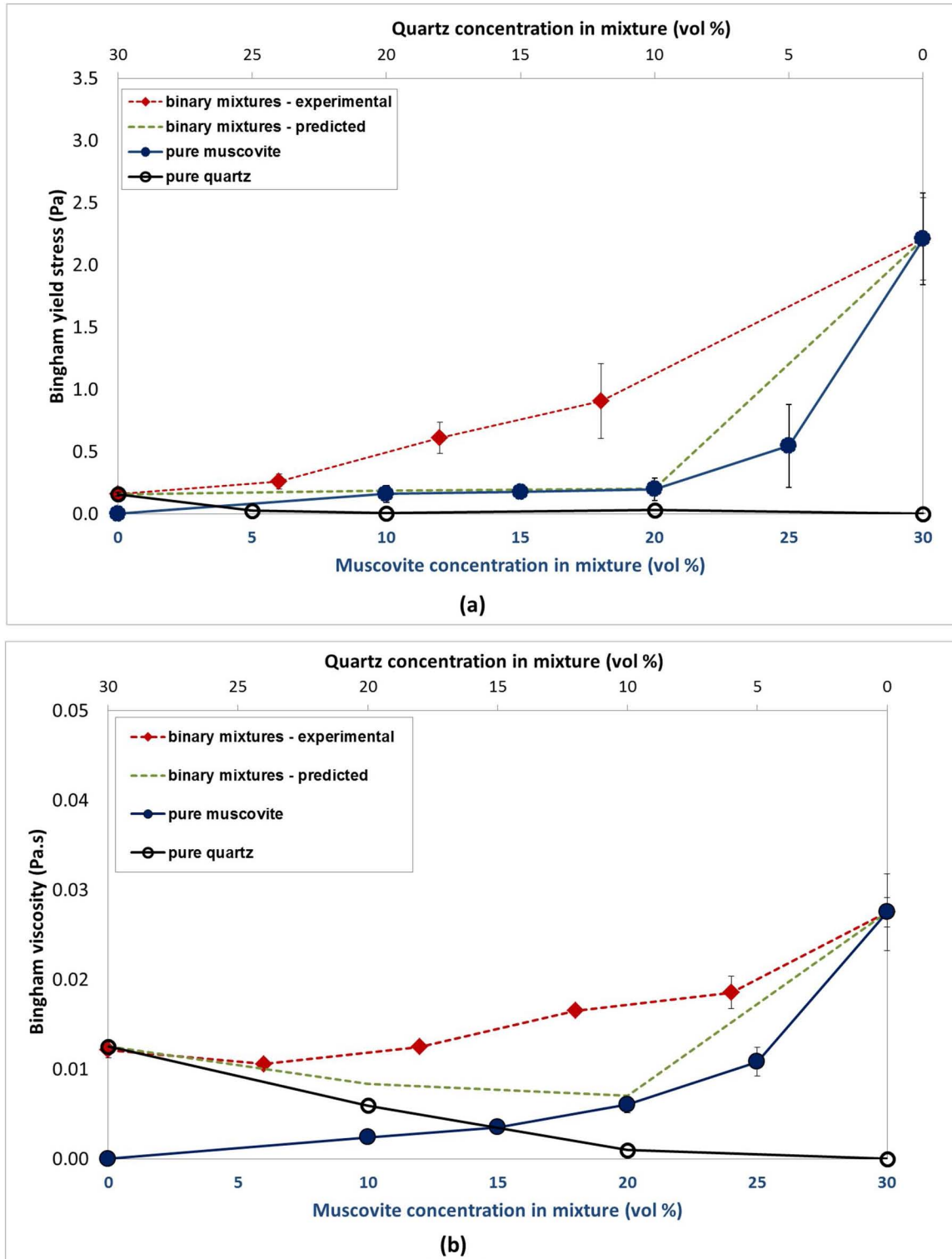


Figure 8.4 - A comparison of the (a) Bingham yield stresses and (b) Bingham viscosities of suspensions of muscovite-quartz mixtures to the predicted model and to suspensions of pure muscovite and pure quartz. The errors bars represent the 95% confidence interval of the average values.

8.4. THE RHEOLOGY OF SUSPENSIONS OF VERMICULITE-QUARTZ MIXTURES

8.4.1. The rheology of suspensions of vermiculite-quartz mixtures as a function of pH

A comparison of the yield stresses of suspensions of vermiculite-quartz mixtures to the yield stresses of pure vermiculite suspensions over the range pH 3 to 11 is shown in Figure 8.5. In each case, tests were conducted at the 'critical' vermiculite-quartz concentration which was determined at a ratio of 70% vermiculite and 30% quartz within a 30% solids by volume mixture (i.e. 21% vermiculite, 9% quartz). Therefore, the suspensions have a much higher proportion of vermiculite relative to quartz and it is expected that the rheology of the binary mixture suspensions (as represented by the yield stress curves as a function of pH), will closely resemble or be largely driven by the vermiculite contained in the mixture.

The binary mixtures show an increase in suspension yield stress from pH 3 to 6. Between pH 6 and pH 8, the yield stress is greatest, with a yield stress peak at circa pH 8. Beyond pH 9, the yield stress decreases. This trend is similar to the trend observed for pure vermiculite suspensions, which also have a yield stress peak range between pH 6 and pH 8. The similarity between these is indicative of the dominance of vermiculite within the mixture. This is more apparent in vermiculite-quartz mixtures than in muscovite-quartz mixtures, probably due to the increased charge anisotropy of the particles which is enhanced by the indicated broader positive edge pH range (Figure 5.10).

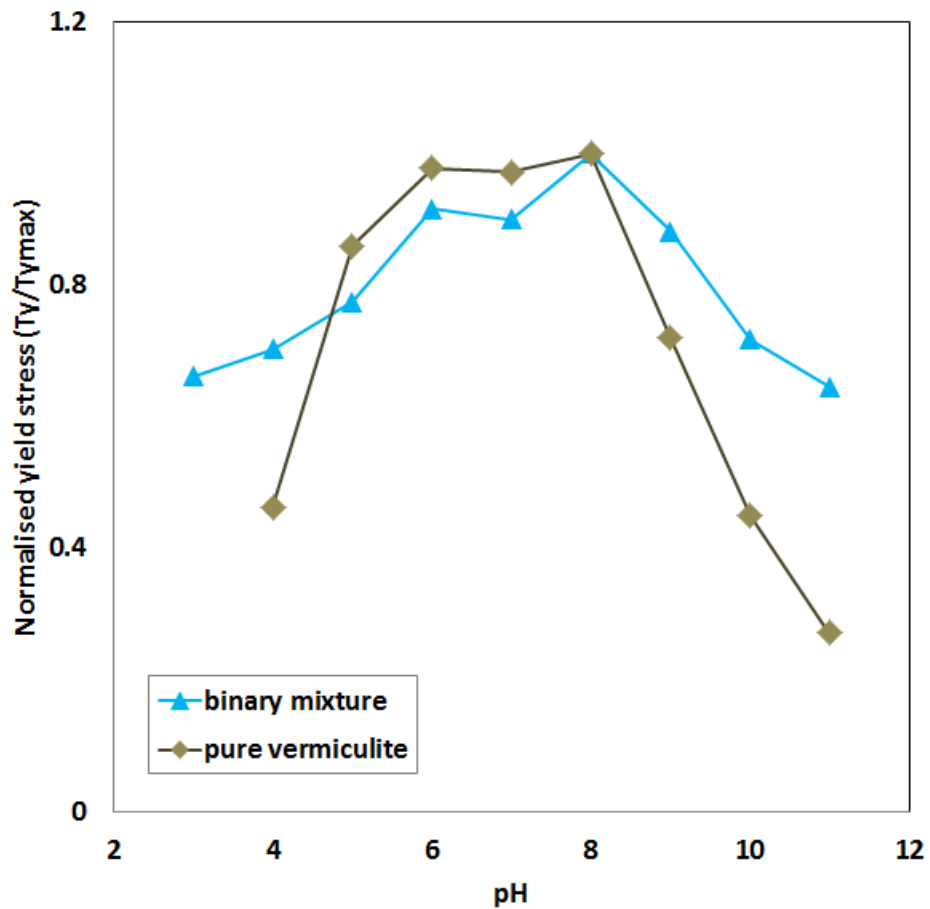


Figure 8.5 - A comparison of the yield stresses of vermiculite-quartz binary mixtures to pure vermiculite suspensions as a function of pH.

A comparison of the yield stress peaks shows that the peak at pH 8 is more apparent in the binary mixtures than in pure vermiculite suspensions. This corresponds with the measured point of zero charge of vermiculite (circa pH 8.4), where the charge differential between oppositely charged vermiculite planes (edges and faces) is large. Indeed high charge differentials may also exist well away from the p.z.c. Highly negative faces with a small number of highly charged positive edges would have a net negative charge, but very strong EF interactions. Therefore high suspension yield stresses may exist over a large pH range (as observed in both the pure minerals and the binary mixtures). In the case of vermiculite, this may be enhanced by the indicated broader positive edge pH range (Figure 5.10) and the comparatively low crystallinity of vermiculite particles resulting in exposed edges on the surface (Figure 4.3). Since quartz particles carry a

strong negative charge, the charge differential between vermiculite edges and quartz particles may also be largest in this range within a binary mixture. Therefore, strong EF and EQ interactions are both expected at this condition, resulting in pronounced maximum suspension yield stress.

The most important aspect of colloidal behaviour of vermiculite particles at low acidic pH conditions is FF agglomeration and is dominant with re-alignment to EF/EE aggregates as the pH is increased. EQ interactions are likely to occur as the charge anisotropy between positively charged edges and negative quartz particles increases. This is likely to occur in the region of maximum yield stress (pH 6 to pH 9). Such interactions may link adjacent vermiculite EE and EF aggregates resulting in voluminous heterocoagulated structures. Beyond this, the charge anisotropy between vermiculite edges and faces and vermiculite edges and quartz particles decreases, resulting in transition to weak EE aggregates and completely dispersed suspensions due to mutual repulsion between negatively charged quartz and vermiculite particles.

The proposed modes of particle association between vermiculite and quartz particles, related to changes in the suspension yield stresses and viscosities over the range pH 3-11 are shown in Figure 8.6.

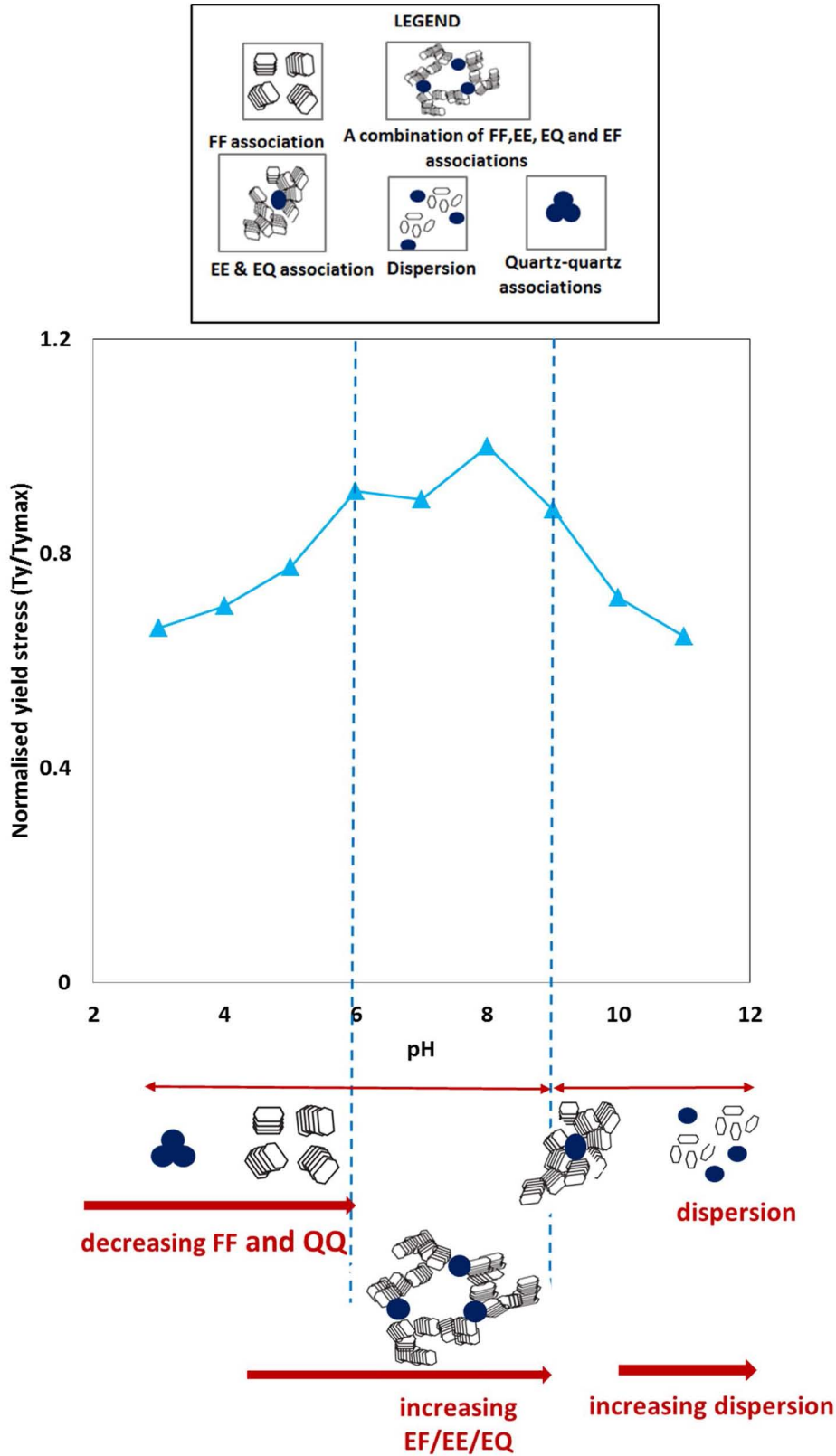


Figure 8.6 - Proposed modes of particle interaction in vermiculite-quartz mixtures as a function of pH.

8.4.2. The rheology of suspensions of vermiculite-quartz mixtures at pH 9

It has been proposed that at pH 9, vermiculite suspensions predominantly comprise EF and EE aggregates. It has also been suggested that additional EQ interactions may form within binary vermiculite-quartz mixtures. Therefore, a combination of EF and EE aggregates is expected with quartz particles linking adjacent EE and EF structures to form heterocoagulated aggregates at pH 9. Figure 8.7a shows the measured suspension yield stresses of vermiculite-quartz suspensions at different mixture ratios at pH 9. This is compared to suspensions of pure vermiculite and quartz and to the predicted yield stresses, derived from the additive effects of each mineral. Figure 8.7b gives a comparison of the suspension viscosities.

At high quartz concentrations (low vermiculite concentrations), the suspension is likely to exist in a dispersed state, shown by the negligible yield stress values. However, an increase in suspension yield stress is observed due to the solids volume replacement with more rheologically complex vermiculite. At any given concentration, vermiculite will be characterized by higher suspension yield stresses/viscosities than quartz. Therefore, based solely on the additive effects which take into consideration the volume contributions of each mineral, rheological behaviour similar to vermiculite is predicted, giving little significance to quartz particles in the mixture. However, the measured values do not correspond with these predicted values and a comparison with the measured rheological properties shows higher yield stresses/viscosities, indicating antagonistic rheological effects between vermiculite and quartz particles.

This finding is in agreement with the antagonistic behaviour observed for muscovite-quartz mixtures and further suggests that it is the interactions between quartz and vermiculite, (possibly through the formation of EQ aggregates), that result in more rheologically complex suspension behaviour. The presence of quartz results in more complex structural formation and significantly exacerbates the rheological behaviour of vermiculite.

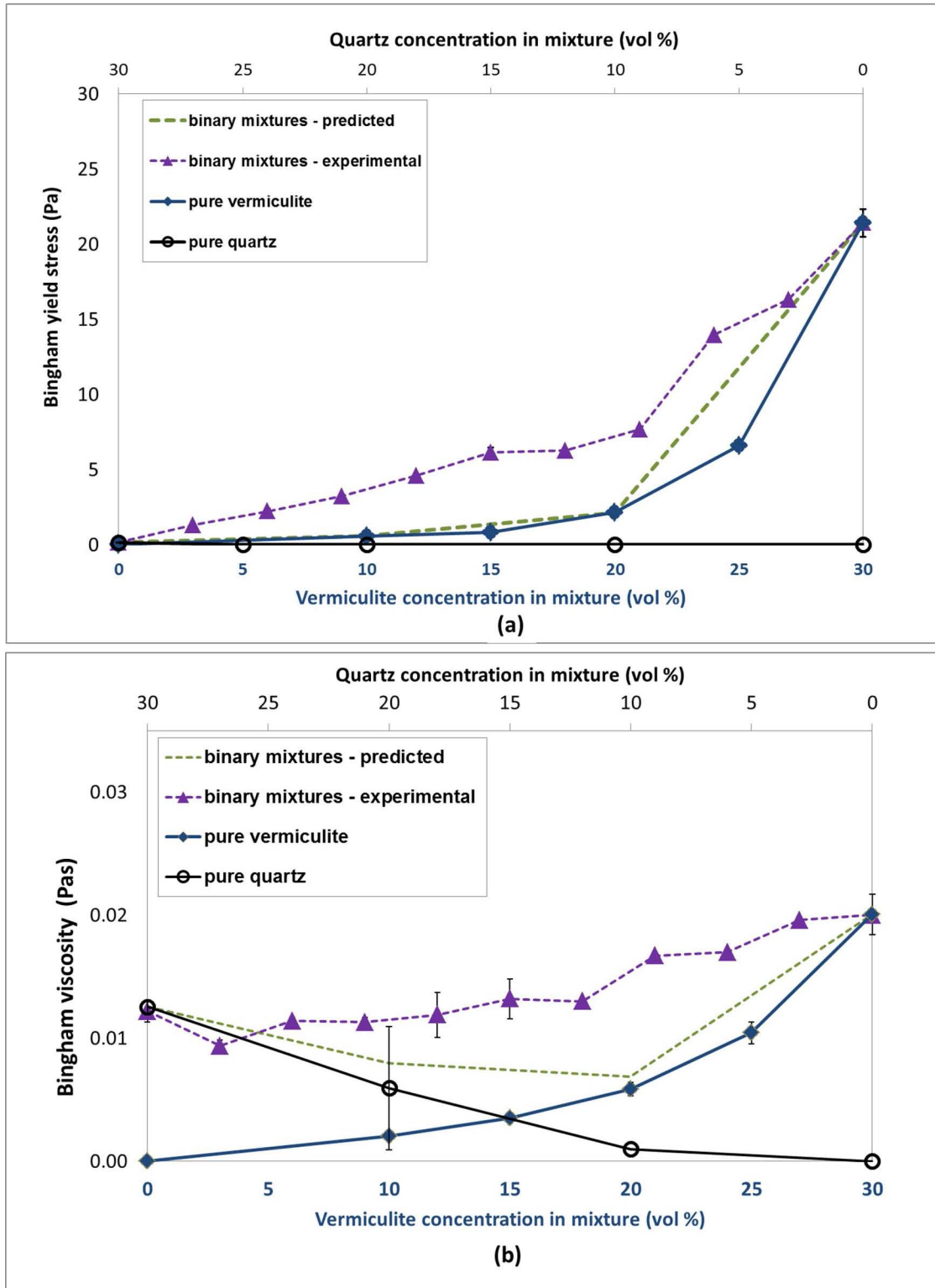


Figure 8.7 - A comparison of the (a) Bingham yield stresses and (b) Bingham viscosities of suspensions of vermiculite-quartz mixtures to the predicted model and to suspensions of pure vermiculite and pure quartz. The errors bars represent the 95% confidence interval of the average values.

8.5. THE RHEOLOGY OF SUSPENSIONS OF CHRYSOTILE-QUARTZ MIXTURES

8.5.1. The rheology of suspensions of chrysotile-quartz mixtures as a function of pH

In order to limit exposure to hazardous chrysotile, rheology tests on suspensions of chrysotile-quartz mixtures were not conducted over the entire range pH 3-11, as was done with the other phyllosilicate-quartz mixtures. It has been demonstrated that chrysotile does not have a single peak value for the point of maximum yield stress. Instead, there exists a pH range over which chrysotile aggregation is most apparent (circa pH 5.5–9) (Figure 6.3). In this range, there is little variation in the rheology of suspensions of pure chrysotile. Therefore, in determining whether this trend is prevalent in mineral mixtures comprising chrysotile, the rheology of suspensions of chrysotile-quartz mixtures was compared at pH 6 and pH 9. This gives an indication of the rheology of the mixtures as a function of pH. A comparison of the Bingham yield stress and viscosity at these conditions is given in Figure 8.8.

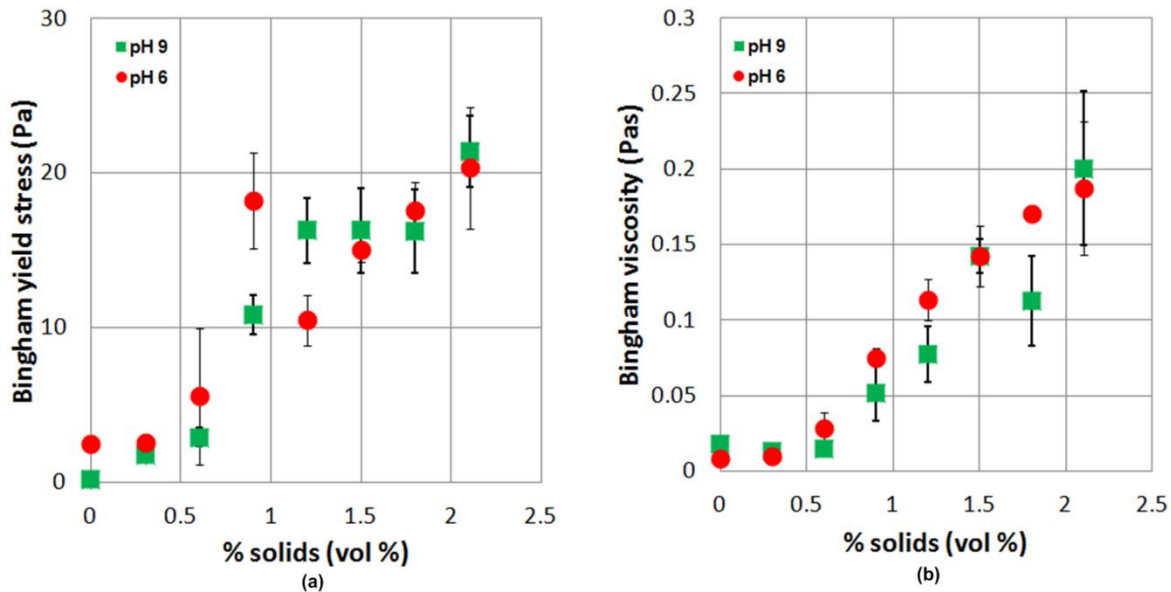


Figure 8.8 - A comparison of the (a) Bingham yield stresses and (b) Bingham viscosities of suspensions of chrysotile-quartz mixtures at pH 6 and pH 9. The error bars represent the 95% confidence interval on the average values. The x-axis only depicts the chrysotile concentration in a total of 30% v/v

In each case, tests were conducted within a 30% total solids volume, varying the proportion of chrysotile and quartz in the mixture. It must be noted that unlike muscovite and vermiculite, tests could not be conducted at high proportions of chrysotile (up to 30% solids by volume chrysotile). In fact, measurements on the chrysotile-quartz binary mixtures were limited to low chrysotile concentrations (< 2.5% by volume chrysotile, 27.5% quartz). Mixtures in this range comprise comparatively low phyllosilicate concentrations where complex suspension behaviour may not be expected. However, high yield stress values (20Pa) were observed, showing similarity to pure chrysotile suspension behaviour. This suggests that even with significantly higher volume concentrations of quartz in the mixture, the suspension behaviour is dominated by chrysotile. Again, this highlights the importance of the effective volume of the chrysotile particles. Although they may essentially exist in low apparent volumes, it is the high effective volume of individual fibres that enhances their effect on suspension flow behaviour.

A comparison of the rheological properties at pH 6 and pH 9 shows similarity in the yield stresses and viscosities of the suspensions. This concurs with findings observed for pure chrysotile suspensions. Together with the low chrysotile concentrations in the mixtures, this behaviour further demonstrates the dominance of chrysotile on the overall flow behaviour of the mineral mixtures. Therefore, although measurements could only be conducted at two pH values, the similarity in the suspension rheology at these conditions suggests that the rheology trend of chrysotile-quartz suspensions as a function of pH is similar to that observed for suspensions of pure chrysotile (Figure 6.3), with a yield stress peak range between pH 5.5 and pH 9.

On this basis, it is proposed that the yield stresses of chrysotile-quartz mixtures as a function of pH can also be viewed in 3 distinct regions similar to pure chrysotile suspensions. It is likely that the yield stress increases with pH in the region pH 4 to pH 5.5, and reaches a maximum at values between pH 5.5 and 9, after which there is a decrease between pH 9 and pH 11. The distinction in these regions is related to differences in the charge differential between quartz and chrysotile particles.

It can be assumed that chrysotile fibres are highly entangled throughout the range (pH 4 to 11), with quartz particles trapped between fibres. However, the degree of entanglement is enhanced

between pH 5.5 and pH 9 due to the large charge differential and strong attractive forces between strongly negative quartz particles and positively charged chrysotile particles. The charge differential (and yield stress) decreases with a characteristic decrease in the positive charge of chrysotile at higher pH (Figure 5.12). The proposed modes of particle association of chrysotile-quartz suspensions are shown in Figure 8.9.

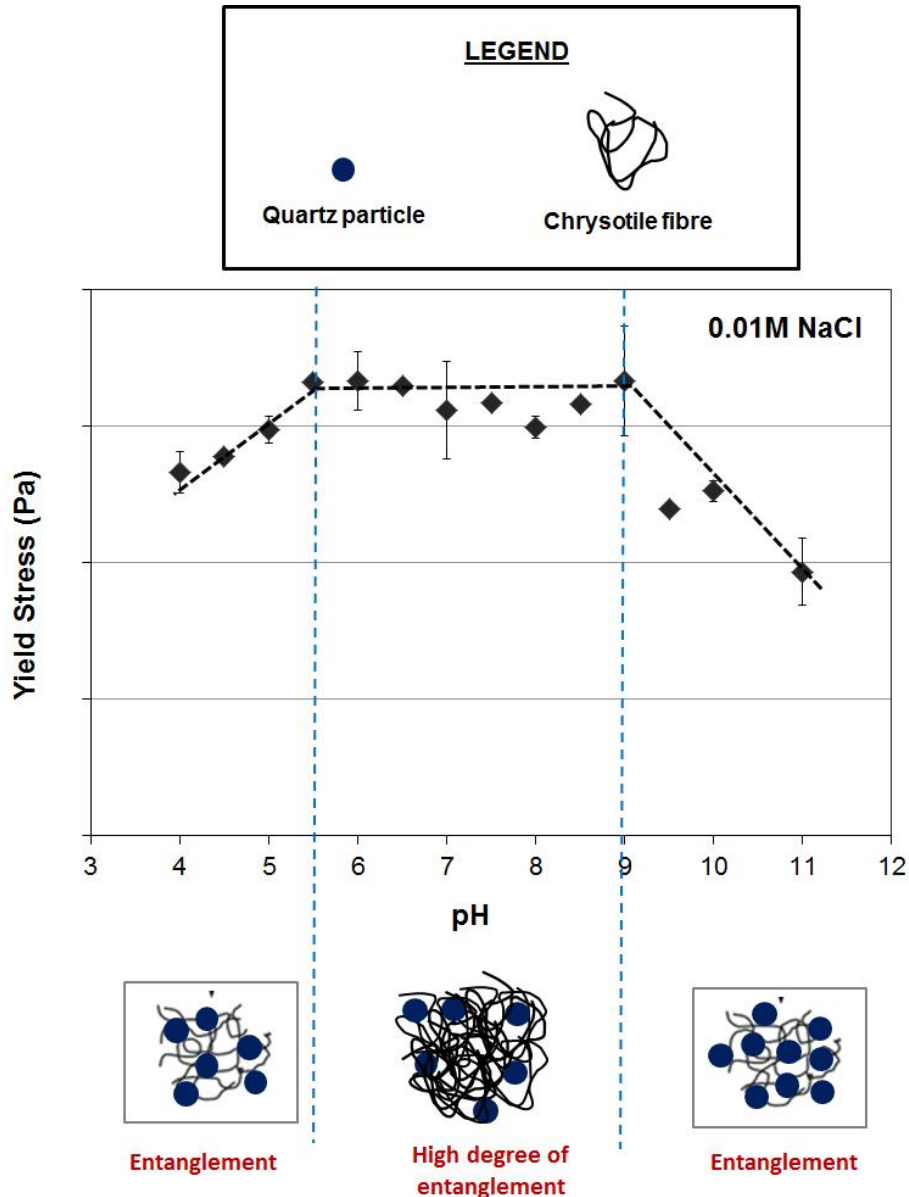


Figure 8.9 - Proposed modes of particle association in chrysotile-quartz mixtures as a function of pH. The yield stress data is for chrysotile only.

8.5.2. The rheology of suspensions of chrysotile-quartz mixtures at pH 9

pH 9 falls within the region of maximum yield stress in pure chrysotile suspension behaviour. It is believed that the aggregation of chrysotile particles is enhanced by the large charge differential between the tube lengths and edges at this pH. Even so, the surface charge is dominated by the exposed brucite layer and chrysotile particles carry an overall positive charge at pH 9. Therefore, within a binary mixture, attractive forces may exist with negatively charged quartz particles, and may enhance aggregation and suspension rheology due to additional chrysotile-quartz coagulation. Even so, it is expected that the fibrous morphology will have a definitive role towards the suspension flow behaviour of the chrysotile-bearing suspensions.

A comparison of the predicted yield stresses and viscosities of chrysotile-quartz mixtures (as dictated by the weighted effects of each mineral) relative to the experimentally determined values is given in Figure 8.10. Since tests were limited to mixtures with low concentrations of chrysotile, this analysis is presented for mixture concentrations within the range of pure quartz (30% quartz, 0% chrysotile) to 29% quartz, 1% chrysotile within 30% total solids by volume. The yield stresses are shown in Figure 8.10a and the viscosities in Figure 8.10b.

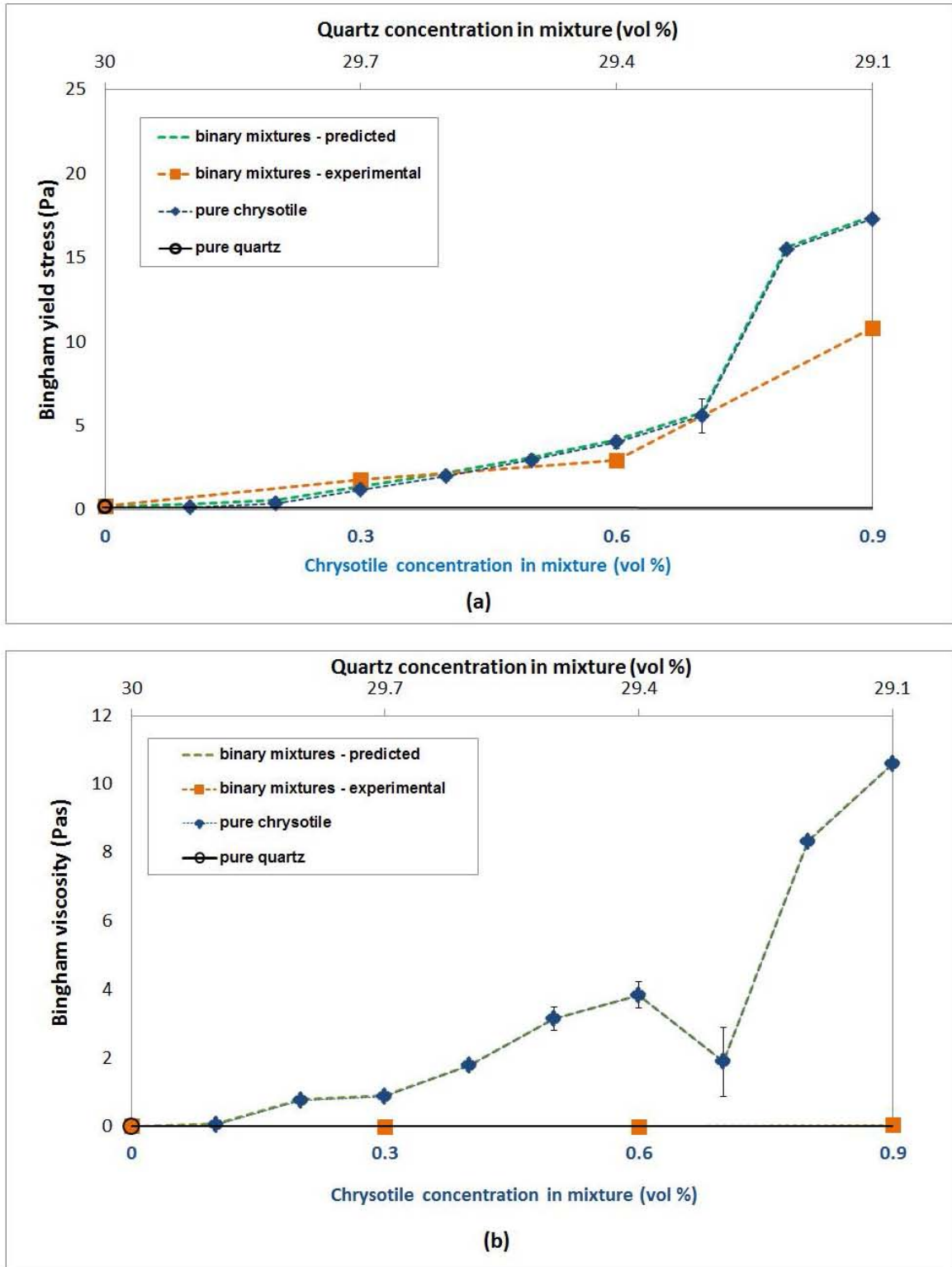


Figure 8.10 - A comparison of the (a) Bingham yield stresses and (b) Bingham viscosities of suspensions of chrysotile-quartz mixtures to the predicted model and to suspensions of pure chrysotile and quartz. The errors bars represent the 95% confidence interval of the average values.

A comparison of the pure minerals to the predicted binary behaviour shows that, at any given concentration, chrysotile will have a considerably higher contribution towards the suspension yield stress than quartz. Therefore, the predicted yield stress values are similar to those observed for pure chrysotile suspensions. This behaviour, is in fact, observed in the measured suspension yield stresses of the binary mixtures, with few discernible differences observed between pure chrysotile and chrysotile-quartz binary mixture behaviour. Lower yield stresses are observed at concentrations of 0.9% chrysotile-29.1% quartz, suggesting synergistic effects. However, based on the behaviour at even lower chrysotile concentrations, the reduction in yield stress may be attributed to experimental error. The similarity in suspension behaviour suggests that the presence of quartz is relatively inconsequential towards the suspension yield stress. Quartz, in this case, may behave as a benign component. Quartz particles are likely to become trapped in the intricate network of fibres and their rheological characteristics become 'masked' by chrysotile. The quartz particles do not significantly detangle or alter the high degree of entanglement, such that the suspension yield stress of chrysotile fibres is not significantly affected.

A comparison of the viscosities, on the other hand, shows different behaviour. Figure 8.10b shows that, based on pure mineral suspension behaviour, high viscosities similar to chrysotile are predicted. However, the binary mixtures are characterized by low suspension viscosities, more closely resembling quartz suspensions. This means that at high shear conditions, an equivalent volume of chrysotile particles will flow with more ease when present in a mineral mixture than in a homogeneous suspension. The reduction in viscosity shows clear synergistic effects between quartz and chrysotile particles. This suggests that upon yielding the quartz particles promote alignment of fibres within the flow field, making the system shear thin more dramatically (as indicated by the low Bingham viscosities) due to reversible structural breakdown.

8.6. DISCUSSION

The rheological properties of suspensions of binary mixtures of each phyllosilicate mineral with quartz have been investigated. In each case, the suspension behaviour of the mixtures has been

compared to that of the pure phyllosilicates as a function of pH, as a means to determine whether the phyllosilicates dominate the rheological behaviour of the mixture suspensions.

In all cases, the yield stress trend of the binary mixtures showed similarity to the component phyllosilicate mineral. This was expected since it had been previously determined that the phyllosilicates result in more rheologically complex suspension behaviour than quartz. The pH range over which the yield stress of vermiculite-quartz mixtures is maximum is similar to pure vermiculite suspensions and a yield stress trend similar to pure chrysotile suspensions could also be assumed for chrysotile-quartz mixtures. However, a deviation in the yield stress peak was observed for muscovite, indicating that when present in a mixture (or multicomponent system), muscovite may not necessarily dominate the suspension behaviour. It has already been shown that muscovite results in the least rheologically complex suspension behaviour when compared to the other phyllosilicates in this study, showing the most rheological similarity to quartz behaviour. Therefore, compared to vermiculite and chrysotile, it is expected that muscovite would present the most sensitivity due to the addition of another mineral. Vermiculite and chrysotile, on the other hand, are expected to dominate the suspension behaviour due to their inherent rheological complexity.

The rheological properties have also been investigated at pH 9, where the measured yield stresses/viscosities have been compared to predicted values based on the additive contributions at each mixture concentration. This is one method that can be used in determining the synergistic or antagonistic effects during blending and has been successfully applied in other industries (e.g. pharmaceuticals) but has found less application in the minerals processing industry. However, as blending techniques are being increasingly used as a means to mitigate the processing issues associated with problematic ores, this simple analysis serves to examine its applicability to rheological predictions.

Table 8.1 gives a summary on the findings of the yield stresses and viscosities of each phyllosilicate-quartz mixture, where synergistic effects are indicative of better suspension behaviour (lower yield stresses and viscosities) than predicted, while antagonistic effects suggest higher yield stresses and viscosities. Within the rheological context, synergistic effects are ideal

as they result in improved and more manageable properties. Antagonistic effects, on the other hand, result in more complex suspension behaviour which cannot be easily estimated based on the concentrations of constituent minerals. Such behaviour would result in less predictable and controllable metallurgical performance.

Table 8.1 – A summary of the rheological effects of mixing each phyllosilicate mineral with quartz.

Mixture	Bingham yield stress	Bingham viscosity	Overall effect
Muscovite-quartz	Antagonistic	Antagonistic	Antagonistic
Vermiculite-quartz	Antagonistic	Antagonistic	Antagonistic
Chrysotile-quartz	Little/no effect	Synergistic	Synergistic

Antagonistic effects were observed for muscovite and vermiculite binary mixtures, indicating that the addition of quartz results in higher yield stresses and viscosities. This has been attributed to the possible development of additional edge-quartz interactions, which may result in additional network structural formation, giving rise to higher suspension yield stresses and viscosities. Even so, the rheological properties of muscovite-quartz mixtures result in suspensions of lower yield stresses and viscosities, which in most cases would be considered rheologically negligible. On this basis, muscovite bearing suspensions are less likely to result in rheologically problematic suspensions. The addition of quartz to vermiculite suspensions, on the other hand, results in significant increases in suspension yield stress and viscosity, and vermiculite bearing suspensions are likely to cause rheological related problems.

The addition of quartz to chrysotile shows little/no effect to the yield stresses, owing to the high effective volume and entanglement of the long, thin fibres. However, synergistic effects are observed with the viscosities, suggesting improved chrysotile flow characteristics in multicomponent systems. This is perhaps the most significant finding in this case as it suggests that the deleterious effects of chrysotile can be controlled or improved through blending techniques.

8.6.1. A comparison of the rheology of suspensions of phyllosilicate-quartz mixtures

Having determined the synergistic and antagonistic interactions within each binary mixture, it is now possible to compare the rheology of all the mixtures for a preliminary indication of the relative rheological behaviour of phyllosilicate bearing ores. Figure 8.11 gives a comparison of the Bingham yield stresses and viscosities of the binary mixtures. The rheological behaviour of the binary mixtures is also evaluated against the rheology of pure mineral suspensions here.

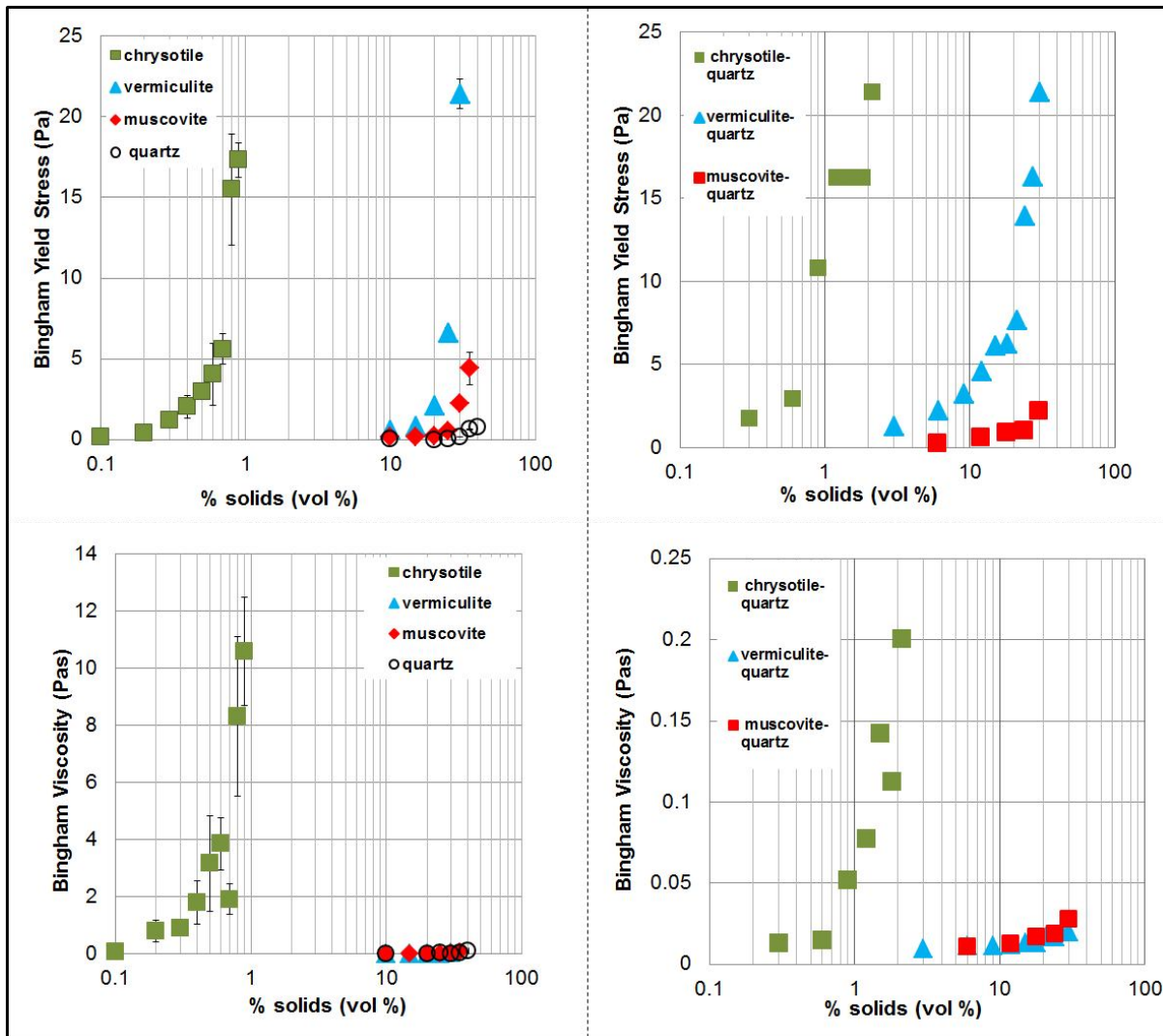


Figure 8.11 – A comparison of the Bingham yield stresses and viscosities of pure mineral suspensions and suspensions of binary mixtures. The mixture data is for % v/v phyllosilicates in a total 30% v/v solids mixture.

A comparison of the Bingham yield stresses of the binary mixtures shows a trend similar to that seen in the rheology of the pure minerals. Suspensions containing muscovite and vermiculite are still characterised by comparatively low yield stresses. Vermiculite-quartz mixtures are characterised by higher yield stresses than suspensions of muscovite-quartz mixtures not only due to differences in particle association between vermiculite particles, but also possibly due to a higher degree of charge anisotropy and attractive forces in vermiculite-quartz flocs. This results in a more defined difference in the suspension yield stresses of vermiculite and muscovite when present in mineral mixtures than was observed in homogeneous suspensions. Nonetheless, suspensions containing muscovite and vermiculite still have comparatively low viscosities similar to those observed in pure suspensions at high shear conditions.

The extremely high yield stresses observed in pure chrysotile suspensions are prevalent in suspensions of chrysotile-quartz mixtures. However, the viscosities of pure chrysotile are reduced drastically when in the presence of quartz. Even so, the occurrence of chrysotile in small amounts results in suspensions which are much more viscous than suspensions containing vermiculite or muscovite at much higher concentrations.

8.6.2. Implications on phyllosilicate mineral behaviour in real ores

The prediction of rheological performance has been based primarily on the volume contributions of each element. This is equivalent to the relative feed proportions of different streams in calculating flotation recoveries or grinding efficiency of blended streams where an analysis such as this has been used (Van Tonder et al., 2010). While this may be adequate for predicting performance in these systems, it does not adequately predict the expected rheological response of blended streams. In this case, blending is not just about mixing a ‘good’ and ‘bad’ ore. Rheological suspension behaviour is also strongly dependent on the particle interactions that are likely to form in suspension, and these contribute towards the observed synergistic or antagonistic responses. These need to be considered when predicting the rheological response of blended streams but cannot be adequately detected by an analysis based on volume/mass

proportion. Therefore, this must be considered when applying blending techniques to rheological systems. Indeed, the suggested additional interactions are inferred and further research would be required to validate the findings. However, as a simplistic analysis, the point made is valid.

Although the binary mixtures used in this study form simple mineral systems, they provide an understanding of the interactions and effects of each mineral when present in real ore systems, on a preliminary basis. The findings of this study can be used to better explain the rheological behaviour of these minerals within the minerals processing industry. This is essential towards the characterisation of the rheological behaviour of ores containing platy, fibrous and swelling clay phyllosilicate gangue minerals.

Suspensions containing muscovite and quartz have comparatively lower yield stresses and viscosities than the other phyllosilicate-quartz mixture suspensions. On this basis, it can be inferred that suspensions containing muscovite (and other micas) are likely to present the least rheological problems during ore beneficiation. This can be related to the metallurgical performance of micaceous bearing ores. The results of this study indicate that the rheological complexity associated with muscovite is alleviated by electrostatic attraction with other minerals at conditions of opposite charge. This is in agreement with previous studies which have attributed the sliming of phyllosilicate particles to valuable minerals during sulphide mineral flotation (Edwards et al., 1980; Bremmell et al., 2005; Mitchell et al., 2005).

It is worth noting, however, that although micaceous minerals do not typically present problematic rheological behaviour (compared to other phyllosilicate minerals), this may not necessarily be the case when present in more complex mineral systems. This is because the interaction between micaceous minerals and other minerals in suspension is dependent on the interfacial chemistry of the other minerals contained in the ore. For example, unexpected heterocoagulation and reduced flotation rates have been observed during sulphide mineral flotation (He et al., 2009). Here, the presence of oxidation, dissolution of the sulphide minerals and specific adsorption of specific hydrolysed ions modify the surface structure of muscovite particles and result in marked increases in shear yield stresses of muscovite in muscovite-sulphide mixtures (Nasroti, 2010). This not only reduces the hydrophobicity of the sulphide

minerals but also reduces collector adsorption and/or selectivity (Ralston and Fornaserio, 2006). Such rheological enhancements will also have implications on hydrometallurgical, separation and smelting operations involving mica rich pulps and may lead to significant economic losses to the minerals industry (He et al., 2009).

There have not been many reports regarding problematic processing behaviour specifically due to vermiculite gangue. Owing to its paragenesis, vermiculite is often classed as micaceous or as a swelling clay. This study has demonstrated that vermiculite displays different colloidal properties to muscovite resulting in more complex suspension flow behaviour. Therefore, classifying it under this group could potentially result in ‘unexpected’ issues. Swelling clays, on the other hand, are known to have deleterious effects particularly during tailings treatment due to their poor compaction and dewatering abilities. Such problems have been encountered in several industries such as the coal industry (de Kretser et al., 1997), the Florida phosphate mining industry (Somasundaran et al., 1975), and the Australian bauxite processing industry (Nguyen and Boger, 1998; Sofrá and Boger, 2002). While vermiculite does display swelling properties, this is to a far less extent than smectites such as montmorillonite and vermiculite bearing ores are not likely to present issues to as great an extent. Even so, the observed rheological complexities, especially above a critical concentration are likely to cause hydrometallurgical processing issues to a much higher degree than muscovitic suspensions. The disposal of vermiculite bearing tailings to other industries (e.g. foundry, paper, cosmetics, insulation, road works and food industries) where they have many applications is preferred as a means to avoid treatment altogether (Schoeman, 1989). Where vermiculite has been observed to report to the concentrate, the elevated quantities of MgO have been known to cause furnace operational problems during smelting and downstream processing. This is due to increased liquidus temperatures, often resulting in smelting penalties for mineral processing companies (Beattie et al., 2006).

The issues that are typically experienced during the beneficiation of ores containing chrysotile have been mentioned briefly in Chapter 2. The high yield stresses and viscosities observed at extremely low solids concentrations concur with the high pulp viscosities (at concentration as low as 8% solids by volume) that have been observed during the flotation of serpentine-rich ores (Genc et al., 2010). The complex rheological behaviour of chrysotile is also evident in decreased

hydrodynamic performance and high power inputs during flotation. The transportation of chrysotile to the concentrate is related to the strong positive charge of chrysotile particles which almost completely depress negatively charged sulphides and report to the concentrate (Edwards et al., 1980). Entrainment of chrysotile has also been reported to be due to the entrapment of floatable sulphides, rendering chrysotile naturally floatable by association (Patra et al., 2010). This leads to impeded flotation kinetics, decreased hydrodynamic performance and froth instability. In comminution, chrysotile bearing ores present decreased grinding efficiency due to the long, thin morphology of the fibres (Connelly, 2011). All these are in support of the complex rheological behaviour observed. The synergistic effects observed could be used as a means to reduce the physical morphological effects of chrysotile in suspension.

University of Cape Town

Chapter 9.

CONCLUSIONS AND RECOMMENDATIONS

The primary objective of this thesis was to characterise the colloidal behaviour of three phyllosilicates, namely muscovite, vermiculite and chrysotile in terms of their surface charge, mineralogical and resultant rheological properties. These minerals commonly exist as gangue material in many low grade ores. The thesis was initiated in order to gain a better understanding of the flow behaviour of these minerals within well-defined model mineral systems, with a longer term view to understanding their impact in complex mineral systems found in mineral processing circuits.

Indeed clay/phyllosilicate colloidal behaviour is a complex field of study, perhaps complicated by the existence of several different schools of thought on important fundamental issues. As such, the subjective and multifaceted behaviour of phyllosilicates is appropriately recognized in this study. Conventional and non-conventional theories and analytical techniques have been considered in seeking to reconcile the respective surface charge analysis, charge anisotropy and aggregation mechanisms in this study. As a result, theories on factors such as the modes of particle interaction can only be inferred, based on the rheological trends observed here. This then makes it difficult to achieve definitive conclusions on phyllosilicate colloidal characteristics on a broad scale and most research in this area can mainly serve as a contribution towards ongoing studies to better isolate the causes of phyllosilicate behaviour. There remains a large scope for continued research and it is acknowledged that further characterization efforts are warranted if the mineral processing industry is to gain a comprehensive understanding of phyllosilicate colloidal behaviour.

This chapter presents a summary of the main findings from this thesis, taking into consideration the analytical techniques and theories which have been implemented. The implications and recommendations for future work are also put forward.

9.1. PHYLLOSILICATE MINERALOGY

In this study, XRD and SEM analyses were used to substantiate existing literature based on the shape and properties specific to each mineral. It was demonstrated that:

- Quartz particles are angular in shape, existing in a combination of hexagonal and cubic particles of comparatively low aspect ratio. These form closely packed clusters.
- Muscovite has a long, thin platy morphology, with an aspect ratio estimated in the range 40-130, making the edge surfaces relatively insignificant to the basal planes.
- Vermiculite particles also have a platy morphology, with sheets of lower aspect ratio (~16-20) and comparatively rougher surfaces than muscovite. The platelets also characteristically expand in a concertina/worm-like manner upon exfoliation.
- Chrysotile particles have a fibrous morphology (aspect ratio estimated at 1000) and form highly entangled meshes with fibres entangled both within themselves and with adjacent fibres.

The observed morphological properties are characteristic of each of the minerals and are in agreement with several other researchers which have found similar properties.

9.2. PHYLLOSILICATE SURFACE CHARGE DISTRIBUTION

The zeta potential measurement has often been used as a sole means of estimating the surface charge properties of phyllosilicates. However, the accuracy of this method and its application to the phyllosilicates in this study is compromised by its inherent assumption of spherical

morphology. In each case, the inaccuracy of the zeta potential measurement has been demonstrated through deviations between the apparent iso-electric point (measured by the zeta potential measurement) and the point of zero charge (estimated from the Roberts Mular titration). Such behaviour is consistent with that of anisotropically charged minerals that carry a different charge on multiple particle planes. This is contrary to what was observed for quartz, which showed a similarity in the point of zero charge and iso-electric point as is commonly observed in isotropically charged minerals. For this reason, quartz served as a good basis for comparison with the phyllosilicate minerals due to its isotropic charge and comparatively regular morphology.

This study has proposed the combined use of the Roberts Mular titration and zeta potential measurements as a means to estimate the *degree of charge anisotropy* of the minerals under study. Herein, a large deviation between the point of zero charge and the iso-electric point is indicative of a high degree of charge anisotropy. This has been supplemented with an estimation of the charge differential between edges and faces by calculation of the permanent negative charge component of the basal plane/face. This charge is attributable to the degree of isomorphous substitution, which in each case, has been approximated using a calculation based on the elemental composition of each mineral. The derivation and dissipation of charge is in line with the proposed charges for kaolinite and talc (phyllosilicate clay minerals) whose charge properties have been studied most extensively and are well documented in literature. The exact magnitude of the electrical charge on the basal planes of each mineral is unknown, but the proposed charge distributions were based on the relative degrees of substitution. Following this analytical approach, it has been proposed that the degree of charge anisotropy increases in the order chrysotile < muscovite < vermiculite. Schematic representations of the comparative charge distributions in summary of the surface charge analysis for each mineral are given in Figure 9.1.

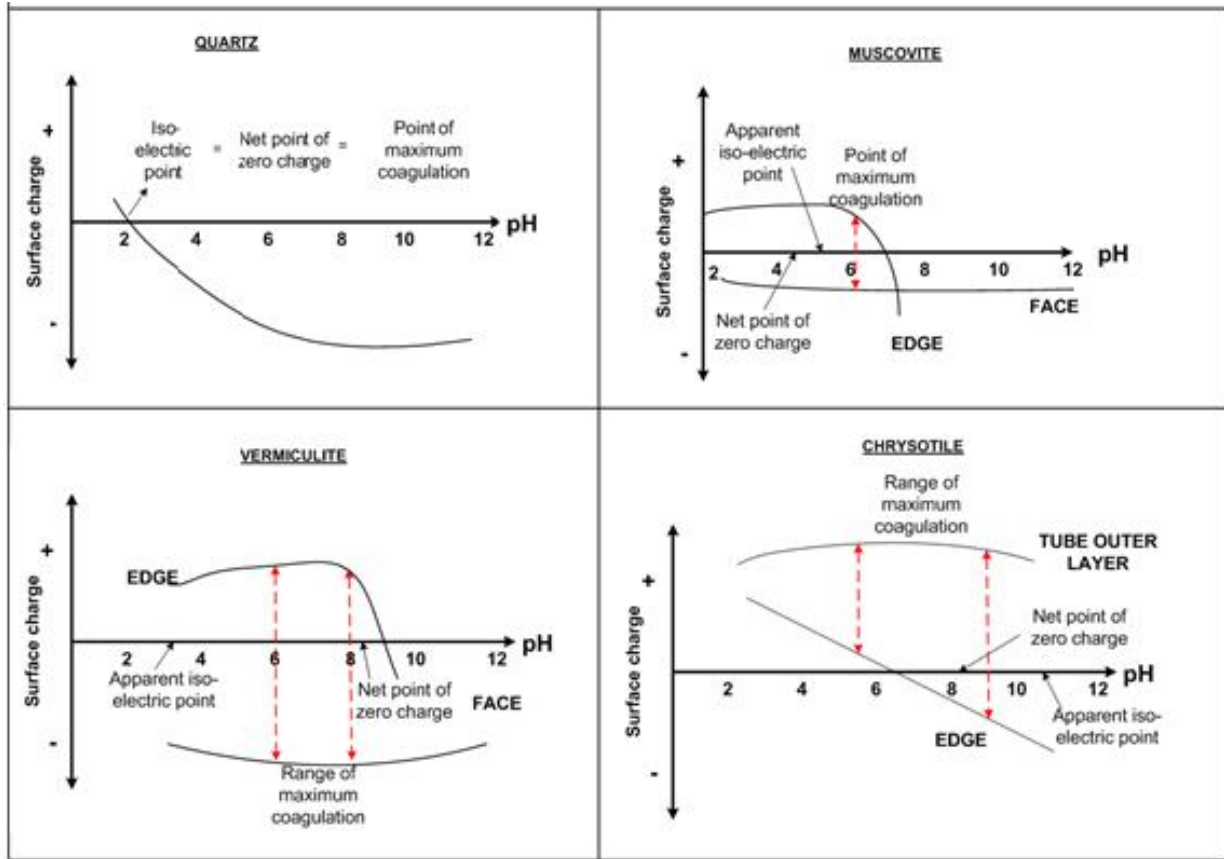


Figure 9.1 – Proposed charge distributions of the phyllosilicate minerals.

9.2.1.1. THE INFLUENCE OF MORPHOLOGY AND SURFACE CHARGE ON SUSPENSION RHEOLOGY

The rheological properties of suspensions of each mineral have been investigated and discussed in terms of the observed and proposed morphological and surface charge characteristics. Indeed both surface charge and particle morphology play an integral role towards the colloidal behaviour of these minerals. However, the flow characteristics of these minerals are also a result of other factors such as electrolyte concentration. In this study, attempts to minimize the influence of these other external factors have been made. Even so, it is difficult to isolate the specific effects of particle morphology and surface charge as they are intrinsically dependent on each other. However, the rheological characteristics differ from phyllosilicate to phyllosilicate, where morphological and surface charge effects may have varying levels of influence.

Chrysotile suspensions are characterized by the most complex suspension rheology, with high yield stresses and viscosities observed at extremely low solid concentrations (< 1% by volume). The flow behaviour in this case can be largely attributed to the long, thin morphology and flexibility of the fibres which enhance entanglement when in suspension. This results in high effective volume of individual fibres, despite their low concentration. Here, surface charge anisotropy does not play a significant role towards the suspension rheology.

Muscovite and vermiculite both have a platy morphology, although muscovite platelets have characteristically higher aspect ratios than vermiculite. This then minimizes the effect of charge anisotropy in muscovite as the basal plane charge dominates such that the edge charge contribution is comparatively insignificant. Face-face aggregation is the dominant mode of particle aggregation, resulting in the least complex suspension rheology. While face-face association is still important for vermiculite suspensions, the edge contribution may be more significant due to the lower aspect ratio of the platelets. Here, particle realignment to edge-face and edge-edge structures is more likely, resulting in the observed higher yield stresses and viscosities.

By considering the morphology of the minerals, the rheological investigations demonstrated that suspension rheology is most complex in suspensions containing fibrous (chrysotile) minerals, followed by platy minerals (vermiculite, muscovite) and finally angular (quartz) minerals. These results are consistent with the premise that suspension rheology is more pronounced if particles are non-spherical and are in agreement with findings from other researchers who have found similar trends using synthetic materials (Barnes et al., 1989).

9.3. THE RHEOLOGICAL BEHAVIOUR OF BINARY MIXTURE SUSPENSIONS

The behaviour of the phyllosilicate minerals in binary mixtures comprising quartz and each phyllosilicate mineral were investigated to gain a preliminary understanding of the effects of the

phyllosilicate minerals when in suspension with minerals of different morphology and surface charge as is typically observed in real ores.

It was demonstrated that the application of robust mixture designs as a means to predict performance is not as simple for rheological systems. The rheology cannot be predicted based solely on the weighted additive concentrations of each mineral in the mixture. Instead, the interactions that are likely to occur between particles in suspension should be taken into account, although these are not easily calculable in mixture design.

In the case of muscovite and vermiculite, the surface charge effects are likely to promote aggregation and formation of complexes with quartz, resulting in higher suspension yield stresses and viscosities (antagonistic effects). The high degree of entanglement in chrysotile suspensions, on the other hand, was unaffected by the presence of quartz. However, the ease of flow (and suspension viscosities) was improved likely due to the detangling of fibres by spherical quartz particles, showing overall synergistic effects. This finding suggests that chrysotile rheological effects may be mitigated through blending techniques. However, further investigation would be required to support this.

The rheological analysis of phyllosilicate-bearing suspensions has facilitated the development of a rheological classification of the minerals studied. This classification serves to demonstrate that phyllosilicates behave differently with some presenting more rheological complexity than others. Such an understanding is beneficial for predicting ore performance based on the phyllosilicate gangue material. Figure 9.2 gives a graphical representation of the classification of chrysotile, vermiculite and muscovite relative quartz, in terms of suspension yield stress and viscosity. It must be noted that this classification is based on high shear systems which are most relevant in mineral processing applications.

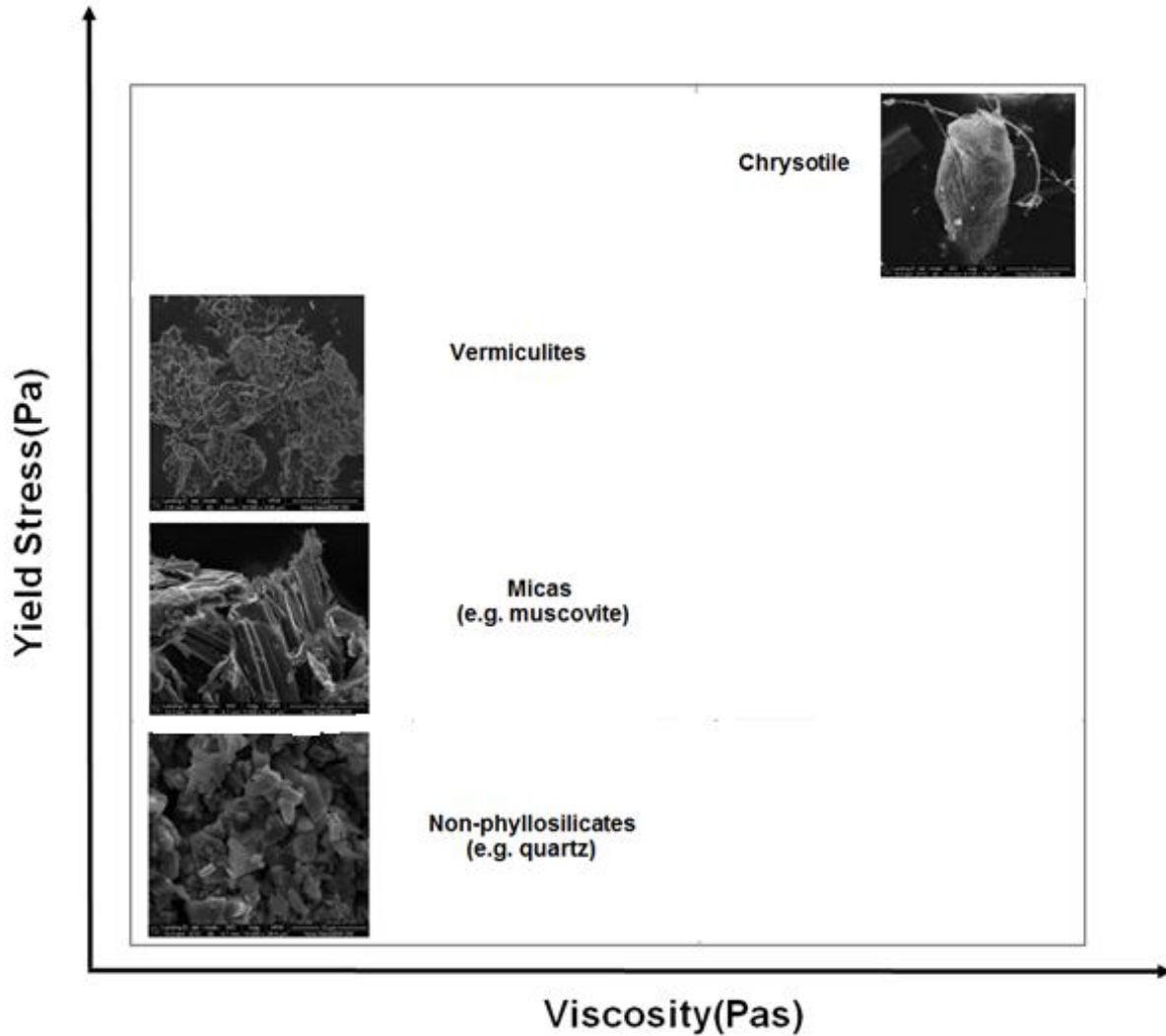


Figure 9.2 – A graphical representation of the classification of chrysotile, vermiculite and muscovite suspension behaviour.

9.4. IMPLICATIONS OF THE STUDY

The motivation behind this research was the increasing need for the beneficiation of low grade ores which contain multiple phases of phyllosilicate gangue minerals. The required fine grinding of these ores results in rheological difficulties. Although there have been several studies which have looked into ways of improving the efficiency and throughput on specific operations which process low grade ores, there is limited knowledge regarding the relationship between pure

phyllosilicate gangue mineralogy and its metallurgical behaviour. Moreover, the accurate analysis of these minerals has been compromised by their irregular morphologies and surface charge properties.

In this thesis, the pivotal role of particle surface charge and mineralogy towards the behaviour of phyllosilicate minerals has been demonstrated. Based on the specific effects of these factors, the results of this study have developed a better understanding of the flow behaviour of each mineral. As a result, the modes of particle association of the phyllosilicate minerals not only in homogenous but also in heterogeneous mineral systems have been proposed. This serves as a basis for further studies into the behaviour of these minerals within complex systems which more closely resemble real ores.

The importance of accurately characterizing the surface charge properties of phyllosilicate group minerals has been highlighted. Indeed accurate surface charge characterization remains a challenge. However, it has been demonstrated in this study that the use of a combination of techniques yields a more comprehensive understanding of the charge distribution. Furthermore, the importance of surface charge and morphology towards suspension behaviour of each mineral has been identified. This could be beneficial towards the formulation of mitigation strategies for dealing with these minerals.

Indeed this study has analysed model mineral systems and the outcomes may not necessarily be directly applicable to specific processes. However, by characterizing the behaviour according to suspension yield stresses and viscosities, the results provide a means to predict issues that may arise in industrial operations. In general, high yield stresses and viscosities are manifest in several operational issues such as high pumping energy requirements, low gas dispersion, high agitation rates, turbulence damping, low grinding performance, low product fineness and poor settling rates. Therefore, for each mineral, the yield stresses and viscosities can be linked to specific processes.

The most practical applications of this study can be seen in the analysis of binary mixtures which has provided an indication of the effects of these phyllosilicate minerals within a mineral mixture

resembling a simple ore. The synergistic effects observed for chrysotile indicate that the rheological effects of this mineral can be mitigated through blending. With a better knowledge of the specific interactions that are likely to occur between minerals, issues that commonly arise such as high pulp viscosities and low settling rates during the processing of phyllosilicate bearing ores can now be better understood.

Finally, this study has been able to establish a link between phyllosilicate mineralogy and rheological performance, demonstrating the importance of using the principles of applied mineralogy and minerals processing in tandem as a means to better understand metallurgical performance. By keeping the same principles in mind, the information provided by this study could be supplemented by coupling with geometallurgical techniques (such as hylogging and automated early mineral detection), with the eventual aim of assessing and if possible predicting ore behaviour on the basis of mineralogical data. In the long run, this could be beneficial for the recognition of potentially problematic minerals upfront and could be important in flow sheet design and plant optimization. Such an understanding could significantly improve downstream effects and result in long term financial savings.

9.5. RECOMMENDATIONS FOR FUTURE WORK

In light of the findings of this thesis, the following recommendations can be made:

- The study of phyllosilicate mineralogy should be extended to include additional factors such as textural analysis and topography for a conclusive mineralogical analysis and to determine whether these factors contribute towards mineral behaviour.
- The application of the zeta potential and Roberts Mular titration measurements in tandem should be used in the surface charge analysis of other phyllosilicates to further validate its effectiveness for anisotropically charged minerals.

- The work presented in this thesis should be extended to other phyllosilicate minerals for an inclusive and broader classification of the behaviour of phyllosilicate group minerals.
- Having gained a better understanding of the effects of these minerals in their pure form and in simple mineral systems, this study could be extended to more complex systems which more closely resemble real ores. A naturally occurring ore containing phyllosilicate minerals could be investigated to determine whether the theoretical findings are in agreement with real ore behaviour.
- The study of the rheological properties is of broad significance as properties such as suspension yield stress and viscosity are reflected in different process parameters such as power draw, breakage rate, fines production, dispersant usage and particle size. In future studies, the effects of the phyllosilicate rheological behaviour on these parameters should be investigated. This would provide a practical link between phyllosilicate rheological properties and metallurgical performance in different phases of the process circuit.
- In the case of chrysotile with detrimental effects at low concentrations, future studies which focus on identifying the critical concentrations in naturally occurring ores beyond which suspension behaviour is no longer manageable could be conducted.
- In depth studies in the form of atomic forces measurements or nano-scaled imaging could be used to investigate the proposed modes of particle interaction within homogeneous and binary mineral systems.

REFERENCES

- Abend, S., and Lagaly, G. 2000, "Sol-gel transitions of sodium montmorillonite dispersions", *Applied Clay Science*, vol. 16, pp. 201-227.
- Abollino, O., Giacomino, A., Malandrino, M. and Mentasti, E. 2008, "Interaction of metal ions with montmorillonite and vermiculite", *Applied Clay Science*, vol. 38, pp. 227-236.
- Addai-Mensah, J. and Ralston, J. 2005, "Investigation of the role of interfacial chemistry on particle interactions, sedimentation and electro osmotic dewatering of model kaolinite dispersions", *Powder Technology*, vol. 160, pp. 35-39.
- Addai-Mensah, J. and Ralston, J. 2004, "Interfacial chemistry and particle interactions and their impact upon dewatering behavior of iron oxide dispersions", *Hydrometallurgy*, vol. 74, pp. 221-231.
- Alderman, N. J., Meeten, G. H., and Sherwood, J. D. 1991, "Vane rheometry of bentonite gels", *Journal of Non-Newtonian Fluid Mechanics*, vol. 39, pp. 291-310.
- Allison, S.A. and O'Connor, C.T. 2011, "An investigation into the flotation behaviour of pyrrhotite", *International Journal of Mineral Processing*, vol. 98, pp. 202-207.
- Alvarez-Silva, M., Uribe-Salas, A., Mirnezami, M. and Finch, J.A. 2010, "The point of zero charge of phyllosilicate minerals using the Mular–Roberts titration technique", *Minerals Engineering*, vol. 23, pp. 383-389.
- Antonijevic, M.M., Dimitrijevic, M.D., Stevanovic, Z.O., Serbula, S.M. and Bogdanovic, G.D. 2008, "Investigation of the possibility of copper recovery from the flotation tailings by acid leaching", *Journal of Hazardous Materials*, 158,1, pp. 23-34.
- Arnold, B.J. and Aplan, F.F. 1986, "The effect of clay slimes on coal flotation, Part 2: The role of water quality", *International Journal of Minerals Processing*, vol. 17, pp. 243-260.
- Arshad, M.A., St. Arnaud, R.J. and Huang, P.M. 1972, "Dissolution of trioctahedral layer silicates by ammonium oxalate, sodium dithionite-citrate-bicarbonate and potassium pyrophosphate", *Canadian Journal of Soil Science*, vol. 25, pp. 19-25.
- Bacchin, P., Bonino, J., Martin, F., Combacau, M., Barthes, P., Petit, S. and Ferret, J. 2006, "Surface pre-coating of talc particles by carboxyl methyl cellulose adsorption: Study of

- adsorption and consequences on surface properties and settling rate", *Colloids and Surfaces A: Physicochemical and Engineering Aspects*, vol. 272, pp. 211-219.
- Bakker, C.W., Meyer, C.J. and Deglon, D.A. 2010, "The development of a cavern model for mechanical flotation cells", *Minerals Engineering*, vol. 23, pp. 968-972.
- Bakker, C.W., Meyer, C.J. and Deglon, D.A. 2009, "Numerical modelling of non-Newtonian slurry in a mechanical flotation cell", *Minerals Engineering*, vol. 22, pp. 944-950.
- Barabaszova, K. and Valaskova, M. 2013, "Characterisation of vermiculite particles after different milling techniques", *Powder Technology*, doi: 10.1016/j.powtec.2013.01.05
- Barnes, H.A. and Nguyen, Q.D. 2001, "Rotating vane geometry – a review", *Journal of Non-Newtonian Fluid Mechanics*, vol. 98, pp. 1-14.
- Barnes, H.A. 1999, "The yield stress—A review or "πανταρει"—Everything flows?", *Journal of Non-Newtonian Fluid Mechanics*, vol. 81 pp. 133-178.
- Barnes, H.A., Hutton, J.F. and Walters, K. 1989, *An Introduction to Rheology*, Elsevier.
- Barton Jr., J.M., Barnett, C.S., Barton, W.P., Barnett, M., Doorgapershad, A., Twiggs, C., Klema, R., Martin, J., Meillonig, J. and Zenglein, R. 2003, "The geology of the area surrounding the Venetia Kimberlite pipes, Limpopo belt, South Africa: A complex interplay of nappe tectonics and granitoid magmatism", *South African Journal of Geology*, vol. 106, pp. 109-128.
- Basset, W.A. 1963, "The geology of vermiculite occurrences", *Clays and Clay Minerals*, vol. 10, pp. 61-96.
- Beattie, D.A., Huynh, L., Kaggwa, G.N. and Ralston, J. 2006, "The effect of polysaccharides and polyacrylamides on the depression of talc and the flotation of sulphide minerals", *Minerals Engineering*, vol. 19, pp. 598-608.
- Becker, M., Harris, P.J., Wiese, J.G. and Bradshaw, D.J. 2009, "Mineralogical characterisation of naturally floatable gangue in Merensky Reef ore flotation", *International Journal of Mineral Processing*, vol. 93, pp. 246-255.
- Benna, M., Kbir-Ariguib, N., Magnin, A. and Bergaya, F. 1999, "Effect of pH on rheological properties of purified sodium bentonite suspensions", *Journal of Colloid and Interface Science*, vol. 218, pp. 442-455.
- Bochart, G. 1989. Chapter 14 – Smectites in Minerals in soil environments, eds. Dixon, J.B. and Weed, S.B. *Soil Science Society of America, Madison, Wisconsin, USA*, pp. 675-727.

- Boersma, W.H., Laven, J. and Stein, H. N. 1990, "Shear thickening (dilatancy) in concentrated dispersions", *AICHe Journal*, vol. 36, pp. 321-332.
- Boger, D.V. 2009, "Rheology and the resource industries", *Chemical Engineering Science*, vol. 64, pp. 4525-4536.
- Boger, D.V.1999, "Rheology and the minerals industry", *Mineral processing and extractive metallurgy review*, vol. 20, pp. 1 - 25.
- Boggs, S. 2006. *Principles of Sedimentology and Stratigraphy*, 4th edition, Pearson Prentice Hall, Upper Saddle River, NJ.
- Bolland, M.D.A., Posner, A.M. and Quirk, J.P.1976, "Surface charge on kaolinites in aqueous suspensions" *Austr. J. Soil Res.*, vol. 14, pp. 197-216.
- Boshoff, E.T., Morkel, J., Vermaak, M.K.G. and Pistorius, P.C. 2007, "Kimberlite degradation: The role of cation type", *Minerals Engineering*, vol. 20, pp. 1351-1359.
- Bourg, I.C., Sposito, G. and Bourg, A.C.M. 2007, "Modelling the acid-base surface chemistry of montmorillonite", *Journal of Colloid and Interface Science*, vol. 312, pp. 297 – 310.
- Bracke, G., Satir, M., Kraub, P.1995, "The cryptand [222] for exchanging cations of micas", *Clay and Clay Minerals*, vol. 43, pp. 732 – 737.
- Brady, P. V. and Krumhansl, J. L. 2001, "The surface chemistry of clay minerals", *Surfactant Sci. Series*, vol. 103, pp. 281-301.
- Brady, P. V., Cygan, R. T. and Nagy, K. L. 1998, "Surface charge and metal sorption to kaolinite", *Adsorption Metals Geomedia*, pp. 371-382.
- Brandenburg, H. and Lagaly, G. 1988, "Rheological properties of sodium montmorillonite dispersions", *Applied Clay Science*, vol. 3, pp. 263-279.
- Breeman, N. and Buurman, P. 1998, *Soil formation*, Kluwer Academic Publishers, Dordrecht, The Netherlands.
- Bremmell, K.E. and Addai-Mensah, J. 2005, "Interfacial chemistry mediated behaviour of colloidal talc dispersions", *J. Colloid and Interface Science*, vol. 283, pp. 1173-1182.
- Bremmell, K.E., Fornaserio, D. and Ralston, J. 2005, "Pentlandite-lizardite interactions and implications for their separation by flotation", *Colloids and Surfaces: A Physiochemical and Engineering Aspects*, vol. 252, pp. 207-212.

- Brewster, G.R. 1980, "Effect of chemical pre-treatment on X-ray powder diffraction characteristics of clay minerals derived from volcanic ash", *Clay and Clay Minerals*, vol. 28, pp. 303-310.
- Brindley, G.W. and Brown, G. 1980, *Crystal structures of clay minerals and their X-ray identification*, eds. Brindley, G.W. and Brown, G. Mineralogical Society, London, UK, pp. 98 – 104; 210-212.
- Brindley, G.W. and Zussman, J. 1957, "Chrysotile cross fibre vein", *Amer. Min*, vol. 42, pp. 461-474.
- Bourg, I.C., Sposito, G. and Bourg, A.C.M. 2007, "Modeling the acid-base surface chemistry of montmorillonite", *Journal of Colloid and Interface Science*, vol. 312, pp. 297-310.
- Bulatovic, S.M., Wyslouzil, D.M. and Kant, C. 1999, "Effect of clay slimes on copper, molybdenum flotation from porphyry ores", In *Proceedings of the Copper '99-Cober '99 International Conference*, Phoenix, pp. 95-111.
- Burdukova, E., Becker, M., Ndlovu, B., Mokgethi, B. and Deglon, D.A. 2008, "Relationship between slurry rheology and its mineralogical content", In *24th International Minerals Processing Congress*, eds. Wang, D.D., Xao, S.C., Wang, F.L., Cheng, Z.U., Long, H. China Scientific Book Service Co.Ltd Beijing, China, pp. 2169 -2178.
- Burdukova, E., Becker, M., Bradshaw, D.J. and Laskowski, J.S. 2007, "Presence of negative charge on the basal planes of New York talc", *Journal of Colloid and Interface Science*, vol. 315, pp. 337-342.
- Burdukova, E. 2007, *Surface properties of New York talc as a function of pH, polymer adsorption and electrolyte concentration*, PhD thesis, Dept. of Chemical Engineering, University of Cape Town.
- Burgess, J. 1978, *Metal ions in solution*, Ellis Norwood, Chichester, England, pp. 178-183.
- Burns, A.F. and White, J.L. 1963, "Removal of potassium alters b-dimension of muscovite", *Science*, vol. 139, pp. 39-40.
- Burt, D.L.R and Sheppy, N.R. 1975, "Mount Keith nickel sulphide deposit". In: Knight, C.L. (Ed.), *Economic Geology of Australia and Papua New Guinea. 1. Metals*. Australasian Institute of Mining and Metallurgy. Melbourne, Victoria, Australia. Monograph, vol. 5, pp. 159–168.

- Callaghan, I.C. and Ottewill, R.H. 1974, "Interparticle forces in montmorillonite gels", *Discussions of the Faraday Society*, vol. 57, pp. 110-118.
- Carty, W.M. 1999, "The colloidal nature of kaolinite", *American Ceramic Society Bulletin*, pp. 72-77.
- Celik, M. S. 2004, "Electrokinetic behaviour of clay surfaces", *Interface Science Technology*, vol. 1, pp. 57-89.
- Cheremisihoff, N.P. 1988, *Encyclopedia of Fluid Mechanics: Rheology and Non-Newtonian Flows*, Houston, Texas: Gulf Publishing Company.
- Christmann, P. 2010, "Importance of the mining sector for the economies and populations of ACP groups of States", *Ministries of Mines Meeting of the group of ACP States*, ACP House, Brussels, Belgium.
- Collins, B., Napier-Munn, T.J. and Sciaronne, M. 1974, "The production, properties and selection of ferrosilicon powders for heavy-medium separation". *Journal of South African Institute of Mining and Metallurgy*, vol. 75, pp. 103-119.
- Collocott, T.C. 1971, *Chambers Dictionary of Science and Technology*, W.R. Chambers, Edinburgh.
- Connelly, D. 2011, "High clay ores – a mineral processing nightmare", In *Australian Journal of Mining*, July/ August edition: Mineral processing-Flotation and Separation, pp. 28-29.
- Coulson, J.M., and Richardson, J.F. 1999, *Coulson and Richardson's Chemical Engineering: Fluid Flow, Heat Transfer and Mass Transfer*, vol. 1, 6th edition, Butterworth-Heinemann, Oxford, pp. 105-120; 195.
- Das, K. K. 2002, "Electrokinetics of mineral particles", *Surfactant Science Series*, vol. 106, pp. 799-824.
- Delgado, A., Gonzalez-Caballero, F. and Bruque, M. 1986, "On the zeta potential and surface charge density of montmorillonite in aqueous electrolyte solutions", *Journal of Colloid and Interface Science*, vol. 113, pp. 203 – 211.
- de Krester, R.G., Scales, P., and Boger, D.V. 1998, "Surface chemistry-rheology inter relationships in clay suspensions", *Colloids and Surfaces A: Physicochemical and Engineering Aspects*, vol. 137, pp. 307-318.
- de Krester, R.G., Scales, P., and Boger, D.V. 1997, "Improving clay-based tailings disposal : a case study on coal tailings", *AIChE Journal*, vol. 43, pp. 1894 – 1903.

- de Kretser, R.G. and Boger, D.V. 1992, "The compression, dewatering and rheology of slurried coal mine tailings", In Proceedings 5th Australian Coal Science Conference, Newcastle, Australia, pp. 422-429.
- Deer, W.A., Howie, R.A. and Zussman, J. 1992, An introduction to rock forming minerals, Addison Wesley Longman Limited, England.
- Deng, Y., White, G.N., and Dixon, J.B. 2009. Soil Mineralogy Laboratory Manual 11, Department of Soil and Crop Sciences, Texas A&M, pp. 26-37. University, College Station, Texas 77843-2474.
- Derjaguin, B.V. and Landau, L. 1941, "Theory of stability of strongly charged lyophobic sols and the adhesion of strongly charged particles in solution of electrolytes", Acta Physicochem 14, pp. 633-662.
- Dippenaar, A. 1988, "The effect of particles on the stability of flotation froth", Report No. 81, IMM, South Africa.
- Dixon, J.B. and Weed, S.B. 1989, Minerals in soil environments, 2nd edition, eds. Dixon, J.B. and Weed, S.B. Soil Science Society of America, Madison, Wisconsin, USA.
- Dixon, J.B. and Weed, S.B. 1977, Minerals in soil environments, eds. Dixon, J.B. and Weed, S.B. Soil Science Society of America, Madison, Wisconsin, USA.
- Doi, M. and Edwards, S.F. 2001. Theory of Polymer Dynamics, Oxford University Press, Oxford.
- Douglas, L.A. 1989, Chapter 13 – Vermiculites in Minerals in soil environments, eds. Dixon, J.B. and Weed, S.B. Soil Science Society of America, Madison, Wisconsin, USA, pp. 635 - 674.
- Du, J., Morris, G., Pushkarova, R.A. and Smart, R.S.C. 2010, "Effect of surface structure of kaolinite on aggregation, settling rate and bed density", Langmuir, vol. 26, pp. 13227-13235.
- Dukhin, S.S. and Derjaguin, B.V. 1976, Electrophoresis, Moscow, Academy of Science, USSR.
- Dunn, F. 2004, A study of the relationship between various slurry material characteristics and the flow behaviour of co-disposed Kimberlite tailings upon deposition, MSc dissertation, University of Witwatersrand, Johannesburg, South Africa.
- Duran, J.D.G., Ramos-Tejada, M. M., Arroyo, F.J. and Gonzalez-Caballero, F. 2000, "Rheological and electrokinetic properties of sodium montmorillonite suspensions: I.

- Rheological properties and interparticle energy of interaction”, *Journal of Colloid and Interface Science*, vol. 229, pp. 107-117.
- Eales, H.V., Cawthorn, R.G., 1996. The Bushveld Complex. In: Cawthorn, R.G. (Ed.), *Layered Intrusions*. Amsterdam, Elsevier, pp. 181–229.
- Edwards, C.R., Kipkie, W.B. and Agar, G.E. 1980, “The effect of slime coatings of the serpentine minerals, chrysotile and lizardite on pentlandite flotation”, *International Journal of Mineral Processing*, vol. 7, pp. 33-42.
- Estelle, P., Lanos, C and Perrot, A., 2008, “Processing the Couette viscometry data using a Bingham approximation in shear rate calculation”, *Journal of Non-Newtonian Fluid Mechanics*, vol. 154, pp. 31-38.
- Fangary, Y.S., Barigou, M., Seville, J.P.K. and Parker, D.J. 2000, "Fluid trajectories in a stirred vessel of non-newtonian liquid using positron emission particle tracking", *Chemical Engineering Science*, vol. 55, pp. 5969-5979.
- Fanning, D.S., Keramidas, V.Z. and El-Desoky, M.A.1989, Chapter 12-Micas in Minerals in soil environments, eds. Dixon, J.B. and Weed, S.B. Soil Science Society of America, Madison, Wisconsin, USA, pp. 551-634.
- Fanning, D.S. and Keramidas, V.Z. 1977, Minerals in soil environments, eds. Dixon, J.B. and Weed, S.B. Soil Science Society of America, Madison, Wisconsin, USA, pp. 195-258.
- Farrokhpay, S. and Bradshaw, D. 2012, “The effect of clay minerals on froth stability in mineral flotation”, In *Proceedings of the 26th International Mineral Processing Congress*, New Delhi.
- Farrokhpay, S. 2012, “The importance of rheology in mineral flotation: A review”, *Minerals Engineering*, vol. 36-38, pp. 272-278.
- Fisher, D.T., Boger, D.V. and Scales, P.J. 2007, “The bucket rheometer for shear stress-shear rate measurements of industrial suspensions”, *Journal of Rheology*, vol. 51, pp. 82-93.
- Flegmann, A.W., Goodwin, J.W. and Ottewill, R. 1969, “Rheological studies on kaolinite suspensions”, *Proc. Br. Ceram. Soc.*, vol. 13, pp. 31-45.
- Fuerstenau, D.W. and Huang, P. 2003, “ Interfacial phenomena involved in talc flotation”, In *Proceedings of the 23rd International Minerals Processing Congress*, Cape Town, Document Transformation Technologies.

- Furlong, D.L., Freeman, P.A. and Lau, A.G.M., 1981, "The adsorption of soluble silica at solid-aqueous solution interfaces, I-Leaching from glass- an electrokinetic study", *Journal of Colloid and Interface Science*, vol. 80, pp. 20-31.
- Gao, M. and Forssberg, E. 1993, "A study on the effect of parameters in stirred ball milling", *International Journal of Mineral Processing*, vol. 37, pp. 45-59.
- Genç, A.M., Kilickaplan, I. and Laskowski, J.S. 2010, "Pulp rheology in the flotation of serpentinised ultramafic nickel sulfide ore and its effect on flotation.", In *Proceedings of the 8th UBC-McGill-UA International Symposium on the fundamentals of mineral processing: rheology and processing of fine particles*, editor. Pawlik, M. The Canadian Institute of Mining, Metallurgy and Petroleum, Vancouver, British Columbia, Canada, pp. 13-20.
- Gomez, C.O., Maldonado, M., Araya, R. and Finch, J.A. 2010, "Frother and viscosity effects on bubble shape and velocity", In *Proceedings of the 8th UBC-McGill-UA International Symposium on the fundamentals of mineral processing: rheology and processing of fine particles*, editor. Pawlik, M. The Canadian Institute of Mining, Metallurgy and Petroleum, Vancouver, British Columbia, Canada, pp. 57-73.
- Govender, I., Mangesana, N., Mainza, A.N. and Franzidis, J.P. 2011, "Measurement of shear rates in a laboratory tumbling mill", *Minerals Engineering*, vol. 24, pp. 225-229.
- Greene, R.S.B., Eggleton, R.A. and Rengasamy, P. 2002, "Relationships between clay mineralogy and the hardsetting properties of soils in the Carnarvon horticultural district of Western Australia", *Applied Clay Science*, vol. 20, 211-223.
- Guggenheim, S. and Martin, R.T. 1995, "Definition of clay and clay minerals Journal report of the AIPEA nomenclature and CMS nomenclature committees", *Clays and Clay Minerals*, vol. 43, pp. 255-256.
- Gupta, V., Hampton, M.A., Stokes, J.R., Nguyen, A.V. and Miller, J.D. 2011, "Particle interactions in kaolinite suspensions and corresponding aggregate structures," *Journal of Colloid and Interface Science*, vol. 359, pp. 95-103.
- Gupta, V. and Miller, J.D. 2010, "Surface force measurements at the basal planes of ordered kaolinite particles", *Journal of Colloid and Interface Science*, vol. 344, pp. 362-371.
- Hamaker, H. C., 1937, "The London-van der Waals attraction between spherical particles", *Physica* 4, pp. 1058-1072.

- Hasselov, M., Layven, B., Bengtsson, H., Jansen, R., Turner, D.R. and Beckett, R. 2001, "Particle size distribution of clay-rich sediments and pure clay minerals: A comparison of grain analysis with sedimentation field-flow fractionation", *Aquatic Geochemistry*, vol. 7, pp. 155-171.
- He, M. Addai-Mensah, J. and Beattie, D. 2009, "Sericite-chalcocite mineral particle interactions and hetero-aggregation (sliming) mechanism in aqueous media", *Chemical Engineering Science*, vol. 64, pp. 3083-3093.
- He, M. and Forssberg, E. 2007, "Influence of slurry rheology on stirred media milling of quartzite", *International Journal of Mineral Processing*, vol. 84, pp. 240-251.
- He, M., Wang, Y. and Forssberg, E. 2004, "Slurry rheology in wet ultrafine grinding of industrial minerals: a review", *Powder Technology*, vol. 147, pp. 94-112.
- Hong, H. L., Xiao, R.J. and Min, X.M. 2003, "Reaction activity of kaolinite surfaces: Quantum Chemistry Calculations", *J. Wuhan University Technology, Materials Science*, vol. 18, pp. 9-12.
- Hussain, S.A., Dermirci, Ş. and Özbayoglu, G. 1996, "Zeta Potential Measurements on Three Clays from Turkey and Effects of Clays on Coal Flotation", *Journal of Colloid and Interface Science*, vol. 184, pp. 535-541.
- Hill, R.E.T., Barnes, S.J., Perring, C.S. 1996, "Komatiite volcanology and the volcanogenic setting of associated magmatic nickel deposits". In: Grimsey, E.J., Neuss, I. (Eds.), *Nickel '96 Mineral to Market*. Kalgoorlie, 27–29 November 1996. Australasian Institute of Mining and Metallurgy, Publication Series, 6/96, pp. 91–95.
- Hoatson, D.M., Jaireth, S. and Jaques, A.L. 2006, "Nickel sulfide deposits in Australia: Characteristics, resources, and potential", *Ore Geology Reviews*, vol. 29, pp. 177-241.
- Hoffman, R.L. 1972, "Discontinuous and dilatant viscosity behavior in concentrated suspensions. I. Observation of a flow instability", *Transactions of the Society of Rheology*, vol. 16, pp. 155-173.
- Hogg, R. 2000, "Flocculation and dewatering", *International Journal of Mineral Processing*, vol. 58, pp. 223-236.
- Hogg, R., Healy, T. W., and Fuerstenau, D.W. 1966, "Mutual coagulation of colloidal dispersions", *Journal of the Chemical Society, Faraday Transactions*, vol. 62, pp. 1638-1651.

- Holwell, D.A., McDonald, I. and Armitage, P.E.B. 2006, "Platinum group mineral assemblages in the Platreef at the Slandslot Mine, in the northern Bushveld Complex, South Africa", *Mineralogical Magazine*, vol. 70, pp. 83-101.
- Horie, M. and Pinder, K.L. 1979, "Time-dependent shear flow of artificial slurries in coaxial cylinder viscometer with a wide gap" .*Canadian Journal of Chemical Engineering*, vol. 57, pp. 125-134.
- Hu, Y. H., Sun, W., Liu, W and Wang, D.Z. 2003, "Cleavage nature, electrokinetics, aggregation and dispersion of kaolinite", *Transactions of Nonferrous Metals Society China*, vol. 13, pp. 1430-1434.
- Hunter, R.J. 1981, *Zeta Potential in Colloid Science – Principles and Applications*, Academic Press, New York.
- Hurlbut, C.S and Sharp, W.E. 1998, *Dana's Minerals and how to study them (After Edward Salisbury Dana)*, 4th edition, John Wiley & Sons, Inc., New York, pp. 248-257.
- Israelachvili, J. N. 1985, *Intermolecular and surface forces with applications to colloidal and biological systems*, Academic Press, London.
- Jackson, M.L. and Sridhar, K. 1974, "Scanning electron microscope and X-Ray diffraction study of natural weathering of phlogopite through vermiculite to saponite", In *Proceedings of the Soil Science Society of America*, vol. 38, pp. 843-847.
- Jackson, M.L., Lee, S.Y., Brown, J.L. Sachs, I.B. and Syers, J.K. 1973, "Scanning electron microscopy of hydrous metal oxide crusts intercalated in naturally weathered micaceous vermiculite", In *Proceedings of the Soil Science Society of America*, vol. 37, pp. 127-131.
- Jackson, M.L. 1973, *Soil Chemical Analysis Advanced Course*, 2nd edition, published by author, Dept. Soil Science, University of Soil Science, Wisconsin Madison, pp. 895.
- Jackson, M.L. 1963, "Interlaying of expansible layer silicates in soils by chemical weathering", In *Proceedings of the 11th Conference of Clays and Clay Minerals*, Pergamon Press, New York, pp. 29-46.
- James, A.E. and Williams, D.J.A. 1982, "Flocculation and rheology of kaolinite/quartz mixtures", *Rheologica Acta*, vol. 21, pp. 176-183.
- Jayasundara, C.T., Yang, R.Y., Guo, B.Y., Yu, A.B. and Rubenstein, J, 2009, "Effect of slurry properties on particle motion in IsaMills", *Minerals Engineering*, vol. 22, pp. 886-892.

- Jogun, S., and Zukoski, C.F. 1996, "Rheology of dense suspensions of platelike particles", *Journal of Rheology*, vol. 40, pp. 1211-1232.
- Johnson, S.B., Franks, G.V., Scales, P.J., Boger, D.V. and Healy, T.W. 2000, "Surface chemistry–rheology relationships in concentrated mineral suspensions", *International Journal of Mineral Processing*, vol. 58, pp. 267-304.
- Johnson, S.B., Russell, A.S. and Scales, P.J. 1998, "Volume fraction effects in shear rheology and electroacoustic studies of concentrated alumina and kaolin suspensions", *Colloids and Surfaces A: Physicochemical and Engineering Aspects*, vol. 141, pp. 119-130.
- Johnson, S.B., 1998, Surface chemistry–rheology relationships in concentrated mineral suspensions, PhD thesis, The University of Melbourne.
- Jorjani, E., Barkhordar, H.R., Tayebi Khormani, M. and Fazeli, A. 2011, "Effects of aluminosilicate minerals on copper-molybdenum flotation from Sarcheshmeh porphyry ores", *Minerals Engineering*, vol. 24, pp. 754-759.
- Kasongo, T., Zhou, Z., Xu, Z. and Masliyah, J. 2000, "Effect of clays and calcium ions on bitumen extraction from Athabasca oil sands using flotation", *The Canadian Journal of Chemical Engineering*, vol. 78, pp. 678-680.
- Kawatra, S.K. and Bakshi, A.K. 1996, "On-line measurement of viscosity and determination of flow types for mineral suspensions", *International Journal of Mineral Processing*, vol. 47, pp. 275-283.
- Keentok, M., Milthorpe, J.F. and O'Donovan, E. 1985, "On the shearing zone around rotating vanes in plastic liquids: Theory and Experiment", *Journal of Non-Newtonian Fluid Mechanics*, vol. 17, pp. 23-35.
- Khraisheh, M.C., Holland, C., Creany, P. Harris, P. and Parolis, L. 2005, "Effect of molecular weight and concentration on the adsorption of CMC onto talc at different ionic strengths", *International Journal of Mineral Processing*, vol. 75, pp. 197-206.
- Kishk, F.M. and Barshad, I. 1969, "Morphology of vermiculite clay particles as affected by their genesis", *The American Mineralogist*, vol. 54, pp. 849-857.
- Kirjavainen, V. and Heiskanen, K. 2007, "Some factors that affect beneficiation of sulphide nickel–copper ores", *Minerals Engineering*, vol. 20, pp. 629-633.

- Klein, B., Alton, N. E., Colebrook, M. and Pawlik, M. 2012, "Electroacoustic measurements of mixed quartz and iron oxide mineral systems", *International Journal of Mineral Processing*, vol. 110-111, pp. 12-17.
- Klein, C. and Dutrow, B. 2008, *Manual of Mineral Science*, 23rd edition, John Wiley and Sons Inc., New York, pp. 456-467; 519-534.
- Klein, C. and Hurlbut, C. S. 1993, *Manual of Mineralogy* (after J.D. Dana), 21st edition .Wiley and Sons, New York.
- Klein, B. and Pawlik, M. 2005, "Rheology modifiers for mineral suspensions", *Minerals and Metallurgical Processing*, vol. 22, pp. 83-88.
- Knecht, V., Risselada, H. J., Mark, A. E. and Marrink, S. J. 2008, "Electrophoretic mobility does not always reflect the charge on an oil droplet", *Journal of Colloid and Interface Science*, vol. 318, pp. 477-486.
- Koopal, L.K., Yang, Y., Minnaard, A.J., Theunissen, P.L.M. and Van Riemsdijk, W.H. 1998, "Chemical immobilisation of humic acid on silica", *Colloids and Surfaces A: Physicochemical and Engineering Aspects*, vol. 141, pp. 385-395.
- Krapiel, A.M.L., Keller, K., Morel, F.M.M. 1998, "On the acid-base chemistry of permanently charged minerals", *Environ. Sci. Technol.*, vol. 32, pp. 2829-2838.
- Krieger, I.M. 1968, "Shear rate in Couette viscometer", *Journal of Rheology*, vol. 12, pp. 5-11.
- Lagaly, G. And Zeisner, S. 2003,"Colloid chemistry of clay minerals: the coagulation of montmorillonite dispersions", *Advances in Colloid and Interface Science*, vol. 100-102, pp.105-128.
- Laird, D.A. 2006, "Influence of layer charge on swelling of smectites", *Applied Clay Science*, vol. 34, pp. 74-87.
- Laskowski, J. S. 2012,"Anisotropic minerals in flotation circuit", *CIM Journal*, vol. 3, pp. 203-213.
- Laskowski, J.S., Ndlovu, B. and Kilickaplan, I. 2010, "Rheology of aqueous suspensions of needle-like mineral particles". In *Proceedings of the 8th UBC-McGill-UA International Symposium on the fundamentals of mineral processing: rheology and processing of fine particles*, editor. Pawlik, M. The Canadian Institute of Mining, Metallurgy and Petroleum, Vancouver, British Columbia, Canada, pp. 193-203.

- Laskowski, J.S. and Pugh, J.S. 1992, Chapter 4- Dispersion stability and dispersing agents in Colloid Chemistry in mineral processing, edited by Laskowski, J.S. and Ralston, J.S. Elsevier Science Publishers B.V., Amsterdam, Netherlands, pp. 151-161.
- Laskowski, J.S. and Sobieraj, S. 1969, "Zero points of charge of spinel minerals", Transactions of Institute of Mining and Metallurgy, vol. 78, C161 - C162.
- Lee, R. J., Strohmeier, B.R. and Bunker, K. L. 2008, "Naturally occurring asbestos: a recurring public policy challenge", Journal of Hazardous Material, vol. 15, pp. 1-21.
- Leong, Y. K. 2005, "Yield stress and zeta potential of nanoparticulate silica dispersions under the influence of adsorbed hydrolysis products of metal ions –Cu(II), Al(III) and Th(IV)", Journal of Colloid and Interface Science, vol. 292, pp. 557-566.
- Leong, Y.K. and Yeow, Y. L. 2003, "Obtaining the shear rate relationship and yield stress of liquid foods from Couette viscometry data", Rheologica Acta, vol. 42, pp. 365-371.
- Leong, Y. K. and Boger, D.V. 1990, "Surface chemistry effects on concentrated suspension rheology", Journal of Colloid and Interface Science, vol. 136, pp. 249-258.
- Leschak, P. and Ferrell, R.E. 1988, "Morphologies of suspended clay-sized quartz particles in Mississippi River and their reaction to sedimentary sources", Geological Society of America, vol. 16, pp. 334-336.
- Liddell, P.V. and Boger, D.V., 1996, "Yield stress measurements with the vane", Journal of Non-Newtonian Fluid Mechanics, vol. 63, pp. 235-261.
- Lifshitz, E. M. 1956, "The theory of molecular attractive forces between solids", Soviet Physics, JETP 2, pp. 73-83.
- Luckham, P.F., Vincent, B. and Tadros, T.F. 1983, "The controlled flocculation of particulate dispersions using small particles of opposite charge. III. Investigation of floc structure using rheological techniques", Colloids and Surfaces, vol. 6, pp. 101-118.
- Luckham, P.F. and Rossi, S. 1999, "The colloidal and rheological properties of bentonite suspensions", Advances in Colloid and Interface Science, vol. 82, pp. 43-92.
- Lui, X., Hu, Y. Huang, S. and Qui, G. 2001, "Chemical composition and surface property of kaolins", Kuangwu Xuebao, vol. 21, pp. 443-447.
- Lyklema, J. 1995, Fundamentals of Interface and Colloid Science, 2nd edition. Academic Press, London.

- Lyons, J.S., Furlong, D.N. and Healy, T.W. 1981, "The electrical double layer properties of the mica (muscovite)-aqueous electrolyte interface", *Australian Journal of Chemistry*, vol. 34, pp. 1177-1187.
- M'Ewen, M.B. and Pratt, M.I. 1957, "The gelation of montmorillonite, Part 1", *Transactions of the Faraday Society*, vol. 53, pp. 535.
- M'Ewen, M.B. and Pratt, M.I. 1957, "The gelation of montmorillonite, Part 2", *Transactions of the Faraday Society*, vol. 53, pp. 549.
- Ma, X., Bruckard, W.J. and Holmes, R. 2009, "Effect of collector, pH and ionic strength on the cationic flotation of kaolinite", *International Journal of Minerals Processing*, vol. 93, pp. 54-58.
- Maslova, M. V., Gerasimova, L. G. and Forsling, W. 2004, "Surface properties of cleaved mica", *Kolloidny Zhurnal*, vol. 66, pp. 364-371.
- McBride, M.B., Baveye, P. 2002, "Diffuse double-layer models, long range forces, and ordering in clay colloids", *Soil Sci. Soc. Am.*, vol. 66, pp. 1207-1217.
- McBride, M.B., Baveye, P. 2003, "Response to Comments on Diffuse double-layer models, long-range forces, and ordering of clay colloids", *Soil Sci. Soc. Am.* vol. 67, pp. 1961-1964.
- McFarlane, A., Bremmell, K. and Addai-Mensah, J. 2005, "Microstructure, rheology and dewatering behaviour of smectite dispersions during orthokinetic flocculation", *Minerals Engineering*, vol. 18, pp. 1173-1182.
- McKeague, J.A. and Day, J.H. 1966, "Ditionite and oxalate extractable Fe and Al as aids in differentiating various classes of soils", *Canadian Journal of Soil Science*, vol. 44, pp. 13-22.
- Mercier, L. and Detellier, C. 1995, "Preparation, characterization and applications as heavy metals sorbents of covalently grafted thiol functionalities on the interlamellar surface of montmorillonite", *Environmental Science Technology*, vol. 29, pp. 1318-1323.
- Meunier, A. 2005, *Clays*, Springer – Verlag, Berlin Heidelberg, pp. 192.
- Miano, F. and Rabaioli, M. R. 1994, "Rheological scaling of montmorillonite suspensions: the effect of electrolytes and polyelectrolytes", *Colloids and Interface Science A: Physicochemical and Engineering Aspects*, vol. 84, pp. 229-237.

- Mikulášek, P., Wakeman, R.J. and Marchant, J.Q. 1997, "The influence of pH and temperature on the rheology and stability of aqueous titanium dioxide dispersions", *Chemical Engineering Journal*, vol. 67, pp. 97-102.
- Miller, J.D., Nalaskowski, J., Abdul, B., Du, H. 2007, "Surface characteristics of kaolinite and other selected two layer silicate minerals", *The Canadian Journal of Chemical Engineering*, vol. 85, pp. 617 – 624.
- Mitchell, T.K., Nguyen, A.V. and Evans, G.M. 2005, "Heterocoagulation of chalcopyrite and pyrite minerals in flotation separation", *Advances in Colloid and Interface Science*, vol. 114-115, pp. 227-237.
- Montgomery, D.C. and Runger, G.C. 2006, *Statistics and Probability for Engineers*, 4th edition, John Wiley and Sons.
- Morkel, J., Pistorius, P.C. and Vermaak, M.K.G. 2007, "Cation exchange behaviour of Kimberlite in solutions containing Cu^{2+} and K^{+} ", *Minerals Engineering*, vol. 20, pp. 1145-1152.
- Motta, M. M. and Miranda, C. F. 1989, "Molybdate adsorption on kaolinite, montmorillonite and illite: Constant capacitance modeling", *Soil Science Soc. Am J.*, vol. 53, pp. 380-385.
- Mpofu, P., Addai-Mensah, J. and Ralston, J. 2004, "Flocculation and dewatering behaviour of smectite dispersions: effect of polymer structure type", *Minerals Engineering*, vol. 17, pp. 411-423.
- Mular, A.L. and Roberts, R.B. 1966, "A Simplified method to determine isoelectric points of oxides", *Transactions of the Canadian Institute of Mining and Metallurgy*, vol. 69, pp. 438 - 439.
- Muster, T.H. and Prestidge, C.A. 1995, "Rheological investigation of sulphide mineral slurries", *Minerals Engineering*, vol. 8, pp. 1541-1555.
- Nalaskowski, J.B., Abdul, B., Du, H. and Miller, J.D., 2007, "Anisotropic character of talc surfaces as revealed by streaming potential measurements, atomic force microscopy and molecular dynamics simulations", *Can. Met. Quarterly*, vol. 46, pp. 227-236.
- Nasser, M.S. and James, A.E. 2006, "Settling and sediment bed behaviour of kaolinite in aqueous media", *Separation and Purification Technology*, vol. 51, pp. 10-17.
- Nasroti, A. 2010, *Particle interactions and processability of aqueous muscovite clay mineral dispersions*, PhD Thesis, Ian Wark Research Institute.

- Navidi, W. 2008. *Statistics for engineers and scientists*, 2nd edition, McGraw Hill International Edition.
- Newman, A.C.D. and Brown, G. 1969, "Delayed exchange of potassium from some edges of mica flakes", *Nature*, vol. 223, pp. 175-176.
- Ney, P. 1973, "Applied mineralogy in zeta potentials and flotability of minerals", Springer-Verlag, Vienna/ New York, vol. 6, pp. 214.
- Nguyen, Q.D. and Boger, D.V. 1998, "Application of rheology to solving tailings disposal problems", *International Journal of Mineral Processing*, vol. 54, pp. 217-233.
- Nguyen, Q.D. and Boger, D.V. 1987, "Characterisation of yield stress fluids in concentric cylinder viscometers", *Rheologica Acta*, vol. 26, pp. 508-515.
- Nguyen, Q.D. and Boger, D.V. 1985, "Direct Yield Stress measurement with the vane rheometer", *Journal of Rheology*, vol. 29, pp. 335-347.
- Nguyen, Q.D. and Boger, D.V. 1983, "Yield Stress measurement for concentrated suspensions", *Journal of Rheology*, vol. 27, pp. 321-349.
- Nishimura, S., Scales, P.J., Tateyama, H., Tsunematsu, K. and Healy, T.W. 1995a, "Cationic modification of muscovite mica ", *Langmuir*, vol. 11, pp. 291-295.
- Nishimura, S., Scales, P.J., Biggs, S.R. and Healy, T.W. 1995b, "AFM studies of amine surfactant hemimicelle structures at the mica-water interface", *Colloids and Interface Surface A: Physicochemical and Engineering Aspects*, vol. 103, pp. 289-298.
- Nishimura, S., Tateyama, H., Tsunematsu, K. and Jinnal, K. 1992, "Zeta potential measurement of muscovite mica basal plane-aqueous solution interface by means of plane interface technique", *Journal of Colloid and Interface Science*, vol. 152, pp. 359-367.
- Norrish, K. 1973, "Factors in the weathering of mica to vermiculite", In *Proceedings of the International Clay Conference, Madrid*, ed. Ciencias, D., C.S.I.C., Madrid, Spain, pp. 417-432.
- O'Brien, R.W. and White, L.R. 1978, "Electrophoretic mobility of a spherical colloidal particle", *Journal of Chemical Society, Faraday Transactions 2: Molecular and Chemical Physics*, vol. 74, pp. 1607-1626.
- Okuda, S., Inoue, K. and Williamson, W.O. 1969, "Negative surface charges of pyrophyllite and talc", In *Int. Clay Conference*, eds. Heller, L., Israel University Press, Tokyo, Japan, pp. 31-p41.

- Otsuki, A., Barry, S. and Fornasiero, D. 2011, "Rheological studies of nickel oxide and quartz/hematite mixture systems", *Advanced Powder Technology*, vol. 22, pp. 471-475.
- Parker, S.P. 1991, *McGraw-Hill Dictionary of Science and Technology*, 4th edition, McGraw-Hill, New York.
- Pashley, R.M. 1985, "Electromobility of mica particles dispersed in aqueous solutions", *Clays and Clay Minerals*, vol. 33, pp. 193-199.
- Pashley, R.M. and Israelachvili, J.N. 1984, "DLVO and hydration forces between mica surfaces in Mg^{2+} , Ca^{2+} , Sr^{2+} and Ba^{2+} chloride solutions", *Journal of Colloid and Interface Science*, vol. 97, pp. 446-455.
- Patra, P., Bhambhani, T., Nagaraj, D.R. and Somasundaran, P. 2010, "Effect of morphology of altered silicate minerals on metallurgical performance: transport of Mg silicates to the froth phase", In *Proceedings of the 8th UBC-McGill-UA International Symposium on the fundamentals of mineral processing: rheology and processing of fine particles*, editor. Pawlik, M. The Canadian Institute of Mining, Metallurgy and Petroleum, Vancouver, British Columbia, Canada, pp. 31-42.
- Permien, T. and Lagaly, G. 1994, "The rheological and colloidal properties of bentonite dispersions in the presence of organic compounds IV. Sodium montmorillonite and acids", *Applied Clay Science*, vol. 9, pp. 251-263.
- Pils, J.R.V., Laird, D.A. and Evangelou, V.P. 2007, "Role of cation demixing and quasicrystal formation and breakup on the stability of smectitic colloids", *Applied Clay Science*, vol. 35, pp. 201-211.
- Pokrovsky, O.S. and Schott, J. 2004, "Experimental study of brucite dissolution in aqueous solutions: surface speciation and chemical affinity control", *Geochemica et Cosmochimica Acta*, vol. 68, pp. 31-45.
- Prakash, S., Das, B., Mohanty, J.K. and Venugapol, R. 1999, "The recovery of fine iron minerals from quartz and corundum mixtures using selective magnetic coating", *International of Mineral Processing*, vol. 57, pp. 87-103.
- Prestidge, C.A. 1997, "Rheological investigations of ultrafine galena particle slurries under flotation-related conditions", *International Journal of Mineral Processing*, vol. 51, pp. 241-254.

- Protz, R. and St. Arnaud, R.J. 1964, "The evaluation of four pretreatments used in particle size distribution analyses", Canadian Journal of Soil Science, vol. 44, pp. 345-351.
- Prutton, M. 1994, Introduction to Surface Physics, Oxford University Press.
- Ralston, J., and Fornaserio, D. 2006, "Effect of MgO minerals on pentlandite flotation", In 23rd International Minerals Processing Congress, Istanbul, Turkey eds. Onal, G., Acarkan, N., Celik, M.S., Arslan, F., Atesok, G., Guney, A., Sirkeci, A.A., Yuce, A.E., Perek, K.T. Promed Advertising Ltd, Istanbul, Turkey, pp. 750- 755.
- Raman, K.V. and Jackson, M.L. 1964, "Vermiculite surface morphology", In Proceedings of the National Conference of Clays and Clay Minerals, vol. 12, pp. 423-429.
- Rand, B. and Melton, I.E. 1977, "Particle interactions in aqueous kaolinite suspensions: I. Effect of pH and electrolyte upon the mode of particle interaction in homoionic sodium kaolinite suspensions", Journal of Colloid and Interface Science, vol. 60, pp. 308-320.
- Rasmusson, M., Rowlands, W.O., O'Brien, R.W. and Hunter, R.J. 1997, "The dynamic mobility and dielectric response of sodium bentonite", Journal of Colloid and Interface Science, vol. 189, pp. 92-100.
- Rawle, A. 2011, "Particle size analysis properties", Malvern talks <http://www.materials-talks.com/blog/2011/01/21/particle-size-analysis-principles/>
- Robinsky, E.I. 1975, "Thickened discharge – A new approach to tailings disposal", CIM Bulletin, vol. 68, pp. 47-53.,
- Robinson, M. 1996, Chambers 21st Century Dictionary, W.R. Chambers, Edinburgh.
- Roth, C.B., Jackson, M.L., Lotse, E.G. and Syers, J.K. 1968, "Ferrous-ferric ratio and CEC changes on deferration of weathered micaceous vermiculite", Isr. J. Chem., vol. 6, pp. 261-273.
- Rubiera, F., Esteban, R., Arenillas, A. and Pis, J.J. 1999, "Effect of blending different rank coals on NO_x emissions, In Prospects for Coal Science in the 21st Century, vol. 1, eds. B.Q. Li and Z.Y. Liu, China: Shanxi and Technology Press, pp. 1501-1504.
- Roth, C.B., Jackson, M.L., De Villiers, J.M. and Volk, V.V., 1966, "Surface colloids on micaceous vermiculite", Trans. Comm. II and IV, International Society of Soil Science, Aberdeen, pp. 217-21.

- Sakairi, N., Kobayashi, M., Adachi, Y., 2005, "Effects of salt concentration on the yield stress of sodium montmorillonite suspension", *Journal of Colloid and Interface Science*, vol. 283, pp. 245-250.
- Scales, P.J., Greiser, F. And Healy, T.W., 1990, "Electrokinetics of the muscovite mica – aqueous solution interface", *Langmuir*, vol. 6, pp. 582-589.
- Scales, P.J., Healy, T. W. and Evans, D. F., 1988, "The zeta potential of muscovite mica: Counterion complexation by a macrocyclic ligand", *Journal of Colloid and Interface Science*, vol. 124, pp. 391-395.
- Scott, A.D. and Smith, S.J. 1966, "Susceptibility of interlayer potassium in micas to exchange with sodium", *Clays and Clay Minerals*, 14th National Conf. Clays and Clay Minerals, pp. 69-81.
- Schainberg, I., Alperovitch, N.I. and Keren, R. 1987, "Charge density and Na-K-Ca exchange in smectites", *Clay and Clay Minerals*, vol. 35, pp. 68-73.
- Schindler, D.W. 1976, "Biogeochemical evolution of phosphorous limitation on nutrient-enriched lakes of the Precambrian Shield", *Environmental Biogeochemistry Ann Arbor Sci.*, pp. 647-667.
- Schoeman, J.J. 1989, "Mica and vermiculite in South Africa", *Journal of South African Institute of Mining and Metallurgy*, vol. 89, pp. 1-12.
- Schofield, R.K. and Samson, H.R. 1954, "Flocculation of kaolinite due to the attraction of oppositely charged crystal faces", *Discussions of the Faraday Society*, vol. 18, pp. 135-145.
- Schouwstra, R.P., Kinloch, E.D. and Lee, C.A. 2000, "A short geological review of the Bushvelt Complex", *Platinum Minerals Review*, vol. 44, pp. 33-39.
- Schroth, B.K. and Sposito, G. 1997, "Surface charge properties of kaolinites", *Clays and Clay Minerals*, vol. 45, pp. 85-91.
- Schubert, H. 2008, "On the optimization of hydrodynamics in fine particle flotation", *Minerals Engineering*, vol. 21, pp. 930–936.
- Schubert, H. and Bischofberger, C. 1978, "On the hydrodynamics of flotation machines", *International Journal of Mineral Processing*, vol. 5, pp. 132-142.
- Secor, R.B. and Radke, C.J. 1985, "Spillover of the diffuse layer on montmorillonite particles", *Journal of Colloid and Interface Science*, vol. 103, pp. 237-244.

- Senapati, P.K., Mishra, B.K. and Parida, A. 2010, "Modelling of viscosity for power plant ash slurry at higher concentrations: Effect of solids volume fraction, particle size and hydrodynamic interactions", *Powder Technology*, vol. 197, pp. 1-8.
- Senior, G.D. and Thomas, S.A. 2005, "Development and implementation of a new flowsheet for the flotation of a low grade nickel ore", *International Journal of Mineral Processing*, vol. 78, 1, pp. 49-61.
- Shabalala, N.Z.P., Harris, M., Leal Filho, L.S. and Deglon, D.A. 2011, "Effect of slurry rheology on gas dispersion in a pilot scale mechanical flotation cell", *Minerals Engineering*, 24, pp. 1448-1453.
- Shainberg, I. 1973, "Rate and mechanism of Na-montmorillonite hydrolysis in suspensions", In *Proceedings of the Soil Sci. Soc. America*, vol. 37, pp. 689-694.
- Shaw, D. J. 1992, *Introduction to colloid and surface chemistry*, Butterworth Heinman.
- Shi, F.N. and Napier-Munn, T.J. 2002, "Effects of slurry rheology on industrial grinding performance", *International Journal of Mineral Processing*, vol. 65, pp. 125-140.
- Sofrá, F. and Boger, D.V. 2002, "Environmental rheology for waste minimization in the minerals industry", *Chemical Engineering Journal*, vol. 86, 3, pp. 319-330.
- Solomon, M. and Boger, D.V. 1998, "The rheology of aqueous suspensions of spindle-like colloidal haematite rods," *Journal of Rheology*, vol. 42, pp. 929-949.
- Somasundaran, P., Smith, E.L. and Harris, C.C. 1975, "Dewatering of phosphate slimes using coarse additives", *Mineral Processing Congress, Caligri, Italy*, pp. 1301.
- Srodon, J. 2006, Quantitative analysis of clay minerals in *Handbook of Clay Science*, ed. Bergaya, F., Theng, B.K.G. and Lagaly, G., *Developments in Clay Science*, 1, Elsevier Ltd, pp. 765-786.
- Steffe, J.F. 1966, *Rheological methods in food engineering process*, 2nd edition, Freeman Press, East Lansing, USA.
- Stokes, J.R. and Telford, J.H. 2004, "Measuring the yield behavior of structured fluids", *Journal of Non-Newtonian Fluid Mechanics*, vol. 124, pp. 137-146.
- Subbanna, M., Pradip and Malghan, S.G. 1998, "Shear yield stress of flocculated alumina-zirconia mixed suspensions: effect of solid loading, composition and particle size distribution", *Chemical Engineering Science*, vol. 53, pp. 3073-3079.

- Sverjensky, D.A. 1994, "Zero-point-of-charge prediction from crystal chemistry and solvation theory", *Geochemica et Cosmochimica Acta*, vol. 58, pp. 3123-3129.
- Swartzen-Allen, S.L. and Matijevic, E. 1974, "Surface and Colloid Chemistry of Clays", *Chemistry Reviews*, vol. 74, pp. 385-400.
- Swartzen-Allen, S.L. and Matijevic, E. 1976, "Colloid and Surface properties of clay suspensions III. Stability of montmorillonite and kaolinite", *Journal of Colloid and Interface Science*, vol. 56, pp. 159 – 167.
- Tangsathitkulchai, C. 2003, "The effect of slurry rheology on fine grinding in a laboratory ball mill", *International Journal of Mineral Processing*, vol. 69, pp. 29-47.
- Tao, D., Dopico, P.G., Hines, J and Kennedy, D. 2010, "An experimental study of clay binders in fine coal froth flotation", In *Proceedings of the International Coal Preparation Congress*, Lexington, USA, pp. 478-487.
- Tarzi, J.G. and Protz, R. 1978, "Characterisation of morphological features of soil micas using scanning electron microscopy", *Clays and Clay Minerals*, vol. 26, pp. 352-360.
- Tateyama, H., Scales, P.J., Ooi, M. Nishimura, S., Rees, K. And Healy, T., 1997, "X-ray diffraction and rheology study of highly ordered clay platelet alignment in aqueous solutions of sodium tripolyphosphate" *Langmuir*, vol.13, pp. 2440-2446.
- Tombácz, E. and Szekeres, M. 2006, "Surface charge heterogeneity of kaolinite in aqueous suspension in comparison with montmorillonite", *Applied Clay Science*, vol. 34, pp. 105-124.
- Tremolada, J., Dzioba, R., Bernardo-Sanchez, A. and Menendez-Aguado, J.M. 2010, "The pre-robbering of gold and silver by clays during cyanidation under agitation and heap leaching conditions", *International Journal of Mineral Processing*, vol. 94, pp. 67-71.
- Triantafillopoulos, N.G. and Smith, K. 1998, "Troubleshooting rheology problems in metered size press", In *Proceedings of Tappi Metered Size Press Forum*, pp. 13-35.
- Van Olpen, H. 1977, *Clay Colloid Chemistry*, 2nd edition, John Wiley & Sons, New York, pp. 318
- Van Olpen, H. 1951, "Rheological phenomena of clay sols in connection with the charge distribution on the micelles", *Discussions of the Faraday Society*, vol. 11, pp. 82-84.
- Van Tonder, E., Deglon, D and Napier-Munn, T. 2010, "The effect of ore blends on the mineral processing of platinum ores", *Minerals Engineering*, vol. 23, pp. 621-626.

- Vanerek, A., Alince, B., and van de Ven, T.G.M. 2006, "Delamination and flocculation efficiency of sodium activated kaolin and montmorillonite", *Colloids and Surfaces A: Physicochem Engineering Aspects*, vol. 273, pp.193-201.
- Vasudevan, M., Nagaraj, D.R., Patra, P. and Somasundaran, P. 2010, "Effect of altered silicates in flotation performance: role of changes in pulp rheology", In Proc. 8th UBC-McGill-UA International Symposium on the fundamentals of mineral processing: rheology and processing of fine particles, editor. Pawlik, M. The Canadian Institute of Mining, Metallurgy and Petroleum, Vancouver, British Columbia, Canada, pp. 21-30.
- Venkata, K.V. and Jackson, M.L. 1963, "Vermiculite Surface Morphology", In Proceedings of the 12th National Conference on Clays and Clay Minerals, pp. 423-429.
- Verma, A.R. 1956, "A phase contrast microscopic study of the surface structure of blende crystals", *Mineralogy Magazine*, vol. 31, pp. 136-144.
- Verwey, E.J.W. and Overbeek, J.T.G. 1948, *Theory Stability of Lyophobic Solids*, Amsterdam, Elsevier.
- Vietti, A.J. 2003, Chapter 1 : Development of thickened tailings technology within the De Beers Group, *Paste and Thickened Tailings Disposal Handbook*, Ed Vietti and Dunn, Technical Support Services, De Beers Consolidated Mines, Johannesburg, South Africa
- Vietti, A.J. 2003, "Surface chemistry effects of kimberlitic clay minerals", In Proceedings of the Fourth One Day Seminar on Hydraulic Transport in the Mining Industry, Hydraulic Conveying Association of South Africa, Johannesburg, South Africa.
- Vuthaluru, H.B., Brooke, R.J., Zhang, D.K. and Yan, H.M. 2003, "Effects of moisture and coal blending on Hardgrove Grindability Index of Western Australian coal", *Fuel Processing Technology*, vol. 81, pp. 67-76.
- Wallace, D., Tipman, R., Komishke, B., Wallwork, V. and Perkins, E. 2004, "Fines/water interactions and consequences of the presence of degraded illite on oil sands extractability", *The Canadian Journal of Chemical Engineering*, vol. 82, pp. 678-680.
- Wiese, J., Harris, P. and Bradshaw, D. 2011, "The effect of the reagent suite on froth stability in laboratory scale batch flotation tests", *Minerals Engineering*, vol. 24, pp. 995-1003.
- Wiese, J.G., Harris, P. and Bradshaw, D.J. 2007, "The response of sulphide and gangue minerals in selected Merensky ores to increased depressant dosages", *Minerals Engineering*, vol. 20, pp. 886-995.

- Williams, D. J. A. and Williams, K. P. 1978, "Electrophoresis and zeta potential of kaolinite", *Journal of Colloid and Interface Science*, vol. 65, pp. 79-87.
- Weisberg, S. 2005, *Applied Linear Regression*, John Wiley & Sons.
- www.wise-uranium.org/mdaf.html Chronology of major tailings dam failures
- Xiao, H., Liu, Z. And Wiseman, N. 1999, "Synergetic effect of cationic polymer microparticles and anionic polymers on fine clay flocculation", *Journal of Colloid and Interface Science*, vol. 216, pp. 409-417.
- Yada, K. 1971, "Study of the microstructure of chrysotile asbestos by high resolution electron microscopy", *Acta Cryst*, A27, pp. 659 - 664.
- Yan, L., Englert, A. H., Masliyah, J. H. and Xu, Z. 2011, "Determination of anisotropic surface characteristics of different phyllosilicates by direct force measurements", *Langmuir*, vol. 27, pp. 12996-13007.
- Yan, D. and Eaton, R. 1994, "Breakage properties of ores blends", *Minerals Engineering*, vol. 7, pp. 185-199.
- Yan, J. and James, A.E. 1997, "The yield surface of viscoelastic and plastic fluids in a vane viscometer", *Journal of Non-Newtonian Fluid Mechanics*, vol. 70, pp. 237-253.
- Yin, X., Gupta, V., Du, H., Wang, X. and Miller, J.D. 2012, "Surface charge and wetting characteristics of layered silicate minerals", *Advances in Colloid and Interface Science*, vol. 179-182, pp. 43-50.
- Yue, J. and Klein, B. 2004, "Influence of rheology on the performance of horizontal stirred mills", *Minerals Engineering*, vol. 17, pp. 1169-1177.
- Zbik, M., Raftery, N.A., Smart, R.S.C. and Frost, R.L. 2010, "Kaolinite platelet orientation for XRD and AFM applications", *Applied Clay Science*, vol. 50, pp. 299-304.
- Zbik, M. and Smart, R. C. 2002, "Dispersion of kaolinite and talc in aqueous solution: nano-morphology and nano-bubble entrapment", *Minerals Engineering*, vol. 15, pp. 277-286.
- Zbik, M. and Smart, R.S.C. 1998, "Nanomorphology of kaolinites: comparative SEM and AFM studies", *Clay and Clay Minerals*, vol. 46, pp. 153-160.
- Zhong, Z., Ooi, J.Y. and Rotter, J.M. 2005, "Predicting the handability of a coal blend from measurements on the source coals", *Fuel*, vol. 84, pp. 2267-2274.
- Zhou, Z. and Gunter, W.D. 1992, "The nature of the surface charge of kaolinite clays", *Clay Miner.*, vol. 20, pp. 365-368.